A ZERO ORDER GPS NETWORK FOR THE AUSTRALIAN REGION

PETER MORGAN, YEHUDA BOCK, RICHARD COLEMAN, PENG FENG, DANIEL GARRARD, GARY JOHNSTON, GEOFF LUTON, BARRY McDOWALL, MERRIN PEARSE, CHRIS RIZOS and RUSSELL TIESLER

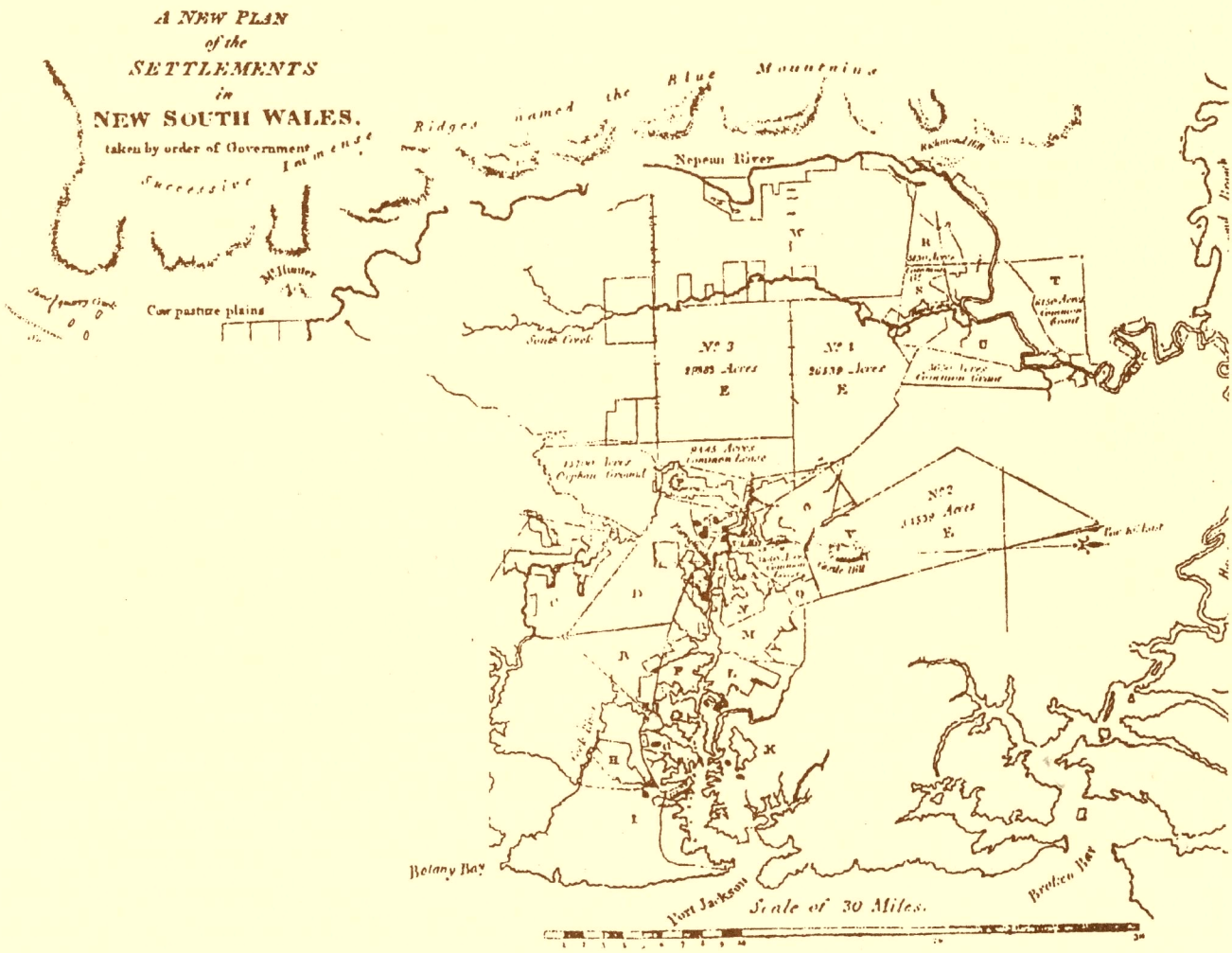

UNISURV S-46, 1996

Reports from

SCHOOL OF GEOMATIC ENGINEERING

THE UNIVERSITY OF NEW SOUTH WALES SYDNEY NSW 2052 AUSTRALIA

UNISURV REPORT S-46, 1996

A ZERO ORDER GPS NETWORK FOR THE AUSTRALIAN REGION

PETER MORGAN, YEHUDA BOCK, RICHARD COLEMAN, PENG FENG, DANIEL GARRARD, GARY JOHNSTON, GEOFF LUTON, BARRY McDOWALL, MERRIN PEARSE, CHRIS RIZOS and RUSSELL TIESLER

Completed, June, 1996
Received: September, 1996

SCHOOL OF GEOMATIC ENGINEERING
UNIVERSITY OF NEW SOUTH WALES
SYDNEY NSW 2052
AUSTRALIA

This report has also been published by the Survey Laboratory of the Faculty of Information Science & Engineering, University of Canberra, and is published in the Unisurv-S Series by permission of the authors.

National Library of Australia

Card No. and ISBN 0 85839 070 1

The Team

Mr Daniel Garrard Mr Barry Mc Dowall A/Prof Peter Morgan Mr Russell Tiesler	School of Computing University of Canberra P.O. Box 1 Belconnen, ACT, 2616 Australia E-Mail: peterm@ise.canberra.edu.au
A/Prof Richard Coleman	Department of Surveying & Spatial Information Science University of Tasmania G.P.O. Box 252C Hobart, Tasmania, 7001 Australia E-Mail: Richard.Coleman@surv.utas.edu.au
A/Prof Chris Rizos	School of Geomatic Engineering University of New South Wales Sydney, NSW, 2052 Australia E-Mail: C.Rizos@unsw.edu.au
Mr Gary Johnston Mr Geoff Luton	AUSLIG P.O. Box 2 Belconnen, ACT, 2616 Australia E-Mail: geoffluton@auslig.gov.au
Mr Merrin Pearse	Department of Survey and Land Information Private Box 170 Wellington New Zealand E-Mail: merrin@wally.gmat.unsw.edu.au
Prof Yehuda Bock Dr Peng Feng	Institute for Geophysics and Planetary Physics, IGPP0225 Scripps Institution of Oceanography La Jolla, CA, 92093, USA E-Mail: bock@pgga.ucsd.edu

Acknowledgements

Major geodetic projects, such as determining a new continent-wide solution or building a major facility, usually appear once in a lifetime. For me this is my second, as I had the privilege of leading the Orroral Geodetic Observatory team in the heady days of the seventies. As in that project, I have had the good fortune to have the unqualified support of the team who participated in the project. They are acknowledged as co-authors. Nevertheless, I again say thank you for your support, given unselfishly, often under considerable stress.

However, the major reason for this section is to acknowledge the contributions that those who supported us in this project. The first vote of thanks goes to my Colleagues in the Faculty of Information Sciences & Engineering at the University of Canberra. To my former Dean, Professor Mary O'Kane, for her understanding of the project and her insistance on rigor and excellence, to Professor Peter Cullen for just plain wisdom, coffee and ears and to Associate Professor Brian Stone, a constant source of encouragement even though bewildered at how fine a wire we often walked.

The project was supported by all state and Commonwealth surveying and mapping authorities. These organisations provided the lion's share of the GPS data which was used in this study. Teams of surveyors and their technical officers and assistants sat on hills and cliffs watching instruments 24 hours a day and then quickly and reliably moving them to new locations. There is a mateship and team spirit that watches over this field work that is often missing from the laboratory. These people are often forgotten, yet without their data and notes the analysis could not be undertaken. I am most grateful for this unsung contribution.

The NSW Land Information Centre at Bathurst and the Queensland Department of Lands played important roles in the early parts of the project with seed funds and a belief that the time was ripe for a radically different approach. I am especially grateful for the support and encouragement given by Charles Zahra at LIC and Jim Hawker at Queensland Lands.

My friends and colleagues at the Department of Earth, Atmosphere and Planetary Sciences at the Massachusetts Institute of Technology were a constant source of assistance and support during the project. The visits to MIT were extremely fruitful and certainly provided stimulation and answers to issues that were of concern in this project. The jam sessions in 611, the MIT Geodesy Lab, were so important. The guidance, help and editorship of Bob King, Tom Herring and Simon McClusky at all stages of the project must be acknowledged.

Another significant input to this project was derived from my membership of the Steering Committee of the International Geodynamics Service. The discussion of common problems relating to large scale networks, orbits and adjustment of results were issues that bound us tightly for two years. One of my old OSU professors, Ivan Mueller, played a significant role in supporting me in this period.

Next I must make mention of AUSLIG and the AUSLIG Geodesy Manager, John Manning. John has asked not to be on the author list because he did no work on the project. Nothing is further from the truth. John managed the important AUSLIG contribution, the AFN, and the coordination of the ANN component for the Intergovernmental Committee for Surveying and Mapping. He also supplied precious money, and committed officers to the project. We met, sometimes irregularly because there were problems to be resolved, other times regularly to keep the task rolling at the momentum that was required. It was indeed wonderful to be working

with a committed manager. John also managed, on behalf of the National Tide Facility, the funds provided by the Greenhouse Advisory Committee of the Department of the Arts, Sport, the Environment, Tourism and Territories.

The penultimate acknowledgement must be to the Australian Research Committee who supported the project by way of ARC grant A49232195. This supported all the development, tests and experiments that were necessary to produce the results of the project.

Finally I must thank my wife Carol for her support and understanding especially in the evenings when I could usually be found glued to the computer rather than caring for other things.

Peter Morgan
Canberra

Abstract

This report describes Global Positioning System work carried out in Australia and its near neighbours, including South East Asia, Papua New Guinea, New Zealand and Antarctica, during the period July 1992 through to October 1994. Much of the work coincided with the initial activities of the International Geodynamics Service. Indeed it was the Epoch campaign of 1992 that provided the impetus for this work.

The field work consisted of two major campaigns. The first was in July 1992 while the second was one year later in August 1993. Additionally, there were several smaller campaigns and data sets including a small 4 day campaign in July 1994. In all, over 200 individual daily solutions for more than 100 regional stations were processed using the GAMIT/GLOBK suite of programs. A significant proportion of the stations were occupied, with time spans greater than nine months, which allowed the determination of plate motion vectors. These vectors are in excellent agreement with the current geophysical models for plate motions and place limits on the precision and quality of the work. We estimate that the horizontal precision of the coordinates is less than 3 centimetres at the 95% confidence level, while the vertical precision is less than 5 centimetres at the same 95% confidence level in the ITRF92 reference system.

Considerable exploratory and comparative work was undertaken to determine the best procedure for analysing the data. This work involved studies into the best sampling interval and the expected quality of orbits with a relatively sparse regional network. The essential findings of these investigations are included in the report.

Also included in the report are essential descriptions of the data collected and details of how and where both the raw and processed data are archived.

The overall result is a network of 127 stations computed in the ITRF92 reference frame, relative to epoch 1994.0, which will serve as a fundamental reference frame for the Australian region for the next 10 years.

Contents

List of Figures

List of Tables

Chapter 1

Introduction

Prior to 1950, Australia possessed no uniform geodetic datum or uniform system covering the full extent of the continent and the surrounding territories. Rather, each state of the Commonwealth had an independent network which generally covered those regions close to the capital, at the expense of the more distant regions. Victoria and New South Wales were connected at two separate places using different levels of trigonometric surveys, while Queensland and New South Wales were connected only at one place using low order surveys. Thus, it was not surprising that Bruce Lambert embarked on a major program to *survey* Australia and provide it with a state-of-the-art geodetic datum. It was Tony Bomford who realised the goal in the first half of 1966 (Bomford, 1967) utilising approximately 50,000 kms of tellurometer observations, in addition to usual voluminous quantities of triangulation data. Bomford's AGD66 work was the first major adjustment to utilise length as one of the dominating observations.

The observational data available to Bomford for his 1966 solution was frozen at the epoch of 1965. It was considered sparse and inadequate in many areas (NMCA, 1976) that were subjected to intense prospecting as Australia entered its mining boom. To overcome the sparse nature of the data set and to improve the overall quality, laser geodimeter surveys were commenced. However, the real impetus occurred when National Mapping entered the satellite era and measured two high precision baselines to support the PAGEOS program (Leppert, 1971). At the same time the Australian Height Datum (Roelse et al., 1971) was completed, enabling a rigorous reduction of observations to the spheroid. Thus, a process of updating and modelling of the Australian continent was instituted through a progressive sequence of models termed Geodetic Models of Australia. The first of these, GMA73, was produced by Bomford (1973). Differences between GMA73 and AGD66 were often in excess of 2 metres with strong regional patterns.

Later in the seventies, portable Doppler observations became routinely available, again showing discrepancies relative to AGD66 and the GMA series. Finally, satellite laser ranging (SLR) (Stolz, 1983) and very long baseline interferometry (VLBI) (Harvey, 1983) data became available. Thus the stage became set for a definite GMA solution, GMA82, (Allman and Veenstra, 1984) to be computed and adopted as the best available national datum. The definition of AGD84 best covers both the spatial distribution of the available observations and the precision of the adjusted quantities. The co-ordinate set from GMA82 was given the name AGD84 at its adoption. AGD84, like its predecessor, AGD66, is primarily derived from terrestrial observations. It uses the Australian National Spheroid to define the semi-major axis and

and flattening of the ellipsoid and the Johnston origin. Thus it is not geocentric but the best local approximation to the geoid.

In the mid seventies, the leadership of National Mapping embarked on a space geodesy program in conjunction with NASA and the Smithsonian Astrophysical Observatory. This program saw the construction of the Orroral Geodetic Observatory and active collaboration between the Division and several US agencies, including the Naval Observatory and Naval Research Laboratories. The TIMATION experiments (Buisson et al., 1977) were at the leading edge of the technology that was to be incorporated into the forthcoming Navstar, or GPS, satellites. This cooperation continued to flourish. In the mid eighties the Australian community, like many others, was quick to embrace the GPS technology, especially since the constellation had very favourable geometry over eastern Australia (Morgan, 1986). Whilst regional programs in general dominated the Australian scene, the emphasis at overseas institutions, such as the US National Geodetic Survey, the Massachusetts Institute of Technology and the Ohio State University, was global. The principal exception was the work in progress at the University of Canberra, where the emphasis was on the relationship of southern hemisphere stations to the global network. The first global campaign was GOTEX conducted in November 1988. This campaign was only marginally successful, due partly to the limited number of satellites and partly to the inhomogeneous nature of the network. Analysis was hindered by the need to physically assemble all the data in a single location and then distribute the assembled data to analysis groups. The next major global campaign was GIG91, run in January 1991. This campaign was very successful and clearly demonstrated the value of a global tracking network for both global and regional campaigns.

The need for global cooperation on an unprecedented level to provide near real-time tracking data and products for high quality projects prompted the setting up of the IGS Oversight Committee (IGS, 1992). The IGS Oversight Committee organised a major 90 day campaign, from 1 June to 1 September 1992, including an intensive epoch component of two weeks commencing 26 July, which allowed non-permanent and non-full P-code instruments to participate, primarily for densification. The major fixed site campaign was so successful that the IGS Oversight Committee immediately moved into the pilot phase of the program and eventually ceased to exist on 1 January 1994 with the introduction of the permanent service and the introduction of the IGS Governing Board. The University of Canberra played a significant role in the campaign, both as an analysis centre interested in Epoch campaigns and as a body interested in the electronic movement of data and the initiation of global resource centres.

Australian resources for the establishment of these networks was considerable. The permanent tracking sites at Yaragadee and Canberra (Tidbinbilla), operated jointly by Australia and NASA, participated in the global or fixed station component of all major campaigns prior to the IGS campaign. This feature, combined with the colocation of other major space geodesy systems and their unique geographical position, resulted in these stations being assigned *core* status in these global networks. Thus Australia had the unique opportunity of referencing other permanent trackers in the region in a global framework during the IGS campaign.

The Australian Surveying and Land Information Group, AUSLIG, which succeeded National Mapping in Commonwealth surveying and mapping functions, along with several of the state agencies saw the significant advantages of participating in the Epoch component of the IGS Campaign. This Epoch component required participants to operate dual-frequency equipment on marks or stations that were expected to be occupied in the future, or which would be upgraded to permanent tracking stations as funds became available. The AUSLIG contribution

to the Epoch campaign was to install permanent pillars at stations that have become known as the Australian Fiducial Network, AFN, and to observe at these marks with dual-frequency instruments. The State Lands Departments of New South Wales and Queensland used a mixture of permanent stations and ground marks. Most of these stations had also participated in the earlier AGD66 and GMA82 solutions and as such provide the essential links between the work of Bomford and Allman and Veenstra. AUSLIG also coordinated the Intergovernmental Committee on Surveying and Mapping (ICSM) activity, including the campaign to establish precision height values for tide gauge bench marks. The early successful analysis of these Epoch92 data within the region in a single unified system provided the impetus for the determination of the 500 km network across Australia and its near neighbours. This led to the 1993 and 1994 campaigns, which were coordinated by AUSLIG in conjunction with state and regional mapping authorities, to extend the initial concepts developed by New South Wales and Queensland into the 500 km Australian National Network, ANN. The aim of the ANN was to provide access to the continent-wide Australian Fiducial Network.

The data from the 1992, 1993 and 1994 campaigns have resulted in Australia again producing a state-of-the-art geodetic reference system. In this case, the observations spanned only two years compared with the decades of data used by Bomford and Allman and Veenstra. This fact, combined with the homogeneity of the technique, means that a true 'snapshot' of the region has been taken. The data and the resultant solutions should be invaluable for the following tasks:

- The establishment of a new, high precision, geocentric reference system capable of serving all surveying and mapping applications well into the next century.
- The characterisation of significant aspects of the Australian environment at discrete epochs with sufficient precision so that the effects of change, especially global change, can be precisely determined.

This report primarily seeks to detail the analysis work carried out at the University of Canberra. In some instances, parallel and complementary work, especially in the archiving of raw data, has occurred in other institutions. However, this work is not described in this report. The report seeks to be self-contained with chapters devoted to essential theory, the technical work undertaken, the organisation and archiving of data and appendices containing detailed listings. Extensive use is made of tables and figures to describe the work undertaken.

Chapter 2 provides some basic GPS theory that is used throughout the report. This theory forms the basis for all work undertaken. In Chapter 3, a basic outline of the GAMIT software suite is given together with the computation and model standards adopted in the solutions. The strategies adopted to produce the highest quality regional solutions are described in Chapter 4. A definition of the data assembly structure and holdings is outlined in Chapter 5 with Chapter 6 detailing data used in other regional networks. Chapter 7 deals with the cleaning of the data. i.e., the preparation of the data for analysis, and the procedures adopted in the GAMIT solutions. Chapters 8, 9 and 10 detail the major investigations that preceded the formalisation of the methodology adopted in the project. Chapter 8 discusses the effect of sampling interval on the recovery of major parameters while Chapter 9 examines the effect of network size and tracking geometry on the recovered orbital parameters. Quality assurance techniques are described in Chapter 10 together with their uses for understanding the variations seen in daily solutions. Chapter 11 outlines the tests conducted on the data collected during the

anti-spoofing days (days 214 and 215 of 1992) and the effects that anti-spoofing and selective availability have on the coordinate solutions. The Tide gauge network, or Australian Baseline Sea Level Monitoring Array, is fully documented in Chapter 12 and includes a description of each site and their computed coordinate solutions. The results, using three years of GPS observations, are summarised in Chapter 13. The GAMIT/GLOBK solutions are given in the ITRF92 reference system at epoch 1994.0. Full listings of all of the cartesian coordinates of these sites are given in Appendix A and the ellipsoidal values, based on the GRS80 ellipsoid, are tabulated in Appendix B. The remaining Appendices give detailed descriptions of the GAMIT solution files and time slice tables and maps of all of the stations used in the solutions.

Chapter 2

Basic Theory

2.1 GPS Theory

GPS theory and technology is now well advanced and there is a large and expanding volume of published literature available. Thus there is no necessity for a full expose of the theory behind positioning from GPS signals. Readers requiring a full treatment are referred to one of the standard texts. The older texts, still quite valid, are by King et al. (1985) and Wells et al. (1986). Newer texts are by, for example, Leick (1995), Hoffmann-Wellenhof et al. (1994) and Kaplan (1996). This last book contains excellent descriptions of the NAVSTAR spacecraft and the L_1 and L_2 signals used in this project.

The following treatment, adapted from King et al. (1985), is intended to set the scene for the many tests that were conducted in order to define a *best* practice for the work. Figure 2.1 shows the relations that exist between a pair of satellites and a pair of ground stations.

2.1.1 The one-way phase observable

King et al. (ibid.) define the carrier beat phase observable between satellite i and ground station j as

$$\begin{aligned}\phi_j^i(t_j) \;=\; & -\left[f_0 + a^i + b^i(t_j - t^0)\right]\tau_j^i(t_j) + \frac{1}{2}b^i(\tau_j^i)^2(t_j) \\ & +\phi_t^i(t^0) + f_0(t_j - t^0) + a^i(t_j - t^0) + \frac{1}{2}b^i(t_j - t^0)^2 \\ & -\phi_{LO_j}(t^0) - f_{LO_j}(t_j - t^0) - f_{LO_j}q_j - f_{LO_j}r_j(t_j - t^0) - \frac{1}{2}f_{LO_j}s_j(t_j - t^0)^2 \\ & +n_j^i + \phi_{noise}\end{aligned} \tag{2.1}$$

where $\phi_j^i(t_j)$ is the phase between satellite i and station j at epoch t_j as recorded by the local receiver oscillator,

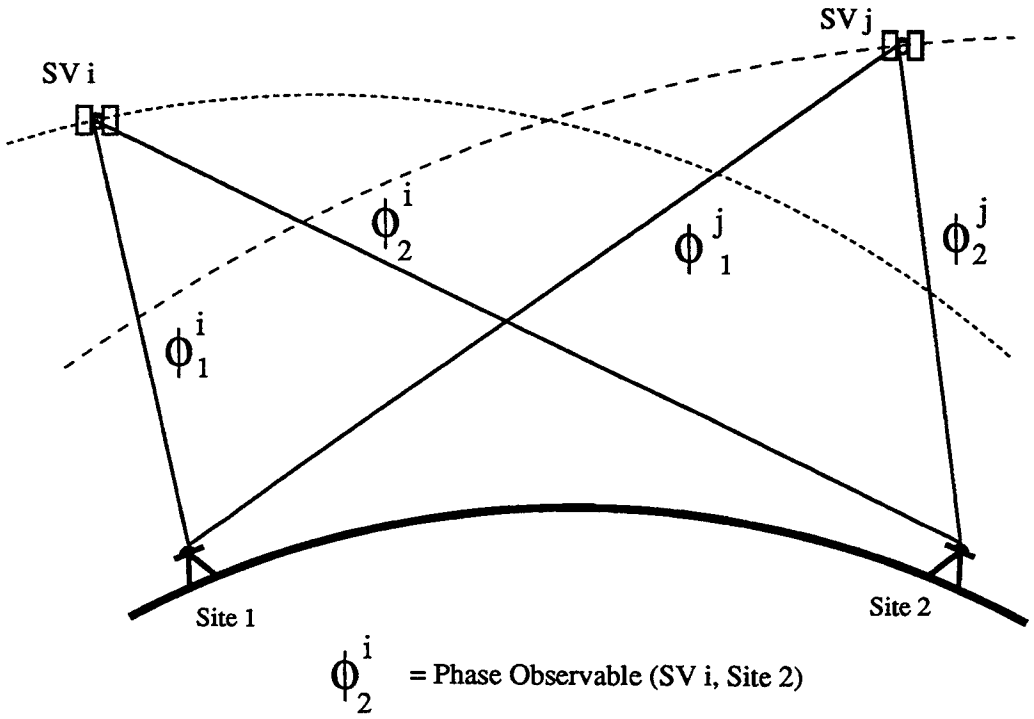

Figure 2.1: Simple schematic of a pair of ground stations simultaneously observing a pair of GPS satellites

τ_j^i is the propagation time delay, including both the geometric delay and the delay introduced by the troposphere and ionosphere,

$\phi_i^i(t^0)$ is the phase of the transmitted signal with respect to the chosen reference epoch t^0,

ϕ_{LO_j} and f_{LO_j} are the phase and frequency of the station (receiver) oscillator, respectively,

q_j, r_j, s_j are the coefficients of the polynomial equation used to model the station oscillator,

n_j^i is an integer representing the n-cycle ambiguity in the observed phase and ϕ_{noise} represents the random measurement noise,

f_0, a^i and b^i are associated with the performance of the satellite clock. f_0 is the nominal frequency of the satellite, a^i is the current offset from the nominal frequency while b^i is the linear drift term. All satellite clocks are driven by cesium standards. The performance of these standards is best modelled by linear equations of the form

$$f^i(t) = f_0 + a^i + b^i(t - t^0)$$

where t^0 is a reference epoch usually chosen to be at the centre of the span, which for daily solutions is 12:00:00 UT.

The station oscillator, like the satellite oscillator, is modelled with a linear parameter model usually a second or third order polynomial. The second order polynomial, typically used for quartz oscillators, has the form

$$t_j' - t_j = \delta t = q_j + r_j(t_j - t^0) + \frac{1}{2}s_j(t_j - t^0)^2$$

This equation, for the difference between the true receiver epoch (t_j) and the observed receiver epoch (t_j') is then used to evaluate the true phase of the local oscillator in the receiver, $\phi_{LO}(t)$.

It is to be noted that Equation 2.1 has the following structure:

- Terms on the first line are proportional to the propagation delay τ_j^i and hence can be interpreted as reflecting the geometry of the satellite and receiver.
- The parameters on line two involve the satellite clock.
- The parameters on line three involve the receiver oscillator.
- The parameters on line four involve the unknown integer ambiguity and the noise in the system as a whole. Note that the integer ambiguity n_j^i is indistinguishable from the phase differences at the reference epoch t^0.

A careful examination of the above equation also indicates that some additional cancellation occurs if the satellite clock and the receiver clocks have the same nominal reference frequency. This assumption is not valid even for satellites or receivers that are connected to atomic standards, due to drift in the clocks.

2.1.2 Between-station differences

It is readily seen from Figure 2.1 that it is possible to take the undifferenced phase between a pair of stations and difference the observations to form a new observable called *between-station differences*. The between-station differences are also known as single differenced observations. It is defined in the following equation, for stations 1 and 2 observing to satellite i, as

$$\Delta\phi_{12}^i = \phi_2^i(t_2) - \phi_1^i(t_1) \tag{2.2}$$

Expanding the above equation, it is usual to make the following assumptions:

- That the phase is sampled at the same epoch at both receivers, except for the fact that the clocks are not perfectly synchronised since they run at different rates. This assumption is not true when mixed instruments, that sample at different epochs, are used in the same network.
- That terms in $(\tau_j^i)^2$ can be neglected as being small.
- That the nominal or base frequency of all satellite and all ground receiver clocks is the same f_0 frequency. This is commonly 5 MHz.
- That the time argument of $\tau_j^i(t_j)$ is neglected for simplicity reducing the delay to τ_j^i.

This leads to an observable of

$$\begin{aligned}
\Delta\phi_{12}^i \;=\; & -f_0\left[\tau_2^i - \tau_1^i\right] - \left[a^i + b^i(t_1 - t^0)\right](\tau_2^i - \tau_1^i) - b^i(t_2 - t_1)\tau_2^i \\
& + a^i(t_2 - t_1) + \frac{1}{2}b^i(t_2 - t_1)\left[2(t_1 - t^0) + (t_2 - t_1)\right] \\
& - f_0(r_2 - r_1)(t_1 - t^0) - f_0 r_2(t_2 - t_1) - \frac{1}{2}f_0(s_2 - s_1)(t_1 - t^0)^2 \\
& - \frac{1}{2}f_0 s_2(t_2 - t_1)\left[2(t_1 - t^0) + (t_2 - t_1)\right] \\
& - \left[\phi_{LO_2}(t^0) - \phi_{LO_1}(t^0)\right] - f_0(q_2 - q_1) + (n_2^i - n_1^i) + \Delta\phi_{noise}
\end{aligned} \tag{2.3}$$

The previous method of collecting terms has been maintained. Thus the first line contains the geometric terms and the second line contains the satellite clock terms. Lines 3, 4 and 5 all relate to the receiver. Only terms involving $(t_j - t^0)$ have been cancelled.

2.1.3 Between-satellite differences

Using Equation 2.1, it is also possible to difference the equation using a pair of satellites to a common ground station. This difference is referred to as the *between-satellite difference* and for satellites i and j with observations to station 1

$$\nabla\phi_1^{ij} = \phi_1^j(t_1) - \phi_1^i(t_1) \tag{2.4}$$

Using the same simplifications as for the between-station differences, the following observable is derived,

$$\begin{aligned}\nabla\phi_1^{ij} \;=\; & -f_0\left[\tau_1^j - \tau_1^i\right] \\ & -\left[a^j\tau_1^j - a^i\tau_1^i\right] - \left[b^j\tau_1^j - b^i\tau_1^i\right](t_1 - t^0) \\ & +(a^j - a^i)(t_1 - t^0) + \frac{1}{2}(b^j - b^i)(t_1 - t^0)^2 \\ & +\left[\phi_t^j(t^0) - \phi_t^i(t^0)\right] + (n_1^j - n_1^i) \\ & +\nabla\phi_{noise}\end{aligned} \tag{2.5}$$

As before, the first line represents the geometric effect. Lines two and three contain the effects of frequency differences between the satellites while line four contains the initial satellite phase differences and the integer part of the phase observations. Note that there are no receiver clock terms in this observable as the sampling is carried out at the same time.

2.1.4 Double differences

Just as it is possible to difference between-satellites and between-stations, it is also possible to difference these differenced observations. That is, use is made of all of the components shown in Figure 2.1. This observable is called the double difference observable and, for stations 1 and 2 and satellites i and j, the observable can be written as

$$\nabla\Delta\phi_{12}^{ij} = \nabla\phi_2^{ij} - \nabla\phi_1^{ij} = \Delta\phi_{12}^j - \Delta\phi_{12}^i \tag{2.6}$$

where

$$\begin{aligned}\nabla\Delta\phi_{12}^{ij} \;=\; & -f_0\left[\tau_2^j - \tau_1^j - \tau_2^i + \tau_1^i\right] \\ & -\left[a^j + b^j(t_2 - t^0)\right](\tau_2^j - \tau_1^j) \\ & +\left[a^i + b^i(t_1 - t^0)\right](\tau_2^i - \tau_1^i) \\ & +(n_2^j - n_1^j - n_2^i + n_1^i) + \nabla\Delta\phi_{noise}\end{aligned} \tag{2.7}$$

As in the previous single difference observables, the arrangements of the terms is to draw attention to the various components. The first line contains the now familiar geometric terms. The second and third lines are associated with the drifting of the satellite clock. These terms are often neglected for short baselines but become important for long baselines. They are also important to account for clock dithering associated with selective availability. Under optimal conditions these terms are small, particulary the b^i and b^j terms, due to onboard rubidium and cesium oscillators. The final line, line 4, is now free of all initial phase unknowns. Indeed, the terms consists simply of the combination of the four unknown integer biases and the system noise. Unfortunately, system noise can be quite large.

2.1.5 Between-epoch differences

This observable uses the difference operator on double difference observables and is known as a *triple difference.* It is defined as:

$$\delta\nabla\Delta\phi = (\nabla\Delta)\phi)_{t+\Delta t} - (\nabla\Delta\phi)_t \tag{2.8}$$

The strength of the triple difference observable lies in the fact that cycle slip editing is very reliable since a single anomalous phase observation effects only two consecutive differences.

2.2 Transformation Theory

In geodesy, considerable use is made of transformations or mapping functions. The most common transformation is the 7 parameter similarity transformation, usually found in the following form (McCarthy, 1992),

$$\begin{bmatrix} X \\ Y \\ Z \end{bmatrix}_{new} = S \cdot \mathbf{R}_x \cdot \mathbf{R}_y \cdot \mathbf{R}_z \cdot \begin{bmatrix} X \\ Y \\ Z \end{bmatrix}_{old} + \begin{bmatrix} \Delta X \\ \Delta Y \\ \Delta Z \end{bmatrix} \tag{2.9}$$

where

$\begin{bmatrix} X \\ Y \\ Z \end{bmatrix}_{new}$ are the transformed geocentric coordinates,

$S = 1 + s$ is the scale factor,

$\mathbf{R}_x, \mathbf{R}_y, \mathbf{R}_z$ are the rotation matrices about the cartesian axes. The convention adopted is for a right-handed coordinate system, with positive counter-clockwise rotations viewed looking towards the coordinate origin,

$\begin{bmatrix} X \\ Y \\ Z \end{bmatrix}_{old}$ are the coordinates of the point to be transformed,

$\begin{bmatrix} \Delta X \\ \Delta Y \\ \Delta Z \end{bmatrix}$ are the translations between the old and new coordinate systems.

A more general form of this process is possible using homogeneous coordinates. The development of homogeneous coordinates for geometric applications was undertaken by E.A. Maxwell while he was Professor of Mathematics, Queens' College, Cambridge (Maxwell, 1946; 1951). They were subsequently applied to projection theory (Noll, 1967) and graphics applications (Blinn, 1977). Equation(2.9) can be rewritten as

$$\begin{bmatrix} X \\ Y \\ Z \\ 1 \end{bmatrix}_{new} = \mathbf{M} \cdot \begin{bmatrix} X \\ Y \\ Z \\ 1 \end{bmatrix}_{old} \tag{2.10}$$

where

M is the 4-by-4 process matrix defined as $\mathbf{S} \cdot \mathbf{R}_x \cdot \mathbf{R}_y \cdot \mathbf{R}_z \cdot \mathbf{T}$

Each of the component matrices is a 4-by-4 matrix. Their homogeneous forms are:

- Scale:

$$\mathbf{S}(s_x, s_y, s_z) = \begin{bmatrix} s_x & 0 & 0 & 0 \\ 0 & s_y & 0 & 0 \\ 0 & 0 & s_z & 0 \\ 0 & 0 & 0 & 1 \end{bmatrix}$$

- Rotation about x-axis:

$$\mathbf{R}_x(\alpha) = \begin{bmatrix} 1 & 0 & 0 & 0 \\ 0 & \cos\alpha & \sin\alpha & 0 \\ 0 & -\sin\alpha & \cos\alpha & 0 \\ 0 & 0 & 0 & 1 \end{bmatrix}$$

- Rotation about y-axis:

$$\mathbf{R}_y(\beta) = \begin{bmatrix} \cos\beta & 0 & -\sin\beta & 0 \\ 0 & 1 & 0 & 0 \\ \sin\beta & 0 & \cos\beta & 0 \\ 0 & 0 & 0 & 1 \end{bmatrix}$$

- Rotation about z-axis:

$$\mathbf{R}_z(\gamma) = \begin{bmatrix} \cos\gamma & \sin\gamma & 0 & 0 \\ -\sin\gamma & \cos\gamma & 0 & 0 \\ 0 & 0 & 1 & 0 \\ 0 & 0 & 0 & 1 \end{bmatrix}$$

- Translation:

$$\mathbf{T}(d_x, d_y, d_z) = \begin{bmatrix} 1 & 0 & 0 & d_x \\ 0 & 1 & 0 & d_y \\ 0 & 0 & 1 & d_z \\ 0 & 0 & 0 & 1 \end{bmatrix}$$

- Shear:
  While no mention has been made of shear in the discussion to this point, it should be noted that homogeneous coordinates readily admit shear between objects. This is

accomplished by incorporating the shear component, **SH**, into the process matrix **M**. The (x, y) shear is represented by

$$\mathbf{SH}_{xy}(sh_x, sh_y) = \begin{bmatrix} 1 & 0 & sh_x & 0 \\ 0 & 1 & sh_y & 0 \\ 0 & 0 & 1 & 0 \\ 0 & 0 & 0 & 1 \end{bmatrix}$$

It is seen from this development that the process matrix, **M**, can be readily thought of as containing 12 unknowns rather than the conventional 7 parameters. However, as well recognised, many of the parameters are set or defined by virtue of the geometry of the coordinate system. In particular, the following relations must be noted:

1. The geocentre is realised, or forced, by selecting the first degree Stokes' coefficients of the gravity field to be zero. Specifically

   $$\bar{C}_{10} = \bar{C}_{11} = \bar{S}_{11} = 0$$

   which implies (Lambeck, 1988)

   $$\iiint x \cdot dM = \iiint y \cdot dM = \iiint z \cdot dM = 0$$

   This implies that there is no translation between any of the networks and that these components can be neglected or set to zero.

2. The scale of GPS networks is realised through the adoption of two constants in the modelling process. The first is the velocity of light used to connect phase to wavelength. The second is the gravitational constant, GM, used in the evaluation of the orbit. The values used in GAMIT for this project were those adopted by the international community for the international collaboration to Monitor Earth-Rotation and Intercompare the Techniques of observation and analysis (MERIT). The MERIT values have subsequently been incorporated into the International Earth Rotation Service (IERS) standards (McCarthy, 1992). A summary of the standards adopted is given in Chapter 3. The implication of this process is that the scale matrix is an identity matrix, **I**. That is

   $$s_x = s_y = s_z = 1$$

3. It is conventional wisdom that there is no shear in well-balanced and uniform GPS networks. Thus, for GPS networks, especially those of considerable extent, the shear matrix would also be the identity matrix, **I**. However, in transforming from three dimensional space onto a projection plane, consideration must be given to shear terms.

From the above statement, it is seen that 9 of the 12 parameters used to define **M** are implicitly defined by our a-priori assumptions, reducing the number of unknowns to three - the three rotations. It is to be noted that the same three unknowns are reached if one starts with the conventional seven parameter model in its standard form.

The implication for this study is that it is theoretically possible to bring two GPS networks into coincidence by using one common point in each of the two networks.

2.2.1 Transformation from 3-D space to 2-D space

There is usually a need to transform from three dimensional space to one of the common two dimensional coordinate systems. The most common systems used are:

- Ellipsoidal:
  This system represents the transformation of the 3-D tuple into latitude and longitude on the surface of the ellipsoid. Ellipsoidal height is usually treated separately from the horizontal curvilinear coordinates. The transformation is considered essential by many users so that mapping coordinates, as used in LIS/GIS, can be effectively computed. The transformation equations usually involve an iterative process and require the parameters of the ellipsoid to be specified - see formulae in Torge (1991) and Bowring (1985).

- Map coordinates:
  This system represents the 3-D tuple as grid coordinates, usually eastings and northings on a plane, and height, perpendicular to the plane. The essential difference between these mapping coordinates and the ellipsoidal coordinates is that they are on a projection plane and hence are subject to distortion. These map coordinate systems are in wide spread use in LIS/GIS systems and other spatial systems.

Our point in discussing them at this stage is to bring attention to the fact that the intermediate step of transforming from the three dimensional system to the mapping coordinate system, via the conventional ellipsoidal system, is not mandatory and that it is possible to hold to existing mapping systems and GPS coordinate systems simultaneously.

This possibility can be understood by again considering the full process matrix M in homogenous coordinates with a second class of process matrices, called projection matrices. Different classes of projection matrices are discussed and illustrated in a comprehensive paper by Carlbom and Paciorek (1978). Thus, it is possible to create projection matrices which will produce most of the azimuthal and equidistant map classes described by Richardus and Adler (1972). The conversion from these classes to other classes, such as the conformal conical and cylindrical classes normally associated with map grid systems, can be achieved using Lauf's divided difference approach (Lauf and Young, 1961). The Lauf technique is only applicable to conformal projections.

The process matrix associated with a stereographic projection is the usual perspective matrix $\mathbf{M}_{per}$ where the distance from the perspective origin to the projection plane, d, is the diameter of a sphere. The precise definition is that the projection centre is diametrically opposite the point of tangency. The form of the projection matrix is:

$$\mathbf{M}_{per} = \begin{bmatrix} 1 & 0 & 0 & 0 \\ 0 & 1 & 0 & 0 \\ 0 & 0 & 1 & 0 \\ 0 & 0 & \frac{1}{d} & 0 \end{bmatrix}$$

This leads to the following matrix equations:

$$\begin{bmatrix} X \\ Y \\ Z \\ W \end{bmatrix}_{map} = \mathbf{M}_{per} \cdot \mathbf{M} \cdot \begin{bmatrix} X \\ Y \\ Z \\ 1 \end{bmatrix}_{gps} \tag{2.11}$$

where W is the homogeneous scale factor.

Thus, the mapping coordinates, still in the global system at this instant, are given by

$$\begin{bmatrix} \frac{X}{W} \\ \frac{Y}{W} \\ \frac{Z}{W} \end{bmatrix} = \begin{bmatrix} x_p \\ y_p \\ z_p \end{bmatrix} = \begin{bmatrix} \frac{x}{d} \\ \frac{y}{d} \\ d \end{bmatrix}$$

The final process, not described here, is to rotate the global mapping coordinates into a local system utilising the projection plane.

2.3 Adjustment Models

It is not possible to observe all the required ground stations in a single session with sufficient precision. It is normal to replicate observations and reductions in order to eliminate random errors and effects which can be minimised by sampling over a larger time interval. Other aspects of the adjustment process are densification or taking the whole to the part.

Several methods of performing adjustments were investigated. It is more common to use the observation equation model approach, with functional models of the form $\mathbf{F}(\mathbf{X}_a) = \mathbf{L}_a$ rather than the full model $\mathbf{F}(\mathbf{X}_a, \mathbf{L}_a) = 0$. Here $\mathbf{X}_a$ represents the parameter vector and $\mathbf{L}_a$ is the observation vector.

2.3.1 The Conventional Approach

The following three observation equations are used in the conventional adjustment approach:

1. The slope distance observation equation

$$l_{ij} = \left[(X_j - X_i)^2 + (Y_j - Yi)^2 + (Z_j - Z_i)^2\right]^{\frac{1}{2}} \tag{2.12}$$

2. The equatorial azimuth equation

$$\alpha_{ij} = \arctan\left(\frac{X_j - X_i}{Y_j - Y_i}\right) \tag{2.13}$$

3. The elevation equation

$$\beta_{ij} = \arctan\left[\frac{Z_j - Z_i}{[(X_j - X_i)^2 + (Y_j - Yi)^2]^{\frac{1}{2}}}\right] \tag{2.14}$$

Of these three models, only the first equation is generally used in GPS processing. The distance equation is invariant to rotational effects. The principal drawbacks of using such equations is:

- Only a third of the available information is used.
- Variances need to be propagated rigorously to maintain the correct weighting.
- All combinations of observation equations need to be used unless the weighting is modified.

The second and third items become significant in large networks, where the number of combinations of distances can reach into the thousands. The technique is only useful in small networks where the GPS observations have been reduced by the single baseline technique rather than the network approach.

2.3.2 The vector approach

The observation equation approach to this model is fully described by Leick (1995). The model is readily written as

$$\begin{bmatrix} \Delta X \\ \Delta Y \\ \Delta Z \end{bmatrix} = \begin{bmatrix} X_j - X_i \\ Y_j - Y_i \\ Z_j - Z_i \end{bmatrix} \tag{2.15}$$

This approach, like the preceeding approach, is also more suited to the baseline approach compared with the network approach. Again the principal reason is that the vector of differences must be formed with all differences and the variances and covariances need to be correctly propagated. This need to propagate the variances is seldom present in the baseline approach where there are only a few baselines.

2.3.3 The network approach

It has been shown in Section 1.2 that it is possible to transform network i to network j using the conventional 7 parameter transformation or the more appropriate reduced model in which the scale parameter is unity and the translations are zero. If the rotations are small, then to first order for the rotation angles α, β, γ, the rotation matrix can be expressed as

$$\mathbf{R} = \mathbf{R}_x(\alpha) \cdot \mathbf{R}_y(\beta) \cdot \mathbf{R}_z(\gamma) = \begin{bmatrix} 1 & \gamma & -\beta \\ -\gamma & 1 & \alpha \\ \beta & -\alpha & 1 \end{bmatrix} \tag{2.16}$$

This model is well suited to network solutions as the variances and covariances do not need to be propagated and the relative weighting is maintained. Moreover, the network geometry is maintained as it is only subject to rotations.

If two networks do not have the same scale and datum definition, then the full 7 parameter model would be needed. One such case is the rotation of a terrestrial network and a GPS

network, or even two GPS networks using the vector approach and inner constraints (Ananga et al., 1993a; 1993b).

2.4 The Adjustment Process

Least Squares adjustment procedures are normally used for the adjustment of all overdetermined systems of equations. For repetitive and replicative observations, sequential least squares techniques are optimal for indicating the quality of a particular replication relative to the mean solution. The addition of information filtering and time series processes offers an attractive alternative approach. Both procedures involve the generation and maintenance of a covariance matrix.

The first option is least squares sequential adjustment. An excellent review of these procedures is given by Gagnon (1976). Lucid working explanations and the design matrix for the observation equation model are given by Cross (1983). The following equations summarise the process.

- The new, epoch 2, least square estimates of the model parameters is given by

$$[\mathbf{X}_a]_2 = [\mathbf{X}_a]_1 + \delta\mathbf{X}_a$$

- The associated covariance matrix is updated in an analogous manner.

$$[\mathbf{C}_{\mathbf{X}_a}]_2 = [\mathbf{C}_{\mathbf{X}_a}]_1 + \delta\mathbf{C}_{\mathbf{X}_a}$$

- The residuals for the new observations can be computed using the associated design and variance-covariance matrix of the new observations, the pre-existing normal equations and the estimate of the parameters at the last state.

The second major method utilises the Kalman filter, which Krakiwsky (1975), shows to be equivalent to conventional least squares. It differs from the above referenced sequential method primarily due to the manner in which the new best parameter estimates are derived. In the case of the Kalman technique, a predictive estimate is first made based on a transition or state information matrix, M, as $\left[\mathbf{X}'_a\right]_2 = \mathbf{M} \cdot \left[\mathbf{X}'_a\right]_1$. This predicted estimate is then refined using a gain matrix, G and observation equation information.

This second method is used in the GLOBK (Herring, 1990) software to join/amalgamate the individual GAMIT solutions. As an introduction to the philosopy and capacity of the GLOBK suite, readers are referred to Herring (1990). A lucid derivation of the standard Kalman filter case with examples, is given by Cross (1983). A brief summary of the features of the solution is given below, based on Cross (ibid.). For simplicity, true values do not have either the a subscript or the $\wedge$ superscript. Estimated values are indicated with the superscript $'$.

1. Compute the starting estimates for epoch i, using the conventional observational model, as

$$\mathbf{X}'_i = -(\mathbf{A}^T\mathbf{P}\mathbf{A})^{-1}\mathbf{A}^T\mathbf{P}\mathbf{L} = -\mathbf{N}_i^{-1}\mathbf{U}_i$$

where $\mathbf{X}'_i$ is a correction vector to the a-priori estimates $\mathbf{X}_0$; $\mathbf{A}$ is the design or Jacobian matrix and consists of the partial differentials with respect to the unknown

parameters; $\mathbf{P}$ is the inverse of the variance-covariance matrix, Σ, of the observed qantities; $\mathbf{L}$ is the difference of the observations computed through the model and the directly observed values; and ^{T} and $^{-1}$ denote the tranpose and inverse of the matrix, respectively.

2. Compute the starting estimate for data set $i+1$ from the transition matrix $\mathbf{M}$ and the estimates for set i. This is usually called a prediction estimate.

$$\mathbf{X}'_{i+1} = \mathbf{M}_i \mathbf{X}'_i$$

3. Compute the associated covariance matrix.

$$\mathbf{C}_{\mathbf{X}'_{i+1}} = \left(\mathbf{N}'_{i+1}\right)^{-1} = \mathbf{M}_i \cdot \mathbf{N}_i^{-1} \cdot \mathbf{M}_i^T + \Sigma_{\mathbf{M}_i}$$

Note the use of the variance-covariace matrix, $\Sigma_{\mathbf{M}_i}$ of the transition matrix and the important role that this plays in the solution. No matrix inversions are necessary in the second form of the above equation as all quantities exist.

4. Compute the gain matrix, $\mathbf{G}$, used to correct the predicted values of set $i+1$. Note that the covariance matrix of the parameters plays an important role in this equation.

$$\mathbf{G} = \left(\mathbf{N}'_{i+1}\right)^{-1} \cdot \mathbf{A}_{i+1}^T \left[\Sigma_{i+1} + \mathbf{A}_{i+1} \cdot \left(\mathbf{N}'_{i+1}\right)^{-1} \cdot \mathbf{A}_{i+1}^T\right]^{-1}$$

5. Compute the corrected state vector utilising the predicted value and the gain matrix multiplied by the adjustment induced by the model for the $i+1$ data set.

$$\mathbf{X}_{i+1} = \mathbf{X}'_{i+1} + \mathbf{G}\left[\mathbf{L}_{i+1} - \mathbf{A}_{i+1} \cdot \mathbf{X}'_{i+1}\right]$$

The second term in the above equation is analogous to the $\delta\mathbf{X}$ correction of the sequential model. This term is also known as the pre-fit differences and can be used to detect data outliers or instability in the estimation process.

6. Compute the associated variance-covariance matrix.

$$\mathbf{C}_{\mathbf{X}_{i+1}} = (\mathbf{I} - \mathbf{G} \cdot \mathbf{A}_{i+1}) \left(\mathbf{N}'_{i+1}\right)^{-1} = \mathbf{N}_{i+1}^{-1}$$

7. A full cycle has now been computed. The cycle is repeated with these last values of $\mathbf{X}_{i+1}$ and $\mathbf{C}_{\mathbf{X}_{i+1}}$ being used to commence the process for the next step which begins at item 2 after updating the step counter i.

When the counter no longer can be updated, the process stops with the last values being the solution required.

At this point we have generated a *forward* solution. Since the final least squares estimate is not available until after the last cycle, no estimates of the residuals can be made as the formal definition of a residual is $v_i = x_a - x_i$.

In order to compute residuals, it is necessary to perform the inverse process, commonly called smoothing, commencing at $i = n$ and proceeding to $n-1$ and finally to where the process commenced at $n = 1$. The reverse stepping uses a smoothing factor,$\mathbf{K}$, analogous to the gain matrix, $\mathbf{G}$, as follows

$$\mathbf{X}_{i-1} = \mathbf{X}'_{i-1} - \left(\mathbf{N}'_{i+1}\right)^{-1} \cdot \mathbf{M}_{i-1}^T \cdot \mathbf{A}_i^T \cdot \mathbf{K}_i$$

where

$$\mathbf{K}_i = -\left[\Sigma_i + \mathbf{A}_i \cdot \left(\mathbf{N}_i'\right)^{-1} \cdot \mathbf{A}_i^T\right]^{-1} \cdot \left[\mathbf{L}_i - \mathbf{A}_i \cdot \mathbf{X}_i'\right]$$

The computation of the residuals, necessary to evaluate repeatabilities, requires the storage of the intermediate variance-covariance matrices determined during the *forward* phase of the process. This demands significant disk storage resources.

Chapter 3

GAMIT

The GAMIT software (GAMIT, 1995) is a comprehensive GPS analysis package, jointly developed at the Massachusetts Institute of Technology (MIT) and the Scripps Institution of Oceanography (SIO), University of California at San Diego. This suite of software was used to compute the network solutions reported in this document.

GAMIT may be split into four main sections. The first is the orbit integration section. This section is usually started with a broadcast orbit which is integrated using conventional procedures. The step size of the integration method was 75 seconds. The ephemeris was tabulated at 22.5 minute intervals. Creation of a tabular ephemeris was one of the first tasks needed in running the solution. It is shown on the lefthand side of Figure 3.1. The task is usually iterated as shown on the left of Figure 3.2 when corrections to the initial conditions exceed 10 metres. In many instances, level 2 and level 3 networks were computed with high quality orbits derived from either a global network or from another higher level network. The output from the ARC module is the tabular ephemeris or *T-file*.

The second major section includes all the preparatory processes that generate the GAMIT file system. Of special importance is the GAMIT specific *X-file* which contains the phase and pseudo-range data in an internal but readable format. The generation of this *X-file* includes the application of a basic filter which compares the observed pseudo-range with the equivalent phase and then looks for the lack of L_2 data. The necessary clock files, for both the ground stations and satellites, are made in this section - see Figure 3.1.

The third section deals with the station modelling. The output from this section includes the *C-files* which contain all the partials required by the least squares solution and the discrepency vector between quantities computed through the a-priori model and those observed. The computation of these *C-files* requires a diverse and complex set of inputs ranging from station-specific information on the instrument setup through to the models for handling the atmosphere and ionosphere and models effecting the terrestrial and celestial reference frames. Changing the a-priori estimates of parameters to be solved for in the final section of the GAMIT process requires iteration of the modelling process. The necessary inputs into the modelling process that generates the *C-files* is shown in the top half of Figure 3.2

The final, or fourth section, involves the solve and cleaning loops shown in the bottom half of Figure 3.2. The figure indicates the role played by the cleaning modules SINCLN

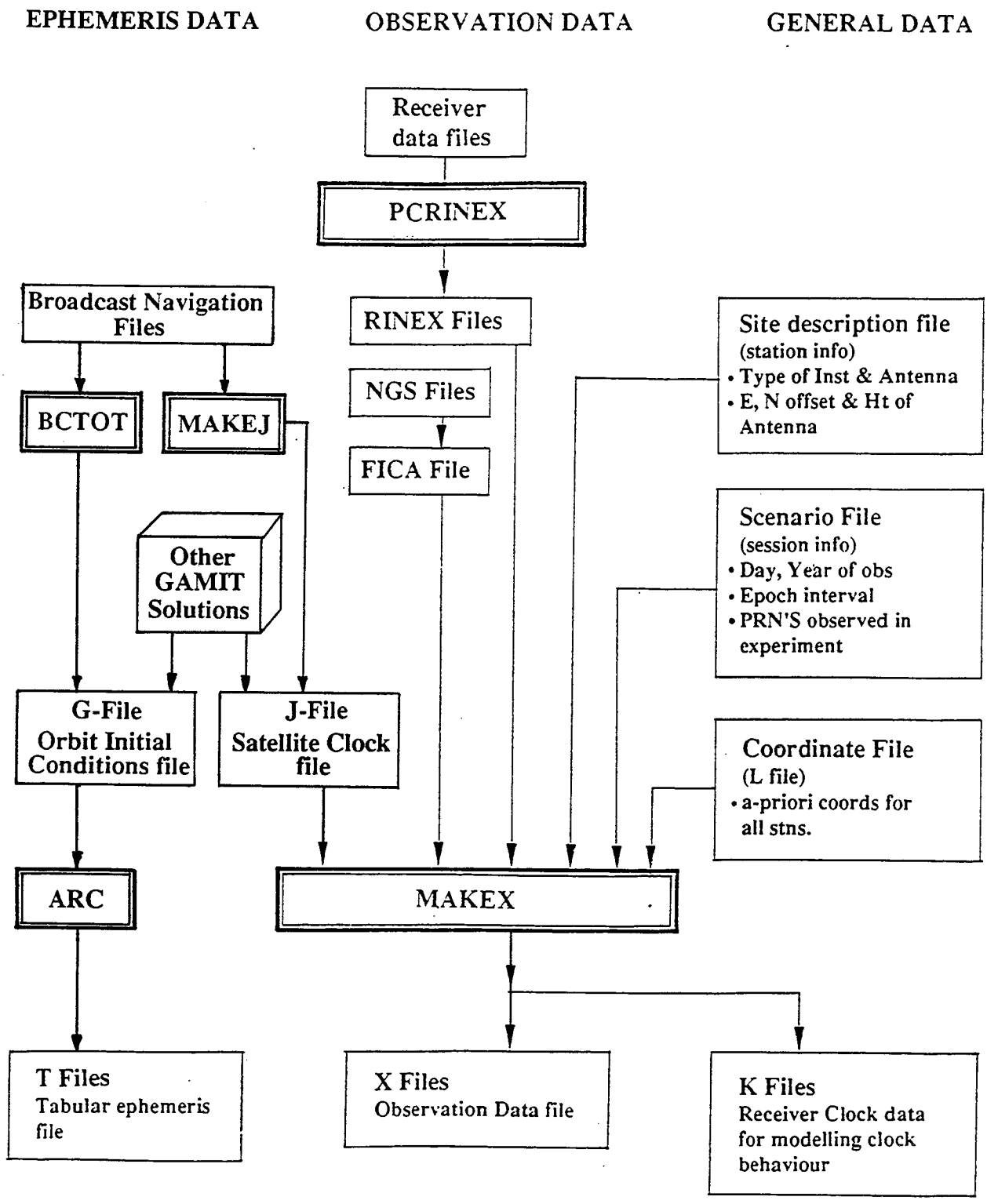

Figure 3.1: Flow chart indicating the files and information required by GAMIT for a standard run. Note the requirements for satellite data, tracking data and general or supporting data.

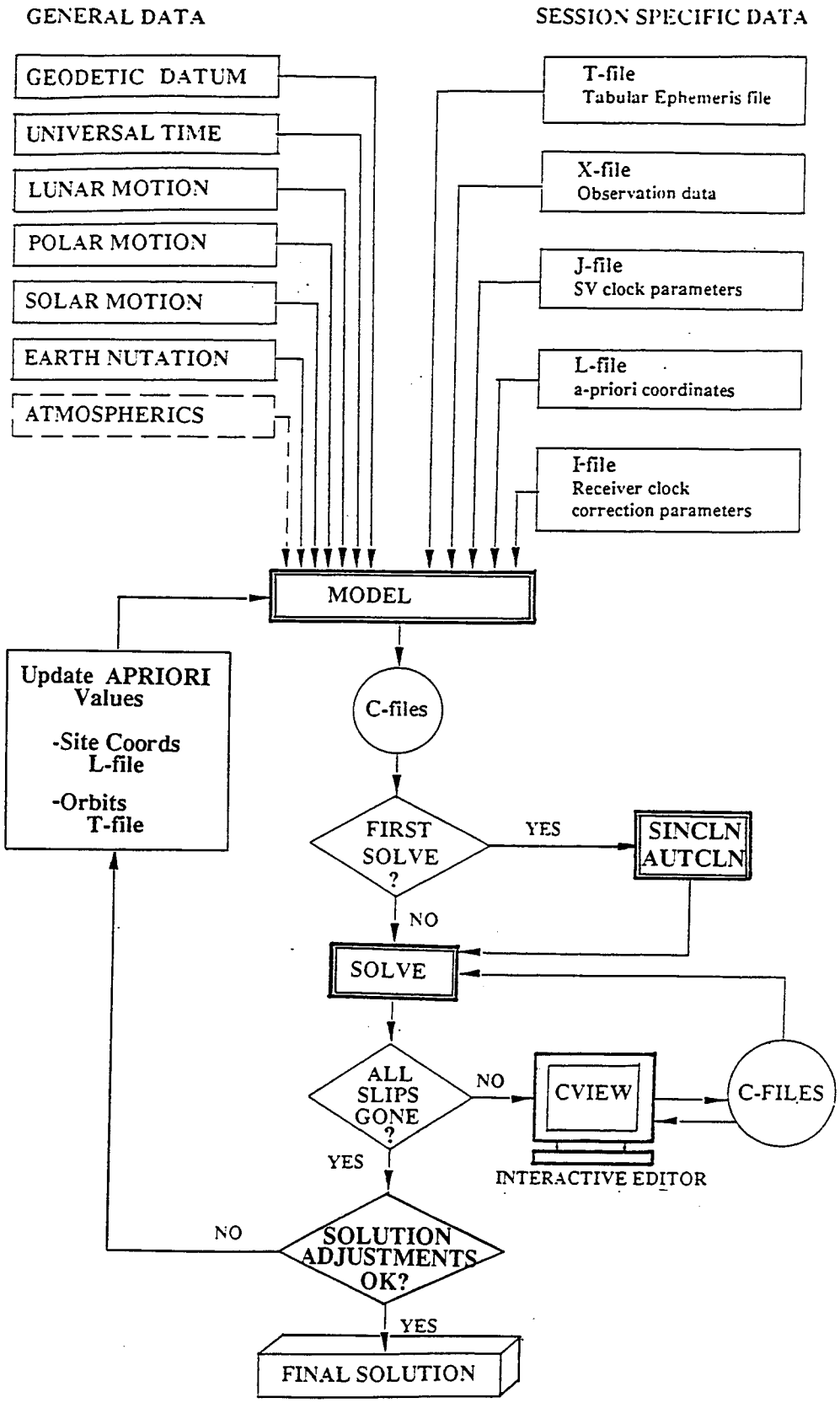

Figure 3.2: Flow chart indicating the dependent and iterative relationships of SOLVE with data cleaning and modelling in GAMIT.

and AUTCLN and their relationship to SOLVE. It is to be noted that the modelling used in the generation of the *C-files* is specific to that modelling process and any change in these parameters that is outside the linear limits requires the modelling process to be iterated. In general, only one iteration was normally required as, after the first occurrence of a site, high quality estimates of the site position vector were available. The re-use of the orbit from a higher level network also provided quality a-priori estimates of the state vector. A secondary benefit of these high quality, a-priori estimates was the manner in which SINCLN operated in that many data problems, which might not have been automatically repaired, were repaired due to the higher levels of confidence under which SINCLN operated.

In general, GAMIT implements the IERS standards as defined in IERS Technical Note 13 (McCarthy, 1992). These standards have been formulated to provide the best consistent set of standards for all IERS functions, including the determination of earth rotation and the maintenance of the terrestrial reference frame.

Implementation of these standards is usually broken up into a number of discrete subsections.

3.1 Orbit Force Modelling

The following parameters and models were invoked in the computation of satellite orbits.

1. The gravitational models used invoked the IGS standards for GM, the velocity of light, and other solar system constants.
2. The geopotential model used is the GEM-T3 model (Lerch et al., 1992). It is truncated to the classical 8-by-8 model.
3. The Bessellian definition of the inertial frame was used.
4. The solid earth tide potential is the IERS standard for the solid body component, the K_1 frequency term and the Pole tide.
5. The third body effects are accounted for using tabular values for the sun and the moon.
6. The solar radiation pressure model implemented was the spherical model, often also called the flat plate model. The direct component is the component along the direction to the sun, the spacecraft y-axis is the y-bias while the third component, the z-bias, is the earth pointing spacecraft axis.
7. The ocean tide potential is the IERS standard.

3.2 Station Modelling

The following parameters and models were invoked in the modelling associated with the correct reference of the station to the non-tidal crust.

1. The inertial reference frame was used for the reductions.
2. UTC time tags were used for the observations rather than GPS time tags.

3. Only the solid body component of the IERS standard was used to model the time series behaviour of the station.
4. No surface meteorological data were used. Standard atmosphere values were used.
5. Atmospheric modelling used the Saastamoinen (1972) and Center for Astrophysics (Davis et al., 1985) models.
6. Only one correction to the nominal model was computed for each 24 hour data span.
7. Station receiver clocks were estimated independently using a nominal orbit such as the broadcast orbit. A third order polynomial was used except for Mini-Mac receivers.
8. The computed position was the station reference point and not the electrical centre.

3.3 Terrestrial Reference Frame

The following parameters and models were used in the alignment of the GAMIT reductions to the terrestrial reference system.

1. The IERS ITRF92 terrestrial reference frame was used.
2. The NUVEL 'no-net-rotation' plate model was used.
3. The GRS80 ellipsoid was used to convert rectangular coordinates to ellipsoidal coordinates.

3.4 GAMIT Options

GAMIT has many options associated with its normal processing mode. The above options refer mainly to modelling issues. There are however several options that change the way the processing is undertaken. The most important of these are the switches used to control SOLVE.

1. **Type of Analysis.** GAMIT allows for two main types of solution, QUICK and FULL. The QUICK solution is not faster to run but more likely to yield better first-cut results by determining the adequacy of the data to perform the desired task. The algorithm places a bias flag at the start of each data gap or jump in the double difference observation series. This lowers the precision of the solution estimate but also makes it insensitive to cycle slips. The FULL option inserts bias flags only when specifically instructed to do so. The FULL options was used for all but the first solution run.
2. **Data Status.** GAMIT acknowledges both raw and clean data. Clean data, or the setting of the CLEAN flag, bypasses the cleaning modules.
3. Choice of Observable. GAMIT allows the adjustment to be performed on a number of observations. Only the LC option was used in this project due to the length of the baselines. Other options include L_1 and an $LC - HELP$ option which seeks to make use of known ionospheric information.
4. **Choice of Experiment.** GAMIT allows three types of experiment. The BASELINE experiment where the orbit is held fixed as well as one station in the network

or alternatively one end of the baseline is held fixed. This type of experiment is useful for short baselines where there is insufficient power to adjust the orbits. The second choice is the RELAX experiment. This is the normal processing option. It involves the simultaneous estimation of the orbit parameters and the station vectors. The third type is the determination of the orbit by holding the tracking station coordinates fixed. It is seldom exercised in networks when station coordinates are the major product to be computed.

5. **Station Error.** This parameter was set at the uniform level of 10 mm. It is the error in the psuedoranges. It is constant, with no distance effect applied in this case.
6. **Ionospheric constant.** This was set to be 8 ppm. This relatively large value is necessitated by stations near the magnetic equator, around Darwin, and the Antarctic sites.
7. **Zenith Delay Estimation.** This turns on or off the estimation of the zenith delay. It was always set on.
8. **Number ZEN.** This is the number of zenith delay parameters and was always set equal to one.
9. **Zenith Constraints.** This was only exercised with an a-priori setting of 0.5. It represents an error bound on the determination of the zenith delay.
10. **The Zenith Model.** Only the piecewise linear model was selected.
11. **Zenith delay.** A rate of variation and a time over which the number is to operate, typically 0.02 m/$\sqrt{hour}$ and 100 hours respectively.
12. **Elevation cut-off.** This was set at 15 degrees elevation. In many instances, the data were delivered with the 20 degree elevation mask having been applied at the instrument.

In the GAMIT manual, section RUNNING FIXDRV (chapter 5.2) is the best information to hand. This and other commands are fully described in the GAMIT manual.

Chapter 4

The Analysis Strategy

4.1 Strategy for Handling the Networks

It is seen from the discussion in Chapter 2 that it sufficient to have just one common station in two GPS networks in order for the two networks to be defined in a unique reference system. Unfortunately, when dealing with observations that form only a part of a fully global network, the resulting network solutions are likely to be sub-optimal. The standard practice is to provide more control points than the minimum requirement and to construct appropriate covariance information of the station coordinates so that the least squares condition is met and all rotations are minimised.

The following three conditions were an essential part of the strategy of handling a network of over 100 stations. The concepts were developed from standard surveying traversing practice where an origin station, usually the commencing station, and a closing station, usually the final station, are used to fix the traverse within the higher level coordinate system. Additional control is often brought into the middle of the traverse to increase the reliability of points. These concepts are illustrated in Figure 4.1 where a three level hierarchical system, starting from the global reference system, is shown.

1. Every lower level network was connected to the higher level network using three well distributed sites. The sites were distributed so as to ensure that the network being attached could not rotate relative to the higher level network in any of the three coordinate axes. In Figure 4.1, the highest level network stations are A, B, C and D whilst stations P, Q, R, S, T and U form the lower level network.
2. When three hierarchical levels are necessay, at least one station must be common to all three levels, i.e., a datum station. This ensures that constraints and other defined values are directly impressed on the network rather than via secondary or deduced values, where error propagation may effect the precision.
3. For lower level networks with changing geometry, each network must be connected to its higher level network by at least three common stations. Additionally, each of these networks must include a common connection to a level one station for origin and constraint enforcement.
4. Distinct intermediate networks should, if possible, also connect laterally with the same level network (for example, other regional networks) as well as vertically to

the higher level, global network. This condition ensures that these regional networks fit both globally and regionally with minimum distortion. The lateral connections enforce an overdetermined solution with the global network.

5. The distinct epochs of the campaigns are only linked at the global level utilising global information. Thus, the quality of repeatability and velocity information can be gauged by examining these deduced parameters at stations that repeat at any of the hierarchical levels.

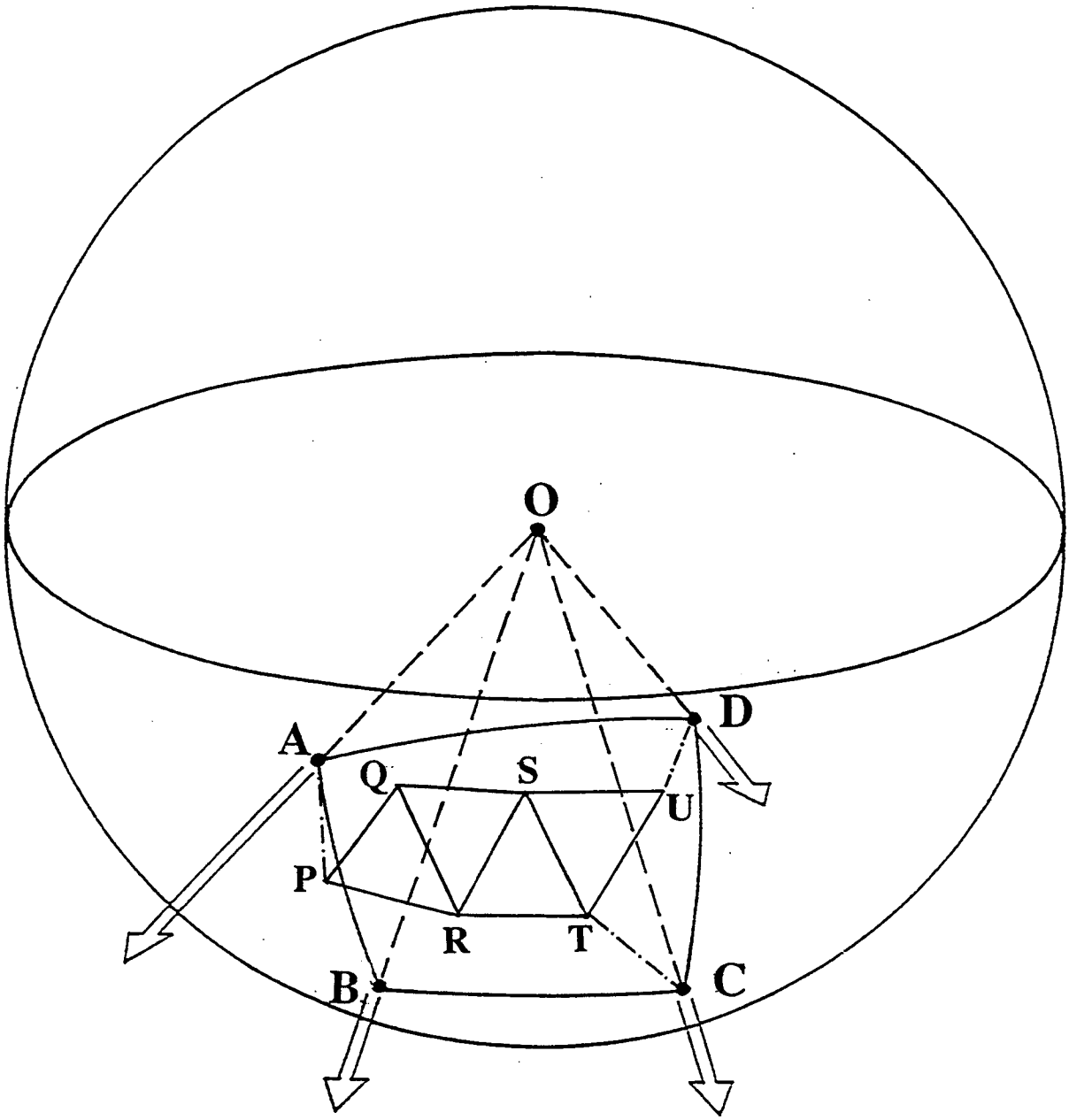

Figure 4.1: Figure illustrating the fiducial control strategy adopted to devolve the global level reference system to the local system within the Australian region

4.1.1 The 1992 Campaign

Figure 4.2 shows the hierarchical connections of the three levels that were used during the IGS Epoch Campaign. The large ARN and Tide networks are connected to the global frame by way of Darwin, Yaragadee and Tidbinbilla (DS42). DS42 is then used, in conjunction with two ARN stations to connect the NSW/Queensland state networks. In this case, DS42 is common to both the ARN (level 2) network and to the NSW (level 3) network.

The DORIS network, which is a weak global network, is connected in the same vertical manner using Fairbanks, Hartebeesthoek and Kokee Park which are also IGS *core* sites. The network is regionally connected in the Australian region using Orroral and Moresby, which are level 2 stations. A similar approach has been taken for the WING network, a regional Western Pacific Network.

The connections between the various level 3 sub-networks observed during the campaign are also shown. Of special importance are the connections between days 207-210 and 216-218 and between the network of days 212-215 and 219-220. All of these sub-networks include the common stations DS42 and BATH.

4.1.2 The 1993 Campaign

Figure 4.3 shows the hierarchical relationships of the networks that form the 1993 campaign. It is important to note that the QLD93 mini-campaign has only two direct connections to the global reference system. However, the NZD campaign, that occurred after the ARN Campaign, was directly linked to the global network using 4 connections. Two of these connections, Hobart and Tidbinbilla, also are part of the ARN solutions and hence the NZD campaign can be considered directly connected to the regional solutions.

4.1.3 The 1994 Campaign

This campaign only spanned four days. Furthermore, the number of participating stations was limited. The Australian stations were solved, along with a global tracking network, in a single GAMIT solution. This eliminated the need for the hierarchical approach taken in the previous years.

4.2 Other Strategies

4.2.1 Frequency of Observations

The epoch interval and number of observations used in GAMIT runs varied from analysis centre to analysis centre. This was partly due to the power of the computing machinery and the available disk storage resources. Our strategy for this important decision was to investigate the effect of the sampling period on the precision and stability of the deduced parameters and

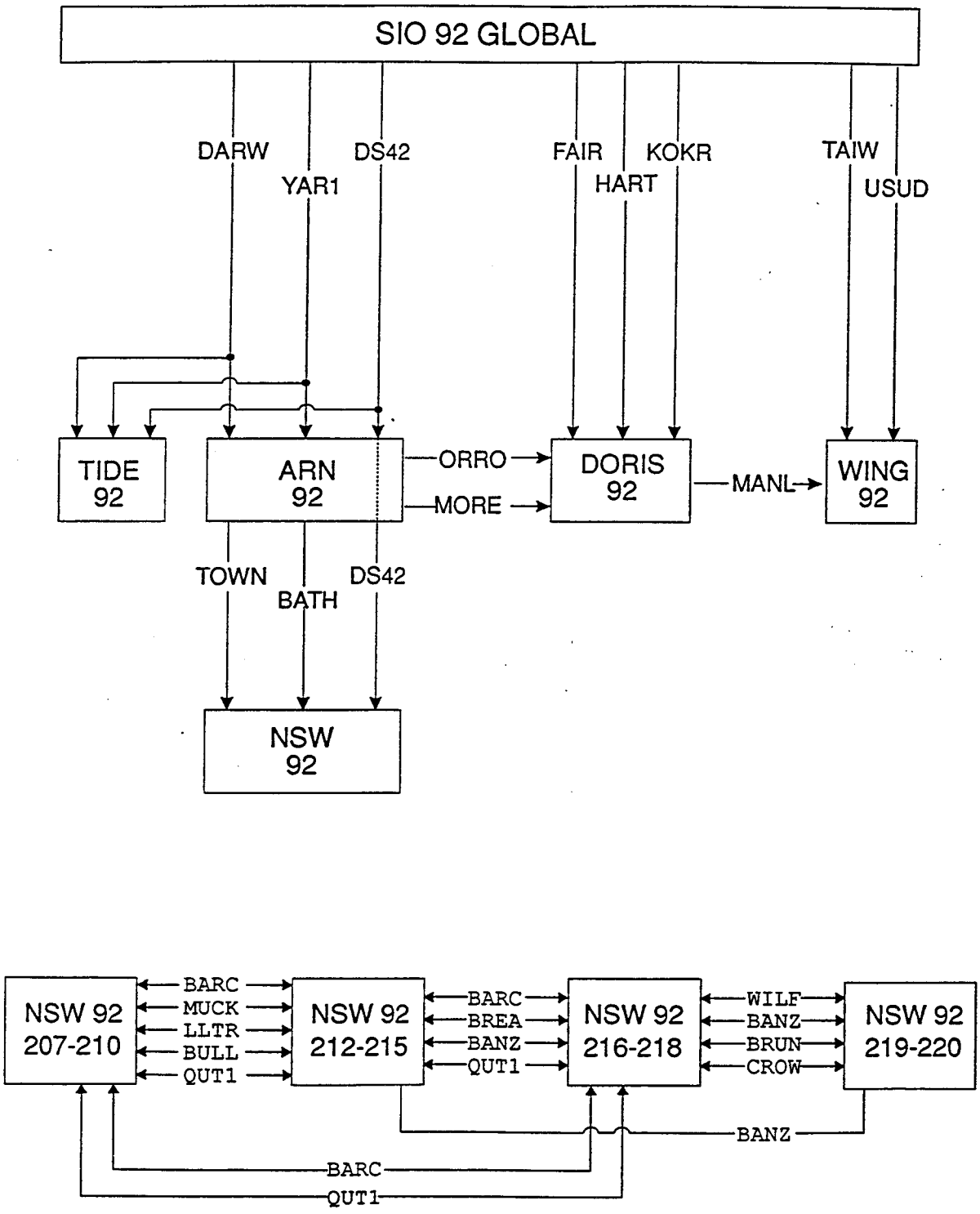

Figure 4.2: Hierarchical diagram of networks and stations used to interconnect the networks participating in the 1992 Campaign.

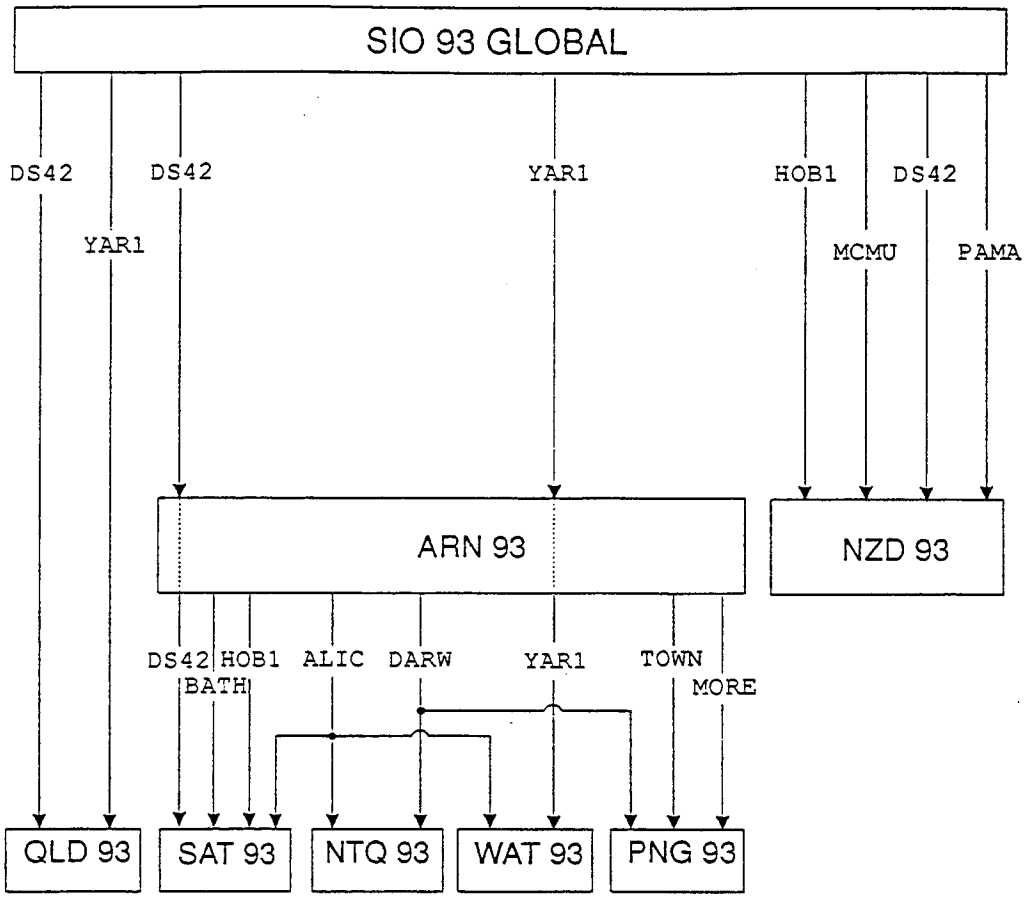

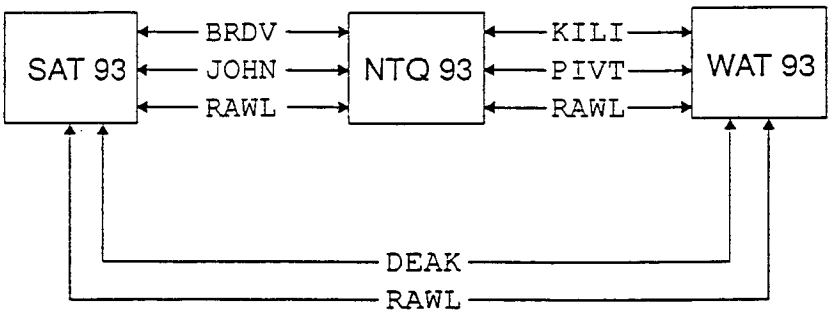

Figure 4.3: Hierarchical diagram of networks and stations used to interconnect the networks participating in the three 1993 campaigns.

then to formulate the best methodology to meet our overall analysis goal of a high precision regional solution. Chapter 8 details the investigation.

4.2.2 Data Cleaning

The strategy adopted for data cleaning was the proven SINCLN module coupled with a complete CVIEW of the resultant output. Early tests on the now-used AUTCLN module indicated that the AUTCLN algorithms rejected data and fragmented the series more than was necessary. The approach taken for data cleaning is outlined in Chapter 7.

4.2.3 Computing Machinery & Resources

SUN hardware was adopted as the basis of our computing machinery. This decision was partly based on compatibility with MIT and the GAMIT software platform, but due consideration was given to system administration and the availability and cost of other packages such as MATLAB for analysis. The System V-based SOLARIS operating system was implemented after determining that this system could be better optimised for the intensive numerical processes involved with GAMIT. Solaris also allowed us to operate with disk partitions of 4 gigabytes compared with the 2.1 gigabytes limit of SunOS. This gave us a better file system.

Computations of high precision networks, such as those performed in this report, are extremely computationally intensive and demanding of computer resources. System design considerations that are important for these types of projects are:

- The amount of available memory must be as large as possible so that paging calls to the disk, for virtual memory, are limited.
- The principal disk storage devices should be directly attached to the main computational CPU's so that network traffic and demands are minimised.
- That system swap space be larger than available memory so that paging can be accomplished in a single call. Ideally, this space should be 4 or 5 times larger than the available computer memory, allowing for concurrent editing or building of run files while the intensive computational processes continue.

Chapter 5

Data

The solutions described in this report were derived from a vast amount of data. These data came from several sources. Unfortunately, a significant portion of the data are not available for public access. The raw data holdings at the University of Canberra are generally in accordance with the IGS RINEX standards. However, a significant amount of the June 1992 data are in the NGS ARGO format. The University of Canberra does not hold any raw receiver data.

- **Level 1, Global data.**
  All of these data are in the public domain. In general they are considered to be part of the IGS data set and hence may be found at IGS data centres and some other sites, such as the University of Canberra, which maintain a complete IGS record. The DORIS data set is also in the public domain. It was collected as part of the IGS 1992 campaign by IGN as part of their contribution to the Epoch92 component. It is available upon request from IGN or University of Canberra (UC).

- **Level 2, Regional data.**
  Data belonging to this class are of mixed ownership. Specifically the following applies. All regional data for 1992, excepting the Tide network, are considered public domain as these data were collected as part of the Australian contribution to the IGS epoch campaign. Data for 1993 and 1994 and the Tide network are administered by AUSLIG and must be requested from this source. Near neighbour data, e.g., New Zealand and Papua New Guinea, were collected by UC directly from the relevant national authorities. These data have been passed on to AUSLIG to maintain regional records and may be requested from either UC, AUSLIG or the appropriate national agency.

- **Level 3, 500 km data.**
  In general, data used to densify the IGS reference frame and establish a 500 km grid spacing over the Australian continent is administered by AUSLIG on behalf of ICSM. These data must be requested from AUSLIG. The small amounts collected independently by UC have been shared with AUSLIG.

The storage of data is based on the assumption that date is a more fundamental attribute than site identification and cataloguing in this way is more amenable to management than a system based on station numbers and/or station names. This is primarily due to the fact that processing is performed according to the day of year (DOY) rather than by site. Thus, a DOY system is amenable to the storage of both raw and processed information.

The data were assembled on hard disk and then written to read/write 512 byte per sector magneto-optical discs, with a capacity of approximately 270 megabytes per side. Each side of the platter was then labelled with a unique seven digit label, **UVYYDDD**, where

U is a disk type with

U=0 representing *raw* RINEX data.

U=1 representing *clean* RINEX data.

U=2 representing *processed* RINEX data.

U=3 representing campaign-orientated backups.

U=4 representing compressed solutions.

U=5 unassigned

U=6 unassigned

U=7 representing software documentation (Readme files) and reports.

U=8 unassigned

U=9 representing scratch and other specialists disks.

V is used to extend or subdivide the **U** label. Specifically for raw and clean RINEX data this field is used to indicate volume overflow. Overflow volumes have an identical directory structure to the primary or base volume.

V=0 is the first volume of a designated directory.

V=i is the i^{th} volume of the directory.

YY is the year, e.g. 92, of the first day directory on the platter.

DDD is the day of the year, e.g., 020 is January 20, of the first directory on the platter. Platters are set up to hold seven days of data and hence labels standardly increment by 7. Data are stored using the same boundaries as the conventional GPS week.

This structure of 'GPS Week per platter side' was principally mandated by the relatively long period over which data arrives at UC and the need to have a system which would allow it to be collocated with similar data. The platter labels are seen as directories when the magneto-optical jukebox, */data3*, is accessed; thereby providing the user with immediate information as to whether the data are mounted and immediately available or if the data are currently off-line.

There are several significant issues that must be dealt with in the management of this database that are unusual to those who maintain commercial transaction-driven databases. Some of the more important issues are:

- Not all parts of the database are mounted at any one time.
- Individual files are about 1.2 megabytes when uncompressed or about 0.4 megabytes in compressed form. These files are generated on a daily basis. It is normal for the file to be processed in time sequential order. It is not uncommon to selectively filter data in these files, especially if the observational frequency exceeds the analysis frequency. Placing time series data into relational data structures and then exporting the required segment demands considerable CPU resources.

- Various combinations of the individual files are required by different analysts depending on their application. It is not common for a small number of subsets to be common to the majority of users. The files are very static since once they are loaded into the database as raw RINEX files, they cannot be modified. A similar situation applies to many of the other components, although data from analysis runs are often subject to revision. This process is infrequent although it may involve large volumes of data.

- While extensive use is made of the data archive in the local geographical region a considerable number of transactions occur over the Internet. Internet bandwidths and general levels of resources are unable to support full graphical user interfaces and other aspects of interactive sessions, although there have been significant steps in this direction with some of the tools like Gopher and Netscape as well as recent improvements in bandwidth.

- There is a small but important component of the data records that relate to the sites. This includes the instrument setup, the instrument serial numbers and operators as well as access diagrams. Experience has shown that these fields are unreliable in the RINEX files. Indeed this component is the most error-prone component and good station logs are necessary to unscramble the conflicts. Both UC and AUSLIG have hard copy records of most sites, but the holdings are far from complete. The appendix section of this report lists the master station.info file used in this study. This file also exists on the 7092000 platter held at UC.

- The cost of maintaining an extensive database on read/write magneto-optical discs is quite high at $ 340 per gigabye. This is to be compared to about $ 10 per gigabyte using Exabyte 8 mm tape. At UC, we have offloaded these data to exabyte in the same structure as was on the magneto-optical platters. Restoration to our cache platter server, which is able to hold 8 platter sides, requires 30 minutes.

5.1 The structure of the Raw RINEX data Platters

Figure 5.1 shows the structure of a typical raw RINEX platter which forms the major component of the database. This structure is repeated for the *clean* RINEX files.

The naming convention within the .94o and .94n directories is strictly in accordance with the RINEX convention (Gurtner, 1989) with the exception that the files are compressed with the UNIX *compress* routine, which adds the extension **.Z** to the end of the filename.

Thus, raw RINEX data are located in the .YYo structure, whilst the broadcast ephemeris data are located in directory .YYn structure. The latter is not complete as the information repeats at each station since it is satellite-dependent and not station-dependent. Thus a composite file for the fictious site 'brdc' is formed. This file contains the broadcast ephemeris for all satellites for the full 24 hours of the day. It can be used in place of a station-collected navigation or ephemeris file. The .sum directory contains housekeeping and other summary files. In particular, ionospheric and other warning and message data are often loaded into this directory.

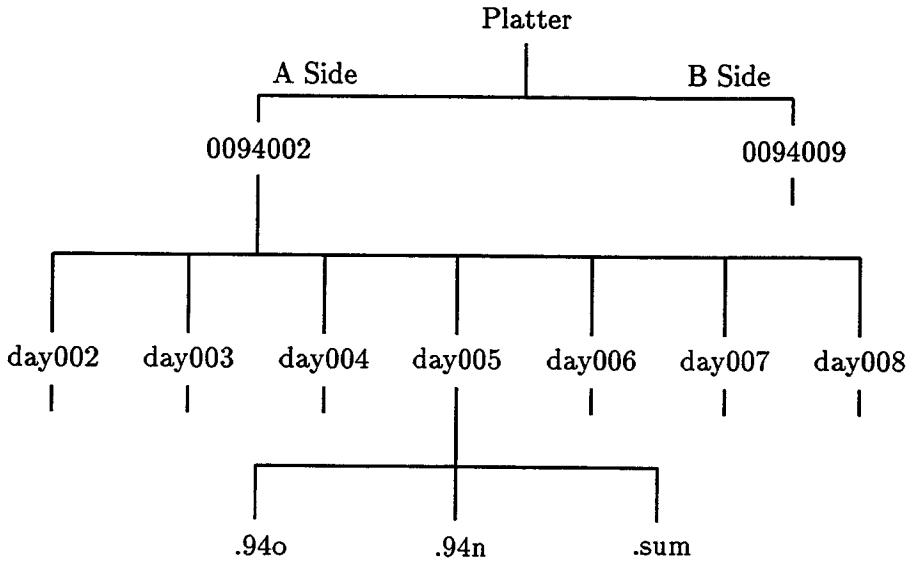

Figure 5.1: Schematic structure of raw RINEX data holdings

Chapter 6

Other Networks

The 1992 IGS Campaign was the catalyst for a significant increase in global GPS activity. In addition to the Australian contribution, there were significant contributions from New Zealand, Papua New Guinea, French and Japanese groups. There were also several other small groups, mainly in Europe but also including a Brazilian team. The analysis of these data collecting contributions was not a high priority in the IGS campaigns partly because of the gains that were being made with the permanent array and partly because of the difficulties associated with the reductions from regional campaigns. One of the immediate difficulties was the organisation of a central data centre, as it was IGS policy that regional data were the responsibility of regional centres. Unfortunately, these regional centres were not as well prepared as the global centres. The University of Canberra collected a significant portion of the non-European IGS 1992 epoch campaign data, primarily due to the fact that this data type was in the southern hemisphere or in vicinity of Australia. With the extension of the Australian network into its near neighbours, Papua New Guinea and New Zealand, much of these data were reduced either to extend the network into the adjacent regions, or to provide confirmation of the procedures and strategies adopted for our reduction and analysis process.

6.1 The Doris Network

This network is due to a French initiative as part of the Epoch component of the IGS Campaign. Appendix F.4 lists the data associated with this network as well as showing a map of the geographical distribution of the stations. The initiative had as its long term aim the study of systematic differences between DORIS and GPS-derived parameters. As such, GPS dual-frequency receivers were run at about 17 DORIS sites for the duration of the IGS 1992 epoch campaign. These sites, together with additional sites in Brazil, constitute what this report calls the DORIS network. It is supported by three stations linked to the global frame. These stations were Hartebeesthoek, Kokee Park and Fairbanks. Other connections are enforced by including observations at Orroral and Port Moresby, which were considered part of the Australian regional network. Thus, while the DORIS network is a global network, it is perhaps better to consider it as a level 2 network similar to the Australian Regional Network. The addition of the Brazilian Trimble data did much to improve the uniformity and stability of the Doris network.

The selection of Hartebeesthoek, Kokee Park and Fairbanks was done mainly to maximise the number of regional double differences. Hartebeesthoek maximised the African region including Reunion, St Helens and Djibouti. Kokee Park maximised the Central American sites of Socorro and Galapagos while Fairbanks maximised Sakalinsk and Arnagador.

The DORIS system, unlike the GPS system, is an uplink system, in that the ground instruments are transmitters while the receiver is on the spacecraft. Two frequencies are used, 401 MHz and 2036 MHz, enabling an ionospheric dispersion to be precisely computed. The spacecraft observes the Doppler shift between the transmitted signal and a reference frequency generated onboard the satellite.

The Doppler frequency is the differential of the phase, i.e., $\int \text{Doppler} \cdot dt = \text{phase}$. This phase must now be treated in an analogous manner to the GPS phase observable.

6.2 The Papua New Guinea Network

Papua New Guinea participated in the IGS 1992 campaign and the subsequent Australian campaigns in close collaboration with the Australian effort. The data used in this analysis was collected by the Papua National Mapping Bureau and forwarded to the University of Canberra. In general, the data were treated differently depending on the amount of data available.

- The 1992 data were directly added to the ARN network, see Appendix F.3.
- The 1993 data were reduced as a level three network due to the increased number of stations observed. In this case, observation at Townsville AFN and Darwin were added to provide, in conjunction with Port Moresby, the necessary hierarchical links to the ARN network at level 2, see Appendix F.10.
- The 1994 data were again directly added to the ARN network, see Appendix F.12.

There is a considerable amount of data collected outside the period of interest to this report. These data are the subject of on-going research at The School of Geomatic Engineering of the University of New South Wales.

The overall conclusion that is to be drawn is that Papua New Guinea data have all the attributes of data pertaining to an Australian state network. It has therefore been treated in exactly the same manner.

6.3 New Zealand

The New Zealand GPS data had quite different characteristics to the other GPS data used in this study. The principal differences which required different strategies and concepts arose partly from the non-coincidence of the observing epochs, the manner in which the data were observed and the tectonic setting of New Zealand, which is vastly different from Australia.

New Zealand's original and still only national geodetic datum, New Zealand Geodetic Datum 1949 (NZGD49), is the result of geodetic surveys undertaken from 1930 to 1946. A full description on NZGD49 can be found in Lee (1978). The land mass of New Zealand is subjected to earth deformation. This earth deformation is primarily a result of the collision between the Pacific and Australian tectonic plates. Reilly (1990) indicates rates between the Australian and Pacific plates of 39 mm/yr in the south, and up to 58 mm/yr in the north of New Zealand. Therefore, it can be expected that between 1949 and 1995 there could be 2 m of deformation between the east coast and the west coast of New Zealand.

The NZGD49 coordinates, which form the datum for all cadastral surveys in New Zealand, have been held fixed at the values determined in 1949. Due to the improvement in the accuracy of survey techniques and the continued earth deformation, surveys carried out today do not fit with the coordinates of the primary NZGD49 stations. When NZGD49 is replaced, the new datum should attempt to take into account the effects of earth deformation so as to prolong the useful lifetime of the new datum.

6.3.1 New Zealand GPS Data

In March 1993, the Department of Survey and Land Information (DOSLI) undertook a 13 day GPS campaign across New Zealand. The GPS network was designed for the six Ashtech LM-XII GPS receivers which DOSLI had available at the time of the campaign. The network design was influenced firstly by the requirement to try and occupy a first or second order station in each of the 28 meridional circuits. The second restriction was the intended GPS post processing software, the Ashtech proprietary software, GPPS. GPPS's main restriction was that a 24 hour data span could not be processed unless broken into sessions, where at least one satellite was present for the entire session. Thus, the observations were chosen to consist of two 4 hour sessions per day.

For the period 8^{th} through 20^{th} March (DOY 067 to 079), 1993, the best satellite constellations for two 4 hour observation sessions, occurred from 2000 to 2400 and 0100 to 0500 New Zealand Summer Time (+13 h). These periods were used for field campaigns. A 9 hour time span, from 2000 to 0500 New Zealand Summer Time, allowed fiducial station observations to be taken during more stable ionospheric conditions and the transportation of the GPS equipment to the next station during the daylight hours.

Three New Zealand fiducial sites were chosen to form the common sites between observation sessions. These sites were Whangaparaoa (D045), Three Sisters (D474) and Heaphy House (WELL = D475), their locations can be seen in Figure F.8. As four of the receivers moved around sites in the South Island, sites D474 and WELL were occupied and when the receivers were in the North Island, sites D045 and WELL were occupied. The fiducial sites were operated continually throughout the nine hours of each observing session. The four new sites for each day were operated for the first 4 hours, then were switched off for an hour, during which time the antenna was set up at a new height, then switched on for the second 4 hour session. The altering of the antenna height was done to detect incorrect height of instrument measurements by having a second occupation at each site. However, the altering of antenna height created some processing problems, as outlined in the following section.

Appendix F.8 tabulates the observed data and shows the geographical distribution of stations in New Zealand for this component of the network.

6.3.2 GAMIT/GLOBK Processing

The analysis strategy undertaken was to use GAMIT in its conventional 24 hour mode to provide maximum strength and efficiency in cleaning with SIO global orbits. This required a station appearing in session one to have a different site name to the same station appearing in session two, primarily because there were different instrument setups in the two sessions. This strategy also enabled us to make maximum use of the extended tracking that occurred at the New Zealand fiducial station, thereby strengthening the relationship of these stations to the global reference frame. GAMIT readily allows each day to have a different instrument setup so only a session one and session two characterisation of the site was necessary. In general, the second session occupation saw the site name's first character change from D to E. This was subsequently taken care of in the GLOBK earthquake file, see Appendix E.

Since the network was not observed coincident with any of the major Australian campaigns, it was directly linked to the global frame using four stations. The increase in the number of stations had nothing to do with the quality of the hierarchical links in this instance, but rather the need to provide double difference observations that would have a full sky coverage, since New Zealand is a small compact country. However, in all other respects, these hierarchical or external fiducial stations work in exactly the same manner as the three layer hierarchical system used in the the Australian case. It could be argued that the use of four stations, especially in the geometry that applies to the New Zealand case, is preferable to the Australian geometry.

6.4 The West Pacific Integrated Network of GPS, (WING)

This network was established by researchers at the Earthquake Research Institute of the University of Tokyo (Kato, 1994) to provide a base from which to investigate the regional tectonics. The data and geographical coverage are shown in Appendix F.5.

The network is rather linear in extent compared to all other networks analysed in this study. Sites USUD and TAIW were added for the hierarchical attachment of this network to the global frame. The linear extent of the network was of concern to us as our hierarchical attachment strategy is to have the third control point well removed from the line joining the other two, so that all rotations are correctly compensated for. Ideally one of the Chinese stations would have helped strengthen the solution. After due consideration, we opted for the Manila station to provide the additional control, this choice was based on having the largest geographical spread. The connection between the DORIS and WING networks was also considered to be a useful benefit.

The data from this network were standard in all respects. The network was routinely processed as a level 2, regional network.

Chapter 7

Data Cleaning and Solution Procedures

7.1 Data Cleaning

The level and expertise associated with data cleaning have long been at the heart of reliable, high-quality GPS results. The literature abounds with *cleaning* algorithms and procedures. An excellent review of methods and procedures that are known to yield acceptable results can be found in the Ph.D. dissertation of Chu (1993). The now classical work of Blewitt (1989; 1990) is also important as the *turbo-edit* algorithm is universally used in most high precision applications involving P_2 observations.

Data cleaning can be accomplished in two main ways. The first is to do data cleaning in what is termed observation space. The method generally does not require orbital information and makes use of linear combinations of observables, including the P_2 observable. It is highly regarded by all concerned with navigation problems, where highest quality orbits are generally not available and processing time is limited. The second processing option is to clean in 'residual' space where a conventional, well understood and defined model is removed from the observations. It is argued that small and difficult to resolve combinations are more readily detected and resolved with this approach, rather than with the observation space model. GAMIT uses the latter approach as it has access to high quality orbits and is not constrained by real-time issues.

The initial GAMIT algorithms were the work of Dong (1989). These algorithms are the SINCLN algorithms. They were most efficient on single difference data. The newer algorithms, AUTCLN, are from the work of Herring. These algorithms incorporate double difference searching and full validation across all double difference combinations. The AUTCLN algorithms were not extensively used for the AFN/ANN solutions. The principal reasons for not using the AUTCLN algorithms was that use of SINCLN coupled with CVIEW hand editing produced data sets that;

- were more continuous in nature with less fragmentation.
- had fewer unresolved phase discontinuities, cycle slips, and hence a smaller number of

free-bias flags. Minimising the number of free-bias flags strengthens the solutions.

AUTCLN has continued to undergo development and is now the major cleaning routine for most GAMIT analysts. This is also partly due to the increased availability of the P_2 pseudo-range and the use of the widelane combination.

Thus it is not surprising that by 1994 AUTCLN had assumed the dominant role in data cleaning. Continued use was made of the SINCLN/CVIEW approach for processing the 1994 data to be consistent with our previous solutions.

Figure 7.1 illustrates the more stringent automatic rejection criteria that is common with AUTCLN processing. With the full GPS constellation now available, the reduction in data is not considered a detrimental effect in processing networks with the AUTCLN routines. To the contrary, it is impossible to devote sufficient time to the more demanding manual processes of SINCLN/CVIEW.

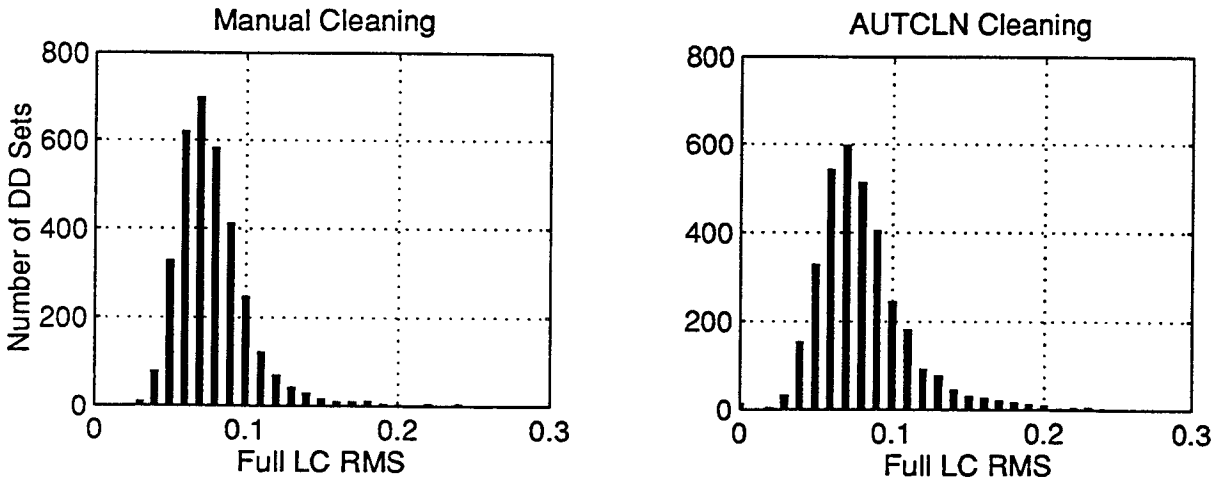

Figure 7.1: Histograms of rms of *LC* combination used by the SOLVE module in GAMIT. The *full* rms statistic which is defined as the rms for each segment of data separated by a bias flag. It is readily seen that the manual SINCLN/CVIEW process produces more double difference observables than the AUTCLN process. However, the distribution of the rms values is very similar.

The normal CVIEW procedures were modified from commencing at the bottom of a strictly numerically and alphabetically ordered stack of satellite numbers and site codes to one in which we : (a) cleaned the Tidbinbilla to Yaragadee baseline first, using the available widelane information, (b) then cleaned the remaining stations against Tidbinbilla and Yaragadee, (c) then cleaned the remaining stations against themselves. In those networks where hierarchical stations were added to the level being cleaned, cleaned files were directly imported from the higher level and cleaned against these stations. In some rare instances, the higher level cleaning scheme was revised due to a clearer picture being obtained in CVIEW editing in the lower level network. This change in procedure was made possible by the practice of keeping cleaning log

books which indicated the cleaning decisions made.

One final comment now needs to be made. There have been major advances in the automation of GPS processing in the last two years, primarily mandated by the sheer volume of data that needs to be processed on a daily schedule. The use of the SINCLN/CVIEW procedures normally required 3 to 5 days of intensive human activity to arrive at a clean daily solution. AUTCLN now accomplishes the same task using 2 hours of moderate speed CPU time.

7.2 Choice of GPS Observable

GPS observations usually involve the following data types:

1. L_1 phase or carrier beat phase of the 1575.42 MHz signal.
2. L_2 phase or carrier beat phase of the 1227.60 MHz signal.
3. C/A pseudo-range based on the 1.023 MHz modulation of the L_1 signal.
4. P_1 pseudo-range based on the 10.23 MHz modulation of the L_1 signal.
5. P_2 pseudo-range based on the 10.23 MHz modulation of the L_2 signal.

GAMIT makes use of only the phase observables in forming the observation equations. However, full use is made of all observables in cleaning the data.

Major sources of errors in most processing schemes revolve around the appropriate choice of observable. These sources include the dispersive effects of the ionosphere, the frequency dependent nature of the position of the electrical phase centre of the antenna and other antenna effects, often highly dependent on antenna design and the gain of the antenna as well as the relative signal to noise ratio of the incoming signal. In general it is well known that the most precise solutions, on short baselines where there is high correlation of ionospheric and other perturbations, are derived from treatments that consider the L_1 and L_2 data independently. However, for baselines beyond even a few hundred metres, the level of correlation is sufficiently reduced that alternative strategies are recommended. The normal counter strategy is to compute the ionospheric free, LC or L_3, combination according to

$$\phi_{LC} = 2.546\phi_{L_1} - 1.984\phi_{L_2} \tag{7.1}$$

Unfortunately this linear combination amplifies the noise on the L_1 and L_2 channels. Again if these noise signals are uncorrelated, then the noise on the ionospheric free combination is almost three times that of the basic channels. This increase in noise is a major concern as some special combinations of L_1 and L_2 phase result in hard to detect *cycle-slips*. We overcame most of these problems by simultaneously considering the LG or L_4 linear combination in which all geometrical and other non-dispersive delays cancel. This combination is represented as

$$\phi_{LG} = \phi_{L_2} - 0.779\phi_{L_1} \tag{7.2}$$

In general we made both the LC and LG combinations smooth and continuous by considering the following table of cycle errors, Table 7.1. Note the consideration of half cycle slips produced by squaring instruments.

Table 7.1: Table of common LC and LG jumps caused by incorrect bias assignment in the L_1 and L_2 phase values. Note that half cycles on L_2 are permitted for squaring-type receivers. LC jumps of less than 1 cycle are potentially dangerous especially when rapid fluctuations of the ionosphere make detection of cycle-slips in L_1, L_2 or LG difficult.

L_1	L_2	LC	LG
-1	-1	-0.56	-0.22
-1	-0.5	-1.55	0.28
-1	0	-2.55	0.78
-1	0.5	-3.54	1.28
-1	1	-4.53	1.78
0	-1	1.98	-1.00
0	-0.5	0.99	-0.50
0	0.5	-0.99	0.50
0	1	-1.98	1.00
1	-1	4.53	-1.78
1	-0.5	3.54	-1.28
1	0	2.55	-0.78
1	0.5	1.55	-0.28
1	1	0.56	0.22
2	1.5	2.12	-0.06
2	2.5	0.13	0.94
2	3	-0.86	1.44
3	4	-0.30	1.66
4	5	0.26	1.88

The success of correctly accounting for slips and other irregularities can be gauged from Figure 7.1 in that the sequence rms is well under 0.3 for all but a few series. This approach may be contaminated by small phase jumps near either end of a large data sequence. Additionally, as pointed out above, there are some gaps that can be difficult to interpret. Nevertheless, the statistics are well behaved with the bulk of the double difference sequences having rms levels well under 0.1 of a cycle or 2 cm.

7.3 The GAMIT Solutions

A standard GAMIT run consists of two parts. The first is run according to conventional weighted least squares practices where the analyst defines the system weights. The second part is also run according to conventional least squares practices but now with loose constraints. For the loosely constrained solution to be effective, it is essential that the data be free from all sources of contamination. We used a-priori coordinate errors of 5 cm in latitude and longitude and 10 cm in height for those stations providing the hierarchial linking between networks as we had high confidence in our knowledge of their positions. In addition, the CIGNET stations at Hobart (TAS1), Townsville (TOWN), and Wellington (WELL) were weighted at 10 cm in latitude and longitude and 20 cm in height, based on our experiences with these stations. The orbital elements were assumed to have 20 part per million errors on the conventional Keplerian

elements and 10% errors on the force parameters. The observations were uniformally weighted at 10 mm.

We solved for the following parameters:

1. The three components of the station vector, $[X, Y, Z]$,
2. One correction to a nominal atmospheric delay,
3. The six conventional components of the satellite state vector, $[X, Y, Z, \dot{X}, \dot{Y}, \dot{Z}]$,
4. Three non-gravitational corrections to the satellite state vector,
5. Biases as appropriate.

Analysis of the results concentrated on the precision of recovery of parameters, the normalised root mean square statistic (nrms) and the quality with which the daily solutions could be adjusted into a single solution using the GLOBK suite. Chapter 10 details these results.

A parameter of interest to analysists invoking least squares procedures is the ratio of observations to unknowns. Conventional wisdom indicates that this ratio should exceed fifty. Higher values do not, in general, guarantee more precise results but rather tend to provide a better base on which to resolve parameters that might otherwise be heavily correlated. In this case, the number of unknown parameters involved in a solution can be formulated as $u = 4 * stations + 9 * satellite + biases$.

Table 7.2 lists the number of parameters belonging to the individual classes for several solutions for days 208, 209, 210 and 211 of 1992 using the ARN network. It is readily seen that the ratio of observations to unknowns is well above the above mentioned levels.

Table 7.2: Tabulation of the number of observations and the number of unknowns in each class for a sample of ARN networks.

day	Obs.	Unknowns				Ratio
		Station	Satellites	Biases	Total	Obs/Total
207	91994	52	162	187	401	229
208	109087	56	162	211	429	254
209	136959	72	162	266	500	273
210	143546	72	162	272	506	283

Chapter 8

Sampling Interval

The analysis of GPS data is traditionally performed on either 30 second data or 120 second data. The choice is usually based on laboratory *best* practice. In Australia, this best practice resulted in the University of Canberra adopting a 30 second standard, while the University of New South Wales adopted a 120 second standard. In order to understand the effects that the sampling interval would have on the results, a four day period in 1992, days 207 through 210, were analysed at 30, 120 and 240 second sampling intervals. This chapter reports the studies associated with these tests.

8.1 Autocorrelation Studies

The autocorrelation function is a measure of the similarity of the function $f_1(t)$ with itself shifted by some fixed interval τ. It is an even function with a maximum at $\tau = 0$. The autocorrelation function can be defined as

$$C_{11}(\tau) = \lim_{T\to\infty} \frac{1}{T} \int_{-\frac{T}{2}}^{\frac{T}{2}} f_1(t) f_1(t+\tau) dt \tag{8.1}$$

where τ is the chosen sampling interval and T is the length of the data record.

Figure 8.1 shows a typical autocorrelation function for the raw, undifferenced L_1 phase for two typical satellites at Tidbinbilla, DS42, and Yaragadee, YAR1. It is seen from the figure that the autocorrelation function remains high for appreciable intervals indicating that there is little to differentiate sampling intervals in the region of 30 to 120 seconds.

Single difference functions can be formed (equations 2.2 and 2.4) from these undifferenced observations. The associated autocorrelation functions are shown in Figure 8.2. The upper two figures show the between-satellite differences while the lower two figures show the between-station differences. It is readily seen that the autocorrelation functions decay more quickly indicating that these functions are likely to contain more independent information than the undifferenced functions for the same amount of data. It is interesting to note that there is

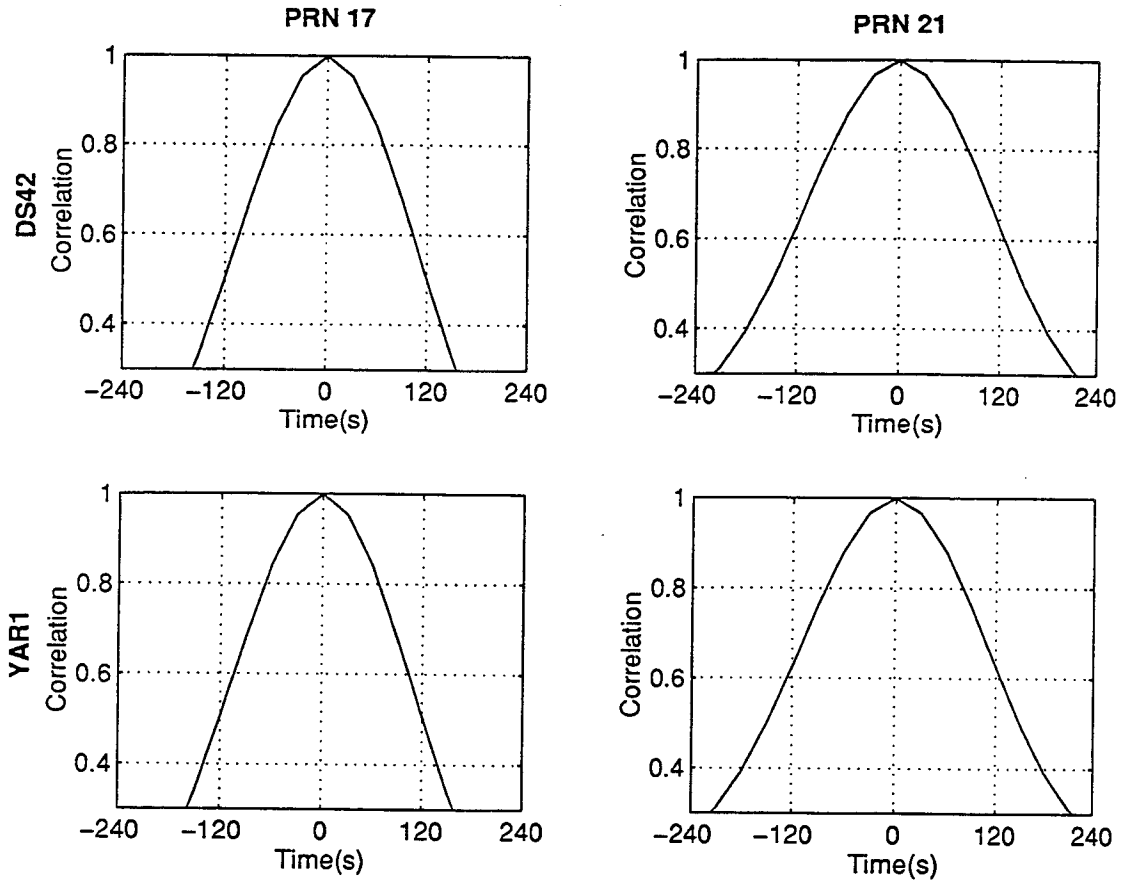

Figure 8.1: Typical autocorrelation functions for raw, undifferenced L_1 phase data for a set of data used to construct single and double differenced observables. The normal sampling interval ranges from 30 to 120 seconds.

a tendency for the between-satellite differences, which remove receiver oscillator errors, to exhibit higher autocorrelations than the between-station differences, which are dominated by the geometrical relationships between the stations.

The double differenced operator can be formed from either of the single differenced pairs. This is shown in Figure 8.3. It is noticed that the autocorrelation function of the double differenced function is higher than that of the single difference functions. This is primarily attributed to the fact that the double differenced function is free of all oscillator effects and other random errors that are cancelled in the double differencing process. The degree of cancellation is dependent on the interstation distance and the level of perturbation of the clocks, with excess in both quantities implying that some a-priori knowledge is desirable.

Finally, the triple difference function, formed by differencing between successive epochs of the double difference function, is shown. As anticipated, this is significantly less autocorrelated than the double difference function from which it was derived as the constant part is removed by differencing.

These studies suggest that there are no appreciable gains in selecting 30 second sampling versus 120 second sampling, or even say, 240 second sampling. The major gains appear to be in the type of observable chosen and its power to achieve the desired result. Clearly, observables

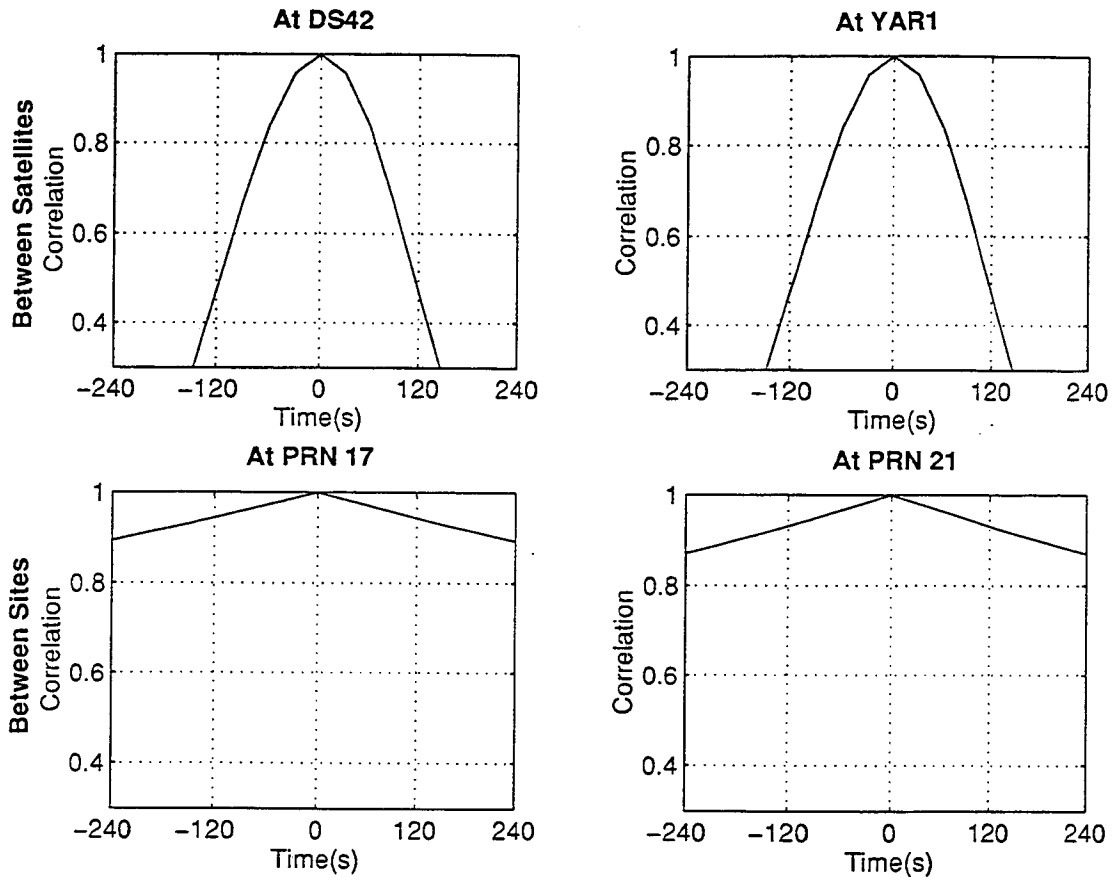

Figure 8.2: Typical autocorrelation functions for single differenced L_1 phase data. The data used is the same as used in Figure 8.1. Note that the autocorrelation function stands higher in these plots compared with the plot of the raw data as shown in Figure 8.1.

that eliminate or lower the impact of selective availability are more desirable to those which require this perturbation to be fully accounted for. It remains to be said that the spectra shown in these figures and discussed here are but a small sample of the wide variety that can result from experimental data. They are, however, representative of the types to be expected.

8.2 Cross Correlation Studies

Since the single difference and double difference functions involve two or more observables, it is possible to cross correlate the component series. The cross correlation coefficient is a measure of the similarity of the two functions. Rapid fall-off of the coefficient indicates that the component functions are independent and/or different. This is not surprising as one observable can be from a rising satellite, while the other can be from a setting satellite. The cross correlation function can be written as

$$C_{12}(\tau) = \int_{-\infty}^{\infty} f_1(t) f_2(t+\tau) dt = \int_{-\infty}^{\infty} f_1(t-\tau) f_2(t) dt \tag{8.2}$$

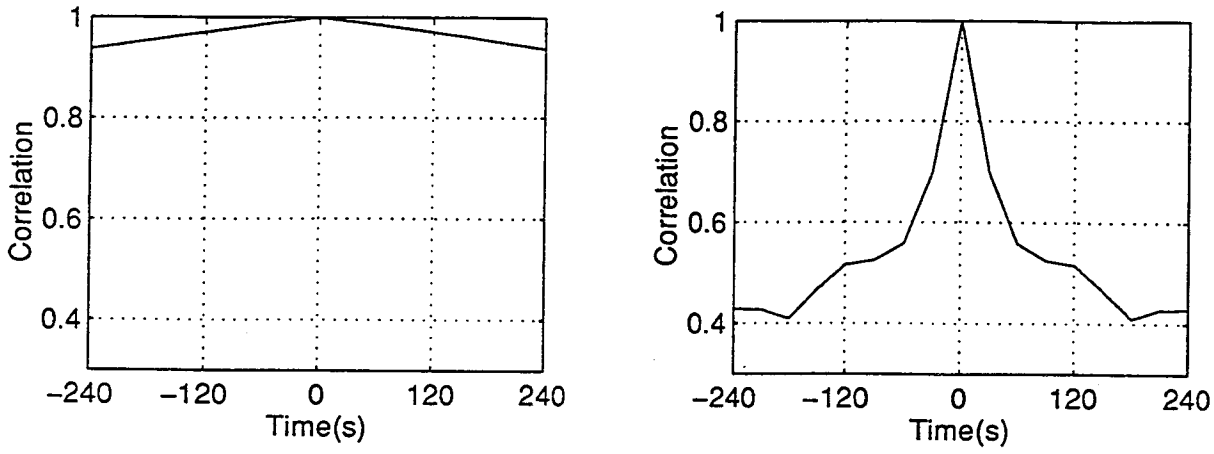

Figure 8.3: Double and triple difference autocorrelation functions for the data of Figure 8.1

Figure 8.4 shows the cross correlation function for the between-satellite and between-station functions and for the double difference operator. It is immediately noted that these functions are not symmetric and that it is the selective availability signal that dominates. The cross correlation of the between-station differences, which eliminates the first order effects of selective availability is non-central and of low magnitude. The between-satellite differences, when considering the same satellite, have high correlation due to the dominant nature of selective availability. It is to be stressed that the functions depicted in Figure 8.4 are typical and the significant variations shown can readily be attributed to the station geometry and the particular satellite configuration available. This is in contrast to the autocorrelation functions which showed only small variations due to station geometry and satellite configuration.

Figure 8.5 shows the cross correlation for the double difference function. It can be seen that this is characterised by a peak correlation much less than 0.9 and that the fall-off is quite rapid. While the peak correlation and the rate of fall off are dependent on the geometry of the ground stations and the configuration of the satellites, the values shown in Figure 8.5 are typical. Thus, while the double difference function may be smooth with a high autocorrelation, the cross correlation coefficient of the components is low. This indicates that even for 30 second samples there is a large measure of independence between the samples since the constituent components of the observations are not highly correlated.

8.3 Review of Auto and Cross Correlation Studies

There is a considerable body of literature on correlations and power spectra and their impact on geophysical phenomena. Important sources are the works of Bath (1974), Claerbout (1985) and the classical text by Bracewell (1978).

Figure 8.6 illustrates some common forms for the autocorrelation function. The data derived from single and double difference algorithms appears to approximate the red noise case of this figure. The most common method of dealing with red noise systems is to increase the length of the sampled interval. In this case, this means that bias flags should be resolved as much as

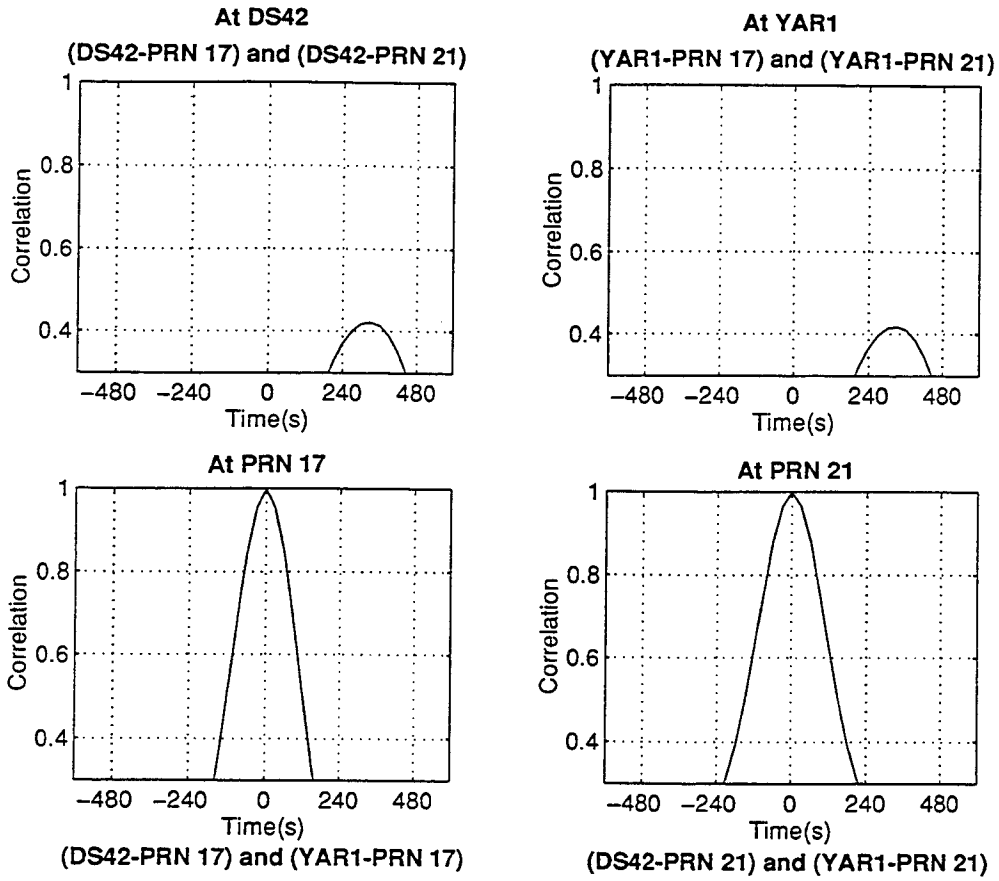

Figure 8.4: Typical cross correlation functions for single differenced L_1 phase data. The data used is the same as used in Figure 8.1.

possible so that the data sets are as long and continuous as possible.

8.4 Power Spectrum

The auto and cross correlation functions are linked to the power spectrum and cross power spectrum as Fourier pairs. For the autocorrelation and power spectrum Fourier pair, the connection is:

$$\begin{aligned} C_{11}(\tau) &= \int_{\infty}^{\infty} f_1(t) f_1(t+\tau) dt \\ &= \frac{1}{2\pi} \int_{-\infty}^{\infty} |F_1(\omega)|^2 e^{i\omega\tau} d\omega \\ &= \frac{1}{2\pi} \int_{-\infty}^{\infty} E_{11}(\omega) e^{i\omega\tau} d\omega \end{aligned} \tag{8.3}$$

and conversely

$$E_{11} = \int_{-\infty}^{\infty} C_{11}(\tau) e^{i\omega\tau} d\tau$$

where $E_{11}(\omega) = |F_1(\omega)|^2 = F_1^* F_1(\omega)$ is the power spectral density and $F_1(\omega) = \int_{-\infty}^{\infty} f_1(t) e^{-i\omega t} dt$.

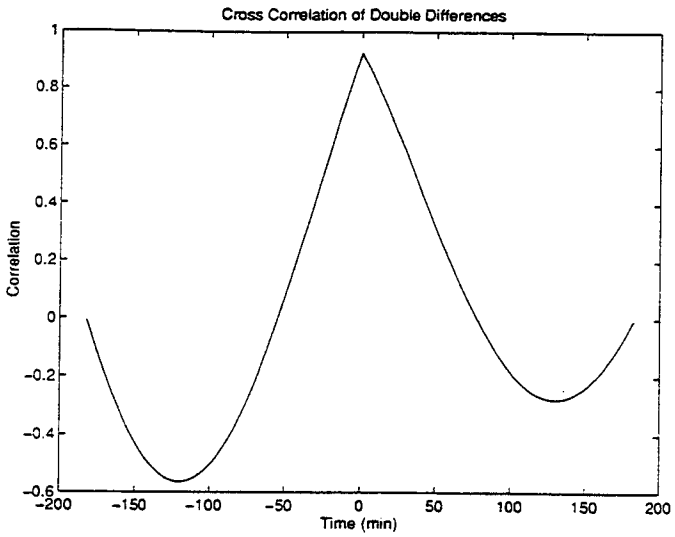

Figure 8.5: A typical cross correlation for the double difference observable as derived from the data of Figure 8.1.

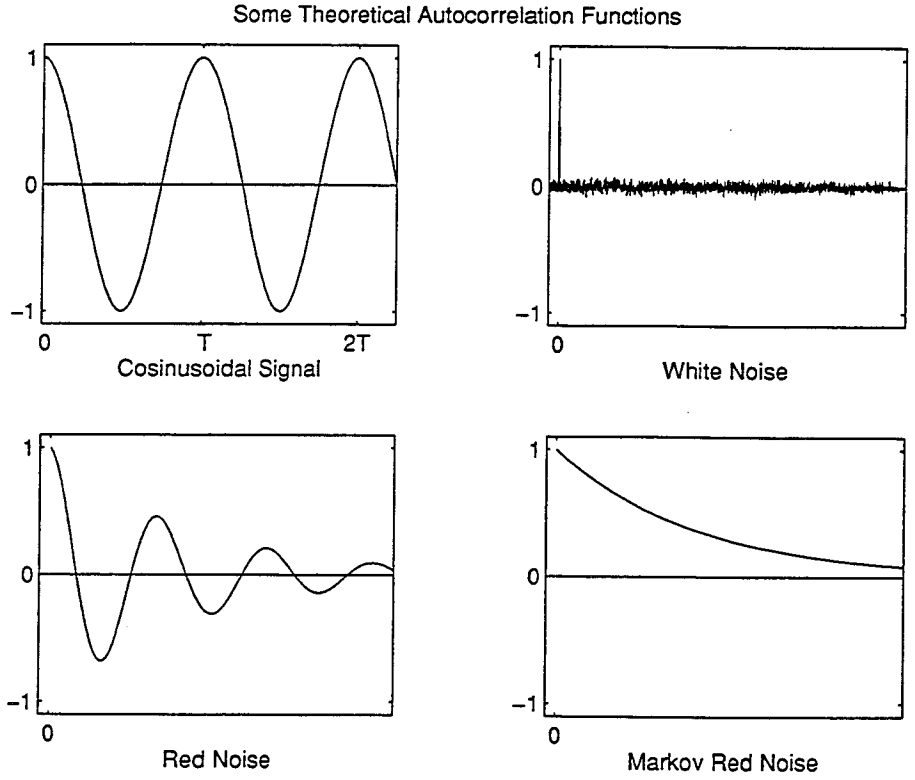

Figure 8.6: Typical auto and cross correlation functions for the four major types of signals (Adapted from Bath (1974).

The above equations provide a convenient method of computing the auto correlation function and power spectral function. The latter has important uses in detecting cyclical events. One form of cyclical event that can be characterized by the power spectrum is multipathing. The power spectrum is also useful for quantifying system noise levels. In this project we were not able to choose instrument types at any stage of the project. Logistical constraints of ownership and operations were always used to locate instruments and hence the relative superiority of one instrument type over another was not made. Nevertheless, Figure 8.7 illustrates the change

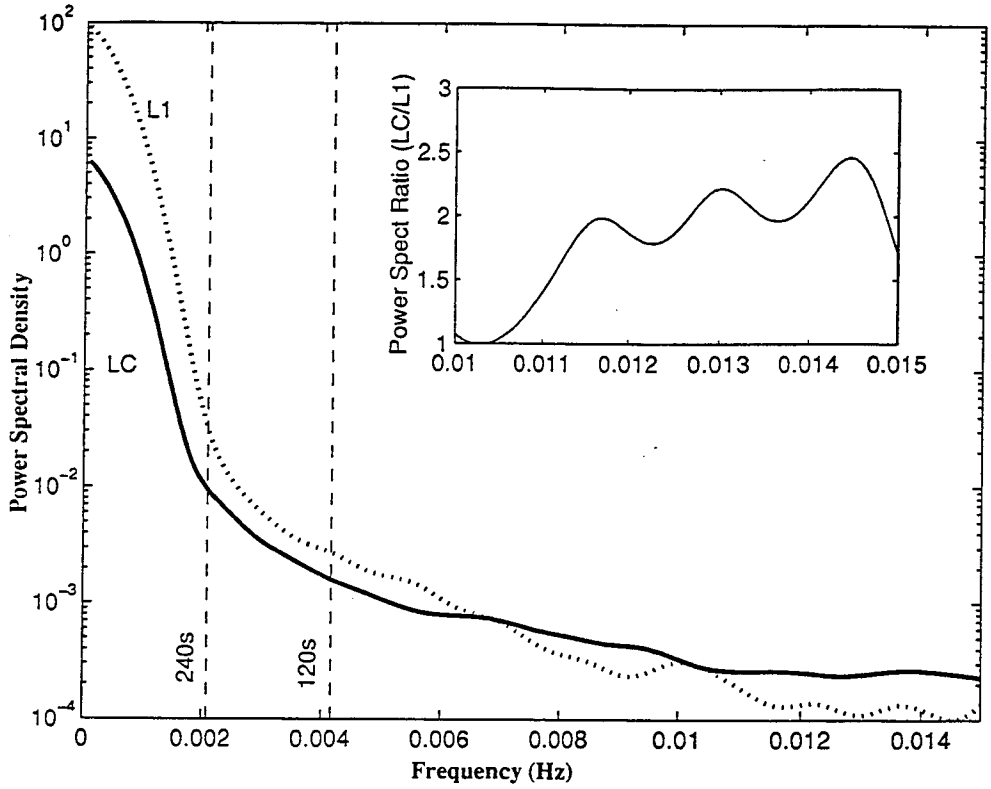

Figure 8.7: Smoothed Power spectra of L_1 and LC double differenced observables between a pair of Rogue receivers at Yaragadee and Tidbinbilla, DS42. The FFT used 512 data points from a 30 second sampling strategy. The vertical lines represent the Nyquist frequencies associated with 240 and 120 second sampling intervals. The small subplot shows the increase in noise in going from the L_1 frequency to the LC frequency. Auto and cross correlation studies indicate that the noise in L_1 and L_2 is highly correlated and hence the noise growth is not a simple linear function.

in system noise that results when the LC observable is used compared to the L_1 observable previously used.

Figure 8.7 clearly shows that LC is less noisy than L_1 at low frequencies, primarily due to removal of ionospheric perturbations that would be expected to appear at the low frequency or *red* end of the spectrum. The reverse occurs at higher frequencies, mainly due to the amplification of what is essentially white noise. It is interesting to note, that apart from the region near the Nyquist limit, the difference between the noise levels of the two spectra is in agreement with theoretical values for the white noise region. Finally, it is clear that the less dense sampling intervals of 240 seconds are approaching the *red* end of the spectrum where simple statistical representations of correlations and weights no longer holds.

8.5 Sampling Interval Tests

The above correlation studies indicate that the double difference observable introduces new information, even at 30 second sampling. To formally test the effect of increasing the sampling interval, we took 4 days of data and subjected this data to analysis at 30 second, 120 second and 240 second intervals. In each case, we started from the same RINEX files and solved for

Table 8.1: The tabulated constraints were used in the Sampling Interval Tests on Days 207, 208, 209 and 210. The a-priori values of the three CIGNET sites were determined from a solution involving the current data, sampled at 30 seconds, and a significant quantity of southern hemisphere data commencing with GIG91 and other Antarctic data

Station	Constraint (m)		
	North	East	Up
Alice Springs	100.0	100.0	100.0
Bathurst	100.0	100.0	100.0
Bakosurtanal	100.0	100.0	100.0
Christmas Is	100.0	100.0	100.0
Cocos Island	100.0	100.0	100.0
Darwin	100.0	100.0	100.0
Hobart AFN	100.0	100.0	100.0
Karratha	100.0	100.0	100.0
Misima Is PNG	100.0	100.0	100.0
Port Moresby	100.0	100.0	100.0
Orroral	100.0	100.0	100.0
Otago NZ	100.0	100.0	100.0
Townsville AFN	100.0	100.0	100.0
Tidbinbilla	0.05	0.05	0.20
Hobart CIGNET	0.05	0.05	0.20
Townsville CIGNET	0.05	0.05	0.20
Wellington CIGNET	0.05	0.05	0.20
Yaragadee	0.05	0.05	0.20

the same number of parameters. The parameters solved for were:

- The three coordinates of each of the 18 trackers.
- One atmospheric delay for each tracker.
- The six Keplerian elements, in state vector format, for each of 18 satellites used.
- Three non-gravitational parameters for each of the 18 satellites.
- Approximately 200 to 250 bias flags.

The modelling used in these tests is described in Chapter 3.

The constraints helped ensure that each of the daily solutions would refer to the same reference frame and hence, simple averaging and statistical analysis could be undertaken without the need to apply a three-dimensional transformation between the reference systems.

We also sought to minimize the magnitude of the correction by setting the a-priori estimates for the positions of the weakly-constrained sites to a value such that the correction vector was less than one metre. This would allow the analysis to proceed using the magnitude of the correction vector, as the a-priori position would act as a constant offset.

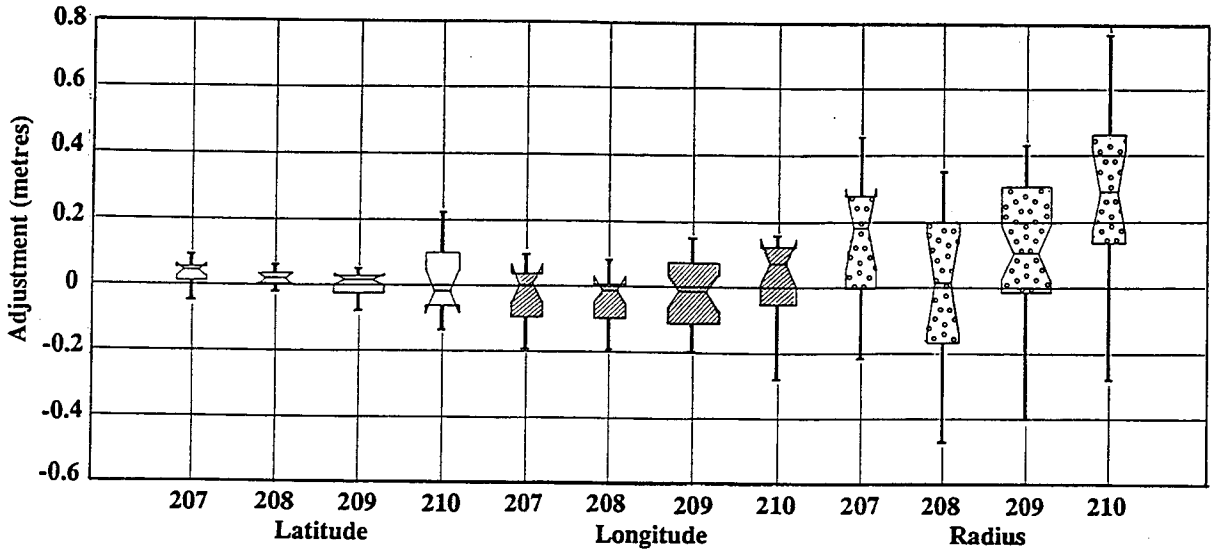

Figure 8.8: Station adjustments, for 30 second sampling, pooled by day. The box & whisker plots are drawn with 95% confidence intervals on the median value

The analysis was conducted in a spherical coordinate reference frame (latitude, longitude, radius) with latitude and longitude being converted to metres at the point of interest. The mode of display chosen was the box and whisker plot developed by Tukey (1967).

8.5.1 The Effect on the Station Vector

The first point to establish was the level of variability that was inherent in the four daily solutions. To do this, the corrections to the adjusted parameters were pooled over the 19 participating stations taking into account the three components of position. Only the results of the 30 second sampling were used. The results are shown in Figure 8.8.

Since the box and whisker plots are pooled corrections relative to an arbitrary a-priori level, it is not so much the absolute size of the boxes and their whiskers that is important but rather the variability of these quantities. In all cases two sample, 95% confidence intervals, overlap between any pair indicating that the sample is homogeneous and consistent at this level.

Figure 8.9 shows the adjustments pooled over all days and all sites for each sampling interval. There is no change in the mean value of latitude and longitude as the sampling interval is increased. However, the changes in the radial or height component are consistent and significant as the interval is increased from 30 seconds to 240 seconds.

There is also a suggestion that precision of the horizontal components improves as the sampling interval increases. This is thought to be due to the uneven manner in which data decimation occurs as the sampling interval increases. The rationale is that the majority of the data are relatively low in elevation. Low elevation data are generally noisier than the high or even moderate elevation data and hence the sampling criteria reject more noisy data than quality data, thereby improving the result. This would tend to improve the horizontal components compared to the height component, which is well known to be sensitive to low elevation data.

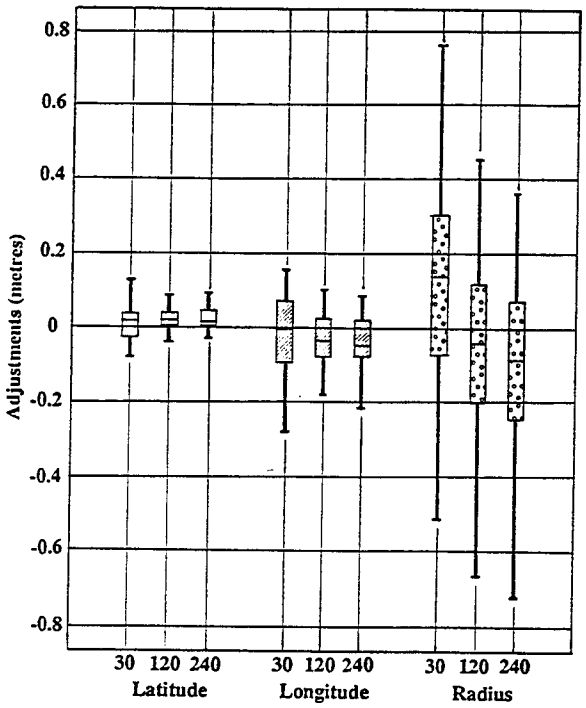

Figure 8.9: Station adjustments pooled over all sites and days to show the effect of changing sampling interval. Individual box and whisker plots in this figure are the composite pooling of plots similar to Figure 8.8

The final figure, Figure 8.10, pools the formal uncertainties associated with the data of Figure 8.9. The distribution of the variables is no longer expected to be a normal distribution. Rather it is likely to be exponential or log-normal in shape as it is the sum of individual estimates which are χ^2 distributed. The striking aspect of the figure is the upward trend of the median and the minimum and maximum values for all three components with the change being greatest for the radial component. The changes are significant, especially in the radial component, for increases in sampling interval from 30 to 120 seconds. It must be noted that precision has two components associated with it (Eisenhart, 1963). The first is the bias or offset from the global mean value. The second is the amount of coherency between replications or the precision of the observation. It is this second concept that is being discussed in this figure.

8.5.2 The Effect on the Satellite State Vector

The methodology for investigating the effect of sampling interval on the quality of the determination of the orbit state vector is analogous to that adopted in the previous study of the site position vector. As in the study of the site position vector, four days of data were processed. However, due to data density, only the first three contiguous days were analysed. In this analysis, the a-priori orbit vector was taken as the SIO global IGS orbit. The network for the local orbit was the extended Regional Network as it had been determined that this network size has an effect on the recovery of the satellite state vector. This effect is described in the following chapter.

The satellite state vector solved in the tests consisted of nine components. The first six components, position and rate of change of position, are related to the conventional gravi-

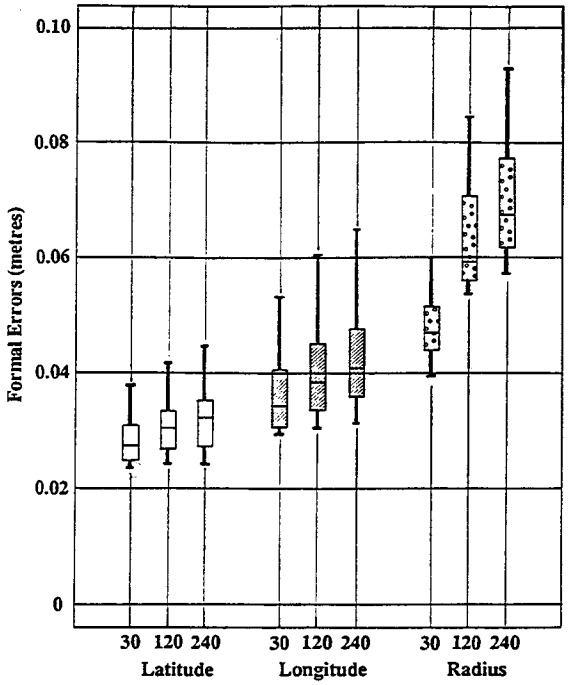

Figure 8.10: The precisions of the corrections to station positions are pooled for all sites and days. This figure complements Figure 8.9

tational Keplerian elements. The final three elements are non-gravitational terms related to other effects. They were the solar radiation pressure, the y-bias term and the orthogonal z-bias term. Only the position component has been analysed in depth.

Figure 8.11 shows that the orbit adjustments to the SIO a-priori input level are all small and of the order of one to two metres. The daily variation of these corrections is small. Likely causes for variation include variable tracking geometry, ionospheric noise and uniformity of the applicability of the single daily troposphere component. It is to be noted that while the plotted figures are corrections to the SIO determined values, no precise statement can be made from the figure as to the absolute nature of either the SIO orbit or the values from the local regional network. It is shown in the next section that the corrections are deemed significant for the case of 30 second data.

Figure 8.12 shows a remarkable level of consistency for all three components. Not only are there no significant statistical differences between the sampling intervals, but the range of variation is remarkably constant. This level of consistency, shown in the magnitude of the adjustments, is not shared by the associated precisions of the corrections. Figure 8.13 shows the almost linear decrease in precision associated with increased sample interval. In all cases, there is considerable upward growth in the median and the minimum and maximum values. This rate of growth is such that the reliability of the correction or adjustment can be seriously questioned for those schemes only utilizing 120 second data, while procedures adopting 240 second sampling should not be used to adjust high quality orbits, such as those determined from global solutions.

The issue of the reliability or the amount of power to correctly determine the state vector with precision is an important issue. This was tackled in the conventional manner by forming the ratio of the adjustment to the formal error, noting that values under three are indicative of a system where the adjustments are not significant. Figure 8.14 shows the pooled X component

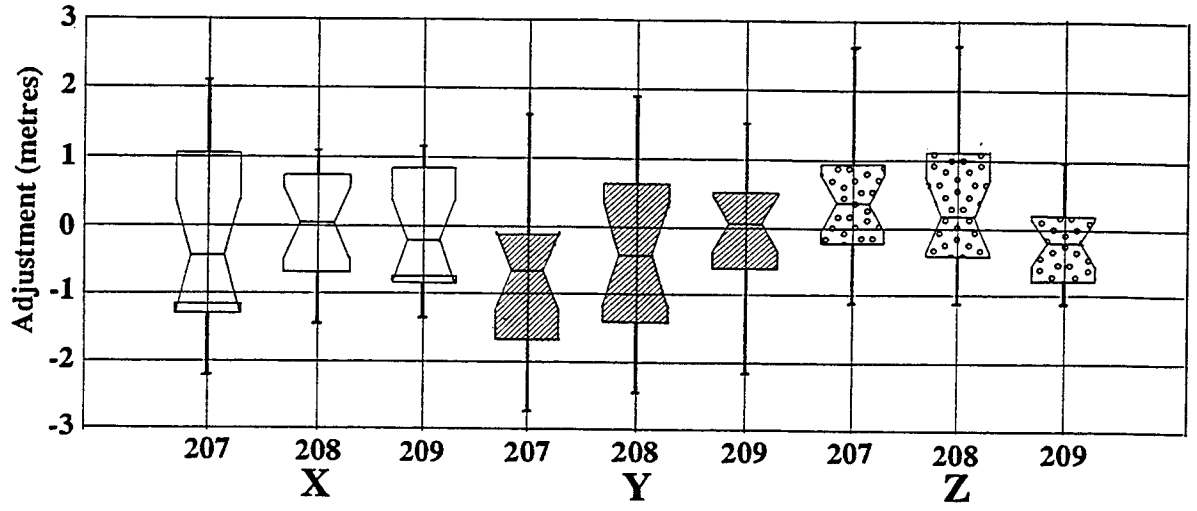

Figure 8.11: The corrections to the position components of 19 satellites relative to the SIO IGS orbit are pooled as a function of day. The box and whisker plots are shown with 95% confidence intervals about their medians which indicates that the overall level of the corrections is not varying significantly on a daily basis.

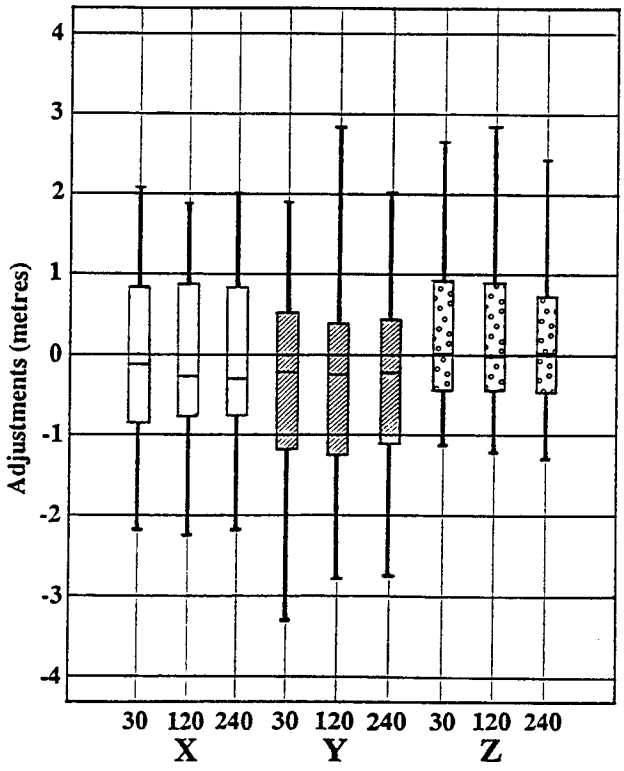

Figure 8.12: The corrections to the SIO a-priori satellite state vector are pooled for each satellite and for the three analysis days.

of the satellite state vector. It is seen that when sampling is at the 240 second level almost all the ratios are less than three indicating the low power of the solution. This is to be compared to the histogram for the 30 second sampling case where it is seen that there are a large number of significant corrections.

The 120 second sampling case is intermediate to these two cases. It is to be pointed out that the area/size of the network also plays a significant role in the size of these ratios, with large networks having considerably more ability to determine an orbit than small networks. This is mainly due to the time extent of the tracking but also due to the all-sky nature of the double differences.

The level of reliability is illustrated in Figure 8.14 for the X-component. The other components of the satellite state vector are similar.

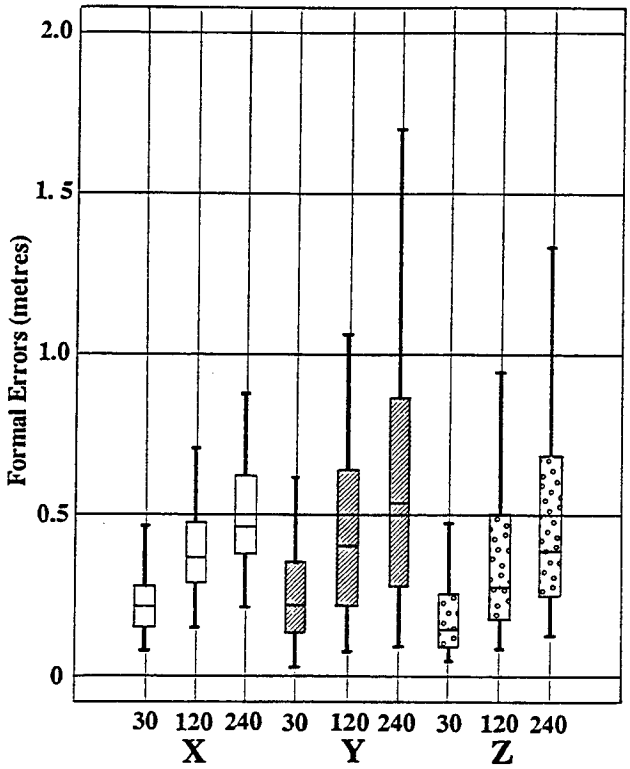

Figure 8.13: Pooled orbit formals for the three positional components of the state vector.

8.6 Conclusion

The overall conclusion from these tests was the requirement to perform all regional work at the 30 second level unless complete reliance was made on overseas orbit products. For Tide Gauge work and other programs, where there is considerable emphasis on the vertical component, 30 second data are also required.

The use of the minimum available sampling interval, 30 seconds, is not intuitive from correlation and spectral studies. Here the dominating aspect is the high autocorrelation function. This high autocorrelation function is not totally unexpected as each satellite's arcs only subtends about $\frac{1}{5}$th of a revolution for typical station configurations. An examination of the cross corre-

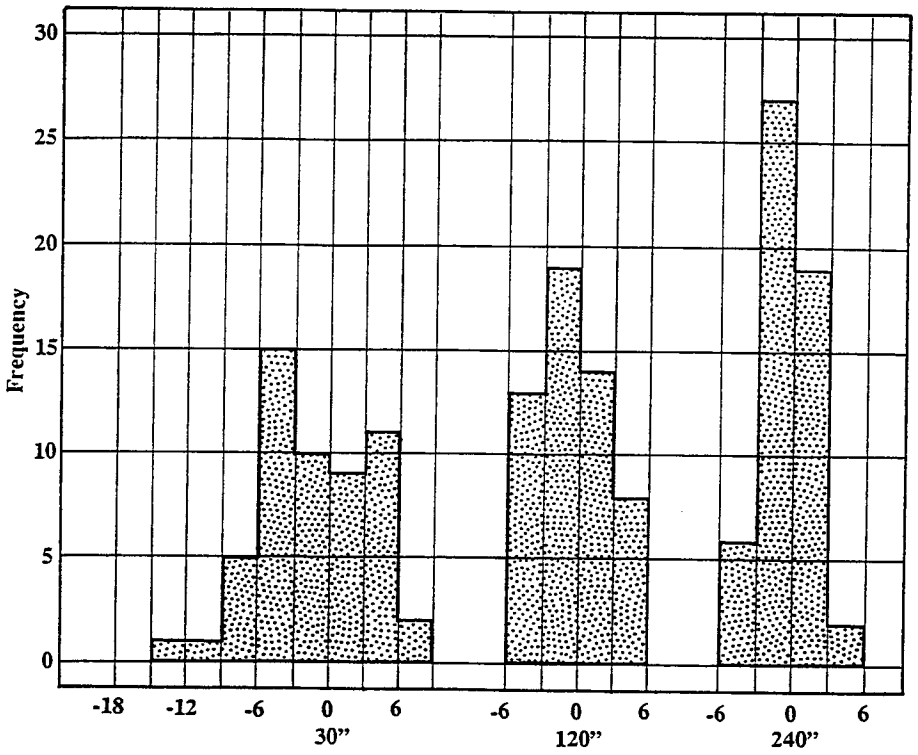

Figure 8.14: The ratio of the corrections to the component of the orbit state vector and its associated formal error are pooled for every satellite over the three analysis days. The resulting histograms, binned at the three sigma level, clearly show that few corrections are statistically meaningful for 240 second sampling procedures, while at the 30 second level the distribution is tending towards a uniform distribution indicating that most corrections are statistically significant.

lation function between the constituent components supports this hypothesis. Additionally, it indicates that there is a rapid fall-off of the cross correlation between the constituent components, indicating their dissimilarity and independence. Thus, significant amounts of information can be introduced at relatively high frequencies without affecting the correct weighting of the adjustment process. It is to be noted that the best accounting method for multipathing and other antenna related effects is to increase the sampling interval so that the effect is covered by the Nyquist theorem and hence is averaged out or correctly modelled.

Finally, a careful analysis of the effects of sampling interval on the major products of station vectors, tropospheric delay and orbit state vector shows that superior results are obtained with 30 second data compared with 120 and 240 second data. For the case of the station vector, the radial or height component is the most affected with the precision of estimating the parameter showing the most significant deterioration. For the satellite state vector, no significant differences are seen in the recovery of the satellite state vector relative to the SIO a-priori values. Again, the significant change is in the precision of recovery of the orbital state vector. This can be so degraded for the 240 second case that there is no rationale and no need to estimate these parameters when using a quality global product, such as an IGS solution or a specific analysis centre solution.

Chapter 9

Orbit Precision & Network Extent

Chapter 8 described tests associated with the precision of recovery of the major parameters as a function of the sampling interval. This chapter extends this work by examining the effect of network size and tracking geometry on the recovery of orbital parameters.

9.1 The effect of increasing the Southern Hemisphere Tracking

This study aims to understand the effect of the limited southern hemisphere tracking on the quality of the orbit. To do this, four days of observations in early 1994 were used. These days had limited southern hemisphere tracking within the IGS Pilot Campaign and a significant southern hemisphere augmentation due to the Scientific Committee for Antarctic Research (SCAR) 1994 campaign. The standard SIO solution was used and then, using the same modelling and analysis procedures, a solution was done using the tracking network augmented by the southern hemisphere stations listed in Table 9.1

Table 9.1: The following stations were observed as part of the SCAR 1994 Artarctic campaign. These stations were not continuously operating in January 1993 and hence were not part of the IGS Pilot campaign.

Station	Instrument	Latitude			Longitude			Height
Macquarie Island	Turbo Rogue	-54	29	58.32454	158	56	9.00000	-6.72
Casey	Turbo Rogue	-66	17	0.12659	110	31	11.02000	23.57
Davis	Turbo Rogue	-68	34	38.36763	77	58	21.40000	44.53
Mawson	Turbo Rogue	-67	36	17.19711	62	52	14.57000	59.25

A two sample analysis of the adjustments to a-priori parameters, X, Y and Z, for 26 satellites for four days indicated that the adjusted quantities from the SIO and the augmented SIO network were statistically equivalent at the 95% confidence level. The analysis of the associated variances was neither as straight forward as the adjustments nor in favour of equivalence. The

correct test for the equivalence of variance is the *F-ratio* test which clearly rejects the equal hypothesis. However, it was felt that other tests are more descriptive as they indicate some of the variability to be found between the satellites and some of the components of the state vector.

9.1.1 Test 1: The distribution of the formal errors

Figure 9.1 shows the distribution of the formal errors for the pooled X, Y and Z components of the satellite state vector. There are 312 observations in the pooled sum. Individual formal errors are normally distributed as a χ^2 function. The summation, or pooling, of these independant quantities leads to a log-normal type distribution which is superimposed over the frequency plots of figure 9.1.

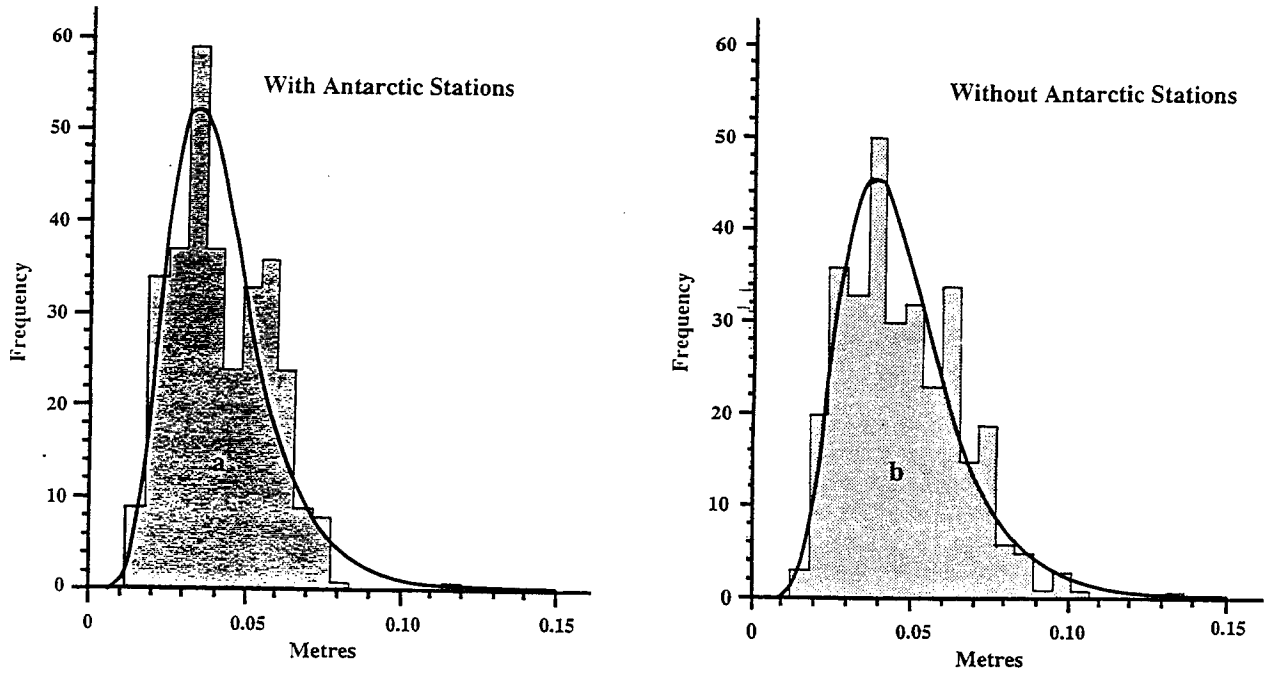

Figure 9.1: Two frequency distribution plots of the formal errors. **A** is the southern hemisphere augmented SIO solution with a mean of 0.0420 m and standard deviation of 0.0170 m. **B** is the standard global SIO solution with a mean of 0.0480 m and standard deviation of 0.0198 m.

9.1.2 Test 2: The distribution of errors for components of the state vector

Figure 9.2 shows box and whisker plots of the pooled X, Y and Z components of the satellite state vector. The box and whisker plots exhibit the log-normal characteristics shown in the previous figure with the distance from the minimum value to the median being, generally, less than the distance from the median value to the maximum value. The reductions are not in the minimum value range, as expected, but in both the median and maximum values. This is due to the nature of the distribution function. The reductions effect all three components more or less equally. The superior nature of the Z component compared to the X and Y components

is not understood. Examination of the standard deviations of the velocity components showed similar patterns.

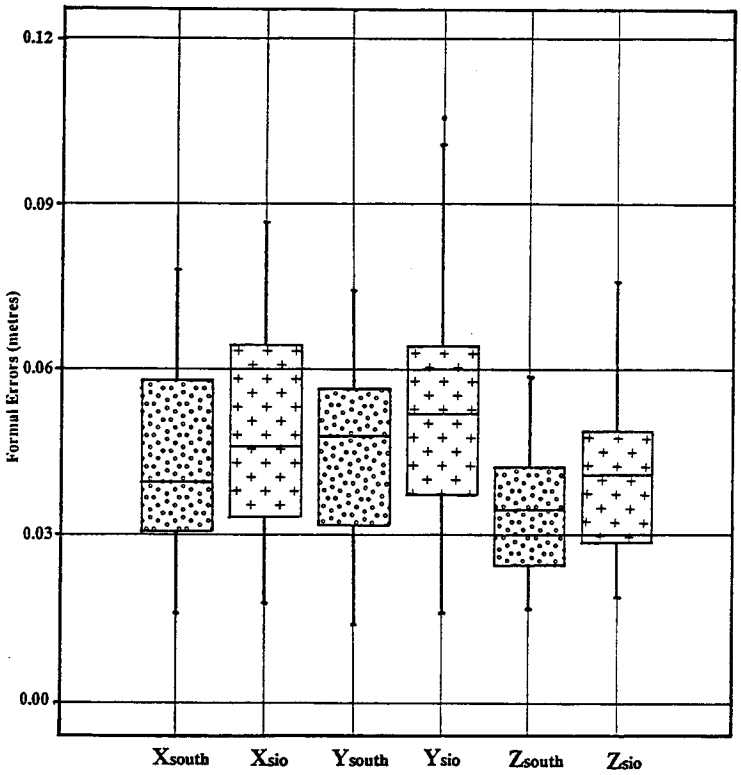

Figure 9.2: A composite box and whisker plot of the distribution of formal errors for the X, Y and Z components of the satellite state vector.

9.1.3 Test 3: The distribution of formal errors by satellite

Figure 9.3 shows a modified box plot of the satellite pooled formal errors. It was shown in figure 9.2 that there was excellent similarity in the X and Y components. The Z component, while smaller, is not dissimilar. Thus, we have pooled the formal errors in the X, Y and Z components of the satellite state vector by satellite number. Only the range of values is shown due to differences in their mean values. Again, it is clearly seen that the augmented network has clearly superior characteristics compared to the standard network.

The figure lists the satellite type and the orbital plane and position that the satellites occupy. There is no systematic trend pertaining to any orbital plane and hence it is concluded that the effect of adding additional tracking data is uniform.

9.1.4 Orbit review

It is clear from the above discussion that additional southern hemisphere tracking improves the quality of the global orbit. Since the quality of this global orbit and its relationship to regional orbits and the reference frame is critical to the methodology adopted in this study, it is also important to consider the effects that these additional tracking stations might have on the reference frame.

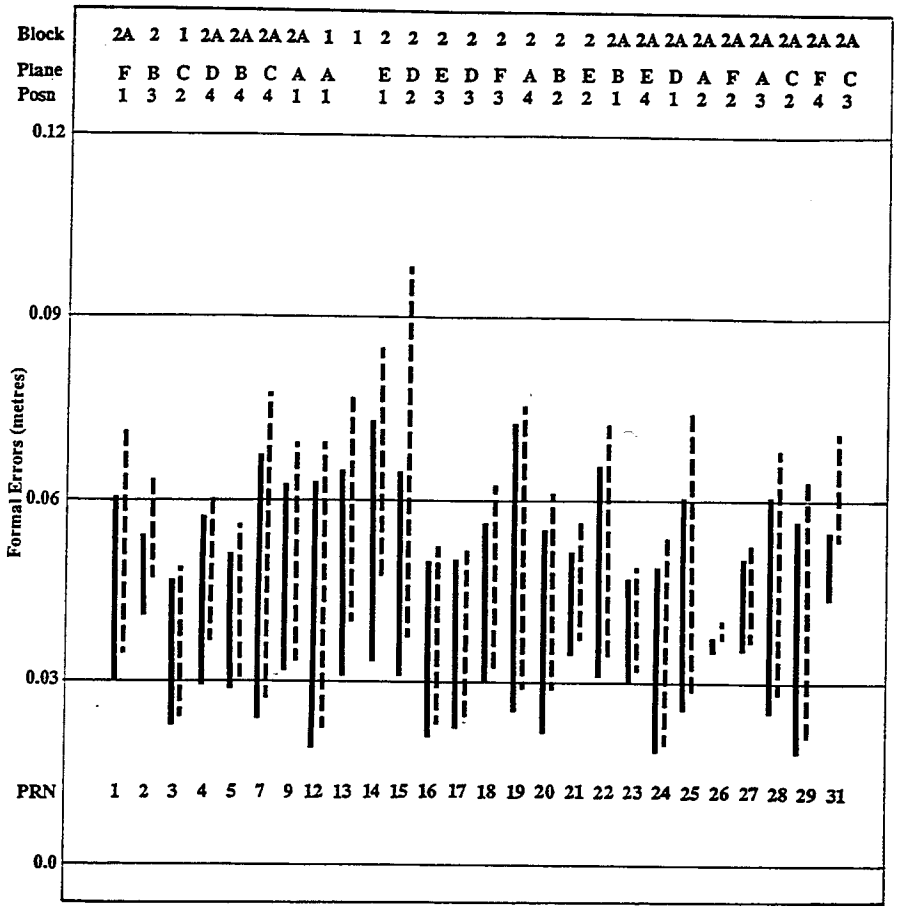

Figure 9.3: A composite box plot pooling the satellite X, Y, and Z formal errors for all four days for each satellite. The solid box is for the augmented southern hemisphere solutions, the dashed boxes refer to the standard SIO solution.

9.2 Southern hemisphere tracking and station coordinates

It is well known that changing the orbit will change the parameters associated with the underlying tracking network. What is more difficult to deduce is the amount of change and whether this change is uniform. The effects are generally thought to be asymmetrical, with a large regional southern hemisphere network being more effected compared to a dense northern hemisphere network. To provide the data for investigating the movement of the tracking network, constrained solutions on a global tracking network were performed. In particular, DS42, SANT, TROM, KOSG, YELL, DS10 and KOKR were constrained to be consistent with ITRF92 - to the one sigma level of 0.05 m in the local north, east, and up solution. The remaining stations were essentially unconstrained with a-priori estimates, in the local system, being set to 9.0 m per component.

9.2.1 Test 1: The effect on IGS northern hemisphere *core* sites

Test stations were chosen at Wetzell, Algonquin and Fairbanks. The corrections to the GAMIT geocentric latitude, longitude and radius for both tracking cases are shown in Figure 9.4. The figure shows small changes in the corrections and the spread or variability of the parameters as

a result of changing the orbit. It is thought that the orbit is well determined for the northern hemisphere. Additionally, each of the stations has other sites around it. In particular, Wetzell has Tromso to the north. In the case of Algonquin, Yellowknife and Tromso are to the north. The conclusion that can be drawn from the test is that increasing the southern hemisphere tracking will have little impact on the northern hemisphere network.

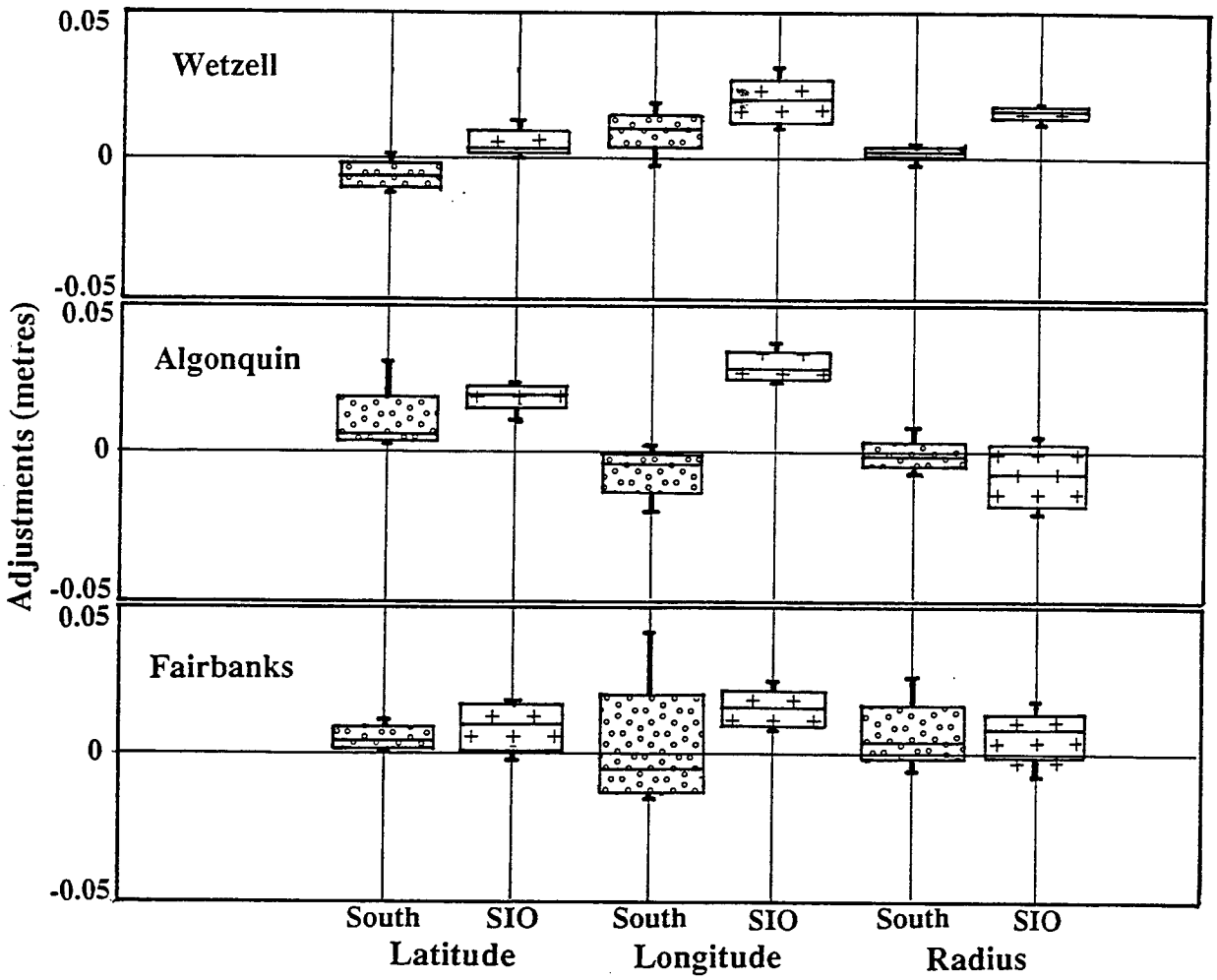

Figure 9.4: Effect of increasing Southern hemisphere tracking on Northern hemisphere stations

9.2.2 Test 2: The effect on Southern hemisphere sites

In evaluating the effect of varying the amount of tracking in the southern hemisphere and the effect on station coordinates, it was not possible to have both constrained and test stations that were IGS *core* stations, as well as being positioned so that these stations were then supported by a more southerly station. Thus, the stations at Hartebeesthoek and Yaragadee, which were previously in a network without tracking to the south, were now included in a network which had more southerly tracking and hence the double difference observable now had a better sky coverage. Hobart was selected as our third station as it had similar geometry, whereas DS42 (Canberra) was supported to the south by Hobart.

The results of intercomparing the two sets of solutions are shown in Figure 9.5. This figure

shows several striking characteristics when compared to Figure 9.4 for the northern hemisphere.

- The scatter associated with the coordinates is very much larger. This is attributed to being directly linked to the number of stations on the northern hemisphere (27) compared to the number of stations (11) in the southern hemisphere for the augmented system.
- The difference between the coordinate parameters for these southern hemisphere sites is much larger than for the northern hemisphere case. Coordinate differences exceed 0.05 m in at least one component for each station.
- The changes in the parameters result from an increase of 8.8% in the number of double difference observables. This change in the number of observations would have been restricted to double differences between the new Antarctic stations and the mid-latitude stations of Yaragadee and Hartebeestoek.

9.2.3 Review

The conclusions that must be drawn from this study include:

1. That our knowledge of the position and precision of IGS *core* stations in the southern hemisphere is inferior to northern hemisphere IGS *core* stations. This lack of precision will unfortunately propagate into the regional coordinates of this study.
2. That there is a variable precision factor in this project due to the upgrading that the global network underwent during the course of this project. This will be difficult to handle. It is expected that as the level of control and tracking approaches that experienced in the northern hemisphere, then the level of variability of these parameters will decrease. However there are extenuating circumstances in the southern hemisphere, such as longer baselines and the necessity to cross the geomagnetic belt.
3. That we can expect the ITRF coordinates of southern hemisphere stations to vary between the annual solutions of the ITRF, with the oscillations or the corrections approaching northern hemisphere levels as stations such as Macquarie, Davis, Casey and Mawson become routine contributors to the IGS.

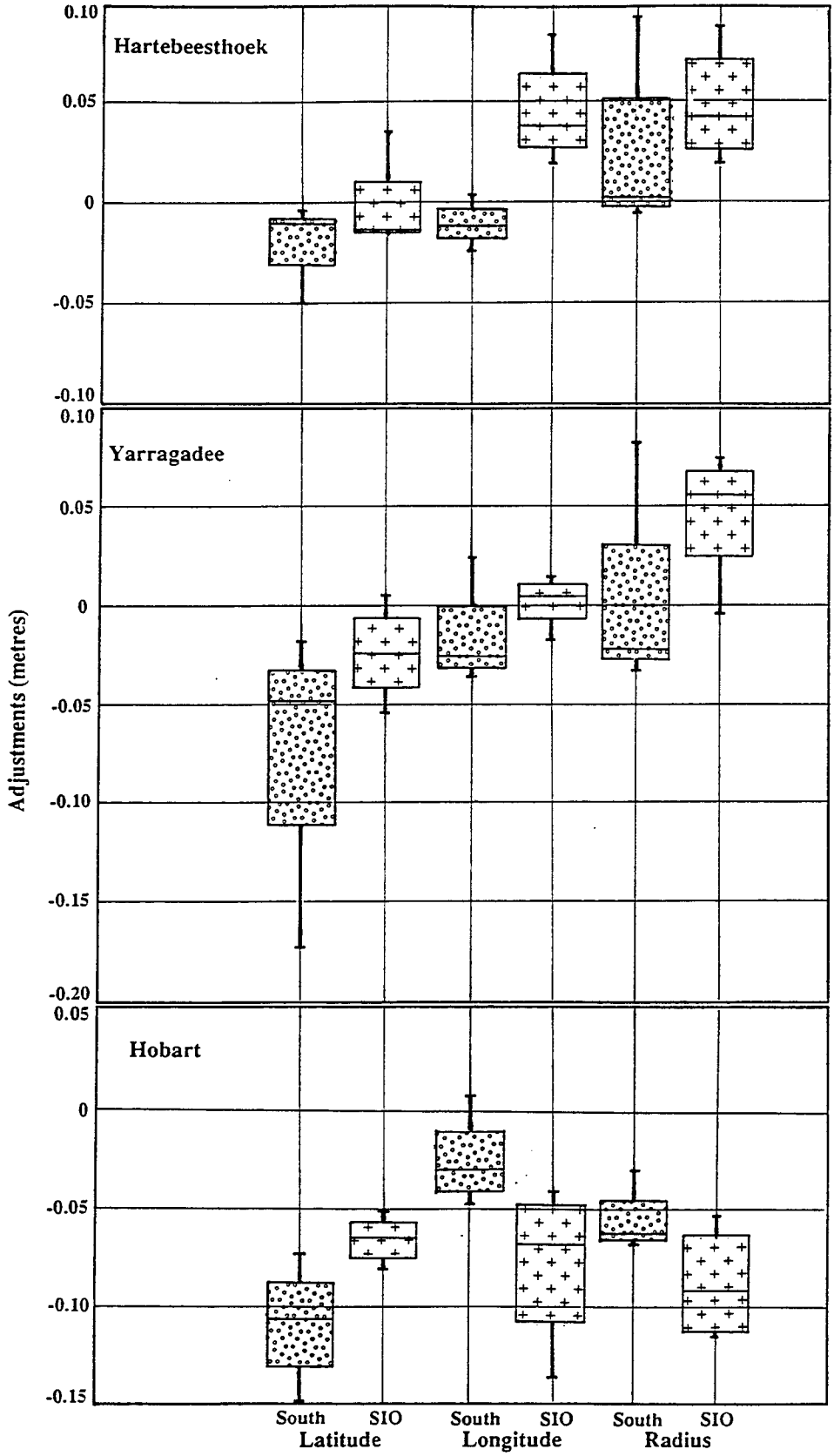

Figure 9.5: Effect of increasing Southern hemisphere tracking on Southern hemisphere stations

Chapter 10

Quality Assurance

Quality assurance (QA) was practiced at a number of levels throughout the processing of the daily files and during the subsequent combination of the daily solutions. This chapter describes the quality assurance steps that preceded the final analysis. It will be seen that there is considerable scope for applying conventional quality assurance procedures for similar size projects in the future using information gathered in this project. In particular, the introduction of QA techniques, such as charting and the monitoring of trends, would assist in understanding variations between daily solutions.

10.1 The Bias Value

It was shown in section 2.1.4 that the double difference observable is especially useful since most of the important frequency terms cancel and there is also complete cancellation of the unknown, but constant, phase difference between the ground receiver clock and the satellite clock. That is, the integer bias term is only contaminated by the noise of the system which includes unmodelled systematic effects. Thus, at first sight, this integer bias parameter appears to be an ideal candidate for quality control as it has known characteristics.

In cleaning the data, particularly for the regional solutions, we adopted the strategy of resolving as many SINCLN-inserted bias flags as we could. In the majority of cases, the double difference time series for a station-satellite combination only had one bias parameter, its initialisation value. The specific methodology adopted to reach this QA level consisted of first cleaning those stations which formed the connections between the higher hierarchical level network and then between stations of the same network level. These network data were used to validate the assignment of uncertain integers. In the case of frequency-doubled L_2 data, half integer values were determined. The remaining stations were then cleaned in a consistent manner against these linking stations. Small, usually less than 20 epoch, segments of data at either the leading or trailing edges of the data run were rejected by unweighting the component that had the lowest elevation. It was usual to check the single difference observation where doubt existed. It is to be noted that the between-station differences (equation 2.2) only cancel out the satellite effects leaving receiver effects to contaminate the phase difference, while the between-satellite differences (equation 2.4) cancel out receiver oscillator errors. This information was used to ascertain whether the problem was a satellite or a receiver problem. In

general, satellite problems affect all receivers. The 'bad' satellite data were generally excluded by unweighting procedures rather than by re-initialisation of the bias flag.

It is important to note that this procedure only resulted in the *bias free* solution. No attempt was made to fix any of the determined biases to integer values, as discussed by Dong and Bock (1989) or Blewitt (1989). This was due to the diverse range of ionospheric conditions that prevailed across the region, the unknown effects of antenna modelling and other station-dependent noise processes, such as multipath and the lack of high quality pseudo-range observations due to the use of squaring receivers. Thus, there can be no expectation that the values of these parameters should be in close proximity to an integer value and hence no quality assurance information can be gleaned from an analysis of these values.

Figure 10.1 is an excerpt from the GAMIT solution for the Australian regional network for day 209 of 1992. Only the non-integer fraction is displayed. It is readily seen that significant noise exists on all baselines from the short 150 metre baseline between two receivers at Hobart, HOBA and TAS1, up to continental-length baselines of 2000 kms between Alice Springs and Darwin. An important observation to note is that most satellite combinations have a consistent pattern, with some cases repeating quite near to an integer value. This could be a valuable observation for bias fixing routines but was not implemented in this study.

10.2 NRMS of the GAMIT Solution

The normalised root mean square, nrms, is a primary solution statistic that was used to ensure quality of each solution. Experience indicates that the normal range for this statistic is between 0.2 and 0.4 for the level of modelling used in these reductions. Lower nrms levels are now common with higher levels of orbit modelling, earth tide modelling and antenna modelling. The a-priori measurement error assigned to the solutions was 10 mm with no distance component. The distance component was purposely set to zero so that this component would not dominate in a solution where long baselines were the rule. Thus values in the above nrms range indicate that the a-priori weighting is loose. Finally, it should be remembered that the nrms value is a scalar.

The above discussion indicates that a sufficient quality assurance procedure has to achieve an nrms value of around 0.3 ± 0.10 for each solution. The nature of the individual perturbations is not well known as the variations can be due to a complex set of interactions between the level of a-priori knowledge and the quality of the data due to its transmission through the ionosphere and troposphere. The SINCLN cleaning algorithm of GAMIT was used for the first level of data cleaning and for resolving data discontinuities. After this step, CVIEW, a manual editing procedure, was used. Several of us participated in this process. It was normal for one operator to be responsible for a level or batch of solutions. It was not feasible to adopt a formal Quality Control approach as might be used in a manufacturing environment due to the variations in the networks, the characteristics of the station location and the GPS instruments used, as well as other undefined parameters. Rather, a rigorous review of the editing was undertaken if nrms values exceeded 0.4 to ensure that potentially damaging observations were excluded.

Figure 10.2 is a plot of nrms for all solutions, except the global SIO solutions. The various networks are identified with unique symbols. It is clear that there are no systematic trends in the figure either between the networks, which would indicate an operator-dependent bias, or as

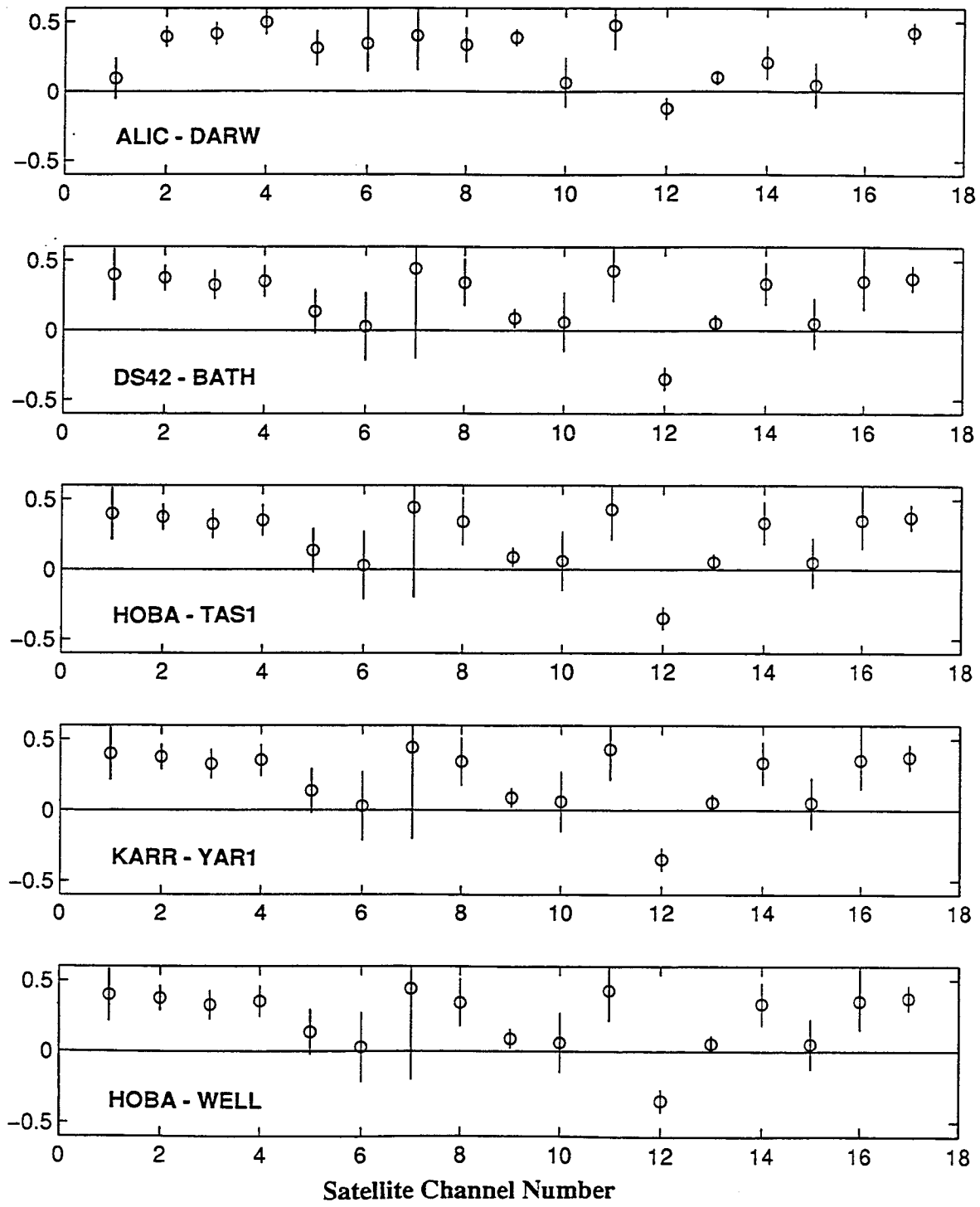

Figure 10.1: Excerpt of L_1 biases from the bias-free solution for the ARN network for day 208 of 1992. The non-integer bias values are plotted, with their formal standard deviations, relative to the nearest integer.

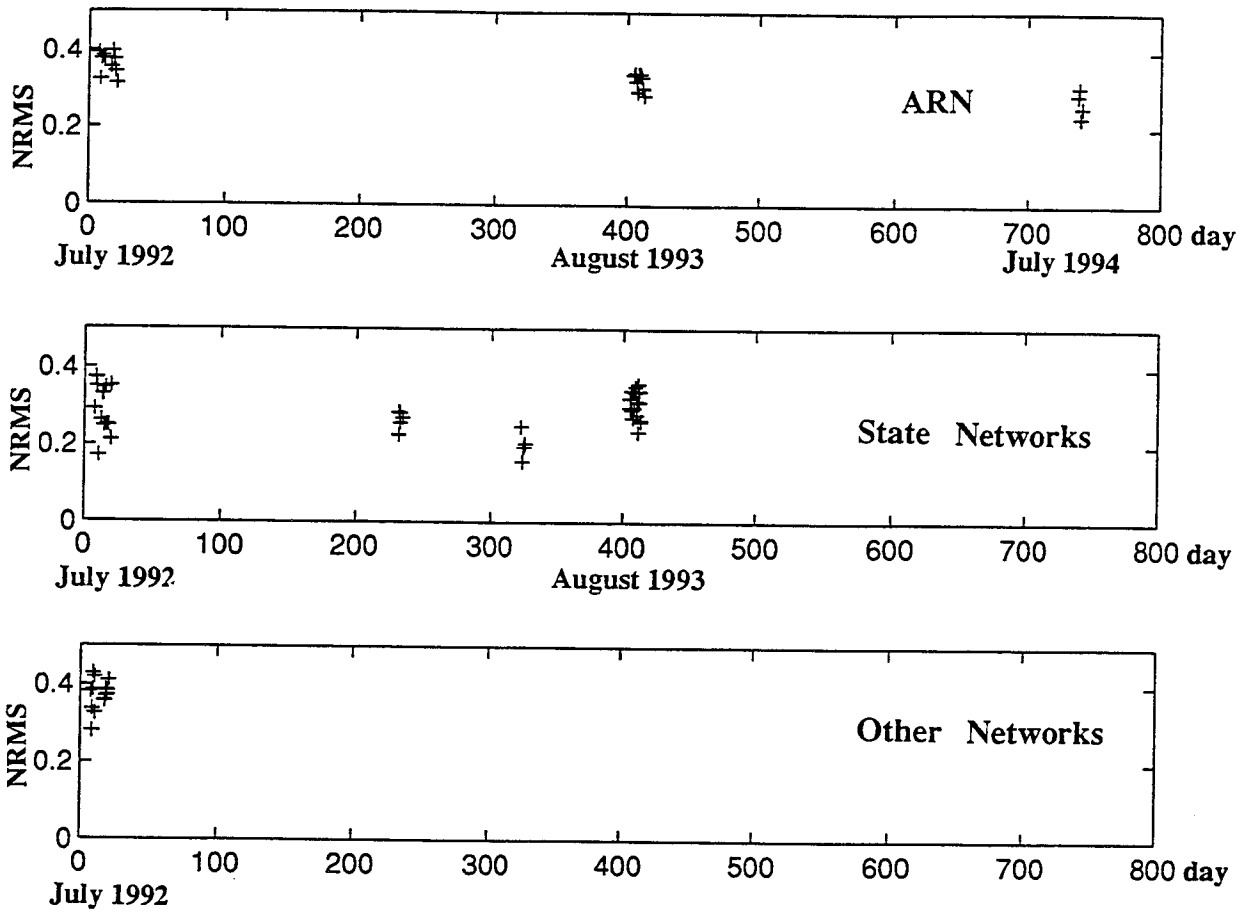

Figure 10.2: Plot of nrms values of solutions as a function of time. The top panel is for the ARN or level two solutions. The middle panel is for the state networks and other level three solutions. The bottom panel is for other solutions, mainly level 2 types, such as the DORIS network. The time axis is with reference to day 200 of 1992.

a function of time, which would indicate procedural changes or the development of increased competency.

10.3 The Formal Uncertainties

The formal uncertainties of both the station coordinates and the satellite orbital parameters are also indicators of the quality of the solution. In this case, the strength of the network plays an important role in limiting the value of these uncertainties. Thus, it is not surprising that weaker networks, such as the DORIS and WING networks, have higher values for these indicators of control.

The value of the formal uncertainities is also tied to the levels of constraint used in the solution. It is considered important for each solution to exceed the level of the a-priori constraint, thereby indicating that the solution has sufficient power to adjust to a true observation-

Table 10.1: Extract of GAMIT formal uncertainties for unconstrained stations. The solution is for the ARN network for day 208 of 1992. All quantities are in metres at the 1 σ level.

Station	Latitude	Longitude	Radius
Alice Springs	0.026	0.031	0.047
Bathurst	0.024	0.030	0.048
Karratha	0.028	0.039	0.048
Hobart AFN	0.025	0.031	0.048
Hobart Cignet	0.025	0.032	0.048

controlled, least squares solution.

Station constraints were generally applied as follows:

- latitude: 0.1 m
- longitude: 0.1 m
- radius or height: 0.2 m

Orbital constraints were generally applied conservatively with the six Keplerian elements constrained to 20 parts per million and a 10% value for the non-gravitational force parameters.

Solutions that did not have formal errors below the a-priori levels were reviewed. In the majority of cases, such flagged solutions also indicated abnormal nrms values. Tables 10.1 and 10.2 are extracts from the Australian Regional solution for day 208 of 1992. The first table shows typical formal errors for the unconstrained stations, while the second table deals with the satellite state vector. These values indicate that the network solution has the necessary power to adjust to a solution without the need for constraints. Note that the solutions carried forward to the GLOBK process are 'relaxed' solutions in which the constraints are considerably relaxed so that distortion, caused by incompatible or overconstrained values, is eliminated.

Table 10.2: Extract of GAMIT formal uncertainties for the satellite state vector. The solution is for the ARN network for day 208 of 1992.

PRN	X	Y	Z	$\dot{X}$	$\dot{Y}$	$\dot{Z}$	*Rad*1	*Rad*2	*Rad*3
	(metres)			(m/s)					
3	0.515	1.319	0.324	0.0001	0.0001	0.0001	0.056	0.0001	0.0001
11	0.478	0.328	0.511	0.0001	0.0001	0.0001	0.007	0.0001	0.0001
14	0.738	0.766	0.689	0.0001	0.0001	0.0001	0.036	0.0001	0.0001
19	0.509	1.711	0.260	0.0001	0.0001	0.0001	0.308	0.0001	0.0001

10.4 The Qcut Process

All daily GAMIT solutions were performed with the same a-priori constraints (see Appendix C) and the same initial starting coordinate values. Hence another indicator of the quality of the analysis process is the quality and repeatability of derived parameters, such as station coordinates and baselines. Baselines, especially their lengths, are often used to check quality as the length is invariant when rotation errors are present. However, it was felt that it was more instructive to monitor parameters that could be contaminated by rotational errors even if these could be minimised later.The most obvious candidate parameter is the adjustment to a-priori station coordinates. All solutions were therefore performed from a constant a-priori set of coordinates and the corrections to these a-priori values were examined as a means of quality assessment.

Table 10.3 is the output of the program which extracts the corrections to a-priori coordinates from the GAMIT *Q-files*. Mean values and standard deviations are also computed. All values are given in metres. These values indicate that there is a high level of repeatability and consistency for station coordinates in the Australian Regional Network for the 1992 period.

Clearly this process of quality checking could not be performed until a significant proportion of the network was reduced and as such the tool is of limited use until the full network is implemented and the variation relative to a reliable mean value assessed. In general, experience with these tables indicated that no unexpected problems with the network are likely to be indicated by the GLOBK process when station variability is less than 0.1 m. Again it is to be stressed that the input to GLOBK is a 'relaxed' solution and as such the corrections will take different values to that indicated in these outputs. Nevertheless, it is seen that raw station variability is generally only a few centimetres in all three components. Daily solutions that indicated a larger than expected variation in the Qcut table were reviewed by looking at the formal errors of the station and the number of double differences associated with the station in order to understand the variation. This procedure was instrumental in augmenting the DORIS network with the KOKE station, this latter station providing additional double difference observables to stations in central and North America.

10.5 The GLOBK χ^2/f Statistic

The final quality assurance statistic that was routinely generated was the GLOBK χ^2/f statistic that GLOBK outputs when it combines networks. A GLOBK analysis was performed at the conclusion of processing each network, i.e., after performing and evaluating the Qcut data. Thus, the overall consistency of the network was checked at this point. It is to be stressed that the relationship of the individual network to other networks was not checked at this stage.

The χ^2/f statistic is a measure of the consistency of the new, loosely-constrained GAMIT solution to GLOBK's knowledge of the parameters being introduced. Ideally, this statistic should be unity. Experience indicates that the χ^2/f statistic is usually less than 4, with most values under 2 for the GLOBK runs associated with the the same network. χ^2/f values larger than 10 generally indicates that there is distortion and strain between one of the introduced parameters and GLOBK's current knowledge of that parameter. Table 10.4 gives the values of the χ^2/f statistic for all of the networks used in this analysis.

Table 10.3: An extract from Qcut when run on the ARN92 Campaign. The residuals, relative to the mean for the days observed, are shown in millimetres along with the standard deviation.

SITE	207	208	209	211	216	217	218	219	220	MEAN	S.D.
ALIC ϕ	13	8	-11	-34	-12	0	-11	22	25	25	18
ALIC λ	0	-25	-13	104	-22	-1	20	-22	-39	40	42
ALIC rad	-121	-200	-47	78	173	118	85	-32	-54	33	121
COCO ϕ	87	63	10	-128	-79	-41	-45	49	85	-2	77
COCO λ	-47	-125	55	-16	66	26	54	15	-27	-63	61
COCO rad	18	-136	8	-58	21	155	72	-64	-16	-217	84
DARW ϕ	25	51	-2	-49	-41	-12	-10	38		-68	35
DARW λ	25	-19	-13	56	-24	-28	23	-20		-487	30
DARW rad	-94	-198	-20	2	111	154	77	-32		413	114
DS42 ϕ	-4	-29	-28	38	10	26	-13	14	-14	48	23
DS42 λ	14	8	-24	99	-27	-12	-39	-10	-7	-93	40
DS42 rad	-60	-187	-56	186	67	63	76	12	-101	241	112
HOBA ϕ	-6	-50	-32	78	22	29	-6	6	-41	59	39
HOBA λ	4	-7	-43	123	-8	4	-42	-18	-13	3	49
HOBA rad	-94	-163	-73	212	66	62	130	-9	-132	95	126
KARR ϕ	38	29	6	-73	-36	-22	-18	29	47	11	40
KARR λ	-20	-68	3	98	68	26	16	-37	-84	62	59
KARR rad	-72	-176	3	7	53	119	114	-16	-31	-137	91
ORRO ϕ	-4	-29	-29	42	6	24	-11	14	-12	53	23
ORRO λ	14	14	-24	90	-26	-13	-37	-11	-8	-4	38
ORRO rad	-64	-172	-67	184	80	53	91	-2	-103	77	112
TAS1 ϕ	-2	-49	-32	78	21	26	-7	5	-40	53	39
TAS1 λ	-19	-2	-40	123	-1	8	-45	-14	-9	-67	49
TAS1 rad	-82	-146	-54	195	92	33	108	-4	-142	360	117
TOWA ϕ	8	17	-25	-26	-29	11	-10	22	33	3	23
TOWA λ	33	6	-44	69	-26	-31	11	-3	-13	-4	35
TOWA rad	-98	-198	-41	96	125	113	71	-15	-52	173	109
WELL ϕ	-10	-23	-60	89	23	28	-42	14	-20	13	44
WELL λ	10	77	16	-69	-76	-46	-46	19	116	-201	66
WELL rad	-85	-185	-104	234	96	63	89	24	-131	536	135
YAR1 ϕ	26	-5	6		-32	-21	-14	11	31	26	22
YAR1 λ	-47	-76	6		82	59	57	-5	-75	143	62
YAR1 rad	-116	-176	12		134	88	138	-28	-53	335	115

Table 10.4: The Chi squared statistic for the individual networks before joining

Network	1	2	3	4	5	6	7	8	9	10
SIO92	0.200	0.853	1.047	1.525	2.609	1.727	1.087	1.467	1.636	2.710
ARN92	0.414	1.484	2.191	3.269	2.709	3.079	2.697	2.887	1.905	1.162
NSW/QLD	0.271	1.213	0.656	0.921	0.921	0.349	1.311	0.218	1.258	1.725
TIDE	0.513	1.341	3.023	2.319						
DORIS	0.031	0.798	1.306	1.469	2.453	2.954				
WING	0.134	1.646	4.332							
QLD93	0.008	0.014	0.079	0.044						
SIO93	0.193	0.802	0.851	1.722	1.558	1.835	0.989	1.644	0.744	
ARN93	1.881	1.794	1.979	1.074	3.057	1.411	1.425	12.765	1.348	
SAT93	0.103	0.207	0.172							
NTQ93				0.282	0.190	0.120				
WAT93							0.146	0.516	0.145	
PNG93	0.191	0.089	0.321	0.749	0.124	0.240	0.091	0.198	0.373	
ARN94	2.706	2.706	2.443	2.110						

Chapter 11

Selective Availability & Anti-Spoofing Days

A major tracking perturbation occurred on day 214 and 215 of 1992 when, for the first time, anti-spoofing was initiated on the fourteen Block 2 and 2A satellites in the 18 strong constellation.

This change to the emitted signals caused severe disruption to global and regional tracking networks as almost all full P-code receivers failed to track correctly or consistently after the change. The constellation reverted to its normal signal structure on day 216.

Table 11.1 lists the status of the constellation during this period. Both Selective Availability and Anti-Spoofing are not implemented on Block 1 satellites.

Table 11.1: GPS Constellation during the IGS 1992 Epoch Campaign.

Satellite PRN	2	3	11	12	13	14	15	16	17	18	19	20	21	23	24	25	26	28
Block Type	2	1	1	1	1	2	2	2	2	2	2	2	2	2A	2A	2A	2A	2A

11.1 Selective Availability

The effect of Selective Availability is fully treated by Feigl (1991a; 1991b). The treatment by Hoffmann-Wellenhof et al. (1994) is based on the treatment of Feigl.

Selective Availability was initially implemented on 25 March, 1990 and has remained in force since that time with various levels of activation. Selective Availability is composed of two processes. The first or δ-process involves the dithering of the satellite clock. The second or ϵ-process involves the truncation of the ephemeris. Thus, the first effect is a high frequency phenomenon effecting all clock functions including the correct estimation of pseudo-ranges derived from the C/A PRN code. The second process effects the position of the satellite.

Clearly in those cases where an external orbit is to be used, this is of no real concern. However, the dithering of the oscillator's basic frequency means that the constants a and b of equation 2.1 are not constant. Furthermore, because stations at opposing ends of large continental baselines, of the order of 3000 km or larger, do not receive the signal at the same instant that it leaves the satellite, the clock contribution is not cancelled. This time difference, 10 milliseconds in the above example, approximately translates to 0.02 cycles or 4 mm if the dithering was ± 2 Hz as normally experienced (Feigel, 1991). This perturbation is a considerable proportion of the rms error budget reported in Section 7.1. Clearly, increasing the level of the perturbation would effect the solutions.

It was not possible to implement any of the standard procedures for minimizing the effect of selective availability as all sites with acceptable, high performance clocks had switched to full P-code receivers. Thus, the effect of selective availability was assumed to be constant at the normal levels of 2 Hz during the anti-spoofing days. Increases in the level of SA would be expected to degrade the results.

11.2 Anti-Spoofing

In a similar manner to selective availability, anti-spoofing is restricted to Block 2 and later satellites. It is dissimilar to selective availability in that it is a binary effect. There are no levels of implementation. There are however different levels of overcoming the the effect and these procedures may have their own 'side effects'.

An important key to understanding anti-spoofing is that code-correlation is used in several steps of the signal processing cycle. The PRN signal needs to be removed before the Doppler-shifted carrier is used to determine the phase measurements. Normally, the coarse C/A code is used, partly because it repeats every millisecond and partly due to the simplicity of implementation. This allows the L_1 frequency to be reconstructed. The process also produces a HOW word in each subframe which is used to position the commencement of the search in the P-code for signal matching.

The encryption of the P-code (more correctly, the Y-code) denied the receivers the essential cross correlation information. All instrument manufacturers were aware of this point. However, receiver firmware was not either able to recognise the change or had to be manually initiated.

This brings the discussion to the four main methods of handling encrypted Y-code signals. A full treatment is given by Ashajee and Lorentz (1992). The treatment by Hoffmann-Wellenhof et al. (1994) is excellent and sufficient for most GPS practitioners.

1. **Squaring.** This technique is the traditional technique implemented in Trimble SST and early Ashtech instruments. The method really does not handle the Y-code at all as it is independent of the PRN code. It allows only the recovery of L_2 phase information. The signal-to-noise ratio is substantially reduced in the squaring process making for an increased number of signal dropouts due to low strength or rapidly varying signals.
2. **Cross correlation.** This technique uses the dispersive delay between the L_1 and L_2 signals due to the ionosphere. Thus, there is a delay between the Y-codes. The delay on the L_2 signal is adjusted to correlate the Y-codes. The technique allows

for both pseudo-ranges and phase observations to be determined. While the signal-to-noise ratio is better than for the squaring technique, it is still substantially lower than for the standard technique, leading to many gaps in the observational series.

3. **Code correlation plus squaring.** This technique uses two important aspects of the Y-code. The first is that the encryption algorithm uses a modulo-2 function of the sum of the P-code and the W-code. The second is that the chipping rate of the W-code is almost 20 times slower than that associated with the Y-code. A correlation is performed and the output then squared to remove the unwanted code. Both pseudo-range and phase observables are determined. The signal-to-noise ratio is improved some 13 db compared to the cross correlation method.
4. **Z-tracking Technique.** This technique, employed on the newer Ashtechs, correlates the Y-code on the L_1 and L_2 signals separately with a locally-generated replica of the P-code, enabling the W-code to be eliminated by low pass filtering. It is to be noted that the W-code is primarily a synchronization code and as such does not contain information. The technique enables pseudo-ranges and phase to be recovered with an improvement of 3 db over the code correlation and squaring techniques. There is still an overall reduction in signal-to-noise ratio of 14 db, compared with pure cross correlation.

Since the networks in Australia, New Zealand and Papua New Guinea were heavily reliant on codeless receivers (Trimble and Ashtech), it was felt that the effect of anti-spoofing should be minimal and hence those regional sites that were observed on these days could be successfully reduced using a locally-generated orbit.

Table 11.2: Qcut variations in corrections to a-priori positions for the ARN network during 1992.

	Day207	Day208	Day209	Day210	Day212	Day213	Day214	Day215
BATH GEOC LAT (DMS)	-0.0269	0.0002	0.0049	0.0246	0.0131	0.0052	-0.1692	0.0536
BATH LONG (DMS)	0.3910	0.0003	-0.0473	-0.0346	0.0382	0.0364	0.0780	-0.0713
BATH RADIUS (KM)	0.0501	-0.0003	-0.0354	0.0528	0.0597	0.1166	1.1269	0.1441
DILL GEOC LAT (DMS)					-0.2603	-0.7687	-0.3328	
DILL LONG (DMS)						-0.0619	0.0276	-0.2375
DILL RADIUS (KM)						0.2325	1.2029	0.4525
HOWI GEOC LAT (DMS)					0.1578	0.1452	-0.2512	
HOWI LONG (DMS)					0.2713	0.2640	0.2521	
HOWI RADIUS (KM)					0.3024	0.4746	1.5015	

Table 11.2 shows the variations in coordinates as given by the QCUT procedure of Section 10.4. The variations in adjustments shown in this table, for sites such as Bathurst, should be compared to Table 10.3. In general, it was the height component that showed the greatest variation. This unexpected variation was the subject of further investigation.

Firstly, we tried to control the variation by adjusting the weights that we applied to the GAMIT solution. The weights and their effects for day 214 ars shown in Table 11.3. The results of this table appear to be counter-intuitive to the use of constraints in that a minimum discrepency is reached when moderate levels of constraints are applied at Townsville and

Table 11.3: Adjustment corrections for Day 214 as a function of the level of constraint applied to Townsville and Wellington. The constraints are expressed in cm.

Label (units) Constraints (cm)	A-priori	Adjust (m)	Loose 5,5,20	Moderate 1,1,7.5	Tight 1,1,5	Absolute 0.1,0.1,0.5
BATH GEOC LAT (DMS)	S33:15:10.76023	0.0415	-0.1692	-0.0287	-0.0307	-0.0332
BATH LONG (DMS)	E149:34:01.44980	-0.0920	0.0780	-0.1011	-0.1155	-0.1356
BATH RADIUS (KM)	6372.4414469000	0.1885	1.1269	0.0667	-0.0286	-0.3232
KARR GEOC LAT (DMS)	S20:51:11.14840	0.0494	-0.4510	0.0023	0.0255	0.0749
KARR LONG (DMS)	E117:05:49.85713	0.0419	0.3814	-0.2296	-0.2583	-0.2017
KARR RADIUS (KM)	6375.5250595000	-0.2095	0.4637	-0.3735	-0.4580	-0.7171
ORRO GEOC LAT (DMS)	S35:27:15.91494	0.0487	-0.1401	-0.0398	-0.0440	-0.0480
ORRO LONG (DMS)	E148:56:22.03817	0.0098	0.1964	-0.0028	-0.0196	-0.0434
ORRO RADIUS (KM)	6372.2745443000	0.0127	0.9449	-0.1189	-0.2147	-0.5170
TOWN GEOC LAT (DMS)	S19:08:25.05604	-0.0071	-0.4041	-0.0068	0.0051	0.0009
TOWN LONG (DMS)	E146:48:50.81090	0.1075	0.1817	0.0004	-0.0065	-0.0005
TOWN RADIUS (KM)	6375.9255519000	0.3156	1.2947	0.3149	0.2266	0.0056
WELL GEOC LAT (DMS)	S41:05:03.04484	0.0035	-0.0254	-0.0061	-0.0146	-0.0008
WELL LONG (DMS)	E174:46:58.61683	-0.1917	-0.2860	-0.0007	0.0103	0.0008
WELL RADIUS (KM)	6368.9131280000	0.4512	1.5028	0.4686	0.3712	0.0134
XMAS GEOC LAT (DMS)	S10:22:52.24786	0.0788	-0.5287	0.1000	0.1359	0.2057
XMAS LONG (DMS)	E105:41:22.58414	0.1542	0.4056	-0.2774	-0.2979	-0.1351
XMAS RADIUS (KM)	6377.7002823000	-0.3108	0.1757	-0.4610	-0.5397	-0.7979

Wellington. The systematic movement of the corrections, from one range to a new range as the station constraint variance is reduced, is indicative of constraining the solution to incorrect values. This effect was also confirmed in the second anti-spoofing day, day215.

After some testing, the moderate level of constraints were chosen as being most representative, as these contraints produced corrections that were in closer agreement with the non-AS days than the other levels. A GLOBK run was then run on all the ARN network for all days between 207 and 220 as described in Section 10.5. The χ^2/f statistic is plotted in Figure 11.1. The figure is to be compared to the values given in Table 10.4 where all values are less than 5 for this network. This clearly indicated that the anti-spoofing reductions (days 214 and 215) were dissimilar to those other daily solutions and that a large amount of contamination was present in the network. The 1 metre height errors, noted in the preceding tables at Bathurst and other sites, are clearly incompatible with those values determined from the earlier days. This is a clear demonstration of the sensitivity of the χ^2/f statistic to errors and strain in the networks being adjusted.

In an effort to reduce this contamination, satellites were identified that might be performing at a lower level than others in the constellation. This was done by comparing the size of the corrections to the a-priori broadcast orbit and the uncertainities associated with these corrections. Satellites 2, 24 and 28 were deemed to be the poorest performing satellites and were subsequently excluded from the GAMIT solutions. We applied the moderate level of constraints and repeated the process. The GLOBK χ^2/f statistic values were not changed significantly because GLOBK requires a weakly-constrained input, not a moderately-constrained input, and

so there was no benefit derived from the constraints. The only benefit was the exclusion of the three poorest performing satellites.

This knowledge, that many of the satellites were performing poorly and that positions and baselines were perturbed from their more normal values, pointed to effects other than anti-spoofing in the data. In particular, it points to the presence of high levels of selective availability. Since this effect could not be controlled, the data for days 214 and 215 were excluded from the solutions. This exclusion necessitated the use of the small 1994 campaign to determine some of the points that were only observed during the implementation of anti-spoofing.

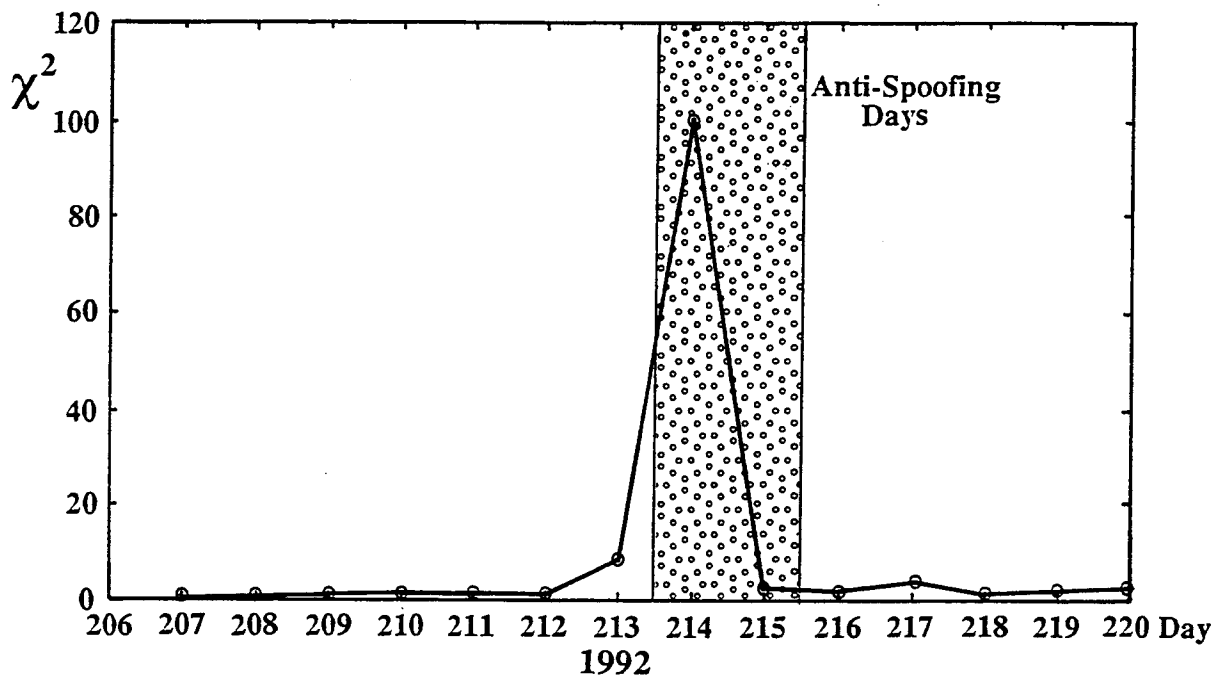

Figure 11.1: The χ^2/f statistic as deduced for the ARN network when the network included data from the anti-spoofing days of 1992.

Chapter 12

The Australian Baseline Sea Level Monitoring Array

As part of Australia's contribution to the Climate Change program, The Department of Sport and Environment (DEST) has funded the National Tidal Facility (NTF) at Flinders University, Adelaide, to install and operate an array of high precision acoustic tide gauges around the Australian coast. This array, The Australian Baseline Sea Level Monitoring Array (ABSLMA), is depicted in Figure 12.1 along with three other gauges of the same type and operated to the same specifications as the national array. Since 1995, gauges at Port Stanvac, Lorne and Burnie have been added to the ABSLMA.

In order to provide geodetic monitoring at the tide gauge sites for the Sea-level program, AUSLIG, with participation from ICSM and the University of Tasmania, arranged GPS observations at each of the principal inland stations associated with each tide gauge to be taken simultaneously with the epoch component of the IGS 1992 campaign and the observation of the AFN network. These observations are known as the Tide network and span days 207 through 210 of 1992. Supplementary and supporting observations, to connect these inland stations to coastal sites closer to the tide gauge, are described in the following sections.

The principal outcome required from these data was a high precision, single epoch solution of the positions of both the inland and coastal marks for the purpose of providing epoch information on the variability of the ground marks used to reference the tide gauge observation. Because of this need, an independent solution to the multi-epoch solution was performed. This solution, in contrast to other solutions, only uses two layers and the days spanning observations at the inland marks. The connection between the global network, used to relate to the ITRF reference frame, and the tide gauge network was provided by incorporating DS42 (Tidbinbilla), Yaragadee and Darwin GPS observations into the tide network. These three stations also appeared in the global solutions performed at the Scripps Institute of Oceanography (SIO) and hence the tide network can be placed in an absolute reference system using three control points that are well distributed. Figure 12.2 shows the hierarchical relationship between the global network and the tide network.

AUSLIG's concept for the control of the tide gauge stations was based on the inland and coastal concept, as developed at the Woods Hole meeting in 1989 (Carter et al., 1989). This concept required the principal mark to be some 10 to 12 kilometres inland, preferably in solid

rock. It is this mark, the *inland* mark, that carries the name of the tide gauge site. The *coastal* mark(s) is used to provide a connection between the tide gauge itself and the inland mark. The connection and use of these coastal stations has been the subject of intense debate and scrutiny, see for example, Morgan (1994). In this reported work, the connections have been performed using the highest quality, global orbit. In all cases, a global tracking network of at least 25 stations using full P-code, permanently operating receivers were analysed to determine the global orbit. Additionally, at least 9 of the IGS *core* stations participated in each of the reductions. In those cases where the connections were coincident with IGS campaigns, the SIO standard product was used. In other situations, orbit computations were done with the same models and procedures as used in computing the standard product. This orbit was then held fixed for the computation of the offset between the inland mark and the coastal mark. All other aspects of the processing and models were as routinely adopted, except that the value of the inland site was also held fixed.

The Tide network is a mixed receiver/antenna network involving most of the common receiver and antenna combinations. The correct manner of handling networks of different receivers and antennae is one of the current unresolved issues in GPS. Many groups avoid the

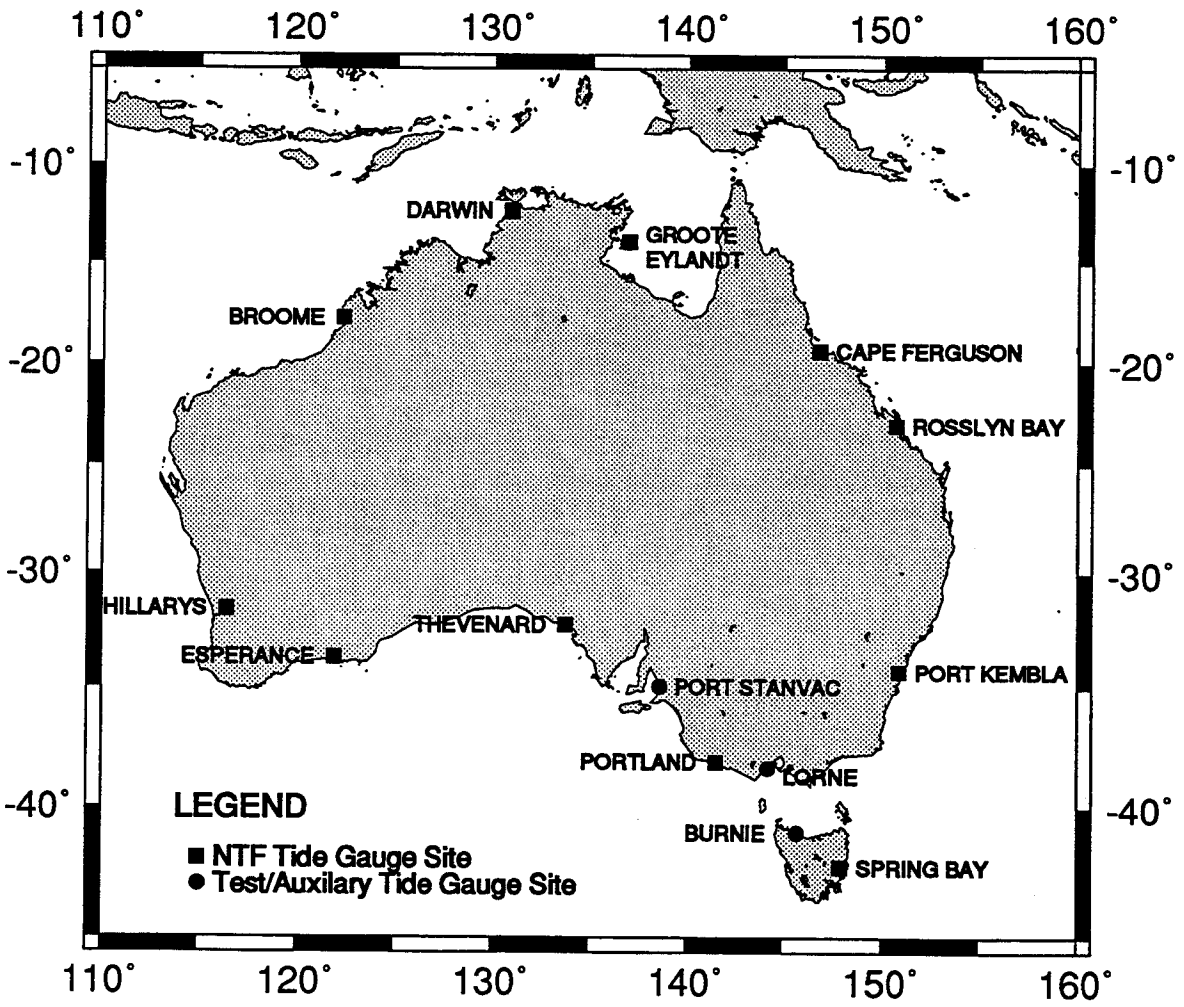

Figure 12.1: Locations of high precision acoustic tide gauges around the Australian coast

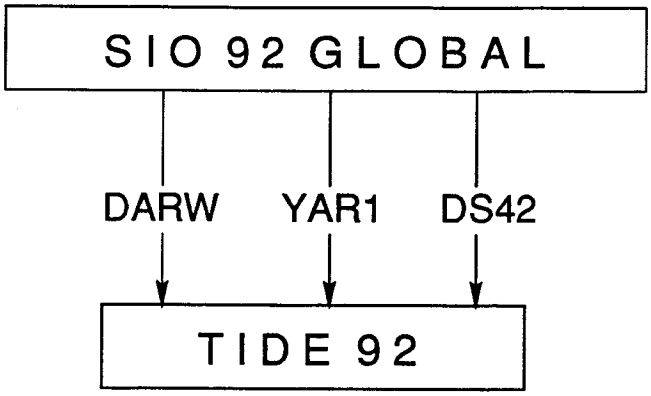

Figure 12.2: Structure and connections between the global SIO network and the regional Tide Gauge Network

problem, or the major part of the problem, by only using receivers and especially antennae of the same brand. The problem is well described by Schupler and Clark (1991). The problem has been recently studied and reviewed by Jaldehag (1995) who detected signal scattering effects that were elevation dependent.

Table 12.1 list the changes in the location of the vertical reference point when antenna modelling is used. The exact value of the correction is still unresolved. Furthermore, it is well known that the GPS network has a small, but detectable, scale difference relative to both the SLR and VLBI networks when antenna phase centre modelling is used. For these reasons, most analysis groups do not implement or consider these corrections.

Table 12.1: Expected changes in height due to antenna phase centre modelling for the *LC* observable. All corrections are in mm.

Antenna Type	Correction for *LC* Observable
TI4000	About 15
Trimble 4000 SST	About 15
Trimble 4000 SSE	Not yet determined
Trimble 4000 SLD	Not determined
Trimble 4000 SDX	Not determined
Ashtec XII	Between -20 and -50
All Dorn-Margolin (Choke)	Between -20 and -30
All Leicas	Not yet determined
Mini-Mac 2816AT	Between 30 and 60

The following modelling issues were considered in computing the Tide Gauge Network:

- **Tides**: Only the major solid body tide was modelled in the solutions. The K_1 frequency correction, the pole tide and the ocean loading effect, (Morgan, 1994) were not implemented. The main reason for not including these few centimetre effect terms was consistency of the reduction process as these terms were only introduced into GAMIT in late 1993 and became part of GAMIT in the early 1994 versions. (The K_1 frequency correction is now part of the standard model invoked in GAMIT).

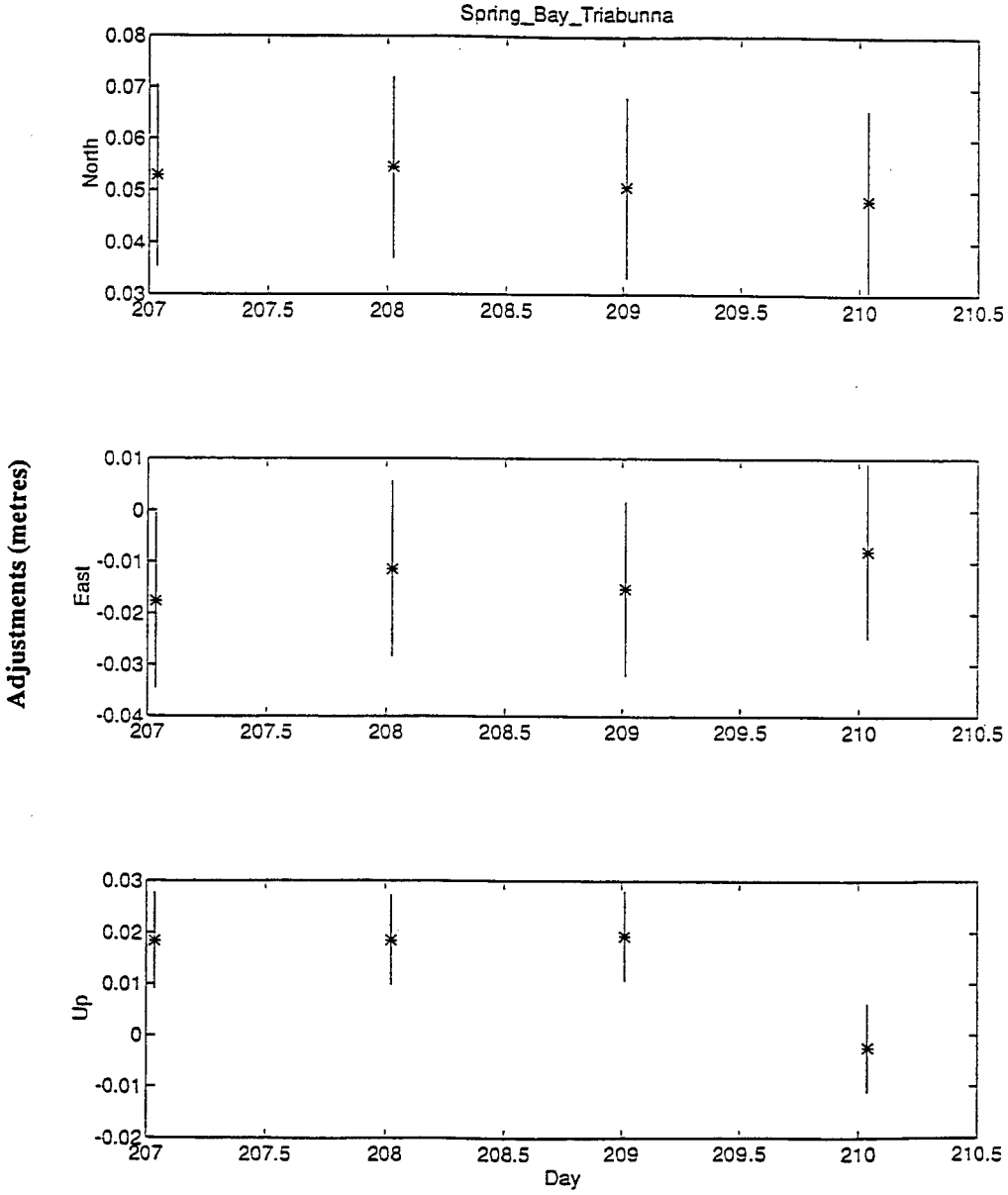

Figure 12.3: Daily repeatability plots for local North, East and Up components of Triabunna during the 1992 Tide campaign.

It must be noted that GPS coordinates are referred to the non-tidal crust, that is, the time-varying as well as the permanent solid tide effects are removed. On the other hand, most sea-level studies use the concept of a mean crust. It is normal to transform from the non-tidal crust to the mean crust for sea-level studies. This is usually done using the work of Ekman (1989). The modified form of the corrected height differences for the southern hemisphere is

$$\Delta h'_{gps} = \Delta h_{gps} + 0.296\, h(\sin^2 \phi_s - \sin^2 \phi_n) \tag{12.1}$$

where
h is the Love number, $h = 0.62$,
ϕ_n and ϕ_s are the latitudes of the station pairs,
Δh_{gps} are GPS height differences between the northern (ϕ_n) and southern (ϕ_s) stations.

- **Antenna Modelling**: No antenna modelling was applied. The main reasons for not applying antenna modelling have been discussed above. Additionally, it is to be noted that antenna modelling, as currently published, did not become part of the modelling options available in GAMIT until early 1994. Recomputation of these data, especially the associated global orbits, was not considered necessary for this analysis.

- **Atmospheric Modelling**: Only a single 24 hour atmospheric delay correction was estimated. Again, a more detailed estimation process, such as the 13 stochastic estimates per day, are now routinely done in GAMIT. However, this was not possible in the GAMIT suite until early 1994. The Saastamoinen *dry* model (Saastamoinen, 1972) was used together with the CfA-2.2 mapping function (Davis et al., 1985).

- **Reference System**: It should be stressed that the coordinates given in the following tables are in the ITRF92 reference system at an epoch of 1992.67, except at Groote Eylandt where the epoch is 1993.57 as Groote Eylandt was observed separately. The coordinates of Tidbinbilla and Yaragadee, which appear in both the global SIO set and the regional Tide Gauge set, were held fixed to their ITRF values at the epoch of 1992.67. Additional stations that were held fixed are listed in Table 13.1. This solution refers to a different epoch but is also much less rigidly attached to the global reference frame as the total span of data was only 4 days. The **GDA** values of these stations are reported for the epoch of 1994.0 as these estimates include tectonic motion. The GRS80 ellipsoid has been used to convert cartesian coordinates into ellipsoidal coordinates.

Figure 12.3 is a plot of the daily repeatability of the observations at the Triabunna ANN site, which is adjacent to the Spring Bay Seaframe gauge. This plot is typical of all other stations. It was constructed by running part of the GLOBK process on the full global and tide networks for days 207 through 210 of 1992. It is readily seen that the repeatability is a few centimetres in each component. The error bars are one sigma error bars.

The following pages give detailed descriptions of each of the tide gauge network sites and a summary of the computed site coordinates (in cartesian and ellipsoidal form).

12.1 Port Kembla

Well defined coastal and inland arrays surround this Seaframe station. The central mark of the inland array is FLAG. This station was previously known as PM7374. The mark is set into basalt rock. Witness marks, PM70943 and PM70944 are close by. The main mark of the coastal array is PM70948, alias 948U at UC. The mark is set into rock using a steel/manganese rod in a covered box. It also has witness marks, PM70947 and PM70946.

The inland mark, FLAG, was observed in the SCAR92 and Epoch92 campaigns and during 1993 on days 264 and 266. The connection between the inland and the coastal stations was observed simultaneously but with significantly reduced data spans.

Precision levelling between the inland array and the coastal array was undertaken in June 1992 and May 1995.

Table 12.2: Coordinates of Port Kembla in ITRF92 at Epoch 1992.67

Station	Cartesian Coordinates		
	X	Y	Z
FLAG	-4597579.5887	2564075.5733	-3589224.2810
948U	-4599796.1110	2558715.5660	-3590124.8577

	Ellipsoidal Coordinates						
	Latitude			Longitude			Height
	Deg	Min	Sec	Deg	Min	Sec	Metres
FLAG	S34	27	57.58103	E150	51	5.54507	73.8247
948U	S34	28	34.01360	E150	54	51.29625	29.7466

12.2 Rosslyn Bay

GPS surveys in the Rosslyn Bay region commenced in July 1992 as part of the IGS epoch campaign when Queensland Lands occupied ID 83091 (OAKS) with a GPS receiver with the view of establishing OAKS as the primary point of the inland array. It was subsequently decided to abandon this station in favour of Mulara (MULA), ID 95189, due to access and stability problems. A connecting survey was performed in June 1993 to link the two locations and to establish two other regional stations.

A geological interpretation of the region indicates that the initial station, OAKS, was sited on Holocene sands, gravel and alluvium, which fill the low lands about Rockhampton and the Fitzroy basin. The newer stations of Mulara and Cobra (COBR), Queensland ID 95196, are on Lower Devonian serpentine which promises to provide a stable basement.

The coastal array stations of Double Head (DBHD), Queensland ID 45202, and Kiosk (KIOS), Queensland ID 82477, are sited on Upper Cretaceous Trachyte plugs and may eventually prove to be unreliable for high precision vertical control. These stations were observed during the October 1993 period utilising low order surveys. However, by joining several of these low order surveys into a span covering 24 hours, it was possible to extract a high precision connection between the inland array and the coastal array.

Spirit levelling between the inland array stations and the coastal stations was performed in early 1994.

Table 12.3: Coordinates of Rosslyn Bay in ITRF92 at Epoch 1992.67

Station	Cartesian Coordinates		
	X	Y	Z
OAKS	-5113582.8816	2874686.8936	-2495475.0698
MULA	-5115155.1227	2872883.3336	-2494382.0889
COBR	-5115677.3740	2872483.4145	-2493738.4279
DBHD	-5121169.7196	2863143.6832	-2493275.5184
KIOS	-5121014.8136	2863071.4616	-2493495.1054

	Ellipsoidal Coordinates						
	Latitude			Longitude			Height
	Deg	Min	Sec	Deg	Min	Sec	Metres
OAKS	S23	11	1.39447	E150	39	24.29176	100.9458
MULA	S23	10	22.50064	E150	40	46.65498	118.6045
COBR	S23	9	59.94581	E150	41	7.90491	103.9597
DBHD	S23	9	43.21824	E150	47	28.73901	129.8932
KIOS	S23	9	51.96026	E150	47	28.29764	59.5557

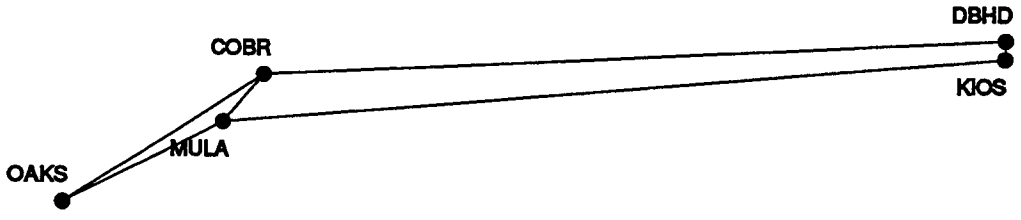

12.3 Cape Ferguson

This is a complex region in that the inland array point differs for GPS and levelling surveys. For the GPS technique, the inland array point for Cape Ferguson is the AFN site at Mt Stewart. It is called AU015 in the AUSLIG system and TOWA at UC. In practice the CIGNET site, TOWN, which has been observed simultaneously with TOWA, is often used, particulary for pre-July 1992 data. The tie between TOWA and TOWN has been performed in both 1992 and 1993 campaigns. It is considered to be of high precision as data spans the full period of both campaigns. The GPS tie from the inland station to the coastal station, Queensland BM 112150(AIM4), was not performed in a conventional period coincident with the operation of the AFN. Rather it was spread between two periods in which only Yaragadee and Tidbinbilla were contributing to the orbit. The GPS station at Mt Stewart was used as the fixed end of the GAMIT baseline solutions. The first period was days 343, 345 and 346 of 1992 while the second observation period was a single day, day 141 of 1993. It is to be noted that the levelling inland array point, Queensland BM 47070(7070), was also observed simultaneously.

For the levelling technique, the inland array point is the Queensland bench mark BM 47070, which is situated on the Bruce Highway. It is part of the national levelling network established along the Queensland coast in the mid-seventies by National Mapping (Morgan, 1992). The tie between this inland array point, and the coastal array point, BM 112150 was performed to a very high standard in early 1994. The suitability of the mark BM 47070 as a stable reference mark cannot be readily determined as the region is characterised by low level sand dunes and low lying swamps overlaying the Thunderbolt Granite suite. At Clevedon, a small village or road junction near the inland levelling bench mark, the granite sequence is clearly seen to the west. It is noted that it is steeply dipping at this point confirming the lack of solid rock along the Bruce Highway on which to anchor long term studies.

The granites are exposed at both Mount Stewart and AIM4 making both points highly suitable as reference marks. Since the granites belong to the Permian and hence should be geologically stable, it is likely that the GPS tie will have much better long term characteristics compared to the levelling tie.

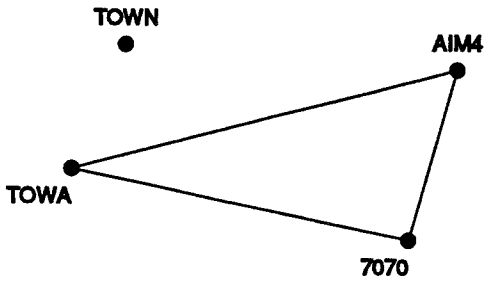

Table 12.4: Coordinates of Cape Ferguson in ITRF92 at Epoch 1992.67

Station	Cartesian Coordinates X	Y	Z
TOWA	-5036492.1195	3298900.1039	-2099859.7555
AIM4	-5054467.8421	3275174.4599	-2092255.9700
7070	-5048726.5539	3275944.8974	-2104777.9432

	Ellipsoidal Coordinates						
	Latitude			Longitude			Height
	Deg	Min	Sec	Deg	Min	Sec	Metres
TOWA	S19	20	50.43089	E146	46	30.78835	587.0273
AIM4	S19	16	34.37223	E147	3	27.81416	64.1601
7070	S19	23	45.98896	E147	1	18.65442	60.3371

12.4 Groote Eylandt

The Seaframe tide gauge station at Groote Eylandt is supported by the coastal and inland array concept. Both sites were observed simultaneously during the 1993 AFN campaign, termed Epoch93. The coastal or near array GPS station is NTS652, called ALYA. The inland station is NTS653, designated as GROO. The tie between the inland and coastal array stations was simultaneous within the Epoch93 campaign and hence is a high quality tie.

Spirit levelling between the inland and coastal arrays was performed in June 1993.

The geology of Groote Eylandt is quite complex. Around Milner Bay there are Quaternary sands and alluvium. This extends some distance inland, especially to the south-east, before the Proterozoic pebbly quartz sandstones are reached. It is not possible to ascertain that the inland array station GROO is indeed on rocks of this formation. It is most likely that both stations are on the Quaternary sands and hence are subject to local motion, especially vertical motion due to the moisture content of the sands that would follow the monsoon cycle.

Table 12.5: Coordinates of Groote Eylandt in ITRF92 at Epoch 1993.67

Station	Cartesian Coordinates						
	X			Y			Z
GROO	-4489874.7964			4265802.4412			-1519918.0535
ALYA	-4487413.8002			4269234.2280			-1517520.6114
	Ellipsoidal Coordinates						
	Latitude			Longitude			Height
	Deg	Min	Sec	Deg	Min	Sec	Metres
GROO	S13	52	41.31411	E136	27	57.50780	88.9352
ALYA	S13	51	21.04833	E136	25	38.20561	78.4478

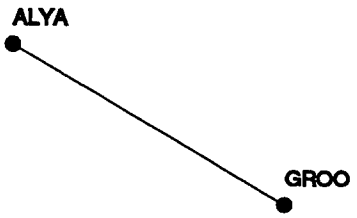

12.5 Darwin

Darwin is a complex GPS site. The AFN station, DARW, is located some 30 km to the south of Darwin at Manton Dam. Manton Dam is in an anomolous area near the extensive Giants Reef Fault which has shown considerable compression immediately to the south. The site appears to be east of the main Archean granites and gneiss sequence of the Rum Jungle Complex and in the more complex metamorphic rocks of the Namoona Group. The Giants Reef Fault has shown considerable movement in historical times and hence the AFN site is not suitable as an inland point. However, it has been used to determine the relationship between the now abandoned inland station Winnellie (WINN) and the coastal array station Pillar (PILL).

The immediate Darwin area is characterised by alluvial plains of mainly uniform loamy, sandy and gravelly soils overlaying Tertiary and Cretaceous sediments. These Cretaceous sediments are quite thin and rest on a platform of Middle Proterozoic rocks of considerable depth, which in turn lie on Early Proterozoic rocks. Both the inland station, Winnellie, and the coastal station, Pillar, are out of the coastal and estuarine plains which are generally unstable. Thus, the regime of the inland and coastal array points is similar. The shallow extent of the upper layers seems to indicate that little extraneous vertical motion should be caused by changes in this layer and that any changes would reflect the basement rocks. Changes to these basement rocks is unlikely making these end points stable.

The spirit levelling connections between the inland and near array points was undertaken in January 1992.

Table 12.6: Coordinates of Darwin in ITRF92 at Epoch 1992.67

Station	Cartesian Coordinates		
	X	Y	Z
DARW	-4091358.6559	4684606.8805	-1408580.7169
PILL	-4073402.3327	4712253.6667	-1367883.4793
WINN	-4077253.7309	4710296.8449	-1363184.1268

	Ellipsoidal Coordinates						
	Latitude			Longitude			Height
	Deg	Min	Sec	Deg	Min	Sec	Metres
DARW	S12	50	37.36100	E131	7	57.84538	125.1835
PILL	S12	28	0.37957	E130	50	27.75079	80.3484
WINN	S12	25	23.75669	E130	52	46.58995	82.8899

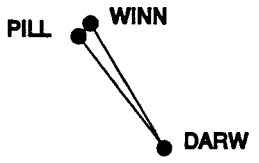

12.6 Broome

The Broome tide gauge is situated on the North West shelf of Australia. It experiences a large tidal range, which can be modified by storm surges especially during the cyclone season. The gauge itself is attached to the wharf. The ANN point (BROO) is labelled BRO173 in the West Australian system. It is about 10 kms to the northeast of Broome. There are three nearby marks, BRO172 and BRO174, both to the west of BRO173. They are, like BRO173, six metre stainless steel rods driven to refusal. BRO45 is an older, shallow reference mark to the southwest of BRO172. It is not considered reliable.

Between the inland array and the coastal array, there is a series of deep marks, similar to BRO172, labelled BRO178, BRO179 and BRO180. Other deep marks along the traverse route provide convenient change points.

The coastal array consists of marks BRO183, BRO184 and BRO185, which are also deep marks. The mark C184 is in close proximity to the coastal stations. The mark BRO186 is on the Broome jetty. It is regarded as the tide gauge bench mark. It has proved to be difficult to tie BRO186 to C184 within conventional survey specifications for closure, due mainly to jetty motion.

The geology of the region consists of red sands of a fine to medium structure of a few tens of metres overlaying pre-Cainozoic rock units. As such there are no stable geological sites within the region. The shallow depth and structure of the sands does not indicate that they are particulary stable and hence no marks can be considered stable. Thus the transfer of heights from the inland array to the coastal array could cause relative and local shifts to contaminate the data. The uniformity of the geology and the expected uniformity of the tidal corrections seems to indicate that a program concentrated at or near the tide gauge would be more appropriate than one based on coastal and inland arrays.

The connecting GPS surveys were done coincidently with the main Epoch92 observations but were unfortunately only done with L1 frequency instruments. Session lengths were about 2 hours. The quality of the reductions is adversely effected by the short period of data and our reliance on 24 hours of data to average out unmodelled tidal effects and the necessity to use the non-ionospherically compensated phase observations.

Spirit Levelling was performed between the coastal and inland arrays in August 1992.

Table 12.7: Coordinates of Broome in ITRF92 at Epoch 1992.67

Station	Cartesian Coordinates X	Y	Z
BROO	-3241494.8674	5134037.3576	-1946745.6129
B180	-3236852.7493	5134271.8838	-1953793.8534
B184	-3234310.3061	5133967.1112	-1958764.1382
R141	-3231915.8311	5136657.8145	-1955686.9319
STAT	-3236209.0070	5136101.0287	-1950160.6334

	Ellipsoidal Coordinates Latitude			Longitude			Height
	Deg	Min	Sec	Deg	Min	Sec	Metres
BROO	S17	53	21.78004	E122	16	2.01607	27.9714
B180	S17	57	22.71515	E122	13	44.36536	28.9239
B184	S18	0	12.68258	E122	12	36.78079	28.5747
R141	S17	58	27.42838	E122	10	39.17744	30.5522
STAT	S17	55	18.22197	E122	12	52.71797	55.5296

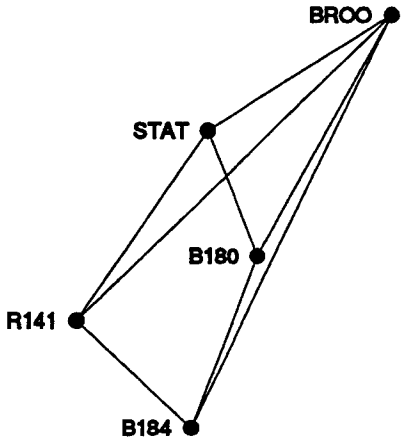

12.7 Hillarys

This is one of the more complex of the Australian GPS regions. In general, the inland array points are all located within the Gnangara telecommunications complex. The distance from the inland array to the coastal array is some 16 kms.

Gnangara 73 is the AFN site and the principle inland array station. It has the aliases GNAN, PER2 and PER3. Each of these represents a unique setup over the Gnangara 73 mark. The ESOC Rogue system, also installed at the site, is called PERT. It occupies the Gnangara 92 mark which is south of Gnangara 73. The mark Gnangara 71 is northwest of Gnangara 73. There are no known GPS occupations of this mark subsequent to July 1992.

The associated coastal array consist of Hamersley 164 (HILS) and DMH20 (MH20). DMH20 is the closest of these points to Tide Hillarys, the Seaframe tide gauge. It is regarded as the primary coastal station.

The connection between the coastal array and the inland array was performed during January 1992 using GPS techniques. Levelling was performed in March 1992.

Both the inland array stations and the coastal stations are to the west of the Darling Fault and hence are on the deep sediments of the region. Considerable extraction of fossil water also occurs in the region which will enhance subsidence and hence could produce anomalous changes in heights.

Table 12.8: Coordinates of Hillarys in ITRF92 at Epoch 1992.67

Station	Cartesian Coordinates		
	X	Y	Z
GNAN	-2368701.3951	4881361.6984	-3341721.1007
HILS	-2355719.2670	4886370.5173	-3343483.0998
MH20	-2355441.6761	4886096.3310	-3344072.4237

	Ellipsoidal Coordinates						
	Latitude			Longitude			Height
	Deg	Min	Sec	Deg	Min	Sec	Metres
GNAN	S31	48	4.21770	E115	53	6.63474	13.1019
HILS	S31	49	12.40190	E115	44	19.37878	-29.9366
MH20	S31	49	34.95108	E115	44	14.39808	-31.4681

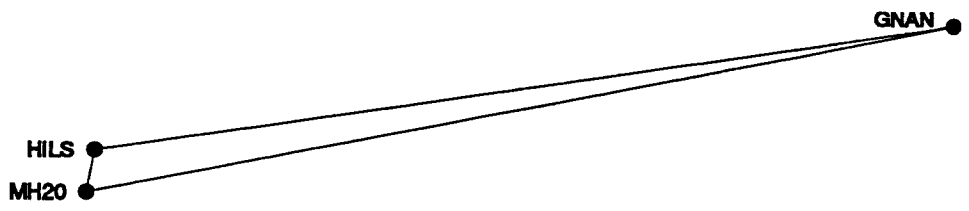

12.8 Esperance

This is quite a simple site with only a local coastal array and the tide gauge bench mark. The marks ESP171, ESP172, and ESP 173 now form the coastal array with the station EPS171 also doubling as the ANN mark, referred to as ESPE. The mark HR4 is on the wharf near the tide gauge.

The coastal array marks are less than 1 km from the tide gauge.

All of these sites are linked by spirit levelling, which is to first order standards. The initial levelling was performed in June 1992. It was subsequently reobserved in September 1993 and June 1995.

The region immediately around Esperance is Pre-Cambrian Migmatite. These rocks are thought to be quite stable. Just out of Esperance there is a rapid change as one moves into sand dunes and lower sandplain deposits. The region is well known for its fossil water supplies, which would significantly alter all gravity observations. This water is regularly and intensely used by the local community.

Table 12.9: Coordinates of Esperance in ITRF92 at Epoch 1992.67

Station	Cartesian Coordinates		
	X	Y	Z
ESPE	-2800864.6361	4500724.6168	-3534886.607

	Ellipsoidal Coordinates						
	Latitude			Longitude			Height
	Deg	Min	Sec	Deg	Min	Sec	Metres
ESPE	S33	52	27.15047	E121	53	40.51991	28.9273

12.9 Thevenard

The Thevenard area is a complicated region for geodesy in that several surveys have been undertaken without too much regard for coordination.

The inland array station for the tide gauge network is Thevenard (THEV), 5633-1475 in the South Australian register. It is some 10 km inland from the coast. It has been observed twice. The first was during January 1992 (SCAR92). The second period of occupation was as part of the Tide network during the IGS epoch campaign. The tie between the inland station and the coastal array site, 5633/1487, close to the Thevenard jetty and the Seaframe gauge, was performed during the January 1992 campaign with dual frequency equipment.

Spirit levelling in the Thevenard region, including the connections between the coastal array and the inland array, is discussed by Ananga et al. (1993). This discussion indicates that the work performed by the S.A. Department of Lands is of a very high quality. It has excellent repeatability when *deep and stable* marks are used. The work of Ananga et. al. (ibid.) was restricted by the following:

- The repeat surveys did not pick up all common stations between the two epochs.
- The route of the two surveys was not the same.
- The same initial and final stations were not observed in the two surveys.

A further GPS development in the region is the establishment of the AUSLIG permanent tracker at the OTC site which is some 35kms inland from the Thevenard Seaframe tide gauge. The connection between this site and the inland and coastal array marks supporting the Thevenard Seaframe gauge were performed in May 1995.

The geology in the region is variable. In the coastal region, including both the coastal and inland array sites, there is a thin layer of sand over the stable Gawler basement rocks. The sand is in ridges which may be subject to irregular motion. At the OTC station, where the AUSLIG station CEDU is located, the Gawler basement rocks are at the surface. These rocks provide an excellent platform for long term studies.

Table 12.10: Coordinates of Thevenard in ITRF92 at Epoch 1992.67

Station	Cartesian Coordinates X	Y	Z
THEV	-3739792.0387	3911197.4232	-3364706.8859
1487	-3730777.6531	3911709.2251	-3373990.1574

	Ellipsoidal Coordinates Latitude			Longitude			Height
	Deg	Min	Sec	Deg	Min	Sec	Metres
THEV	S32	2	43.03106	E133	42	59.81518	33.6894
1487	S32	8	39.35541	E133	38	37.70890	5.4900

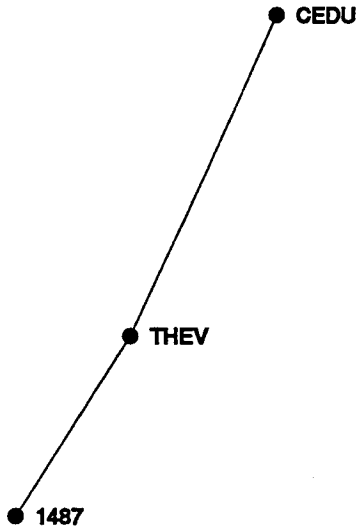

12.10 Port Stanvac

Port Stanvac is the NTF test site at Port Adelaide. The inland array point, 6627/20445 in the South Australian register, is called STAN at UC. The principal coastal array point, 6527/8115 or RFNG, is near the Seaframe gauge on what appears to be filled land, or at least adjacent to land that has been subject to extensive filling.

The GPS connection between the inland and coastal arrays was observed in March 1995 (Days 74 and 75). Levelling between the two sites has not be performed subsequent to September 1990.

The geology of the region is not conducive to the maintenance of an independent vertical datum in that the inland station is in the Adelaide fold belt while the near station is down on the sedimentary plain adjacent to areas extensively filled. It is thought that both the inland station, STAN, and the coastal station, RFNG, can be moving independently and at different rates. The only way that such movements can be deduced is to directly observe both stations in a full global network as outlined by Morgan (1994).

Table 12.11: Coordinates of Port Stanvac in ITRF92 at Epoch 1992.67

Station	Cartesian Coordinates		
	X	Y	Z
STAN	-3916469.8650	3455298.5412	-3649 242.7352
RFNG	-3911226.4955	3462978.1648	-3647 147.6656

	Ellipsoidal Coordinates						
	Latitude			Longitude			Height
	Deg	Min	Sec	Deg	Min	Sec	Metres
STAN	S35	7	23.98454	E138	34	46.95006	306.5489
RFNG	S35	6	6.78136	E138	28	42.60221	47.8952

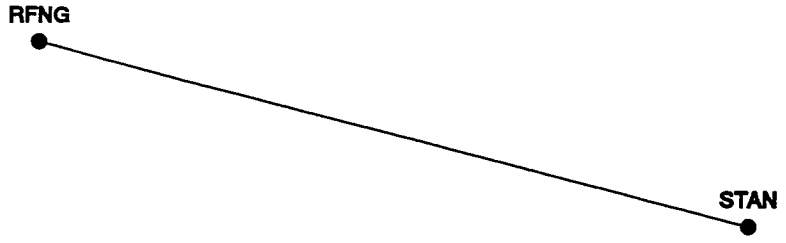

12.11 Portland

The Portland tide gauge is situated at the western entrance of Bass Strait.

The ANN mark, PORT, is designated Trewalla PM80 in the Victorian system. An adjacent witness mark is Trewalla, PM82. The station was observed during Epoch92 in association with other tide gauge stations. It was reoccupied in the 1994 ANN campaign.

The coastal array consists of three permanent marks with Portland PM387 and Portland PM393 being observed by GPS relative to the inland array stations on days 138 to 141 of 1993. The sessions were only 1.5 hours in length. Portland PM387 is closer to the tide gauge than Portland PM393 and as such is regarded as the principal coastal mark. Spirit levelling was done in the same period as Lorne, that is, April to June 1993.

The geology of the Portland region is Quaternary volcanics consisting of olivine and iddingsite basalt. There are no faults in the region. Since the geology is stable and uniform in the region there appears to be no gain in establishing and using the inland array concept as both sites would be equally effected by tidal loadings and other perturbing effects.

Table 12.12: Coordinates of Portland in ITRF92 at Epoch 1992.67

Station	Cartesian Coordinates		
	X	Y	Z
PORT	-3922961.9451	3117568.4903	-3932953.8433
TR82	-3922782.6457	3117631.5178	-3933084.1510
P387	-3925791.3756	3110755.2045	-3935430.8855
P393	-3925545.5325	3110564.8329	-3935824.0542

	Ellipsoidal Coordinates						
	Latitude			Longitude			Height
	Deg	Min	Sec	Deg	Min	Sec	Metres
PORT	S38	18	53.46838	E141	31	33.30515	47.4010
TR82	S38	18	58.81815	E141	31	26.68196	48.8232
P387	S38	20	37.09226	E141	36	25.45328	-0.0571
P393	S38	20	53.34851	E141	36	25.31023	0.0234

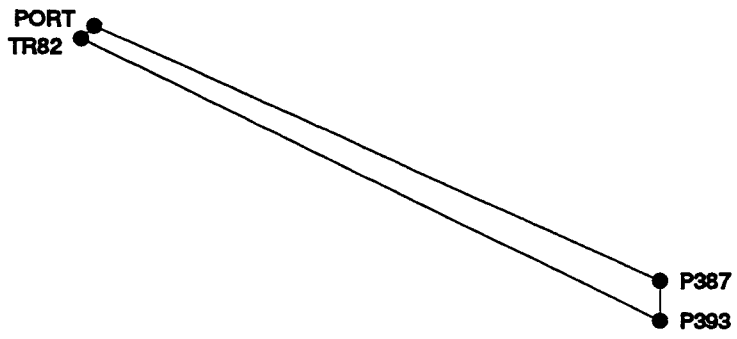

12.12 Lorne

The Lorne tide gauge is part of the Port of Melbourne array. It is operated at standards that allow it to be included in the Australian Baseline array. The site is on the north western edge of Bass Strait and as such can be expected to be subjected to storm surges and other specific Bass Strait events.

The principal ANN or inland array site, Lorne PM76 (BENW), is located some 15 km inland. The associated witness mark is Lorne PM77, which is within 100 metres of the main inland mark, Lorne PM76. The coastal array consists of marks Lorne PM86 and Lorne PM82. These two marks are also within 100 metres of each other.

The inland array points are about 10 kms from the coastal array by direct line but much longer by road due to the steep nature of the Otway Ranges at this point. The elevation difference of 500 metres makes levelling difficult without providing any significant variation in load contributions. The basement material in the area is lower Cretaceous consisting of sandstones, mudstones, and siltstones. The inland array points are situated well away from from the Bambra Fault which has historical vertical motion. The Boonnah anticline is also to the west of the array indicating that homogeneous geology exists between the inland and coastal array points. Since uniform geology exists in the area, there appears to be little gain in establishing inland and coastal arrays, especially when spirit levelling is difficult and costly to perform.

The measurements to BENW were made during the IGS epoch campaign. The connections of the inland array stations to the coastal array stations were made on days 138 to 141 of 1993, the same days as used at Portland. The observation spans were of similar duration to those used at Portland. Spirit levelling connections occurred over a 3 month period, April to June in 1993. This spirit levelling involved an additional station at both the inland and coastal arrays. The length of time to accomplish the task is believed to be indicative of its difficulty.

Table 12.13: Coordinates of Lorne in ITRF92 at Epoch 1992.67

Station	Cartesian Coordinates X	Y	Z
BENW	-4040118.7016	2944818.6160	-3948080.7624
PM77	-4040149.9333	2944824.4700	-3948044.8643
PM82	-4040118.5031	2936777.7849	-3953251.1228
PM86	-4040065.2445	2936781.4235	-3953301.4049

	Ellipsoidal Coordinates Latitude			Longitude			Height
	Deg	Min	Sec	Deg	Min	Sec	Metres
BENW	S38	29	8.02227	E143	54	42.89007	491.3955
PM77	S38	29	6.53212	E143	54	43.45388	491.5107
PM82	S38	32	54.78045	E143	59	11.22614	8.6349
PM86	S38	32	56.88316	E143	59	9.81139	7.9514

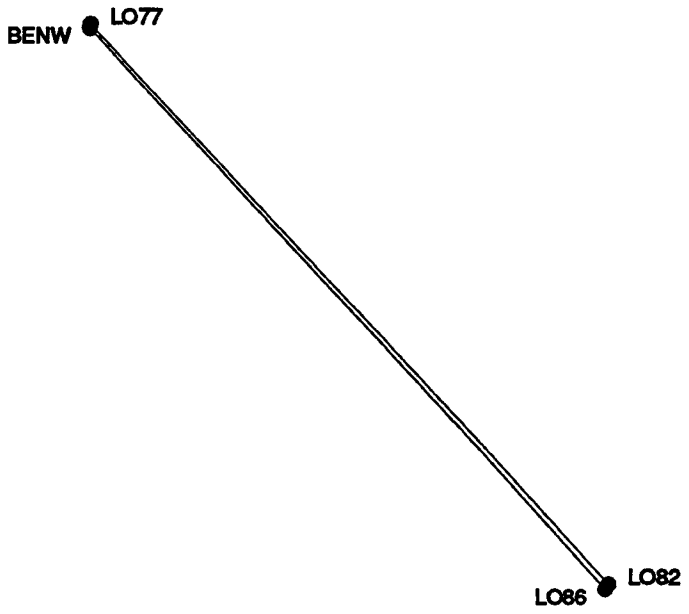

12.13 Burnie

The Burnie site was installed as part of a calibration/verification project for the TOPEX/Poseidon satellite altimeter mission, being the only southern hemisphere site. The project was funded largely from CSIRO Office for Space Science and Applications and coordinated by CSIRO Division of Oceanography with assistance from a number of other agencies - NTF, Tasmanian Department of Environment and Land Management and University of Tasmania. Data from the Burnie tide gauge is now included as part of the NTF ABSLMA network. Early TOPEX/Poseidon calibration results are given in White et al. (1994). However, this site remains an extremely important verification installation for continuous monitoring of the altimeter drift rate, the drift rate being essential for computing reliable sea-level rise estimates from altimetry.

This is a simple station. The TGBM, SPM9089 (SPM9), is situated adjacent to the Burnie wharf and the Seaframe tide gauge. That is, there are no inland/coastal array stations. The station was observed during Epoch92 and hence is rigorously tied to the adopted reference system. Some later data, not as yet processed, is also available.

The geology of the region is late Proterozoic. The exact tie of SPM9 to basement is uncertain at this instant.

Table 12.14: Coordinates of Burnie in ITRF92 at Epoch 1992.67

Station	Cartesian Coordinates		
	X	Y	Z
SPM9	-3989108.2296	2699944.0232	-4166666.7789

	Ellipsoidal Coordinates						
	Latitude			Longitude			Height
	Deg	Min	Sec	Deg	Min	Sec	Metres
SPM9	S41	3	1.97090	E145	54	31.39098	13.1361

12.14 Spring Bay

The GPS picture in the Hobart/Spring Bay region is complicated due to changes in instruments and operating agencies. Historically, the CIGNET site at the University of Tasmania's Mount Pleasant Observatory was designated TAS1 when operated with a MiniMac receiver. The same mount point was used for a NOAA (CIGNET) Rogue installation with the designation of HOB1. Most solutions of the location of TAS1 and HOB1 showed horizontal agreement but vertical disagreement when corrected to the mount point.

During the IGS epoch campaign and the latter local Epoch93 campaign, the AFN pillar was occupied by AUSLIG using Ashtech receivers. Data from this pillar, utilising Ashtech receivers, have generally been designated HOBA. Recently the AFN pillar was permanently occupied by an AUSLIG Rogue receiver. Data from the AFN pillar using the AUSLIG Rogue is generally referred to as HOB2 in most data bases.

The Spring Bay Seaframe tide gauge inland array point is SPM9261 in the Tasmanian system. Its four letter code is TRIA. It is surrounded by four reference marks designated RM1, RM2, RM3 and RM4. The latter is a concrete pillar with stainless steel plate and spigot. The other RMs are domed, galvanised bolts cemented to rock. The main mark is a stainless steel rod in dolerite with a box cover.

Spring Bay was observed during the IGS Epoch92 campaign and hence has been well determined relative to both the MiniMac and AFN sites. This site is some 52 kms distant from Mount Pleasant. The coastal array site is SPM9259, which is almost 2 kms away from the Seaframe tide gauge. GPS connections between the coastal and inland array sites were observed in May 1991. These data were observed during a period of poor global tracking and hence the amount of data from which to compute a global orbit is minimal.

The nearest bench mark to the Seaframe installation is SPM9258 which is situated adjacent to the tide gauge. Station SPM9257 is at the end of the service road adjacent to the wharf, while SPM8522 and SPM8521 are further away from the wharf. There are spirit levelling connections between these stations.

The new mark, SPM9259, has been constructed with similar properties to SPM9261. The mark is a stainless steel rod in dolerite and is supported by four reference marks, one of which is a pillar with a stainless steel plate. RM1 and RM3 are on different rock outcrops to SPM9259.

The geology of this part of Tasmania is mainly basic intrusive rocks of the Mesozoic era. Sediments are shallow and are not expected to be playing a major role in loading. Thus all sites rigidly connected to bedrock are expected to yield rates representative of the general area. The major concern is the degree of connectivity of floating boulders to the basement. A floating boulder was used for SPM9259, the preferred near array station.

Table 12.15: Coordinates of Spring Bay in ITRF92 at Epoch 1992.67

Station	Cartesian Coordinates X	Y	Z
HOB2	-3950071.2636	2522415.2075	-43116 38.4989
SBCP	-3988841.4510	2499449.7399	-42893 49.8302
TRIP	-3990829.6629	2501497.6603	-42863 41.2703
TRIA	-3990830.5875	2501499.2983	-4286 339.0220

	Ellipsoidal Coordinates Latitude			Longitude			Height
	Deg	Min	Sec	Deg	Min	Sec	Metres
HOB2	S42	48	16.98509	E147	26	19.43562	41.1075
SBCP	S42	31	55.87749	E147	55	41.92280	-0.6044
TRIP	S42	29	43.29468	E147	55	12.15789	9.763
TRIA	S42	29	43.20476	E147	55	12.11861	9.4636

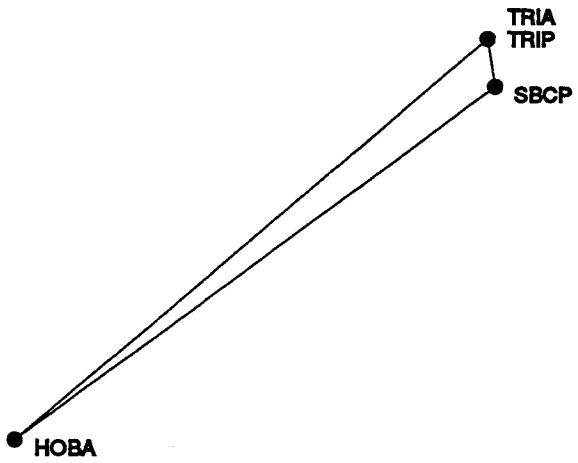

12.15 Other Tide Studies

12.15.1 NRMS and Modelling Improvements

It was previously stated that the above analysis was performed with only the standard solid body model activated. This was partly due to the fact that all the 1992 and 1993 data were reduced with software that only had this model implemented and it was not feasible to revisit the reductions with a rapidly changing software suite. The compatibility of the modelling process between the two network levels was also of concern as any modelling difference between the networks could strain or tension the adjustment process.

Thus, it was decided to monitor the NRMS statistic from the GAMIT solutions as better or more complete modelling of the process should reduce the residuals by reducing the magnitude of the computed minus observed vector used in the least squares process.

Figure 12.4 shows the effect of increasing the modelling complexity from the simple solid body model up to the now fully complete model. The increase in nrms that occurs when the ocean tide correction is added is thought to be due to the inadequacies of this model in shallow coastal waters, as present in the north of Australia. The model used was developed by Scherneck (1983) using the Schwiderski Ocean Tide Model. This model is well known for its inability to correctly represent shallow coastal waters. Thus when the ocean tide is neglected, it is seen that there is a general reduction in nrms with increasing model complexity. Unfortunately there is also increased daily scatter of the nrms value.

While these trends are promising, the conservative view is that the sample is too small to draw any conclusive evidence from at this stage and that a much larger sample and more carefully controlled experimentation is needed.

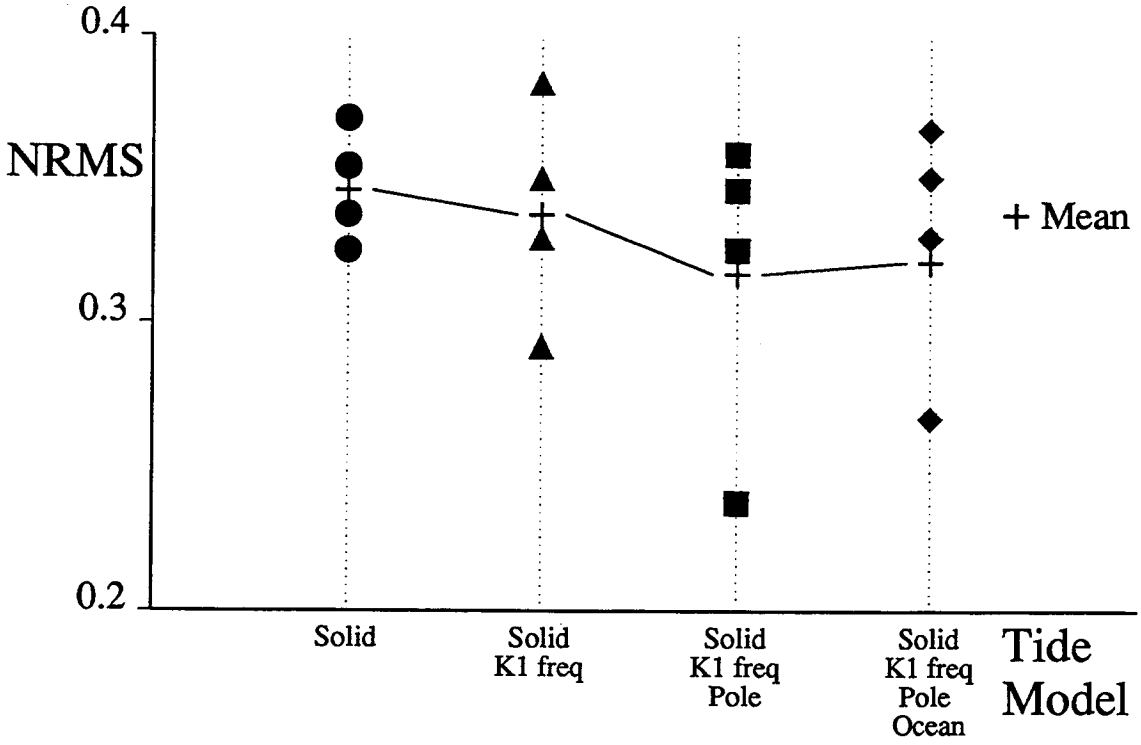

Figure 12.4: NRMS for GAMIT solutions for the four days of the Tide campaign for different levels of implementing the earth tide model.

12.15.2 Mean Height and Tide Modelling

As an extension of the processing that was carried in the previous section, the four daily solutions of the Tide network were unified using the GLOBK suite using the conventional solid tide model and the full earth tide model, including ocean tide effects. The GLOBK process used Yaragadee, Tidbinbilla and Darwin for constraints, being set at the 0.05 m per component in the local North, East and Up system.

Each GLOBK process had the same a-priori values and hence the corrections can be used as a measure of the difference of the two systems.

The results are plotted in Figure 12.5 as a function of latitude. It is seen that the sign of the correction changes near latitude 30°S from a negative correction to a positive correction with the exception of OAKS, where the effects of the Barrier Reef may not be correctly accounted for.

This result is in agreement with general tidal theory which shows that the semi-diurnal, sectorial components M_2, S_2 and N_2 dominate at the equator, while the tesseral, diurnal waves K_1, O_1 and P_1 dominate at latitudes of 45° with the opposite sign.

The importance of this result is that the determination of an appropriate ocean tide model is required to understand the fluctuations in the GPS data. Changes in corrections of the order of 0.05 m are important although it might be argued that a significant portion of this correction is due to the pole tide component which has a 14 month period. The magnitude of this term and the way it acts is the main cause for the smaller positive difference at Darwin and Broome compared with the mid-latitude sites.

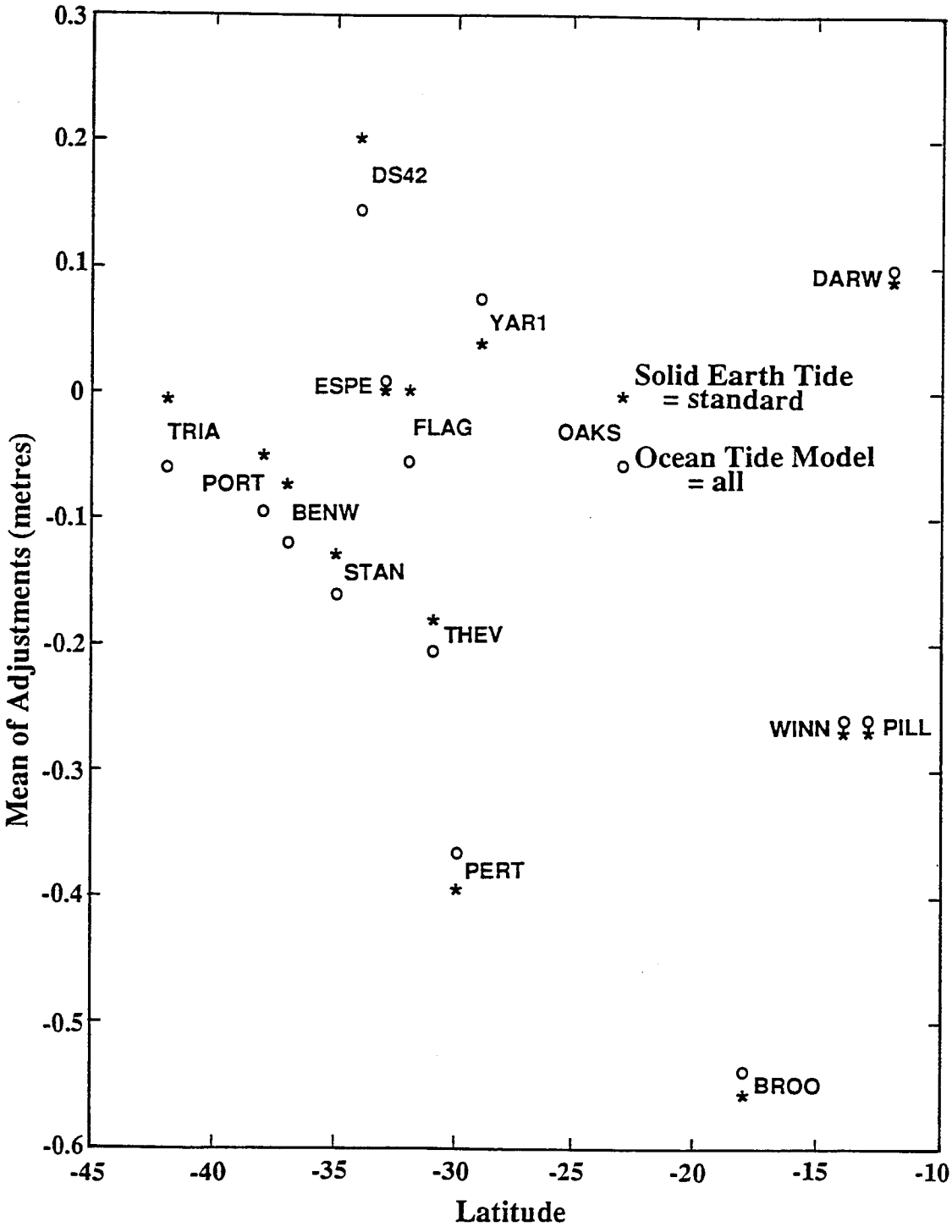

Figure 12.5: Differences in adjusted heights for the Tide gauge network between the standard solution only invoking the principal solid body tide and the full model with all terms including an ocean tide component.

Chapter 13

Results and Analysis

The results of the three years of observations and GAMIT analyses described in the preceding chapters were brought together using the GLOBK program suite developed by Herring to support the analysis of VLBI data (Herring et al., 1990).

Three important considerations were enforced at this stage of the project.

1. The χ^2/f statistic should be, as far as possible, under 10 between the participating solutions.

2. The positions and rates of change of both Yaragadee and Tidbinbilla had to be coincident with their ITRF92 values.

3. The station velocities had to be consistent with the current NUVEL plate model.

The first condition required the recomputation of several of the individual solutions and the resolution of mainly heighting and setup errors. The 'earthquake file' route was adopted for campaign-wide errors caused by incomplete or inexact initial knowledge of the instrument setups. The 'earthquake file' is part of the attached Appendices - see Appendix E.

The latter two conditions were enforced through the application of constraints and the careful resolution of conflicts in the data by use of the 'earthquake file' which allows sites to be renamed and known adjustments applied. Several recording errors were located and resolved by minimizing the χ^2/f statistic and examining plots of station repeatabilities for those sites with multiple occupancies.

The results of the GLOBK solutions are tabulated in two appendices. The first, Appendix A: Cartesian Coordinates and Rates, provides the results in the X,Y,Z nomenclature in the ITRF92 reference frame at epoch 1994.0. The second, Appendix B: Ellipsoidal Coordinates, provides ellipsoidal coordinates referenced to the GRS80 ellipsoid in the ITRF92 reference frame at epoch 1994.0.

13.1 The Reference Frame

The Reference Frame chosen for the results was the International Terrestrial Reference Frame: 1992, ITRF92 (Boucher et al., 1993). This reference frame is generally accessed through the adoption of one or more published coordinates. In the case of GPS, thirteen stations are designated as *core* stations by the IGS, the major contributor to the ITRF solutions. The position and rate of change of these *core* stations is well established within the ITRF and hence these stations are ideal for attaching networks and campaigns, such as this Australian Regional Network, to the ITRF.

Table 13.1: The thirteen IGS *core* stations used to apply constraints. The first four form the Southern Hemisphere ring used to control rotation about the Z-axis. The next group of five were used to control the X and Y rotations and to supply strong velocity information on the North American and Eurasian plates. Tidbinbilla and Yaragadee supply the same information on the Australian plate. The final group of four sites, two from each of the North American and Eurasian plates, were used as test points. Note that DS1B replaced DS10 after the 1992 IGS Campaign

Station	Plate	Latitude		Longitude	
		deg	min	deg	min
Hartebeesthoek	AFRC	-25	53	27	42
Yaragadee	AUST	-29	05	115	25
Tidbinbilla (DS42)	AUST	-35	35	148	59
Santiago	SOAM	-33	09	289	20
Algonquin	NOAM	45	57	281	56
Fairbanks	NOAM	64	58	212	29
Koke Park	PCFC	22	08	200	20
Kootwijk	EURA	52	11	5	49
Tromso	EURA	69	40	18	56
DS60 (Madrid)	EURA	40	26	355	44
Wettzell	EURA	49	09	12	53
Yellowknife	NOAM	62	29	245	42
DS1B (Goldstone)	NOAM	35	20	243	06

Several different strategies exist when applying constraints. The most important differences relate to the level at which the constraints are applied and whether or not the network solution is allowed to adjust as a free network or is forced to a pre-conceived or fiducial network. This work uses the latter approach at the request of ICSM. Consequently the first two groups of the points listed in Table 13.1 were held fixed. However, regardless of the method used, it is necessary to consider the underlying aims of applying the constraints. In this study the aims were:

- To ensure that the solution was consistent with the ITRF, i.e., there is no net rotation between the network solution and the ITRF.

- To ensure that the geophysical velocities of the Australian sites were in accordance with current estimates from the NUVEL models.

The first aim requires that the rotation matrix between the ITRF and the network solution be well determined. The rotation matrix, as demonstrated in chapter 2, is composed of three terms:

1. The rotation about the z-axis, due to errors in UT1, can be controlled by constraining a small number of stations, preferably in a constant latitude belt not too far removed from the equator. Maximum strength is provided when stations are separated by 180° in longitude. The four southern hemisphere stations meet these conditions. Their relationship to each other is shown in Figure 13.1

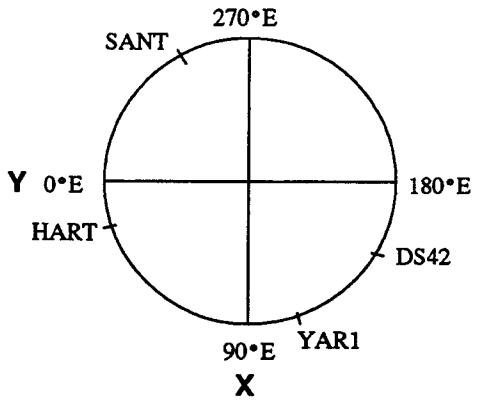

Figure 13.1: Sketch of station distribution to constrain the rotation about the Z-axis

2. The rotation about the x and y-axis, due mainly to errors in polar motion, can be controlled by constraining stations in the y-z and x-z planes respectively. Again the maximum effect is achieved for stations that are diametrically opposite each other in the plane. The rotation about the x-axis has the station pair Yaragadee and Algonquin, while the rotation about the y-axis has the station pair Tidbinbilla and Kootwijk. These conditions are illustrated in Figure 13.2

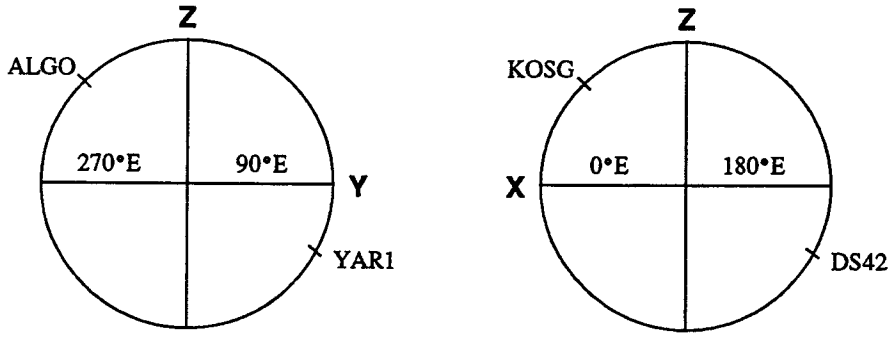

Figure 13.2: Sketch of Station distributions to constrain the rotations about the X and Y-axis

In addition to fitting the station coordinates, it is also possible to supply additional constraining information on the earth rotation parameters, UT1 and x and y pole. This was done

using a special, high-quality VLBI solution provided by Herring (personel communication, 1995).

The second aim is generally thought to be a by-product of the correct specification of the terrestrial reference frame. Thus, it is possible to take data from other techniques, for example VLBI and SLR, and to enforce the results of the reference frame that has such data embeded in it. Indeed, the ITRF solutions have major contributions from VLBI and SLR. Furthermore, the velocity field is consistent with the NNR-NUVEL model. Thus by using a constraint for station velocities, additional information for the determination and maintenance of a consistent frame over the period of interest is obtained.

It is seen from Table 13.1 that constraints have been exercised on the North American, Eurasian and Australian plates. This should ensure that velocities determined for the Australian region are consistent with NNR-NUVEL.

13.1.1 The χ^2/f Statistic

Figure 13.3 shows the performance of the χ^2/f statistic when all the subnetworks are unified in an optimal manner. The striking features of this plot are:

- That the χ^2/f less than 10 rule could not be enforced. This violation imposes considerable distortion and misalignment between the global system, the SIO solution, and all regional solutions, but particularly the Australian regional solution. No specific cause could be found for this discrepancy. The following comments apply:

  (i) The SIO network is both more global and more consistent in its characteristics and components compared to the ARN network. In particular, the ARN is a constantly varying mixture of instruments and sites only covering about $1/16^{th}$ of the earth's surface.

  (ii) The SIO network is composed mainly of Rogue or Turbo Rogue receivers capable of generating high quality pseudo-range observations. These observations play a fundamental role in determining and resolving bias flags and other data irregularities. By way of comparison, the codeless receivers typified by the Trimble SST, only generate the low quality C/A pseudo-range which is often significantly contaminated.

  (iii) The level of the mismatch between the SIO global network and the ARN solution is somewhat dependent on the level of the constraints applied to the southern hemisphere IGS *core* stations. This suggests that these stations are not as well determined as their northern hemisphere counterparts. Previous discussions, especially those undertaken in Chapters 8 and 9 support this hypothesis.

- When the global SIO orbit was not available, the χ^2/f statistic was within the above bounds indicating that no disparity between the systems was present.

- The smaller regional networks, with less power to define the orbits of the satellites, fit better or have less distortion compared to the larger ARN networks. The relationship of the size of the network to the power to adequately determine the orbit parameters was discussed in Chapter 9.

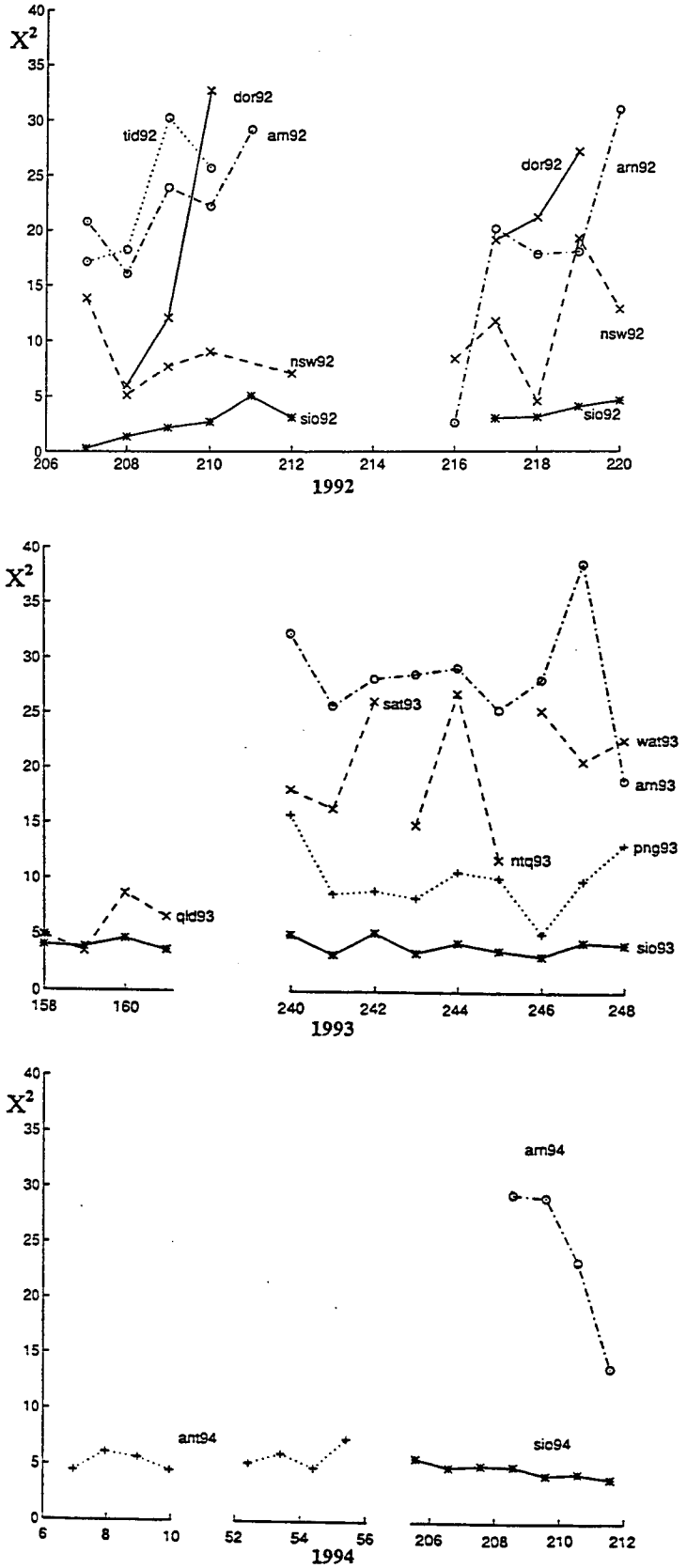

Figure 13.3: Plot of χ^2/f statistic for the final GLOBK run incorporating all sub-networks

13.1.2 Comparison at Test Stations

As mentioned at the beginning of this chapter, four IGS *core* sites were not constrained so that they could be used to test the quality of the solution. The corrections to these four unconstrained ITRF92 values are given in Table 13.2. The important results appear to be more discernible when the corrections to the cartesian X, Y, Z coordinates are transformed into local North, East and Up values. When expressed in the local reference frame, it is seen that both the Up component and the Up rate are much larger than for the horizontal North and East components. In all cases, the formal errors are small indicating that the solution has sufficient power to determine the corrections listed.

The conclusion that can be drawn from this is that the solution has excellent horizontal resolution but is less reliable in the vertical component. This could be due to an inferior a-priori knowledge of this latter component as the formal errors attached to the Up and Up Rate components are also larger. However, it is generally thought that problems relating to modelling still effect the vertical component. Some of the concerns include tropospheric modelling, as only one 24 hour term was solved for in this project, and antenna phase offsets were not applied.

Table 13.2: Corrections in metres or m/yr in both the Cartesian and local coordinate systems for the four IGS *core* stations unconstrained for testing the quality of the solution.

	DS60 (Madrid)	Yellowknife	Wettzell	Goldstone (DS10)
X Coordinate	0.0887 ±0.0025	-0.0147 ±0.0012	0.0259 ±0.0020	-0.0596 ±0.0017
Y Coordinate	-0.0013 ±0.0014	-0.0556 ±0.0015	0.0280 ±0.0013	-0.0592 ±0.0023
Z Coordinate	0.0417 ±0.0021	0.1078 ±0.0025	0.0022 ±0.0023	0.0297 ±0.0018
X Rate	0.0371 ±0.0021	-0.0099 ±0.0009	0.0141 ±0.0017	-0.0210 ±0.0014
Y Rate	-0.0114 ±0.0012	-0.0252 ±0.0012	0.0245 ±0.0011	-0.0335 ±0.0021
Z Rate	0.0484 ±0.0018	0.0418 ±0.0021	-0.0024 ±0.0019	0.0168 ±0.0016
N Coordinate	-0.0254 ±0.0007	-0.0043 ±0.0006	-0.0223 ±0.0006	-0.0218 ±0.0006
E Coordinate	0.0052 ±0.0014	-0.0301 ±0.0008	0.0215 ±0.0012	-0.0264 ±0.0014
U Coordinate	0.0944 ±0.0031	0.0639 ±0.0013	0.0223 ±0.0030	0.0822 ±0.0031
N Rate	0.0010 ±0.0006	-0.0010 ±0.0007	-0.0063 ±0.0005	-0.0090 ±0.0005
E Rate	-0.0086 ±0.0012	0.0101 ±0.0011	0.0008 ±0.0010	-0.0036 ±0.0011
U Rate	0.0505 ±0.0027	0.1222 ±0.0029	0.0115 ±0.0026	0.0418 ±0.0028

13.1.3 Regional Geophysics

The basic assumption in this section is that any regional distortion of either a spatial or temporal nature will enter into the computation of the velocity field and thereby perturb it relative to the known NUVEL model. Determining the rate of change or velocity components in GLOBK generally requires at least two observations with a minimum 1 year between the observations. The data set (Appendix F) clearly shows that the major AFN sites have at

least three occupations at approximately annual intervals. Thus, the velocities should be well defined at these sites.

Three figures are now presented. The first, Figure 13.4, shows the computed horizontal velocity field. There is a high level of uniformity of the velocities and this is what was expected from past geophysical results. The exceptions are the stations of Broome, Esperance and Oaks. These three sites are associated with the Tide network described in Chapter 12.

Extensive consultation with the field crews and data checking did not reveal any irregularities at Oaks or Esperance. At Broome, the height was incorrectly recorded but the intended value was readily discernible. As all sites are only double occupancies, no information is available to suggest which epoch is likely to be in error. It is considered unlikely that there is any local movement at the computed rates.

The second figure, Figure 13.5, shows the height rates expressed in cm/yr. The expected values of these rates are close to zero. High rates, like that shown for Wellington, are indicative of unresolved systematic errors. These errors are likely to be due to incorrect specification of the antenna reference point, the type of antenna used and incorrect recording of antenna heights. The mean of the absolute value of the height rates, excluding Wellington, is 3.9 cm/yr. This represents an average random error of 2.8 cm in the height of these stations. However, if only the AFN and other known pillar stations are considered, then the mean of the absolute value of the height rate is 0.2 cm/yr with a strong preference for negative values. This value is consistent with subsidence due to the mass of the mark, as most of the marks were constructed to the massive NASA/JPL standard rather than the less massive Canadian standard. The errors at the non-pillar stations are thought to be primarily due to changes in antenna types as there was no attempt to maintain consistent instrument types at these stations. However, there were permanent receivers and fixed antenna types at the AFN stations.

Pearse (1995) compared the adjusted heights with the AHD71 (Roelse et al., 1971) and the gravimetrically determined ellipsoidal separation. Pearse found that the mean error was of the order of 30 cm. A substantial component of this error budget is due to the gravimetric estimation process, again supporting the view that the heights as determined from this analysis are of a uniform high quality.

It is clear that the behavior of the Wellington mark on top of Heafy House is anomolous. It is not clear whether the subsidence rate does indeed reflect the load of the structure on the surrounding soils or is due to other yet-to-be determined effects. However, additional data are now available to confirm this anomolous behaviour. Additionally, the mark is about to be transferred to a bedrock site.

The third figure, Figure 13.6, shows the residual horizontal velocity field after subtracting the NUVEL model. The results of this figure emphasise the irregularities at Broome, Esperance and Oaks as well as confirming the generally-held view that, at some level, the Australian continent is behaving as a rigid plate. Excluding stations Broome, Esperance and Oaks, the mean (absolute value) residual of Australian stations is 1.1 cm/yr after removing the NUVEL model.

Several striking features are revealed by the figure. The first is the spatial coherence of stations in western and eastern Australia. This coherence suggests that the Australian plate is undergoing compression. This compressional state was first deduced by Lambeck et

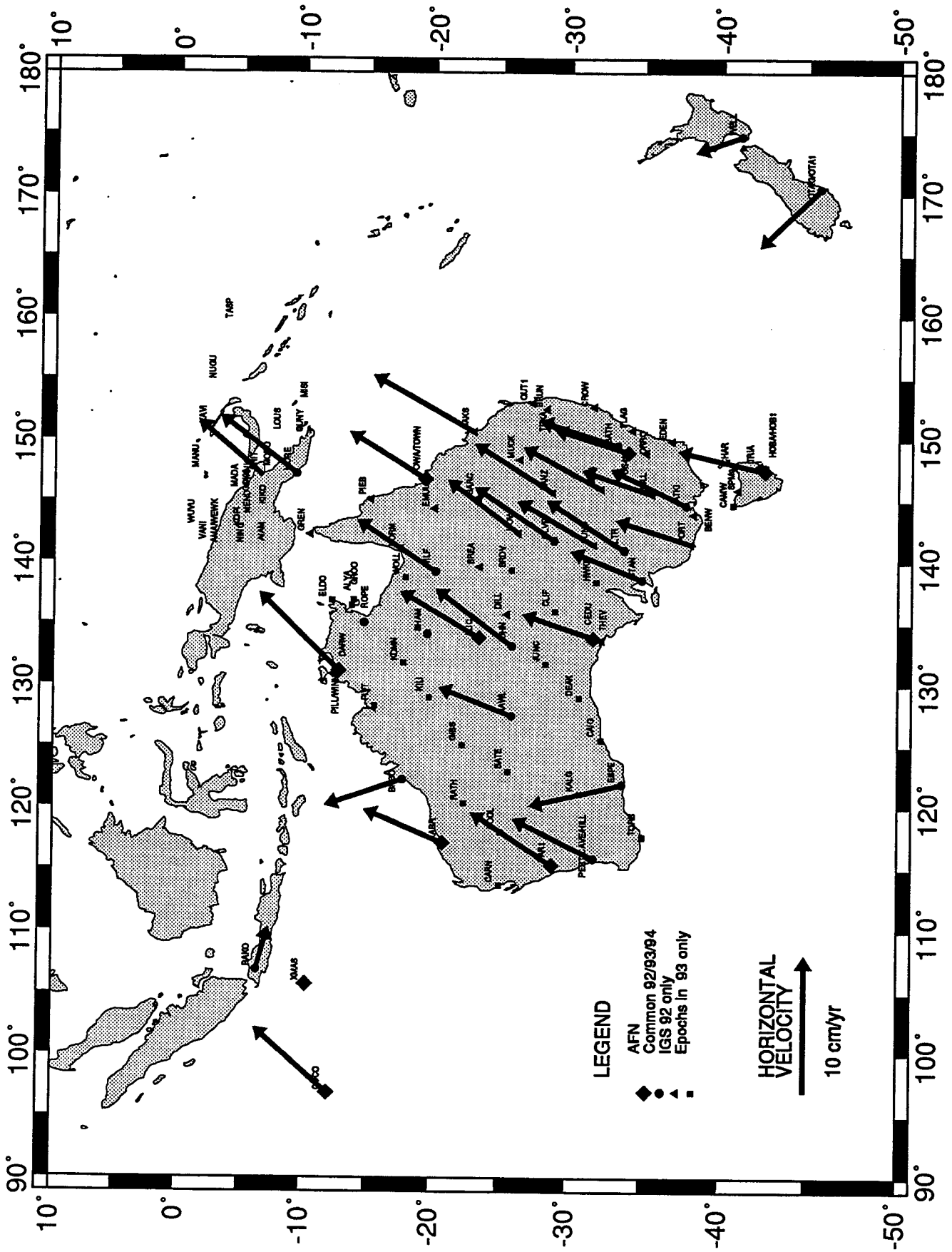

Figure 13.4: Plot of the local North and East components of the station velocity over the Australian region for all multiple-occupation stations with a time interval of at least 6 months. Figure 13.5 shows the complementary vertical component.

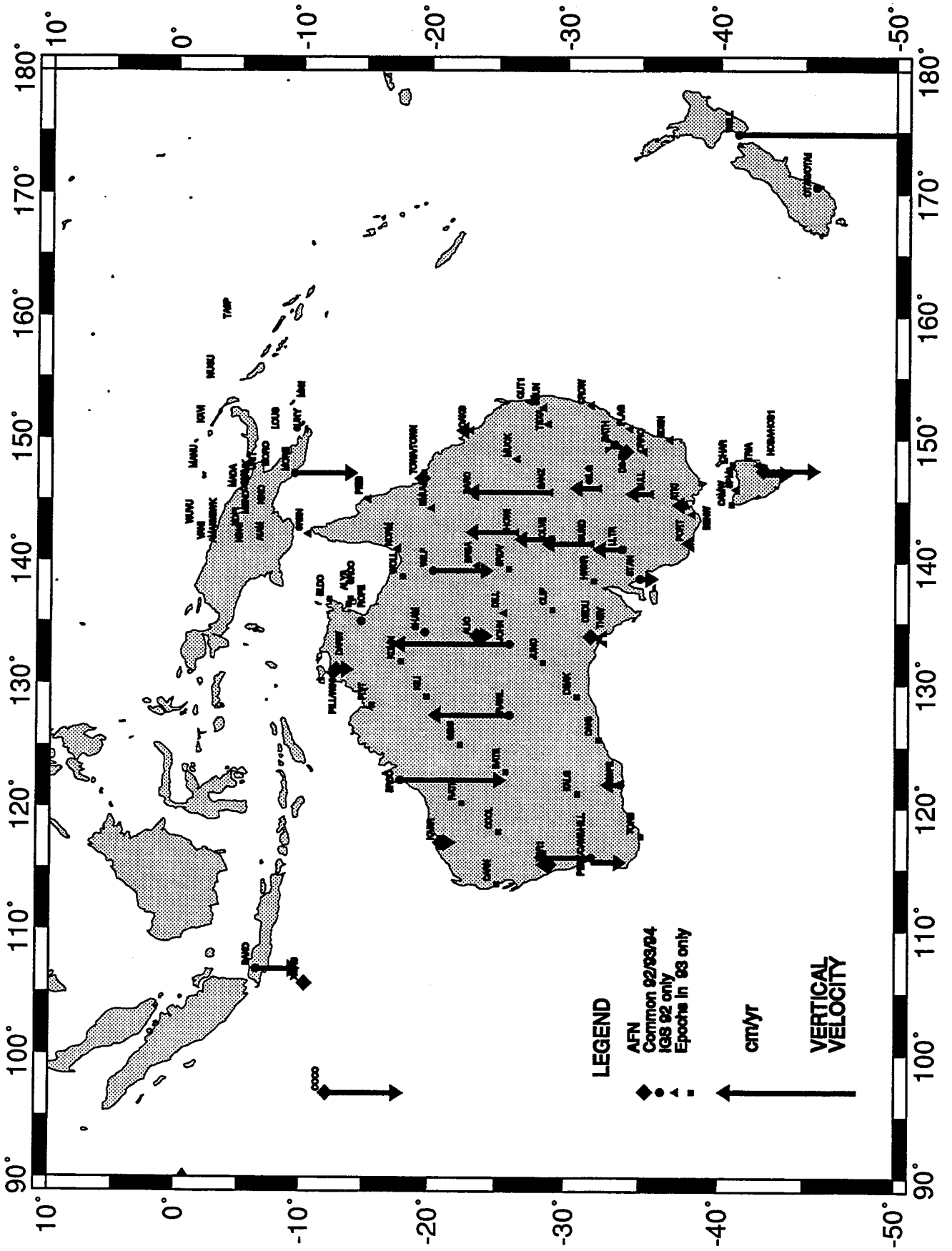

Figure 13.5: Plot of the local Up component of the station velocity over the Australian region for all multiple-occupation stations with a time interval of at least 6 months. Figure 13.4 shows the complementary horizontal components.

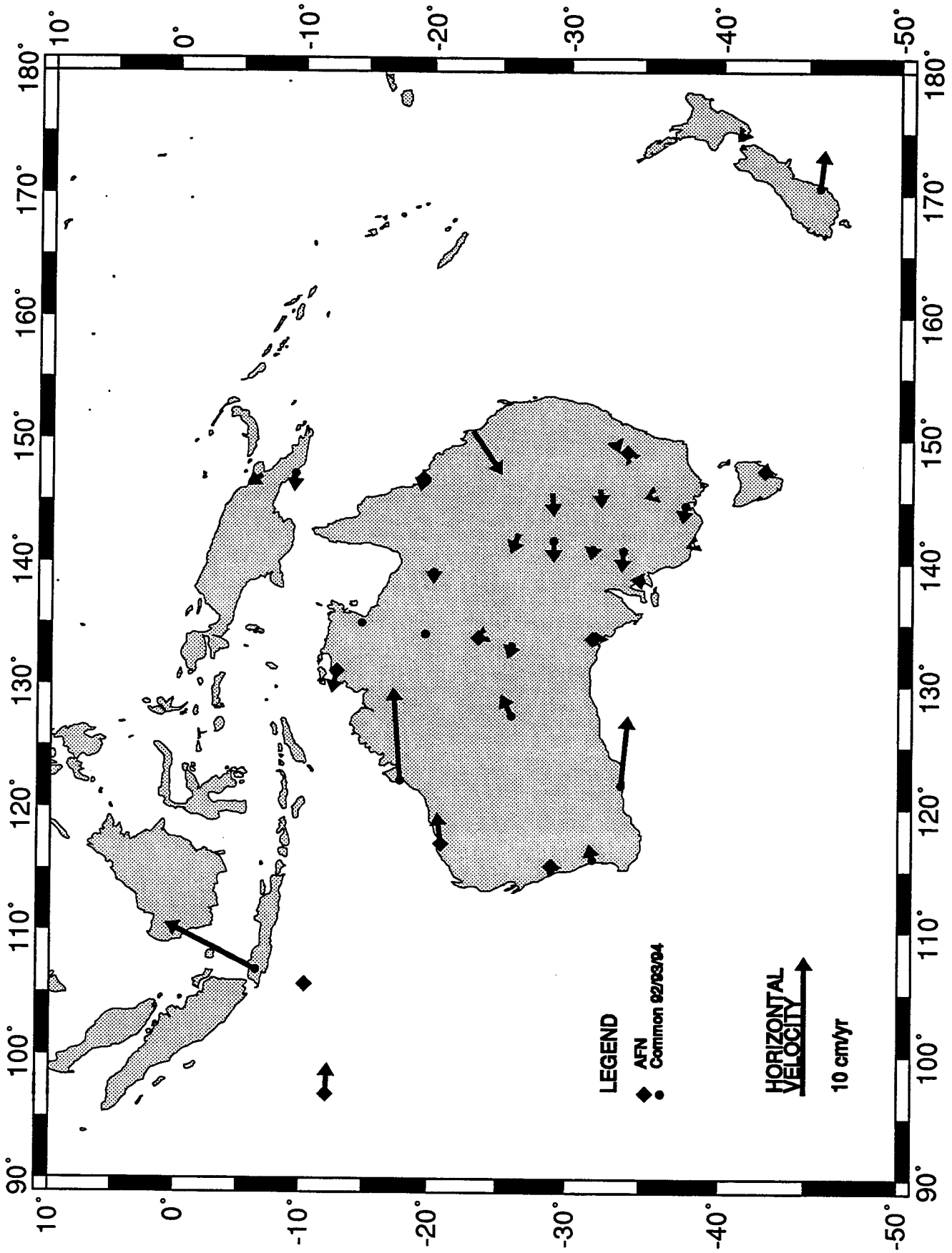

Figure 13.6: Plot of the residual horizontal field between the field of Figure 13.4 and the field as determined from the NUVEL model for the Australian plate. Stations not on the Australian plate show motion with respect to the Australian plate.

al. (1984) after considering seismicity, fault plane solutions to earthquakes and *in situ* stress measurements. The quality and reliability of these vectors is expected to improve as additional data become available. Nevertheless, the agreement suggests that the horizontal positions and their associative velocities are correct.

The second feature to note is the behaviour of some of the stations at the margins of the Australian continent. Clearly, Bakosurtanal is on the Eurasian plate while Otago is on the Pacific plate. The location of Wellington and Lae is not conclusive or alternatively both stations lie in active deformation zones. Additional data would help clarify the geophysics of these areas.

The overall message of this figure and analysis is that there is significant non-rigid behaviour of the Australian continent. This result will become even clearer after a further reoccupation of stations contributing to the solution.

Figure 13.7 is a typical plot of the output of the GLOBK back-solution, with a Gauss-Markov process applied to all the non-fixed stations. The analysis of plots, such as Figure 13.7 enabled many inconsistencies to be addressed.

13.2 Conversion of data to the Epoch 1994.0

The GLOBK solutions refer to two distinct epochs. The first is the solution epoch, which is the last day of data used by GLOBK. The second epoch is the mean uncorrelated time. It is the mean time where the position vector and its rate are uncorrelated. GLOBK only determines this uncorrelated time when velocities are estimated. The problem that needed to be addressed was that many of the ANN stations were only observed once and hence additional information was needed to get these estimates to a common epoch, along with those stations at which it was possible to estimate velocity.

Several methods are available to force GLOBK to provide velocity estimates. The following two options were investigated.

- Solve for velocities at all stations. In those cases where only one epoch was observed, the determined velocity was discarded in favour of the velocity estimated from supplementary information. These supplementary values could be from the NUVEL model itself or an area average of the velocity determined from other nearby stations. It was this later approach that was subsequently adopted in this project.

- Set the a-priori velocity estimates to zero and tightly constrain the velocities so that they remain zero. Then estimate the velocity field from external information, such as the NUVEL model and replace the a-priori zero estimates with the NUVEL model estimates.

The former option was chosen primarily because there was a better recovery or precision of the position components when they were now fixed with both bias free and external bias flags set. The determined velocity estimates are given in Appendix A and B. Note there were were no constraints placed on the velocity values and hence the model was not constrained to follow a particular hypothesis.

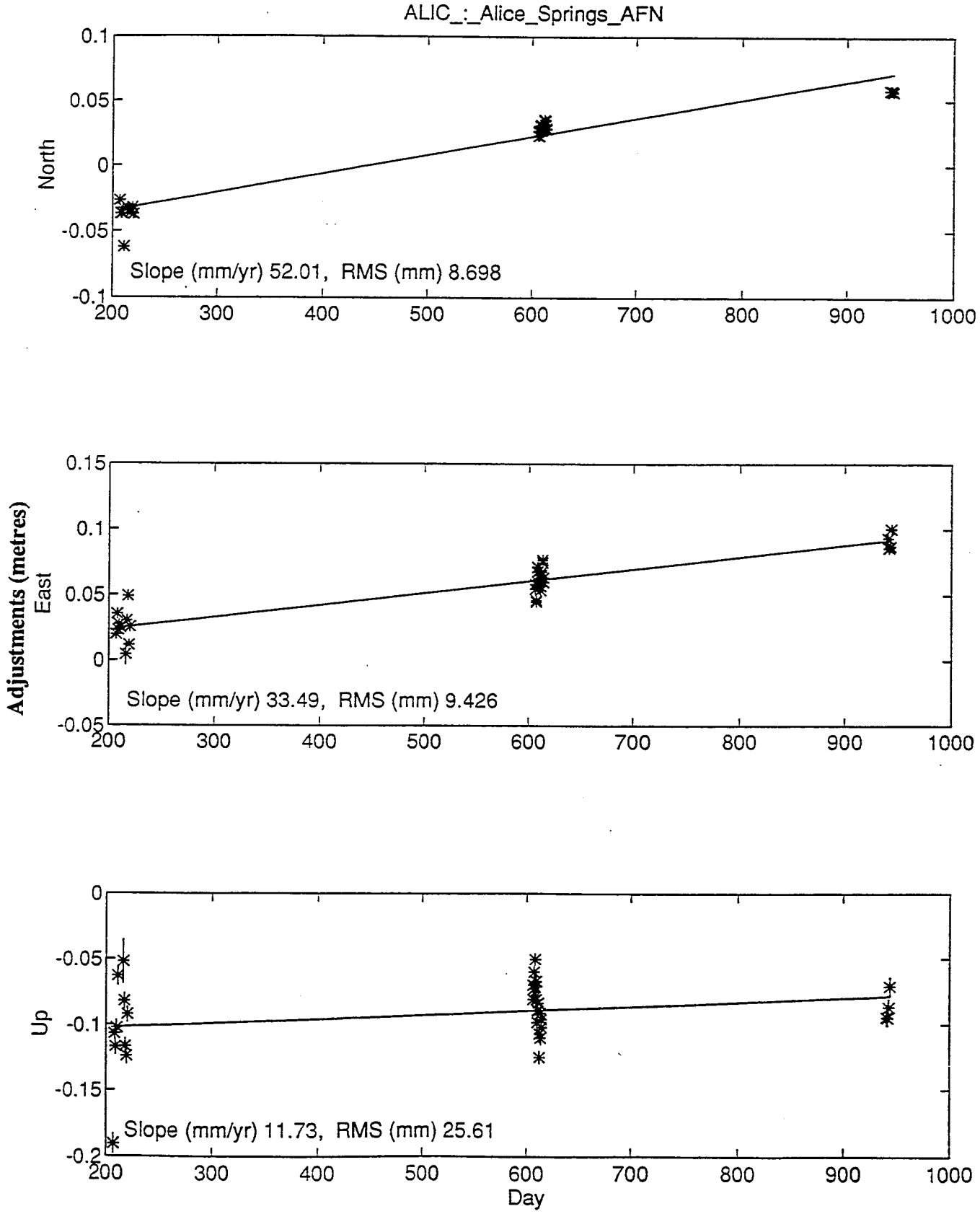

Figure 13.7: Plot of North, East and Up component repeatabilites at Alice Springs

The choice of the area size over which the velocity field was considered uniform considered two criteria. These were the radii of the rings and the number of stations within the enclosed area. The ring radii started at 250 km and increased to 1000 km in steps of 250 km. At least two stations, with velocity estimates, were required to form a mean value which was then used to compute the velocity field at the site. Tests showed that the largest radii did not exceed 750 km. At this stage, it was possible to estimate the 1994.0 values of all sites as all sites had position and rate estimates.

This procedure has several drawbacks. Chief amongst these is the precision of the transformation and its uniform applicability over the region. Other problems included the number of stations that should contribute to the enclosed area or whether one should wait for an opportunity to get the required information.

13.3 Future Prospects

GPS theory and practice have advanced at a rapid rate over the last 4 years. The primary cause of rapid development is almost certainly the demonstrations, pilot programs and introduction of the International Geodynamics Service (IGS) Bureau, with its archive and combination, high-quality, global orbits and other products.

At the University of Canberra, all of the data sets described in this report, plus many others, have been recomputed. Specifically, we have changed the way the orbits are modelled and computed, used upgraded software and decoupled the determination of the tropospheric function with the determination of height for major networks such as described above. This has resulted in nrms values now being close to 0.20, on average, and all χ^2 values being well under 5. The mean nrms value is near 1.8 compared to a value in excess of 12 in previous solutions.

Of the available data, there is a significant data set from May 1995 that needs to be included in the solution as this will provide the third epoch at most of the Tide gauge sites.

The ITRF94 values for *core* stations have been used in the solution and it is found that our global solutions had an rms fit to the global frame of less than 1 cm with very small scale errors. Additionally the scale error and the ties to the global frame were well within current expectations. Specifically the scale is 0.2 ppb different from that defined in ITRF94.

This new work has been mainly done by Russell Tiesler and should be available shortly. Thus the cycle of defining new GDA's, first established by Tony Bomford in the early seventies shortly after the release of his model, is again emulated.

Much work still remains to be done. Of special interest are more frequent and more precise connections of the tide gauge stations and those stations that will add to the determination of a stress map for Australia. These coordinate solutions can be used for geophysical as well as climate studies. It is the latter that requires a long and stable baseline of observations. The data reported here clearly fulfills the first epoch role on all accounts and will remain an important dataset for some time to come.

Chapter 14

Bibliography

Allman, J.S. and Veenstra, C., 1984. Geodetic Model of Australia 1982, *Technical Report 33*, Division of National Mapping, Canberra, Australia.

Ananga, N., 1993. Geodetic Positioning and Monitoring of Tide Gauge Datums, *Ph.D. Thesis*, University of Sydney, Sydney, Australia.

Ananga, N., Coleman, R. and Rizos, C., 1993. Monitoring of Levelling Networks. *Aust.J.Geod.* Photo.Surv., 58: 9-22.

Ananga, N., Coleman, R. and Rizos, C., 1994a. Variance-Covariance Estimation of GPS Networks. *Bulletin Géodésique*, 68(2): 77-87.

Ananga, N., Coleman, R. and Rizos, C., 1994b. Zero-Epoch HeigGeodetic Fixing of Tide Gauge Bench Marks, –More–(30hts and Height Velocities. *Survey Review,*, 32(251): 307-313.

Ashjaee, J. and Lorenz, R., 1992. Precision GPS surveying after Y-code, *Proceedings* of ION GPS-92, Fifth International Technical Meeting of the Satellite Division of the Institute of Navigation, Albuquerque, New Mexico, September 16-18, pp. 657-659.

Bath, M., 1974. *Spectral Analysis in Geophysics*, Elsevier Scientific, Amsterdam, The Netherlands

Blinn, J.F., 1977. A Homogeneous Formulation for Lines in 3D-Space, *Proceedings:* SIGGRAPH'77, also published as *Computer Graphics*, 10(2): 229-234.

Bomford, A.G., 1967. The geodetic adjustment of Australia, *Survey Review*, 114: 52-71.

Bomford, A.G., 1973. Geodetic Models of Australia, *Technical Report 17*, Division of National Mapping, Canberra, Australia.

Boucher, C., Altamimi, Z. and Duhem, L., 1993. ITRF92 and its associated velocity field, *Technical Note 15*, Central Bureau of IERS - Observatoire de Paris, Paris, France.

Bowring, B.R., 1985. The accuracy of geodetic latitude and height equations, *Survey Review*, 28: 202-206.

Bracewell, R.N., 1978. *The Fourier Transform and its Applications*, McGraw-Hill New York, New York.

Buisson, J., McCaskill, T., Humphry Smith, D.C., Morgan, P. and Woodger, J., 1977. Precise worldwide station synchronization via the Navstar GPS, Navigation Technology Satellite (NTS-1), *Proceedings* 8^{th} Annual Precise Time and Time Interval Applications and Planning Meeting, NASA Document X-814-77-149, Goddard Space Flight Center, Greenbelt, Maryland, USA.

Carlbom, I. and Paciorek, J., 1978. Planar Geometric Projections and Viewing Transformations, *ACM Computing Surveys*, 10(4): 465-502.

Carter, W.E., Aubrey, D.G., Baker, T., Boucher, C., LeProvost, C., Peltier, W.R., Zumberge, M., Rapp, R.H., Schutz, B.E., Emery, K.O., and Enfield, D.B., 1989. Geodetic Fixing of Tide Gauge Bench Marks, *Technical Report WHO-89-31*, Woods Hole Oceanographic Institution, Woods Hole, Massachusetts, USA.

Claerbout, J.F., 1976. *Fundamentals of Geophysical Data Processing with Aplications to Petroleum Prospecting*, Blackwell Scientific, Oxford, United Kingdom.

Cross, P.A., 1983, Advanced least squares applied to position-fixing, *Working Paper 6*, Department of Surveying, North East London Polytechnic, United Kingdom.

Davis, J.L., Herring, T.A., Shapiro, I.I., Rogers, A.E.E. and Elgered, G., 1985. Geodesy by radio interferometry: Effects of atmospheric modelling errors on estimates of baseline length, *Radio Science*, 20: 1593-1607.

Eisenhart, C., 1963. Realistic Evaluation of the Precision and Accuracy of Instrument Calibration Systems, *Journal of Research of national Bureau of Standards*, 67C(2): 161-187.

Ekman, M., 1989. Impacts of geodynamic phenomena on systems for height and gravity, *Bulletin Geodesique*, 63: 281-296.

Gagnon, P., 1976. Step-by-step adjustment procedures for large horizontal geodetic networks, *Technical Report 38*, Department of Surveying Engineering, University of New Brunswick, Fredericton, New Brunswick, Canada.

Gurtner, W., 1989. The receiver independent RINEX format, *CSTG GPS-Bulletin*, 2(3): x-x.

Harvey, B.R., Stolz, A., Jauncey, D.L., Niell, A.E., Morabito, D.D. and Preston, R.A., 1983. Results of the Australian Geodetic VLBI Experiment, *Aust.J.Geod.Photo.Surv.*, 38: 39-51.

Harvey, B.R., 1985. The combination of VLBI and ground data for Geodesy and Geophysics, *UNISURV S-27*, School of Surveying, University of New South Wales, New South Wales, Australia.

Heiskanen, W. A. and Moritz, H., 1967. *Physical Geodesy*, Freeman and Co., San Francisco, California, USA.

Herring, T.A., Davis, J.L. and Shapiro, I.I., 1990. Geodesy by Radio Interferometry *Journal of Geophysical Research*, 95: 12,561-12,581.

Hofmann-Wellenhof, B., Lichtenegger, H. and Collins, J., 1994. *GPS Theory and Practice*, 3^{rd} *Ed.*, Springer-Verlag, Wien.

Jaldehag, R.T.K., 1995. Space Geodesy Techniques: An Experimental and Theoretical Study of Antenna Related Error Sources, *Technical Report 276* School of Electrical and Computer Engineering, Chalmers University of Technology, Göteborg, Sweden.

Kaplan, E.D., Ed., 1996. *Understanding GPS Principles and Applications*, Artech House, Norwood, Massachusetts.

Krakiwsky, E.J., 1976. A synthesis of recent advances in the method of least squares, *Technical Report 42*, Department of Surveying Engineering, University of New Brunswick, Fredericton, New Brunswick, Canada.

Lambeck, K., McQueen, H.W.S., Stephenson, R.A. and Denham, D., 1984. *Annales Geophysicae*, 2(6):723-742

Lambeck, K., 1988. *Geophysical Geodesy*, Clarendon Press, Oxford, United Kingdom.

Lee, L.P., 1978. First Order Geodetic Triangulation of New Zealand 1909-49 1973-74, *Technical Series No. 1*, Department of Lands and Survey, Wellington, New Zealand.

Lerch, F.J., Nerem, R.S., Putney, B.H., Felsentreger, T.L., Canchez,B.V., Klosko, S.M., Patel, G.B., Williamson, R.G., Chin, D.S., Chan, J.C., Rachlin, N.L., Chandler, N.L., McCarthy, J.J., Marshall, J.A., Luthcke, S.B., Pavlis, D.W., Robbins, J.W., Kapoor, S. and Pavlis, E.C., 1992. Geopotential Models for the Earth from Satellite Tracking, Altimeter and Surface Gravity Observations: GEM-T3 and GET-T3S, *NASA Technical Memorandum 104555*, NASA Goddard Space Flight Center, Greenbelt, Maryland, USA.

Leppert, K., 1972. Two Australian Baselines for the Pageos World Triangulation, *Technical Report 11*, Division of National Mapping, Canberra, Australia.

Maxwell, E.A., 1946. *Methods of Plane Projective Geometery based on the Use of General Homogeneous Coordinates*, Cambridge University Press, Cambridge.

Maxwell, E.A., 1951. *General Homogeneous Coordinates in Space of Three Dimensions*, Cambridge University Press, Cambridge.

McCarthy, D., 1992. IERS Standards (1992), *IERS Techninal Note 13*, Central Bureau of IERS - Observatoire de Paris, Paris, France.

Morgan, P., 1992. An Analysis of the Australian Height Datum: 1971, *The Australian Surveyor*, 37(1): 46-63.

Morgan, P., Xing, C., Rogers, C. and Larden, D.R., 1986. Validation Procedures in GPS Surveys *Australian Journal of Geodesy, Photogrammetry and Surveying*, 45: 1-35.

Morgan, P., 1994. National Baseline Sea-level Monitoring Program: FXSinal report University of Canberra, Faculty of Information Sciences & Engineering, 86 pp.

NMCA., 1976. *Report on Work Completed During the Period 1945-1975* National Mapping Council of Australia, Canberra, Australia.

Noll, M., 1967. A Computer technique for Displaying N-dimensional Hyperobjects, *Communications of the ACM*, 10(8): 469-473.

Pearse M.B., Kearsley A.H.W. and Morgan P. 1995. Height comparisons on the Australian National GPS Network (ANN): First Results, *Proceedings: Gravity and Geoid*, Joint Symposium of the International Gravity Commission and the International Geoid Commission, Graz Austria Sept 11-17 1994, In Press.

Reilly, W.I., 1990. Horizontal Crustal Deformation on the Hikurangi Margin, *New Zealand Journal of Geology and Geophysics*, 33: 393-400

Richardus, P. and Adler, R.K., 1972. *Map Projections*, North-Holland, Amsterdam, the Netherlands.

Roelse, A., Granger, H.W. and Graham, J.W., 1971. The Adjustment of the Australian Levelling Survey 1970-1971, *Technical Report 12*, Division of National Mapping, Canberra, Australia.

Saastamoinen, J., 1972. Atmospheric correction for the troposphere and stratosphere in radio ranging of satellites, in *The use of Artificial Satellites for Geodesy, Geophys. Monogr. Ser.*, Vol 15, edited by S. W. Hendriksen et al., pp 247-251, American Geophysical Union, Washington, D.C.

Scherneck, H.-G., 1983. Crustal Loading Affecting VLBI Sites, *Report 20*, Department of Geodesy, University of Uppsala, Uppsala, Sweden.

Schupler, B.R. and Clark, T.A., 1991. How Different antennas affect the GPS Observable *GPS World*, pp 32-36, Nov/Dec 1991

Stolz, A., Harvey, B.R., Jauncey, D.L., Niell, A.E., Morabito, D.D. and Preston, R.A., 1983. Australian Baselines Measured by Radio Interferometry, *Australian Surveyor*, 31(8): 563-566.

Torge, W., 1991. *Geodesy*, de Gryuter, New York.

Tukey, J.W., 1977. *Exploratory data Analysis*, Addison-Wesley, Reading, Massachusetts, USA.

Wells, D., Ed., 1986. *Guide to GPS Positioning*, Canadian GPS Associates, Fredericton, New Brunswick.

White, N.J., Coleman, R., Church, J.A., Morgan, P.J. and Walker, S.K., 1994. A Southern Hemisphere Verification for the TOPEX/POSEIDON Satellite Altimeter Mission. *J.Geophys.Res.*, 99(C12): 24505-24516.

Appendix A

Cartesian Coordinates and Rates

Table A.1: Cartesian Coordinates and Rates for Australian regional stations at the epoch 1994.0 in the ITRF92 Terrestrial Reference System

Station	X (metres)	Y (metres)	Z (metres)	$\dot{X}$ (m/yr)	$\dot{Y}$ (m/yr)	$\dot{Z}$ (m/yr)
D078-GPS	-5042730.9900	140230.6848	-3890300.2427	0.1013	-0.0122	0.1371
D100-GPS	-4989460.3973	191252.5830	-3955756.5149	0.1013	-0.0122	0.1371
D431-GPS	-4922647.6720	265115.0836	-4033578.8105	0.1013	-0.0122	0.1371
D072-GPS	-5039298.7131	311182.3088	-3884430.1479	0.1013	-0.0122	0.1371
D473-GPS	-4977955.0840	355512.0562	-3959577.5284	0.1013	-0.0122	0.1371
D143-GPS	-4794050.6415	364491.7157	-4177890.1801	0.1013	-0.0122	0.1371
D131-GPS	-4860522.4524	383529.0984	-4098473.5172	0.1013	-0.0122	0.1371
D452-GPS	-5041354.9592	441059.3926	-3869624.5997	0.1013	-0.0122	0.1371
D045-GPS	-5105842.3286	461788.3347	-3781953.3181	0.1013	-0.0122	0.1371
WELL-GPS	-4780648.7245	436507.1571	-4185440.2946	0.1013	-0.0122	0.1371
D482-GPS	-4780644.8729	436500.5397	-4185441.7187	0.1013	-0.0122	0.1371
D483-GPS	-4780653.0685	436501.1891	-4185431.5747	0.1013	-0.0122	0.1371
D026-GPS	-5167214.2279	496239.2231	-3693852.2384	0.1013	-0.0122	0.1371
D105-GPS	-4929039.9701	498221.5952	-4004033.2328	0.1013	-0.0122	0.1371
D425-GPS	-4741512.8455	480470.7058	-4225018.4664	0.1013	-0.0122	0.1371
D158-GPS	-4763996.1858	561250.8914	-4190671.3317	0.1013	-0.0122	0.1371
D191-GPS	-4660964.2794	571445.5828	-4302316.2717	0.1013	-0.0122	0.1371
D212-GPS	-4590224.0472	585796.1568	-4375478.4298	0.0169	0.0156	0.0634
D469-GPS	-4802026.0179	617521.3076	-4138427.8733	0.1013	-0.0122	0.1371
D309-GPS	-4616400.1424	745241.6630	-4324328.3276	0.0169	0.0156	0.0634
OTA1-GPS	-4387888.2924	733420.7713	-4555178.3895	-0.0676	0.0435	-0.0103
OTAG-GPS	-4388297.1286	733507.2537	-4554771.8134	-0.0676	0.0435	-0.0103
D229-GPS	-4519608.8594	774369.4541	-4419877.1168	-0.0676	0.0435	-0.0103
D320-GPS	-4566344.3399	808430.3739	-4364476.8205	0.0169	0.0156	0.0634
D474-GPS	-4303267.1586	894811.2808	-4606633.4229	-0.0676	0.0435	-0.0103
MCM1-GPS	-1310621.8456	310414.1786	-6213400.5028	0.0885	0.1059	0.1617

Station	X (metres)	Y (metres)	Z (metres)	$\dot{X}$ (m/yr)	$\dot{Y}$ (m/yr)	$\dot{Z}$ (m/yr)
MCMZ-GPS	-1310620.7356	310413.8581	-6213395.5260	-0.0337	0.1694	0.0143
MCMU-GPS	-1310696.2575	310469.1539	-6213368.3784	0.0060	-0.0010	-0.0005
MAC1-GPS	-3464038.4875	1334172.7432	-5169224.4229	0.0252	0.0287	0.0797
BRUN-GPS	-5020720.6887	2499067.3824	-3027805.1424	-0.0604	-0.0135	0.0522
QUT1-GPS	-5046767.6356	2568457.2423	-2925288.0198	-0.0604	-0.0135	0.0522
MISI-GPS	-5576759.3149	2862001.0982	-1175220.9941	0.0010	-0.0606	0.0625
CROW-GPS	-4821560.5349	2482901.7885	-3345746.2911	-0.0445	-0.0026	0.0448
SUGA-GPS	-5126895.1908	2689409.7223	-2667603.4023	-0.0763	-0.0244	0.0595
EC19-GPS	-4644354.4306	2549989.7035	-3539040.9586	-0.0417	0.0007	0.0434
TEXA-GPS	-4899985.7139	2692597.6207	-3060138.8690	-0.0604	-0.0135	0.0522
FLAG-GPS	-4597579.6442	2564075.5742	-3589224.2233	-0.0417	0.0007	0.0434
KAVI-GPS	-5562412.8934	3107929.9853	-285346.1430	0.0346	-0.0790	0.0556
MULA-GPS	-5115155.0414	2872883.2597	-2494381.9443	-0.0763	-0.0244	0.0595
OAKS-GPS	-5113583.0076	2874686.8657	-2495474.9939	-0.0763	-0.0244	0.0595
GUNY-GPS	-5453535.7761	3105804.8345	-1134062.6702	0.0010	-0.0606	0.0625
EDEN-GPS	-4408335.6554	2554609.0262	-3823983.7456	-0.0390	0.0040	0.0420
BATH-GPS	-4594786.6787	2699295.9223	-3494244.2603	-0.0445	-0.0026	0.0448
BASS-GPS	-5113385.2659	3047287.0377	-2283502.2418	-0.0561	-0.0188	0.0523
DS42-GPS	-4460996.0690	2682557.1440	-3674443.8750	-0.0390	0.0040	0.0420
ORRO-GPS	-4446478.9991	2678112.6547	-3696270.2442	-0.0390	0.0040	0.0420
MUCK-GPS	-4860805.1238	2991738.3613	-2837860.6892	-0.0763	-0.0244	0.0595
CHAR-GPS	-4101998.2962	2566148.2099	-4141759.1625	-0.0287	-0.0033	0.0581
TRIA-GPS	-3990830.5766	2501499.2998	-4286339.0565	-0.0287	-0.0033	0.0581
HOB1-GPS	-3950184.0211	2522364.5031	-4311588.3595	-0.0284	-0.0002	0.0491
TAS1-GPS	-3950184.1718	2522364.5982	-4311588.5165	-0.0287	-0.0033	0.0581
HOBA-GPS	-3950071.2739	2522415.2177	-4311638.5118	-0.0289	-0.0064	0.0670
MANU-GPS	-5367596.3793	3437943.3333	-226704.9152	0.0346	-0.0790	0.0556
MORE-GPS	-5288519.1495	3409952.8442	-1038574.3025	0.0010	-0.0606	0.0625
UNIT-GPS	-5313156.6724	3450683.5537	-736065.7174	0.0346	-0.0790	0.0556
TOWN-GPS	-5041025.0099	3296980.3260	-2090553.2964	-0.0484	-0.0124	0.0477
TOWA-GPS	-5036492.2153	3298900.0894	-2099859.6998	-0.0436	-0.0196	0.0496
WANK-GPS	-5262950.4891	3539058.6433	-678565.2911	0.0346	-0.0790	0.0556
GILG-GPS	-4470744.2846	3016577.4932	-3394500.2156	-0.0547	0.0047	0.0360
SPM9-GPS	-3989108.2925	2699944.0419	-4166666.7211	-0.0287	-0.0033	0.0581
MADA-GPS	-5252527.3738	3571989.7005	-575482.7035	0.0346	-0.0790	0.0556
BANZ-GPS	-4610424.0573	3148699.8001	-3073895.9791	-0.0715	0.0014	0.0339
BULL-GPS	-4271156.7001	2929587.3610	-3710093.7300	-0.0525	0.0086	0.0300
GOKA-GPS	-5221573.4302	3603226.5357	-671387.0314	0.0346	-0.0790	0.0556
BARC-GPS	-4808764.1872	3330247.5313	-2535054.5179	-0.0585	-0.0084	0.0398
PIEB-GPS	-5045675.9581	3522171.1643	-1674322.6483	-0.0460	-0.0160	0.0486
CAMW-GPS	-3942894.7653	2790759.3801	-4151125.7085	-0.0409	0.0014	0.0464
ATKI-GPS	-4119867.9459	2918876.4103	-3884282.5049	-0.0569	0.0012	0.0341
EMUU-GPS	-4867427.1051	3487912.8351	-2191805.0680	-0.0460	-0.0160	0.0486
KIKO-GPS	-5133225.7538	3695553.7380	-818612.3235	0.0178	-0.0698	0.0590
BENW-GPS	-4040118.7907	2944818.6419	-3948080.7284	-0.0531	0.0060	0.0347

Station	X (metres)	Y (metres)	Z (metres)	$\dot{X}$ (m/yr)	$\dot{Y}$ (m/yr)	$\dot{Z}$ (m/yr)
MEND-GPS	-5109574.8990	3759378.9127	-678236.4787	0.0346	-0.0790	0.0556
WUVU-GPS	-5080554.9817	3851303.5880	-191868.9911	0.0346	-0.0790	0.0556
HOWI-GPS	-4523298.6557	3485332.8222	-2832259.2522	-0.0734	0.0027	0.0299
GREN-GPS	-4955371.5138	3842257.5162	-1163835.1673	0.0178	-0.0698	0.0590
OLVE-GPS	-4384863.2839	3448388.9492	-3082582.1579	-0.0695	0.0000	0.0379
PORT-GPS	-3922962.0275	3117568.5233	-3932953.8073	-0.0493	0.0108	0.0352
SUND-GPS	-4239032.1574	3377934.9506	-3351167.9153	-0.0714	0.0113	0.0284
VANI-GPS	-4972629.8542	3983208.0945	-296767.1498	0.0178	-0.0698	0.0590
AIAM-GPS	-4934886.4567	3958248.6276	-810301.0775	0.0178	-0.0698	0.0590
NORM-GPS	-4730120.0312	3818318.6256	-1924292.9059	-0.0134	-0.0424	0.0707
LLTR-GPS	-4117215.8359	3333728.2826	-3539972.6089	-0.0662	0.0020	0.0347
BREA-GPS	-4451878.8249	3786508.9281	-2546090.3718	-0.0434	-0.0198	0.0503
BRDV-GPS	-4355678.9694	3740239.9054	-2769201.3854	-0.0715	0.0014	0.0339
WILF-GPS	-4529722.3703	3909094.1985	-2203537.4758	-0.0134	-0.0424	0.0707
STAN-GPS	-3916469.9306	3455298.5594	-3649242.6864	-0.0376	0.0023	0.0433
HWKR-GPS	-4055042.3969	3597135.1672	-3350585.2553	-0.0566	0.0046	0.0386
WOLL-GPS	-4523681.4818	4083441.9674	-1876187.1840	-0.0134	-0.0424	0.0707
ELDO-GPS	-4543818.3826	4263716.3100	-1358180.7404	-0.0455	-0.0325	0.0585
GROO-GPS	-4489874.8421	4265802.3329	-1519917.9740	-0.0455	-0.0325	0.0585
ALYA-GPS	-4487413.8457	4269234.1196	-1517520.5319	-0.0455	-0.0325	0.0585
CLIF-GPS	-4018348.2663	3874926.6863	-3075181.8976	-0.0716	0.0290	0.0303
ROPE-GPS	-4365327.2981	4355926.9921	-1623109.7841	-0.0455	-0.0325	0.0585
SHAM-GPS	-4189540.2937	4309929.9144	-2127995.3602	-0.0372	-0.0117	0.0569
ALIC-GPS	-4052051.7667	4212836.2154	-2545106.0270	-0.0372	-0.0117	0.0569
CEDU-GPS	-3753472.1258	3912741.0400	-3347961.0314	-0.0384	0.0072	0.0485
THEV-GPS	-3739792.1066	3911197.4469	-3364706.8290	-0.0384	0.0072	0.0485
JOHN-GPS	-3929600.9087	4183187.9321	-2774030.9686	-0.1049	0.0508	0.0121
JUNC-GPS	-3733309.6434	4184348.0072	-3029196.8511	-0.0716	0.0290	0.0303
DARW-GPS	-4091358.7443	4684606.8443	-1408580.6421	-0.0455	-0.0325	0.0585
KDMN-GPS	-4017368.7006	4629016.3761	-1759073.4150	-0.0455	-0.0325	0.0585
WINN-GPS	-4077253.8165	4710296.8045	-1363184.0506	-0.0455	-0.0325	0.0585
PILL-GPS	-4073402.4180	4712253.6263	-1367883.4031	-0.0455	-0.0325	0.0585
KILI-GPS	-3777444.0303	4668166.3353	-2143627.2037	-0.0168	0.0009	0.0539
DEAK-GPS	-3448618.5488	4265480.0042	-3244110.0545	-0.0384	0.0072	0.0485
RAWL-GPS	-3586428.2710	4539145.9159	-2678896.4702	-0.0657	0.0499	0.0236
PIVT-GPS	-3806295.3980	4823694.5992	-1704766.4978	-0.0455	-0.0325	0.0585
CAIG-GPS	-3137868.7025	4393013.3631	-3385234.0926	-0.0140	0.0474	0.0484
GIBS-GPS	-3365970.1336	4763630.5436	-2572813.4470	-0.0657	0.0499	0.0236
BATE-GPS	-3124556.0462	4828049.6623	-2750068.6197	-0.0657	0.0499	0.0236
BROO-GPS	-3241494.8130	5134037.3208	-1946745.5098	0.0524	-0.0356	0.0812
ESPE-GPS	-2800864.6674	4500724.7038	-3534886.5540	-0.0140	0.0474	0.0484
KALG-GPS	-2853510.9353	4665806.4059	-3271380.8174	-0.0140	0.0474	0.0484
RATH-GPS	-2979541.6801	5090380.5135	-2420393.9051	-0.0216	0.0013	0.0593
COOL-GPS	-2711522.9806	5098133.3635	-2700765.2415	-0.0333	0.0046	0.0561
TORB-GPS	-2422745.3976	4630068.1973	-3645119.6094	-0.0294	0.0309	0.0482

Station	X (metres)	Y (metres)	Z (metres)	$\dot{X}$ (m/yr)	$\dot{Y}$ (m/yr)	$\dot{Z}$ (m/yr)
KARR-GPS	-2713832.1548	5303935.1866	-2269515.1969	-0.0216	0.0013	0.0593
CAVE-GPS	-2375390.5822	4875553.9136	-3345387.2311	-0.0372	0.0226	0.0480
PERT-GPS	-2368686.8464	4881316.5734	-3341796.3393	-0.0511	0.0401	0.0336
PER2-GPS	-2368701.4393	4881361.7213	-3341721.0234	-0.0232	0.0052	0.0625
YAR1-GPS	-2389025.3940	5043316.8520	-3078530.8610	-0.0450	0.0080	0.0530
CARN-GPS	-2325633.2766	5290021.9041	-2690511.0450	-0.0450	0.0080	0.0530
CAS1-GPS	-901776.2214	2409383.4976	-5816748.4875	0.0789	0.0254	0.0635
BAKO-GPS	-1836968.8853	6065617.2539	-716257.7371	-0.0055	-0.0254	-0.0026
XMAS-GPS	-1696463.0894	6039563.0380	-1149236.1540	-0.0055	-0.0254	-0.0026
COCO-GPS	-741949.8528	6190961.6634	-1337768.7238	-0.0213	-0.0298	0.0640
DAV1-GPS	486854.4996	2285099.3657	-5914955.7712	0.0879	0.0413	0.0907
MAW1-GPS	1111287.1375	2168911.2969	-5874493.6449	-0.0682	0.2827	-0.1131

Appendix B

Ellipsoidal Coordinates

Table B.1: Ellipsoidal Coordinates for Australian regional stations at the epoch 1994.0 in the ITRF92 Terrestrial Reference System using the GRS80 ellipsoid

Station	Latitude ° ' "			Longitude ° ' "			Height (m)
D078-GPS	-37	49	28.35304	178	24	25.56709	360.4046
D100-GPS	-38	34	30.55098	177	48	17.46739	323.3581
D431-GPS	-39	28	44.35127	176	55	2.08344	119.1917
D072-GPS	-37	45	34.08616	176	27	59.07120	95.7400
D473-GPS	-38	36	57.77646	175	54	54.09498	760.2960
D143-GPS	-41	10	48.51645	175	39	7.79799	590.7335
D131-GPS	-40	14	24.72023	175	29	17.92278	143.5113
D452-GPS	-37	35	21.78987	175	0	0.08182	318.9152
D045-GPS	-36	36	0.79634	174	49	55.38454	141.7072
WELL-GPS	-41	16	29.61840	174	46	58.63710	37.6903
D482-GPS	-41	16	29.74798	174	46	58.90521	35.2948
D483-GPS	-41	16	29.32507	174	46	58.90944	34.7814
D026-GPS	-35	37	2.08620	174	30	51.69149	174.3308
D105-GPS	-39	8	2.40608	174	13	41.56679	263.0298
D425-GPS	-41	44	56.57194	174	12	49.71581	254.4628
D158-GPS	-41	19	53.84777	173	16	51.24571	791.6599
D191-GPS	-42	41	14.71038	173	0	37.00849	405.3861
D212-GPS	-43	35	20.28650	172	43	38.37828	510.3047
D469-GPS	-40	42	46.81161	172	40	19.95151	169.4509
D309-GPS	-42	57	11.69538	170	49	46.76628	919.3539
OTA1-GPS	-45	52	10.21097	170	30	39.32228	25.8608
OTAG-GPS	-45	51	51.33602	170	30	38.49251	24.7680
D229-GPS	-44	8	19.85883	170	16	39.36634	1005.8357
D320-GPS	-43	27	20.86207	169	57	37.17235	114.6616
D474-GPS	-46	32	12.95240	168	15	12.38563	176.4384
MCM1-GPS	-77	50	55.12506	166	40	31.12990	-0.9271

Station	Latitude °	'	"	Longitude °	'	"	Height (m)
MCMZ-GPS	-77	50	55.12765	166	40	31.13849	-6.0353
MCMU-GPS	-77	50	52.22506	166	40	25.56417	-14.4224
MAC1-GPS	-54	29	58.32004	158	56	9.00266	-6.6970
BRUN-GPS	-28	31	29.59007	153	32	17.30597	135.6274
QUT1-GPS	-27	28	38.50976	153	1	37.34165	92.9494
MISI-GPS	-10	41	19.90490	152	49	58.93878	87.4564
CROW-GPS	-31	50	36.58469	152	45	12.34357	84.2702
SUGA-GPS	-24	53	7.18107	152	19	11.61938	110.8009
EC19-GPS	-33	55	8.39942	151	13	51.40996	83.4636
TEXA-GPS	-28	51	19.62316	151	12	38.54610	538.2668
FLAG-GPS	-34	27	57.57857	150	51	5.54610	73.8323
KAVI-GPS	-2	34	53.06528	150	48	22.53578	78.8282
MULA-GPS	-23	10	22.49768	150	40	46.65585	118.4490
OAKS-GPS	-23	11	1.39095	150	39	24.29479	101.0041
GUNY-GPS	-10	18	37.50877	150	20	18.09080	94.8706
EDEN-GPS	-37	4	27.40104	149	54	28.50180	17.3258
BATH-GPS	-33	25	46.83164	149	34	1.46525	756.6148
BASS-GPS	-21	7	0.30552	149	12	26.85779	122.2681
DS42-GPS	-35	23	57.15627	148	58	47.98425	665.4397
ORRO-GPS	-35	38	11.11630	148	56	22.05628	1356.2943
MUCK-GPS	-26	35	24.69731	148	23	18.41369	393.4747
CHAR-GPS	-40	45	12.62805	147	58	13.88724	51.2338
TRIA-GPS	-42	29	43.20575	147	55	12.11831	9.4803
HOB1-GPS	-42	48	14.30120	147	26	23.98712	56.7413
TAS1-GPS	-42	48	14.30101	147	26	23.98716	56.9787
HOBA-GPS	-42	48	16.98506	147	26	19.43548	41.1263
MANU-GPS	-2	3	2.29337	147	21	37.63577	129.7507
MORE-GPS	-9	26	2.76968	147	11	12.20017	116.6098
UNIT-GPS	-6	40	16.96985	146	59	52.37457	130.3893
TOWN-GPS	-19	15	35.33064	146	48	50.83207	97.8212
TOWA-GPS	-19	20	50.42839	146	46	30.79057	587.0769
WANK-GPS	-6	8	52.07208	146	4	52.44226	510.0151
GILG-GPS	-32	21	35.60370	145	59	27.58343	544.3694
SPM9-GPS	-41	3	1.96813	145	54	31.39183	13.1450
MADA-GPS	-5	12	41.28824	145	46	56.19305	73.2927
BANZ-GPS	-28	59	56.69551	145	40	7.63275	172.7741
BULL-GPS	-35	47	51.10212	145	33	13.55344	171.7434
GOKA-GPS	-6	4	53.07151	145	23	30.44618	1664.5802
BARC-GPS	-23	34	20.05634	145	17	45.46539	308.9165
PIEB-GPS	-15	19	9.27718	145	4	57.89985	482.2619
CAMW-GPS	-40	51	50.61387	144	42	33.65441	164.7047
ATKI-GPS	-37	45	26.78865	144	40	58.40926	145.1206
EMUU-GPS	-20	13	42.56447	144	22	31.01084	1029.3539
KIKO-GPS	-7	25	24.65305	144	14	55.76611	88.9646
BENW-GPS	-38	29	8.01962	143	54	42.89137	491.4423

Station	Latitude °	'	"	Longitude °	'	"	Height (m)
MEND-GPS	-6	8	36.73422	143	39	22.16540	1815.1543
WUVU-GPS	-1	44	7.59465	142	50	10.07846	79.0563
HOWI-GPS	-26	32	3.93095	142	23	4.94019	227.0781
GREN-GPS	-10	35	2.60770	142	12	39.57623	130.0452
OLVE-GPS	-29	5	16.66830	141	49	2.71231	323.8375
PORT-GPS	-38	18	53.46573	141	31	33.30620	47.4451
SUND-GPS	-31	53	57.29431	141	26	59.62844	408.7922
VANI-GPS	-2	41	5.28039	141	18	15.65564	80.5157
AIAM-GPS	-7	20	51.81934	141	16	1.44646	95.4652
NORM-GPS	-17	40	34.44714	141	5	17.93669	64.2569
LLTR-GPS	-33	55	45.90840	141	0	9.90541	34.4842
BREA-GPS	-23	40	53.17727	139	37	2.80928	196.5645
BRDV-GPS	-25	54	2.59091	139	20	49.82785	67.3920
WILF-GPS	-20	20	34.96747	139	12	22.37156	554.1586
STAN-GPS	-35	7	23.98207	138	34	46.95124	306.5707
HWKR-GPS	-31	53	36.62709	138	25	28.20983	328.9838
WOLL-GPS	-17	13	13.77943	137	55	40.90319	106.7987
ELDO-GPS	-12	22	36.51110	136	49	17.53688	158.1425
GROO-GPS	-13	52	41.31191	136	27	57.51147	88.8758
ALYA-GPS	-13	51	21.04613	136	25	38.20927	78.3881
CLIF-GPS	-29	0	44.70598	136	2	27.43939	158.6511
ROPE-GPS	-14	50	26.70919	135	3	42.32485	140.3899
SHAM-GPS	-19	37	2.26629	134	11	18.58482	469.7934
ALIC-GPS	-23	40	12.44592	133	53	7.84757	603.3580
CEDU-GPS	-31	52	0.01664	133	48	35.37527	144.8021
THEV-GPS	-32	2	43.02837	133	42	59.81642	33.7132
JOHN-GPS	-25	56	49.10537	133	12	34.73757	572.1019
JUNC-GPS	-28	32	18.44138	131	44	22.57652	283.0071
DARW-GPS	-12	50	37.35839	131	7	57.84838	125.1969
KDMN-GPS	-16	6	56.74843	130	57	13.03673	125.8544
WINN-GPS	-12	25	23.75409	130	52	46.59297	82.8984
PILL-GPS	-12	28	0.37696	130	50	27.75380	80.3566
KILI-GPS	-19	46	1.84282	128	58	46.25763	496.4282
DEAK-GPS	-30	46	13.00604	128	57	19.29696	143.8142
RAWL-GPS	-24	59	41.11412	128	18	45.52085	825.2427
PIVT-GPS	-15	36	20.45568	128	16	34.93457	86.0525
CAIG-GPS	-32	15	48.94197	125	32	15.70268	93.8260
GIBS-GPS	-23	56	39.45238	125	14	41.77508	413.6373
BATE-GPS	-25	42	25.54927	122	54	34.65078	480.2142
BROO-GPS	-17	53	21.77744	122	16	2.01517	27.8824
ESPE-GPS	-33	52	27.14736	121	53	40.51916	28.9722
KALG-GPS	-31	3	19.19831	121	26	56.74414	446.4700
RATH-GPS	-22	26	47.68187	120	20	29.86357	532.7493
COOL-GPS	-25	12	51.30660	118	0	25.14925	468.5455
TORB-GPS	-35	4	42.02314	117	37	17.10430	237.9792

Station	Latitude °	'	"	Longitude °	'	"	Height (m)
KARR-GPS	-20	58	53.17004	117	5	49.87255	109.2463
CAVE-GPS	-31	50	24.69345	115	58	31.94599	-6.5496
PERT-GPS	-31	48	7.09697	115	53	6.88607	12.8498
PER2-GPS	-31	48	4.21487	115	53	6.63587	13.0949
YAR1-GPS	-29	2	47.61687	115	20	49.10049	241.2905
CARN-GPS	-25	6	50.39917	113	43	53.60955	-7.3505
CAS1-GPS	-66	17	0.08957	110	31	10.94259	22.5518
BAKO-GPS	-6	29	27.79329	106	50	56.06875	158.2226
XMAS-GPS	-10	26	58.57131	105	41	22.60130	260.3867
COCO-GPS	-12	11	18.06832	96	50	2.27115	-35.2212
DAV1-GPS	-68	34	38.36100	77	58	21.41472	44.5035
MAW1-GPS	-67	36	17.15953	62	52	14.58011	59.1845

Appendix C

The Site Table File: *sittbl.*

The following tabular information is a modified copy of the GAMIT sittbl. file which is used to specify the type of modelling applied to a station. Later entries have precedence over earlier entries. In general, only one global sittbl. file exists in the GAMIT structure and hence it is usually global in character.

The following explanations apply:

FIX Fix one or more of the three station coordinates. NNN = none fixed.

WFILE Does a weather file exist? NONE = none exist.

COORD.CONSTR Coordinate constraint, in metres to apply to the station. Coordinates are the GAMIT latitude, longitude and radius.

EPOCH The epoch range of the Xfile. In this case the range is 1-2880 which is equivalent to 30 second data.

CUTOFF The elevation cutoff applied to the Xfile.

CLK The type of modelling to be applied to the receiver clock. This is now a discontinued option.

KLOCK The type of modelling applied to the receiver clock. Also synonymous with the order of polynomial fit.

DZEN Model to be used to evaluate dry zenith delay. SAAS = Saastamoinen model.

WZEN Model to be used to evaluate wet zenith delay. SAAS = Saastamoinen model.

DMAP Mapping function to be used for the dry component. CFA = Center for Astrophysics (Davis et al., 1985).

WMAP Mapping function to be used for the wet component. CFA = Center for Astrophysics (Davis et al., 1985)

MET. VALUE Standard atmosphere values of pressure, temperature and relative humidity.

```
SITE             FIX  WFILE  --COORD.CONSTR.-- --EPOCH--  CUTOFF  CLK KLK DZEN  WZEN  DMAP  WMAP
     ---MET. VALUE----

       << ITRF CORE SITES >>
YAR1 Yaragadee   NNN   NONE  0.20  0.20  0.20   001-  *    15.0   NNN  3  SAAS  SAAS  CFA   CFA
     1013.25 20.0 50.0
SANT Santiago    NNN   NONE  0.20  0.20  0.20   001-  *    15.0   NNN  3  SAAS  SAAS  CFA   CFA
     1013.25 20.0 50.0
HART Hartebeestho NNN  NONE  0.20  0.20  0.20   001-  *    15.0   NNN  3  SAAS  SAAS  CFA   CFA
     1013.25 20.0 50.0
DS42 CANBERRA NEW NNN  NONE  0.20  0.20  0.20   001-  *    15.0   NNN  3  SAAS  SAAS  CFA   CFA
     1013.25 20.0 50.0
TIDB CANBERRA NEW NNN  NONE  0.20  0.20  0.20   001-  *    15.0   NNN  3  SAAS  SAAS  CFA   CFA
     1013.25 20.0 50.0
ALGO Algonquin   NNN   NONE  0.20  0.20  0.20   001-  *    15.0   NNN  3  SAAS  SAAS  CFA   CFA
     1013.25 20.0 50.0
DS1B Goldstone   NNN   NONE  0.20  0.20  0.20   001-  *    15.0   NNN  3  SAAS  SAAS  CFA   CFA
     1013.25 20.0 50.0
GOLD Goldstone   NNN   NONE  0.20  0.20  0.20   001-  *    15.0   NNN  3  SAAS  SAAS  CFA   CFA
     1013.25 20.0 50.0
DS60 MADRID      NNN   NONE  0.20  0.20  0.20   001-  *    15.0   NNN  3  SAAS  SAAS  CFA   CFA
     1013.25 20.0 50.0
MADR MADRID      NNN   NONE  0.20  0.20  0.20   001-  *    15.0   NNN  3  SAAS  SAAS  CFA   CFA
     1013.25 20.0 50.0
FAIR Fairbanks   NNN   NONE  0.20  0.20  0.20   001-  *    15.0   NNN  3  SAAS  SAAS  CFA   CFA
     1013.25 20.0 50.0
KOKB Kokee Rogue NNN   NONE  0.20  0.20  0.20   001-  *    15.0   NNN  3  SAAS  SAAS  CFA   CFA
     1013.25 20.0 50.0
KOKR Kokee Rogue NNN   NONE  0.20  0.20  0.20   001-  *    15.0   NNN  3  SAAS  SAAS  CFA   CFA
     1013.25 20.0 50.0
KOSG Kootwijk    NNN   NONE  0.20  0.20  0.20   001-  *    15.0   NNN  3  SAAS  SAAS  CFA   CFA
     1013.25 20.0 50.0
TROM Tromso      NNN   NONE  0.20  0.20  0.20   001-  *    15.0   NNN  3  SAAS  SAAS  CFA   CFA
     1013.25 20.0 50.0
WTZ1 Wettzell    NNN   NONE  0.20  0.20  0.20   001-  *    15.0   NNN  3  SAAS  SAAS  CFA   CFA
     1013.25 20.0 50.0
WETT Wettzell    NNN   NONE  0.20  0.20  0.20   001-  *    15.0   NNN  3  SAAS  SAAS  CFA   CFA
     1013.25 20.0 50.0
YELL Yellowknife NNN   NONE  0.20  0.20  0.20   001-  *    15.0   NNN  3  SAAS  SAAS  CFA   CFA
     1013.25 20.0 50.0

       << ROGUE FIDUCIALS >>
DRAO Penticton   NNN   NONE  5.00  5.00  5.00   001-  *    15.0   NNN  3  SAAS  SAAS  CFA   CFA
     1013.25 20.0 50.0
ONSA Onsala      NNN   NONE  5.00  5.00  5.00   001-  *    15.0   NNN  3  SAAS  SAAS  CFA   CFA
     1013.25 20.0 50.0
USUD Usuda       NNN   NONE  5.00  5.00  5.00   001-  *    15.0   NNN  3  SAAS  SAAS  CFA   CFA
     1013.25 20.0 50.0
HONE Honefuss    NNN   NONE  5.00  5.00  5.00   001-  *    15.0   NNN  3  SAAS  SAAS  CFA   CFA
     1013.25 20.0 50.0
HERS Herstmonceux NNN  NONE  5.00  5.00  5.00   001-  *    15.0   NNN  3  SAAS  SAAS  CFA   CFA
     1013.25 20.0 50.0
NALL Ny Allesund NNN   NONE  5.00  5.00  5.00   001-  *    15.0   NNN  3  SAAS  SAAS  CFA   CFA
     1013.25 20.0 50.0
NYAL Ny Allesund NNN   NONE  5.00  5.00  5.00   001-  *    15.0   NNN  3  SAAS  SAAS  CFA   CFA
     1013.25 20.0 50.0
SANG Santiago    NNN   NONE  5.00  5.00  5.00   001-  *    15.0   NNN  3  SAAS  SAAS  CFA   CFA
     1013.25 20.0 50.0
MCM1 McMurdo     NNN   NONE  5.00  5.00  5.00   001-  *    15.0   NNN  3  SAAS  SAAS  CFA   CFA
     1013.25 20.0 50.0
MCM4 McMurdo     NNN   NONE  5.00  5.00  5.00   001-  *    15.0   NNN  3  SAAS  SAAS  CFA   CFA
     1013.25 20.0 50.0
```

```
MCMR McMurdo       NNN   NONE  5.00  5.00  5.00   001-  *    15.0   NNN  3  SAAS  SAAS  CFA   CFA
     1013.25 20.0 50.0
MATE Matera        NNN   NONE  5.00  5.00  5.00   001-  *    15.0   NNN  3  SAAS  SAAS  CFA   CFA
     1013.25 20.0 50.0
ARON Algonquin     NNN   NONE  5.00  5.00  5.00   001-  *    15.0   NNN  3  SAAS  SAAS  CFA   CFA
     1013.25 20.0 50.0
MATG Matera        NNN   NONE  5.00  5.00  5.00   001-  *    15.0   NNN  3  SAAS  SAAS  CFA   CFA
     1013.25 20.0 50.0
YKN1 Yellowknife   NNN   NONE  5.00  5.00  5.00   001-  *    15.0   NNN  3  SAAS  SAAS  CFA   CFA
     1013.25 20.0 50.0
KOKB Kokee Rogue   NNN   NONE  5.00  5.00  5.00   001-  *    15.0   NNN  3  SAAS  SAAS  CFA   CFA
     1013.25 20.0 50.0
USUG Usuda         NNN   NONE  5.00  5.00  5.00   001-  *    15.0   NNN  3  SAAS  SAAS  CFA   CFA
     1013.25 20.0 50.0
WETB Wettzell      NNN   NONE  5.00  5.00  5.00   001-  *    15.0   NNN  3  SAAS  SAAS  CFA   CFA
     1013.25 20.0 50.0

       << SOUTHERN CALIFORNIA PERMANENT GPS GEODETIC ARRAY >>
PIN1 PINON FLAT 1  NNN   NONE  5.00  5.00  5.00   001-  *    15.0   NNN  3  SAAS  SAAS  CFA   CFA
     1013.25 20.0 50.0
PIN2 PINON FLAT 2  NNN   NONE  15.00 5.00  5.00   001-  *    15.0   NNN  3  SAAS  SAAS  CFA   CFA
     1013.25 20.0 50.0
ROCH Roches        NNN   NONE  5.00  5.00  5.00   001-  *    15.0   NNN  3  SAAS  SAAS  CFA   CFA
     1013.25 20.0 50.0
SIO1 SCRIPPS 1     NNN   NONE  5.00  5.00  5.00   001-  *    15.0   NNN  3  SAAS  SAAS  CFA   CFA
     1013.25 20.0 50.0
SIO2 SCRIPPS 2     NNN   NONE  5.00  5.00  5.00   001-  *    15.0   NNN  3  SAAS  SAAS  CFA   CFA
     1013.25 20.0 50.0
SIO3 SCRIPPS 2     NNN   NONE  5.00  5.00  5.00   001-  *    15.0   NNN  3  SAAS  SAAS  CFA   CFA
     1013.25 20.0 50.0
JPL1 JPL MESA      NNN   NONE  5.00  5.00  5.00   001-  *    15.0   NNN  3  SAAS  SAAS  CFA   CFA
     1013.25 20.0 50.0
JPLM JPL MESA      NNN   NONE  5.00  5.00  5.00   001-  *    15.0   NNN  3  SAAS  SAAS  CFA   CFA
     1013.25 20.0 50.0
PGC0               NNN   NONE  5.00  5.00  5.00   001-  *    15.0   NNN  3  SAAS  SAAS  CFA   CFA
     1013.25 20.0 50.0

       << DSN Network >>
DS10 GOLDSTONE     NNN   NONE  0.20  0.20  0.20   001-  *    15.0   NNN  3  SAAS  SAAS  CFA   CFA
     1013.25 20.0 50.0
GOLD Goldstone     NNN   NONE  0.20  0.20  0.20   001-  *    15.0   NNN  3  SAAS  SAAS  CFA   CFA
     1013.25 20.0 50.0
MADR Madrid        NNN   NONE  0.20  0.20  0.20   001-  *    15.0   NNN  3  SAAS  SAAS  CFA   CFA
     1013.25 20.0 50.0
TIDB CANBIERS      NNN   NONE  0.20  0.20  0.20   001-  *    15.0   NNN  3  SAAS  SAAS  CFA   CFA
     1013.25 20.0 50.0 Y
DS40 CANBERRA      NNN   NONE  5.00  5.00  5.00   001-  *    15.0   NNN  3  SAAS  SAAS  CFA   CFA
     1013.25 20.0 50.0
CANB CANBGIG       NNN   NONE  5.00  5.00  5.00   001-  *    15.0   NNN  3  SAAS  SAAS  CFA   CFA
     1013.25 20.0 50.0
DS41 CANBERRA TMP  NNN   NONE  5.00  5.00  5.00   001-  *    15.0   NNN  3  SAAS  SAAS  CFA   CFA
     1013.25 20.0 50.0
TAIW Taiwan        NNN   NONE  5.00  5.00  5.00   001-  *    15.0   NNN  3  SAAS  SAAS  CFA   CFA
     1013.25 20.0 50.0
WES2 Westford      NNN   NONE  5.00  5.00  5.00   001-  *    15.0   NNN  3  SAAS  SAAS  CFA   CFA
     1013.25 20.0 50.0

       << Other mainly global network stations >>
VNDP Vandenberg    NNN   NONE  5.00  5.00  5.00   001-  *    15.0   NNN  3  SAAS  SAAS  CFA   CFA
     1013.25 20.0 50.0
METS Metsahovi     NNN   NONE  5.00  5.00  5.00   001-  *    15.0   NNN  3  SAAS  SAAS  CFA   CFA
     1013.25 20.0 50.0
```

```
PAMA CNES Tahiti      NNN   NONE  5.00  5.00  5.00  001-  *    15.0  NNN  3  SAAS  SAAS  CFA  CFA
     1013.25 20.0 50.0
MASP Maspalomas       NNN   NONE  5.00  5.00  5.00  001-  *    15.0  NNN  3  SAAS  SAAS  CFA  CFA
     1013.25 20.0 50.0
MAS1 Maspalomas       NNN   NONE  5.00  5.00  5.00  001-  *    15.0  NNN  3  SAAS  SAAS  CFA  CFA
     1013.25 20.0 50.0
GRAZ Graz             NNN   NONE  5.00  5.00  5.00  001-  *    15.0  NNN  3  SAAS  SAAS  CFA  CFA
     1013.25 20.0 50.0
STJO St. Johns        NNN   NONE  5.00  5.00  5.00  001-  *    15.0  NNN  3  SAAS  SAAS  CFA  CFA
     1013.25 20.0 50.0
DARW Darwin           NNN   NONE  5.00  5.00  5.00  001-  *    15.0  NNN  3  SAAS  SAAS  CFA  CFA
     1013.25 20.0 50.0
ALBH Albert           NNN   NONE  5.00  5.00  5.00  001-  *    15.0  NNN  3  SAAS  SAAS  CFA  CFA
     1013.25 20.0 50.0
ARGE Buenos Aires     NNN   NONE  500.  500.  500.  001-  *    15.0  NNN  3  SAAS  SAAS  CFA  CFA
     1013.25 20.0 50.0
RCM5 Richmond         NNN   NONE  5.00  5.00  5.00  001-  *    15.0  NNN  3  SAAS  SAAS  CFA  CFA
     1013.25 20.0 50.0
SHAO China            NNN   NONE  5.00  5.00  5.00  001-  *    15.0  NNN  3  SAAS  SAAS  CFA  CFA
     1013.25 20.0 50.0
TSKB Tsukuba          NNN   NONE  5.00  5.00  5.00  001-  *    15.0  NNN  3  SAAS  SAAS  CFA  CFA
     1013.25 20.0 50.0

       << CIGNET FIDUCIALS >>
TOWN Townsville       NNN   NONE  5.00  5.00  5.00  001-  *    15.0  NNN  3  SAAS  SAAS  CFA  CFA
     1013.25 20.0 50.0
WELL Wellington       NNN   NONE  5.00  5.00  5.00  001-  *    15.0  NNN  3  SAAS  SAAS  CFA  CFA
     1013.25 20.0 50.0
TAS1 Tasmania         NNN   NONE  5.00  5.00  5.00  001-  *    15.0  NNN  1  SAAS  SAAS  CFA  CFA
     1013.25 20.0 50.0
HOB1 Tasmania         NNN   NONE  5.00  5.00  5.00  001-  *    15.0  NNN  3  SAAS  SAAS  CFA  CFA
     1013.25 20.0 50.0

       << NSW IGS 92 STATIONS >>
OLVE Olive            NNN   NONE  100.  100.  100.  001-  *    15.0  NNN  3  SAAS  SAAS  CFA  CFA
     1013.25 20.0 50.0
BANZ BarrigunZero     NNN   NONE  100.  100.  100.  001-  *    15.0  NNN  3  SAAS  SAAS  CFA  CFA
     1013.25 20.0 50.0
TEXA Texas Pillar     NNN   NONE  100.  100.  100.  001-  *    15.0  NNN  3  SAAS  SAAS  CFA  CFA
     1013.25 20.0 50.0
BRUN Brunswick        NNN   NONE  100.  100.  100.  001-  *    15.0  NNN  3  SAAS  SAAS  CFA  CFA
     1013.25 20.0 50.0
SUND Sundown          NNN   NONE  100.  100.  100.  001-  *    15.0  NNN  3  SAAS  SAAS  CFA  CFA
     1013.25 20.0 50.0
GILG Gilgunnia        NNN   NONE  100.  100.  100.  001-  *    15.0  NNN  3  SAAS  SAAS  CFA  CFA
     1013.25 20.0 50.0
CULG Culgoora         NNN   NONE  100.  100.  100.  001-  *    15.0  NNN  3  SAAS  SAAS  CFA  CFA
     1013.25 20.0 50.0
CROW Crowdy           NNN   NONE  100.  100.  100.  001-  *    15.0  NNN  3  SAAS  SAAS  CFA  CFA
     1013.25 20.0 50.0
LLTR Lake Littra      NNN   NONE  100.  100.  100.  001-  *    15.0  NNN  3  SAAS  SAAS  CFA  CFA
     1013.25 20.0 50.0
BULL Bullanginya      NNN   NONE  100.  100.  100.  001-  *    15.0  NNN  3  SAAS  SAAS  CFA  CFA
     1013.25 20.0 50.0
EDEN Eden             NNN   NONE  100.  100.  100.  001-  *    15.0  NNN  3  SAAS  SAAS  CFA  CFA
     1013.25 20.0 50.0
MUCK Muckadilla       NNN   NONE  100.  100.  100.  001-  *    15.0  NNN  3  SAAS  SAAS  CFA  CFA
     1013.25 20.0 50.0
HOWI Howitt           NNN   NONE  100.  100.  100.  001-  *    15.0  NNN  3  SAAS  SAAS  CFA  CFA
     1013.25 20.0 50.0
```

```
      << TIDE GAUGE STATIONS >>
FLAG Port Kembla  NNN   NONE  100.  100.  100.   001-  *    15.0   NNN  3  SAAS  SAAS  CFA   CFA
     1013.25 20.0 50.0
PORT Porland VIC  NNN   NONE  100.  100.  100.   001-  *    15.0   NNN  3  SAAS  SAAS  CFA   CFA
     1013.25 20.0 50.0
BENW Lorne        NNN   NONE  100.  100.  100.   001-  *    15.0   NNN  3  SAAS  SAAS  CFA   CFA
     1013.25 20.0 50.0
ESPE Esperance    NNN   NONE  100.  100.  100.   001-  *    15.0   NNN  3  SAAS  SAAS  CFA   CFA
     1013.25 20.0 50.0
PILL Darwin pill  NNN   NONE  100.  100.  100.   001-  *    15.0   NNN  3  SAAS  SAAS  CFA   CFA
     1013.25 20.0 50.0
PERT Pert         NNN   NONE  0.20  0.20  0.20   001-  *    15.0   NNN  3  SAAS  SAAS  CFA   CFA
     1013.25 20.0 50.0
TRIA Triabunna    NNN   NONE  100.  100.  100.   001-  *    15.0   NNN  3  SAAS  SAAS  CFA   CFA
     1013.25 20.0 50.0
WINN Darwin TG    NNN   NONE  100.  100.  100.   001-  *    15.0   NNN  3  SAAS  SAAS  CFA   CFA
     1013.25 20.0 50.0
THEV Thevenard    NNN   NONE  100.  100.  100.   001-  *    15.0   NNN  3  SAAS  SAAS  CFA   CFA
     1013.25 20.0 50.0
STAN Pt Stanvac   NNN   NONE  100.  100.  100.   001-  *    15.0   NNN  3  SAAS  SAAS  CFA   CFA
     1013.25 20.0 50.0
BROO Broome       NNN   NONE  100.  100.  100.   001-  *    15.0   NNN  3  SAAS  SAAS  CFA   CFA
     1013.25 20.0 50.0
OAKS Oaks QLD     NNN   NONE  100.  100.  100.   001-  *    15.0   NNN  3  SAAS  SAAS  CFA   CFA
     1013.25 20.0 50.0
SPM9 Burnie TAS   NNN   NONE  100.  100.  100.   001-  *    15.0   NNN  3  SAAS  SAAS  CFA   CFA
     1013.25 20.0 50.0

      << AUSTRALIAN FIDUCIAL NETWORK STATIONS >>
ALIC AliceSprings NNN   NONE  5.00  5.00  5.00   001-  *    15.0   NNN  3  SAAS  SAAS  CFA   CFA
     1013.25 20.0 50.0
BATH Bathurst     NNN   NONE  5.00  5.00  5.00   001-  *    15.0   NNN  3  SAAS  SAAS  CFA   CFA
     1013.25 20.0 50.0
COCO Cocos Is     NNN   NONE  5.00  5.00  5.00   001-  *    15.0   NNN  3  SAAS  SAAS  CFA   CFA
     1013.25 20.0 50.0
HOBA Hobart       NNN   NONE  5.00  5.00  5.00   001-  *    15.0   NNN  3  SAAS  SAAS  CFA   CFA
     1013.25 20.0 50.0
HOB2 Hobart       NNN   NONE  5.00  5.00  5.00   001-  *    15.0   NNN  3  SAAS  SAAS  CFA   CFA
     1013.25 20.0 50.0
KARR Karratha     NNN   NONE  5.00  5.00  5.00   001-  *    15.0   NNN  3  SAAS  SAAS  CFA   CFA
     1013.25 20.0 50.0
ORRO Orroral      NNN   NONE  5.00  5.00  5.00   001-  *    15.0   NNN  3  SAAS  SAAS  CFA   CFA
     1013.25 20.0 50.0
TOWA Townsville   NNN   NONE  5.00  5.00  5.00   001-  *    15.0   NNN  3  SAAS  SAAS  CFA   CFA
     1013.25 20.0 50.0
AUST Smithfield   NNN   NONE  5.00  5.00  5.00   001-  *    15.0   NNN  3  SAAS  SAAS  CFA   CFA
     1013.25 20.0 50.0

      << AUSTRALASIAN REGIONAL STATIONS IN ARN  SET >>
AIAM Aiambak PNG  NNN   NONE  100.  100.  100.   001-  *    15.0   NNN  3  SAAS  SAAS  CFA   CFA
     1013.25 20.0 50.0
LOSU Losuia PNG   NNN   NONE  100.  100.  100.   001-  *    15.0   NNN  3  SAAS  SAAS  CFA   CFA
     1013.25 20.0 50.0
MISI MisimaIs PNG NNN   NONE  100.  100.  100.   001-  *    15.0   NNN  3  SAAS  SAAS  CFA   CFA
     1013.25 20.0 50.0
MORE Moresby PNG  NNN   NONE  100.  100.  100.   001-  *    15.0   NNN  3  SAAS  SAAS  CFA   CFA
     1013.25 20.0 50.0
OTAG Otago Uni NZ NNN   NONE  100.  100.  100.   001-  *    15.0   NNN  3  SAAS  SAAS  CFA   CFA
     1013.25 20.0 50.0
VANI Vanimo PNG   NNN   NONE  100.  100.  100.   001-  *    15.0   NNN  3  SAAS  SAAS  CFA   CFA
     1013.25 20.0 50.0
XMAS Christmas Is NNN   NONE  100.  100.  100.   001-  *    15.0   NNN  3  SAAS  SAAS  CFA   CFA
```

```
     1013.25 20.0 50.0
BAKO Bakosurtanal NNN   NONE  100.  100.  100.   001-  *    15.0   NNN  3  SAAS  SAAS  CFA   CFA
     1013.25 20.0 50.0

       << OTHER MID-LATITUDE STATIONS >>
WSAM West. Samoa  NNN   NONE  20.0  20.0  20.0   001-  *    15.0   NNN  3  SAAS  SAAS  CFA   CFA
     1013.25 20.0 50.0
EISL Easter Is.   NNN   NONE  20.0  20.0  20.0   001-  *    15.0   NNN  3  SAAS  SAAS  CFA   CFA
     1013.25 20.0 50.0

       << Antarctic 91 STATIONS >>
DOVE Dovers       NNN   NONE  20.0  20.0  20.0   001-  *    15.0   NNN  3  SAAS  SAAS  CFA   CFA
     1013.25 20.0 50.0
MCMU McMurdo      NNN   NONE  20.0  20.0  20.0   001-  *    15.0   NNN  3  SAAS  SAAS  CFA   CFA
     1013.25 20.0 50.0
NEUL Neumayer024p NNN   NONE  20.0  20.0  20.0   001-  *    15.0   NNN  3  SAAS  SAAS  CFA   CFA
     1013.25 20.0 50.0
NEUM Neumayer025a NNN   NONE  20.0  20.0  20.0   001-  *    15.0   NNN  3  SAAS  SAAS  CFA   CFA
     1013.25 20.0 50.0
NEUN Neumayer025p NNN   NONE  20.0  20.0  20.0   001-  *    15.0   NNN  3  SAAS  SAAS  CFA   CFA
     1013.25 20.0 50.0
NEUO Neumayer026a NNN   NONE  20.0  20.0  20.0   001-  *    15.0   NNN  3  SAAS  SAAS  CFA   CFA
     1013.25 20.0 50.0
NEUP Neumayer026p NNN   NONE  20.0  20.0  20.0   001-  *    15.0   NNN  3  SAAS  SAAS  CFA   CFA
     1013.25 20.0 50.0
NEUQ Neumayer027a NNN   NONE  20.0  20.0  20.0   001-  *    15.0   NNN  3  SAAS  SAAS  CFA   CFA
     1013.25 20.0 50.0
NEUR Neumayer027p NNN   NONE  20.0  20.0  20.0   001-  *    15.0   NNN  3  SAAS  SAAS  CFA   CFA
     1013.25 20.0 50.0
NEUS Neumayer028a NNN   NONE  20.0  20.0  20.0   001-  *    15.0   NNN  3  SAAS  SAAS  CFA   CFA
     1013.25 20.0 50.0
NEUT Neumayer028p NNN   NONE  20.0  20.0  20.0   001-  *    15.0   NNN  3  SAAS  SAAS  CFA   CFA
     1013.25 20.0 50.0

       <<  ANTARCTIC 92 SITES >>
amun Amundsen     NNN   NONE  500.  500.  500.   001-  *    20.0   NNN  3  SAAS  SAAS  CFA   CFA
     1013.25 20.0 50.0
byrd Byrd base    NNN   NONE  500.  500.  500.   001-  *    20.0   NNN  3  SAAS  SAAS  CFA   CFA
     1013.25 20.0 50.0
case Casey        NNN   NONE  500.  500.  500.   001-  *    20.0   NNN  3  SAAS  SAAS  CFA   CFA
     1013.25 20.0 50.0
davi Davis        NNN   NONE  500.  500.  500.   001-  *    20.0   NNN  3  SAAS  SAAS  CFA   CFA
     1013.25 20.0 50.0
dece Deception Is NNN   NONE  500.  500.  500.   001-  *    20.0   NNN  3  SAAS  SAAS  CFA   CFA
     1013.25 20.0 50.0
fors Forster      NNN   NONE  500.  500.  500.   001-  *    20.0   NNN  3  SAAS  SAAS  CFA   CFA
     1013.25 20.0 50.0
gnan Gnangara     NNN   NONE  500.  500.  500.   001-  *    20.0   NNN  3  SAAS  SAAS  CFA   CFA
     1013.25 20.0 50.0
grun Grunenhogna  NNN   NONE  500.  500.  500.   001-  *    20.0   NNN  3  SAAS  SAAS  CFA   CFA
     1013.25 20.0 50.0
hils Hillarys     NNN   NONE  500.  500.  500.   001-  *    20.0   NNN  3  SAAS  SAAS  CFA   CFA
     1013.25 20.0 50.0
kerg Kerguelen Is NNN   NONE  500.  500.  500.   001-  *    20.0   NNN  3  SAAS  SAAS  CFA   CFA
     1013.25 20.0 50.0
livi LivingstonIs NNN   NONE  500.  500.  500.   001-  *    20.0   NNN  3  SAAS  SAAS  CFA   CFA
     1013.25 20.0 50.0
maws Mawson       NNN   NONE  500.  500.  500.   001-  *    20.0   NNN  3  SAAS  SAAS  CFA   CFA
     1013.25 20.0 50.0
mcmg McMurdo      NNN   NONE  500.  500.  500.   001-  *    20.0   NNN  3  SAAS  SAAS  CFA   CFA
     1013.25 20.0 50.0
ohig O'Higgins    NNN   NONE  500.  500.  500.   001-  *    20.0   NNN  3  SAAS  SAAS  CFA   CFA
```

```
     1013.25 20.0 50.0
riog Rio Grande   NNN  NONE  500.  500.  500.  001-  *    20.0  NNN  3  SAAS  SAAS  CFA  CFA
     1013.25 20.0 50.0
syow Syowa        NNN  NONE  500.  500.  500.  001-  *    20.0  NNN  3  SAAS  SAAS  CFA  CFA
     1013.25 20.0 50.0
tno1 Terra Nova   NNN  NONE  500.  500.  500.  001-  *    20.0  NNN  3  SAAS  SAAS  CFA  CFA
     1013.25 20.0 50.0
ushu Ushuaia      NNN  NONE  500.  500.  500.  001-  *    20.0  NNN  3  SAAS  SAAS  CFA  CFA
     1013.25 20.0 50.0

       << ANTARCTIC 94 Automatic AUSLIG Rogue SITES >>
cas1 Casey        NNN  NONE  100.  100.  100.  001-  *    20.0  NNN  3  SAAS  SAAS  CFA  CFA
     1013.25 20.0 50.0
dav1 Davis        NNN  NONE  .001  .001  .001  001-  *    20.0  NNN  3  SAAS  SAAS  CFA  CFA
     1013.25 20.0 50.0
mac1 Macquarie Is NNN  NONE  100.  100.  100.  001-  *    20.0  NNN  3  SAAS  SAAS  CFA  CFA
     1013.25 20.0 50.0
mcm1 McMurdo      NNN  NONE  100.  100.  100.  001-  *    20.0  NNN  3  SAAS  SAAS  CFA  CFA
     1013.25 20.0 50.0
maw1 Mawson       NNN  NONE  500.  500.  500.  001-  *    20.0  NNN  3  SAAS  SAAS  CFA  CFA
     1013.25 20.0 50.0

       << SIMPSON DESERT SITES >>
dill McDills      NNN  NONE  500.  500.  500.  001-  *    15.0  NNN  3  SAAS  SAAS  CFA  CFA
     1013.25 20.0 50.0
trk1 Trk1 Simpson NNN  NONE  500.  500.  500.  001-  *    15.0  NNN  3  SAAS  SAAS  CFA  CFA
     1013.25 20.0 50.0
bm26 BM26 Simpson NNN  NONE  500.  500.  500.  001-  *    15.0  NNN  3  SAAS  SAAS  CFA  CFA
     1013.25 20.0 50.0
bm55 BM55 Simpson NNN  NONE  500.  500.  500.  001-  *    15.0  NNN  3  SAAS  SAAS  CFA  CFA
     1013.25 20.0 50.0
trk3 TRK3 Simpson NNN  NONE  500.  500.  500.  001-  *    15.0  NNN  3  SAAS  SAAS  CFA  CFA
     1013.25 20.0 50.0
sml1 SML1 Simpson NNN  NONE  500.  500.  500.  001-  *    15.0  NNN  3  SAAS  SAAS  CFA  CFA
     1013.25 20.0 50.0
bm46 BM46 Simpson NNN  NONE  500.  500.  500.  001-  *    15.0  NNN  3  SAAS  SAAS  CFA  CFA
     1013.25 20.0 50.0
bm45 BM45 Simpson NNN  NONE  500.  500.  500.  001-  *    15.0  NNN  3  SAAS  SAAS  CFA  CFA
     1013.25 20.0 50.0


       << QUEENSLAND SITES  >>
qut1 QUT1 QLD     NNN  NONE  500.  500.  500.  001-  *    15.0  NNN  3  SAAS  SAAS  CFA  CFA
     1013.25 20.0 50.0
barc barc QLD     NNN  NONE  500.  500.  500.  001-  *    15.0  NNN  3  SAAS  SAAS  CFA  CFA
     1013.25 20.0 50.0
brea brea QLD     NNN  NONE  500.  500.  500.  001-  *    15.0  NNN  3  SAAS  SAAS  CFA  CFA
     1013.25 20.0 50.0
wilf wilf QLD     NNN  NONE  500.  500.  500.  001-  *    15.0  NNN  3  SAAS  SAAS  CFA  CFA
     1013.25 20.0 50.0
norm norm QLD     NNN  NONE  500.  500.  500.  001-  *    15.0  NNN  3  SAAS  SAAS  CFA  CFA
     1013.25 20.0 50.0
pieb pieb QLD     NNN  NONE  500.  500.  500.  001-  *    15.0  NNN  3  SAAS  SAAS  CFA  CFA
     1013.25 20.0 50.0
gren gren QLD     NNN  NONE  500.  500.  500.  001-  *    15.0  NNN  3  SAAS  SAAS  CFA  CFA
     1013.25 20.0 50.0
emuu emuu QLD     NNN  NONE  500.  500.  500.  001-  *    15.0  NNN  3  SAAS  SAAS  CFA  CFA
     1013.25 20.0 50.0
bass bass QLD     NNN  NONE  500.  500.  500.  001-  *    15.0  NNN  3  SAAS  SAAS  CFA  CFA
     1013.25 20.0 50.0
mula mula QLD     NNN  NONE  500.  500.  500.  001-  *    15.0  NNN  3  SAAS  SAAS  CFA  CFA
     1013.25 20.0 50.0
```

```
suga suga QLD      NNN   NONE  500.  500.  500.   001-  *    15.0   NNN  3  SAAS  SAAS  CFA   CFA
     1013.25 20.0 50.0

       << WING SITES >>
beij beij China    NNN   NONE  500.  500.  500.   001-  *    15.0   NNN  3  SAAS  SAAS  CFA   CFA
     1013.25 20.0 50.0
wuha wuha China    NNN   NONE  500.  500.  500.   001-  *    15.0   NNN  3  SAAS  SAAS  CFA   CFA
     1013.25 20.0 50.0
shan shan China    NNN   NONE  500.  500.  500.   001-  *    15.0   NNN  1  SAAS  SAAS  CFA   CFA
     1013.25 20.0 50.0
s102 s102 Taiwan   NNN   NONE  500.  500.  500.   001-  *    15.0   NNN  3  SAAS  SAAS  CFA   CFA
     1013.25 20.0 50.0
daen daen Korea    NNN   NONE  500.  500.  500.   001-  *    15.0   NNN  3  SAAS  SAAS  CFA   CFA
     1013.25 20.0 50.0
manl manl P'pines  NNN   NONE  500.  500.  500.   001-  *    15.0   NNN  3  SAAS  SAAS  CFA   CFA
     1013.25 20.0 50.0

       << DORIS SITES >>
arlt arlt          NNN   NONE  500.  500.  500.   001-  *    15.0   NNN  3  SAAS  SAAS  CFA   CFA
     1013.25 20.0 50.0
arna arna          NNN   NONE  500.  500.  500.   001-  *    15.0   NNN  3  SAAS  SAAS  CFA   CFA
     1013.25 20.0 50.0
cach cach          NNN   NONE  500.  500.  500.   001-  *    15.0   NNN  3  SAAS  SAAS  CFA   CFA
     1013.25 20.0 50.0
colb colb          NNN   NONE  500.  500.  500.   001-  *    15.0   NNN  3  SAAS  SAAS  CFA   CFA
     1013.25 20.0 50.0
djib djib          NNN   NONE  500.  500.  500.   001-  *    15.0   NNN  3  SAAS  SAAS  CFA   CFA
     1013.25 20.0 50.0
gala gala          NNN   NONE  500.  500.  500.   001-  *    15.0   NNN  3  SAAS  SAAS  CFA   CFA
     1013.25 20.0 50.0
ineg ineg          NNN   NONE  500.  500.  500.   001-  *    15.0   NNN  3  SAAS  SAAS  CFA   CFA
     1013.25 20.0 50.0
libv libv          NNN   NONE  500.  500.  500.   001-  *    15.0   NNN  3  SAAS  SAAS  CFA   CFA
     1013.25 20.0 50.0
nmn1 nmn1          NNN   NONE  500.  500.  500.   001-  *    15.0   NNN  3  SAAS  SAAS  CFA   CFA
     1013.25 20.0 50.0
reun reun          NNN   NONE  500.  500.  500.   001-  *    15.0   NNN  3  SAAS  SAAS  CFA   CFA
     1013.25 20.0 50.0
sakl sakl          NNN   NONE  500.  500.  500.   001-  *    15.0   NNN  3  SAAS  SAAS  CFA   CFA
     1013.25 20.0 50.0
soco soco          NNN   NONE  500.  500.  500.   001-  *    15.0   NNN  3  SAAS  SAAS  CFA   CFA
     1013.25 20.0 50.0
sthl sthl          NNN   NONE  500.  500.  500.   001-  *    15.0   NNN  3  SAAS  SAAS  CFA   CFA
     1013.25 20.0 50.0
kour kour          NNN   NONE  500.  500.  500.   001-  *    15.0   NNN  3  SAAS  SAAS  CFA   CFA
     1013.25 20.0 50.0
para para          NNN   NONE  500.  500.  500.   001-  *    15.0   NNN  3  SAAS  SAAS  CFA   CFA
     1013.25 20.0 50.0
bras bras          NNN   NONE  500.  500.  500.   001-  *    15.0   NNN  3  SAAS  SAAS  CFA   CFA
     1013.25 20.0 50.0
add1 add1          NNN   NONE  500.  500.  500.   001-  *    15.0   NNN  3  SAAS  SAAS  CFA   CFA
     1013.25 20.0 50.0
rich rich          NNN   NONE  500.  500.  500.   001-  *    15.0   NNN  1  SAAS  SAAS  CFA   CFA
     1013.25 20.0 50.0
gala gala          NNN   NONE  500.  500.  500.   001-  *    15.0   NNN  1  SAAS  SAAS  CFA   CFA
     1013.25 20.0 50.0
nmn1 nmn1          NNN   NONE  500.  500.  500.   001-  *    15.0   NNN  1  SAAS  SAAS  CFA   CFA
     1013.25 20.0 50.0

       << ANN 93 >>
ALYA Alyangula     NNN   NONE  100.  100.  100.   001-  *    15.0   NNN  3  SAAS  SAAS  CFA   CFA
     1013.25 20.0 50.0
```

```
ATKI Atkinson      NNN   NONE  100.  100.  100.  001-  *    15.0  NNN  3  SAAS  SAAS  CFA  CFA
     1013.25 20.0 50.0
BATE               NNN   NONE  100.  100.  100.  001-  *    15.0  NNN  3  SAAS  SAAS  CFA  CFA
     1013.25 20.0 50.0
BRDV Birdsville    NNN   NONE  100.  100.  100.  001-  *    15.0  NNN  3  SAAS  SAAS  CFA  CFA
     1013.25 20.0 50.0
BROO Broome        NNN   NONE  100.  100.  100.  001-  *    15.0  NNN  3  SAAS  SAAS  CFA  CFA
     1013.25 20.0 50.0
CAIG               NNN   NONE  100.  100.  100.  001-  *    15.0  NNN  3  SAAS  SAAS  CFA  CFA
     1013.25 20.0 50.0
CAMW Cameron west  NNN   NONE  100.  100.  100.  001-  *    15.0  NNN  3  SAAS  SAAS  CFA  CFA
     1013.25 20.0 50.0
CARN               NNN   NONE  100.  100.  100.  001-  *    15.0  NNN  3  SAAS  SAAS  CFA  CFA
     1013.25 20.0 50.0
CAVE Caversham     NNN   NONE  100.  100.  100.  001-  *    15.0  NNN  3  SAAS  SAAS  CFA  CFA
     1013.25 20.0 50.0
CEDU Ceduna        NNN   NONE  100.  100.  100.  001-  *    15.0  NNN  3  SAAS  SAAS  CFA  CFA
     1013.25 20.0 50.0
CHAR Charmouth     NNN   NONE  100.  100.  100.  001-  *    15.0  NNN  3  SAAS  SAAS  CFA  CFA
     1013.25 20.0 50.0
CLIF Low cliff     NNN   NONE  100.  100.  100.  001-  *    15.0  NNN  3  SAAS  SAAS  CFA  CFA
     1013.25 20.0 50.0
COOL               NNN   NONE  100.  100.  100.  001-  *    15.0  NNN  3  SAAS  SAAS  CFA  CFA
     1013.25 20.0 50.0
DEAK Deakin        NNN   NONE  100.  100.  100.  001-  *    15.0  NNN  3  SAAS  SAAS  CFA  CFA
     1013.25 20.0 50.0
ELDO Gove          NNN   NONE  100.  100.  100.  001-  *    15.0  NNN  3  SAAS  SAAS  CFA  CFA
     1013.25 20.0 50.0
ESPE               NNN   NONE  100.  100.  100.  001-  *    15.0  NNN  3  SAAS  SAAS  CFA  CFA
     1013.25 20.0 50.0
GIBS               NNN   NONE  100.  100.  100.  001-  *    15.0  NNN  3  SAAS  SAAS  CFA  CFA
     1013.25 20.0 50.0
GROO Groote Is     NNN   NONE  100.  100.  100.  001-  *    15.0  NNN  3  SAAS  SAAS  CFA  CFA
     1013.25 20.0 50.0
HWKR Hawker        NNN   NONE  100.  100.  100.  001-  *    15.0  NNN  3  SAAS  SAAS  CFA  CFA
     1013.25 20.0 50.0
JOHN Johnston      NNN   NONE  100.  100.  100.  001-  *    15.0  NNN  3  SAAS  SAAS  CFA  CFA
     1013.25 20.0 50.0
JUNC Junction      NNN   NONE  100.  100.  100.  001-  *    15.0  NNN  3  SAAS  SAAS  CFA  CFA
     1013.25 20.0 50.0
KALG Kalgoorlie    NNN   NONE  100.  100.  100.  001-  *    15.0  NNN  3  SAAS  SAAS  CFA  CFA
     1013.25 20.0 50.0
KDMN Kidman Sprng  NNN   NONE  100.  100.  100.  001-  *    15.0  NNN  3  SAAS  SAAS  CFA  CFA
     1013.25 20.0 50.0
KILI Tanami        NNN   NONE  100.  100.  100.  001-  *    15.0  NNN  3  SAAS  SAAS  CFA  CFA
     1013.25 20.0 50.0
RAWL Rawlinson     NNN   NONE  100.  100.  100.  001-  *    15.0  NNN  3  SAAS  SAAS  CFA  CFA
     1013.25 20.0 50.0
ROPE Roper Rvr     NNN   NONE  100.  100.  100.  001-  *    15.0  NNN  3  SAAS  SAAS  CFA  CFA
     1013.25 20.0 50.0
PERR Perth ROGUE   NNN   NONE  100.  100.  100.  001-  *    15.0  NNN  3  SAAS  SAAS  CFA  CFA
     1013.25 20.0 50.0
PER2 Perth TRM     NNN   NONE  100.  100.  100.  001-  *    15.0  NNN  3  SAAS  SAAS  CFA  CFA
     1013.25 20.0 50.0
PIVT Pivot         NNN   NONE  100.  100.  100.  001-  *    15.0  NNN  3  SAAS  SAAS  CFA  CFA
     1013.25 20.0 50.0
RATH Rat Hill      NNN   NONE  100.  100.  100.  001-  *    15.0  NNN  3  SAAS  SAAS  CFA  CFA
     1013.25 20.0 50.0
SHAM Shamrock      NNN   NONE  100.  100.  100.  001-  *    15.0  NNN  3  SAAS  SAAS  CFA  CFA
     1013.25 20.0 50.0
TORB Torbat        NNN   NONE  100.  100.  100.  001-  *    15.0  NNN  3  SAAS  SAAS  CFA  CFA
     1013.25 20.0 50.0
```

```
OTA1 Otago New      NNN   NONE  100.  100.  100.  001-  *    15.0  NNN  3  SAAS  SAAS  CFA  CFA
     1013.25 20.0 50.0
WOLL Wollogorang    NNN   NONE  100.  100.  100.  001-  *    15.0  NNN  3  SAAS  SAAS  CFA  CFA
     1013.25 20.0 50.0

       << PNG 93 >>
AMAN Amanab         NNN   NONE  100.  100.  100.  001-  *    15.0  NNN  3  SAAS  SAAS  CFA  CFA
     1013.25 20.0 50.0
CART Carteret       NNN   NONE  100.  100.  100.  001-  *    15.0  NNN  3  SAAS  SAAS  CFA  CFA
     1013.25 20.0 50.0
GOKA Goroka         NNN   NONE  100.  100.  100.  001-  *    15.0  NNN  3  SAAS  SAAS  CFA  CFA
     1013.25 20.0 50.0
GUNY Guny           NNN   NONE  100.  100.  100.  001-  *    15.0  NNN  3  SAAS  SAAS  CFA  CFA
     1013.25 20.0 50.0
JACQ JacquinotBay   NNN   NONE  100.  100.  100.  001-  *    15.0  NNN  3  SAAS  SAAS  CFA  CFA
     1013.25 20.0 50.0
KAVI Kavieng        NNN   NONE  100.  100.  100.  001-  *    15.0  NNN  3  SAAS  SAAS  CFA  CFA
     1013.25 20.0 50.0
KIKO Kiko PNG       NNN   NONE  100.  100.  100.  001-  *    15.0  NNN  3  SAAS  SAAS  CFA  CFA
     1013.25 20.0 50.0
KOPI Kopiago        NNN   NONE  100.  100.  100.  001-  *    15.0  NNN  3  SAAS  SAAS  CFA  CFA
     1013.25 20.0 50.0
LOUS LosuiaIs PNG   NNN   NONE  100.  100.  100.  001-  *    15.0  NNN  3  SAAS  SAAS  CFA  CFA
     1013.25 20.0 50.0
MADA Madeni PNG     NNN   NONE  100.  100.  100.  001-  *    15.0  NNN  3  SAAS  SAAS  CFA  CFA
     1013.25 20.0 50.0
MEND Mendi PNG      NNN   NONE  100.  100.  100.  001-  *    15.0  NNN  3  SAAS  SAAS  CFA  CFA
     1013.25 20.0 50.0
MANU Manus          NNN   NONE  100.  100.  100.  001-  *    15.0  NNN  3  SAAS  SAAS  CFA  CFA
     1013.25 20.0 50.0
MORO Morobe         NNN   NONE  100.  100.  100.  001-  *    15.0  NNN  3  SAAS  SAAS  CFA  CFA
     1013.25 20.0 50.0
MORE Port Moresby   NNN   NONE  100.  100.  100.  001-  *    15.0  NNN  3  SAAS  SAAS  CFA  CFA
     1013.25 20.0 50.0
NING Ningerum       NNN   NONE  100.  100.  100.  001-  *    15.0  NNN  3  SAAS  SAAS  CFA  CFA
     1013.25 20.0 50.0
NUGU Nuguria        NNN   NONE  100.  100.  100.  001-  *    15.0  NNN  3  SAAS  SAAS  CFA  CFA
     1013.25 20.0 50.0
RABL Rabaul         NNN   NONE  100.  100.  100.  001-  *    15.0  NNN  3  SAAS  SAAS  CFA  CFA
     1013.25 20.0 50.0
TASP Tasman isl     NNN   NONE  100.  100.  100.  001-  *    15.0  NNN  3  SAAS  SAAS  CFA  CFA
     1013.25 20.0 50.0
UNIT Unit           NNN   NONE  100.  100.  100.  001-  *    15.0  NNN  3  SAAS  SAAS  CFA  CFA
     1013.25 20.0 50.0
WANK Wankun Vill    NNN   NONE  100.  100.  100.  001-  *    15.0  NNN  3  SAAS  SAAS  CFA  CFA
     1013.25 20.0 50.0
WEWK Wewak          NNN   NONE  100.  100.  100.  001-  *    15.0  NNN  3  SAAS  SAAS  CFA  CFA
     1013.25 20.0 50.0
WUVU Wuvulu         NNN   NONE  100.  100.  100.  001-  *    15.0  NNN  3  SAAS  SAAS  CFA  CFA
     1013.25 20.0 50.0

       << New Zealand Datum 1993 >>
D026 Pukearenga 2   NNN   NONE  100.  100.  100.  001-  *    15.0  NNN  3  SAAS  SAAS  CFA  CFA
     1013.25 20.0 50.0
D045 Whangaparaoa   NNN   NONE  100.  100.  100.  001-  *    15.0  NNN  3  SAAS  SAAS  CFA  CFA
     1013.25 20.0 50.0
D072 F Maketu       NNN   NONE  100.  100.  100.  001-  *    15.0  NNN  3  SAAS  SAAS  CFA  CFA
     1013.25 20.0 50.0
E072 F Maketu       NNN   NONE  100.  100.  100.  001-  *    15.0  NNN  3  SAAS  SAAS  CFA  CFA
     1013.25 20.0 50.0
D078 201 Te Pohue   NNN   NONE  100.  100.  100.  001-  *    15.0  NNN  3  SAAS  SAAS  CFA  CFA
     1013.25 20.0 50.0
```

```
E078 201 Te Pohue NNN   NONE 100. 100. 100. 001- *  15.0 NNN 3 SAAS SAAS CFA CFA
     1013.25 20.0 50.0
D100 1060kahuatiu NNN   NONE 100. 100. 100. 001- *  15.0 NNN 3 SAAS SAAS CFA CFA
     1013.25 20.0 50.0
E100 1060kahuatiu NNN   NONE 100. 100. 100. 001- *  15.0 NNN 3 SAAS SAAS CFA CFA
     1013.25 20.0 50.0
D105 A Huirangi   NNN   NONE 100. 100. 100. 001- *  15.0 NNN 3 SAAS SAAS CFA CFA
     1013.25 20.0 50.0
E105 A Huirangi   NNN   NONE 100. 100. 100. 001- *  15.0 NNN 3 SAAS SAAS CFA CFA
     1013.25 20.0 50.0
D131 Mt Stewart   NNN   NONE 100. 100. 100. 001- *  15.0 NNN 3 SAAS SAAS CFA CFA
     1013.25 20.0 50.0
E131 Mt Stewart   NNN   NONE 100. 100. 100. 001- *  15.0 NNN 3 SAAS SAAS CFA CFA
     1013.25 20.0 50.0
D143 Eringa       NNN   NONE 100. 100. 100. 001- *  15.0 NNN 3 SAAS SAAS CFA CFA
     1013.25 20.0 50.0
E143 Eringa       NNN   NONE 100. 100. 100. 001- *  15.0 NNN 3 SAAS SAAS CFA CFA
     1013.25 20.0 50.0
D158 Jenkins Hill NNN   NONE 100. 100. 100. 001- *  15.0 NNN 3 SAAS SAAS CFA CFA
     1013.25 20.0 50.0
E158 Jenkins Hill NNN   NONE 100. 100. 100. 001- *  15.0 NNN 3 SAAS SAAS CFA CFA
     1013.25 20.0 50.0
D172 Mt Murchison NNN   NONE 100. 100. 100. 001- *  15.0 NNN 3 SAAS SAAS CFA CFA
     1013.25 20.0 50.0
E172 Mt Murchison NNN   NONE 100. 100. 100. 001- *  15.0 NNN 3 SAAS SAAS CFA CFA
     1013.25 20.0 50.0
D191 Isolated Hil NNN   NONE 100. 100. 100. 001- *  15.0 NNN 3 SAAS SAAS CFA CFA
     1013.25 20.0 50.0
E191 Isolated Hil NNN   NONE 100. 100. 100. 001- *  15.0 NNN 3 SAAS SAAS CFA CFA
     1013.25 20.0 50.0
D212 Mt Pleasant  NNN   NONE 100. 100. 100. 001- *  15.0 NNN 3 SAAS SAAS CFA CFA
     1013.25 20.0 50.0
E212 Mt Pleasant  NNN   NONE 100. 100. 100. 001- *  15.0 NNN 3 SAAS SAAS CFA CFA
     1013.25 20.0 50.0
D229 Mt Mary      NNN   NONE 100. 100. 100. 001- *  15.0 NNN 3 SAAS SAAS CFA CFA
     1013.25 20.0 50.0
E229 Mt Mary      NNN   NONE 100. 100. 100. 001- *  15.0 NNN 3 SAAS SAAS CFA CFA
     1013.25 20.0 50.0
D233 A MtHorrible NNN   NONE 100. 100. 100. 001- *  15.0 NNN 3 SAAS SAAS CFA CFA
     1013.25 20.0 50.0
E233 A MtHorrible NNN   NONE 100. 100. 100. 001- *  15.0 NNN 3 SAAS SAAS CFA CFA
     1013.25 20.0 50.0
D253 T Hyde Rock  NNN   NONE 100. 100. 100. 001- *  15.0 NNN 3 SAAS SAAS CFA CFA
     1013.25 20.0 50.0
E253 T Hyde Rock  NNN   NONE 100. 100. 100. 001- *  15.0 NNN 3 SAAS SAAS CFA CFA
     1013.25 20.0 50.0
D269 A Nth Taier  NNN   NONE 100. 100. 100. 001- *  15.0 NNN 3 SAAS SAAS CFA CFA
     1013.25 20.0 50.0
E269 A Nth Taier  NNN   NONE 100. 100. 100. 001- *  15.0 NNN 3 SAAS SAAS CFA CFA
     1013.25 20.0 50.0
D286 X The Bluff  NNN   NONE 100. 100. 100. 001- *  15.0 NNN 3 SAAS SAAS CFA CFA
     1013.25 20.0 50.0
D302 Mt York      NNN   NONE 100. 100. 100. 001- *  15.0 NNN 3 SAAS SAAS CFA CFA
     1013.25 20.0 50.0
E302 Mt York      NNN   NONE 100. 100. 100. 001- *  15.0 NNN 3 SAAS SAAS CFA CFA
     1013.25 20.0 50.0
D309 HB Greenland NNN   NONE 100. 100. 100. 001- *  15.0 NNN 3 SAAS SAAS CFA CFA
     1013.25 20.0 50.0
E309 HB Greenland NNN   NONE 100. 100. 100. 001- *  15.0 NNN 3 SAAS SAAS CFA CFA
     1013.25 20.0 50.0
D320 JF Gillespes NNN   NONE 100. 100. 100. 001- *  15.0 NNN 3 SAAS SAAS CFA CFA
     1013.25 20.0 50.0
```

```
E320 JF Gillespes NNN   NONE 100. 100. 100.  001- *   15.0 NNN 3 SAAS SAAS CFA  CFA
     1013.25 20.0 50.0
D338 8471         NNN   NONE 100. 100. 100.  001- *   15.0 NNN 3 SAAS SAAS CFA  CFA
     1013.25 20.0 50.0
E338 8471         NNN   NONE 100. 100. 100.  001- *   15.0 NNN 3 SAAS SAAS CFA  CFA
     1013.25 20.0 50.0
D425 Cape Campbel NNN   NONE 100. 100. 100.  001- *   15.0 NNN 3 SAAS SAAS CFA  CFA
     1013.25 20.0 50.0
E425 Cape Campbel NNN   NONE 100. 100. 100.  001- *   15.0 NNN 3 SAAS SAAS CFA  CFA
     1013.25 20.0 50.0
D431 Bluff Hill 3 NNN   NONE 100. 100. 100.  001- *   15.0 NNN 3 SAAS SAAS CFA  CFA
     1013.25 20.0 50.0
E431 Bluff Hill 3 NNN   NONE 100. 100. 100.  001- *   15.0 NNN 3 SAAS SAAS CFA  CFA
     1013.25 20.0 50.0
D452 79 Rangiriri NNN   NONE 100. 100. 100.  001- *   15.0 NNN 3 SAAS SAAS CFA  CFA
     1013.25 20.0 50.0
E452 79 Rangiriri NNN   NONE 100. 100. 100.  001- *   15.0 NNN 3 SAAS SAAS CFA  CFA
     1013.25 20.0 50.0
D469 I Parapara   NNN   NONE 100. 100. 100.  001- *   15.0 NNN 3 SAAS SAAS CFA  CFA
     1013.25 20.0 50.0
E469 I Parapara   NNN   NONE 100. 100. 100.  001- *   15.0 NNN 3 SAAS SAAS CFA  CFA
     1013.25 20.0 50.0
D473 Marotiri #2  NNN   NONE 100. 100. 100.  001- *   15.0 NNN 3 SAAS SAAS CFA  CFA
     1013.25 20.0 50.0
E473 Marotiri #2  NNN   NONE 100. 100. 100.  001- *   15.0 NNN 3 SAAS SAAS CFA  CFA
     1013.25 20.0 50.0
D474 3 Sisters    NNN   NONE 100. 100. 100.  001- *   15.0 NNN 3 SAAS SAAS CFA  CFA
     1013.25 20.0 50.0
D481 Marotiri Ecc NNN   NONE 100. 100. 100.  001- *   15.0 NNN 3 SAAS SAAS CFA  CFA
     1013.25 20.0 50.0
E481 Marotiri Ecc NNN   NONE 100. 100. 100.  001- *   15.0 NNN 3 SAAS SAAS CFA  CFA
     1013.25 20.0 50.0
D482 HH R9        NNN   NONE 100. 100. 100.  001- *   15.0 NNN 3 SAAS SAAS CFA  CFA
     1013.25 20.0 50.0
E482 HH R9        NNN   NONE 100. 100. 100.  001- *   15.0 NNN 3 SAAS SAAS CFA  CFA
     1013.25 20.0 50.0
D483 HH R9A       NNN   NONE 100. 100. 100.  001- *   15.0 NNN 3 SAAS SAAS CFA  CFA
     1013.25 20.0 50.0
E483 HH R9A       NNN   NONE 100. 100. 100.  001- *   15.0 NNN 3 SAAS SAAS CFA  CFA
     1013.25 20.0 50.0
D484 F Maketu Ecc NNN   NONE 100. 100. 100.  001- *   15.0 NNN 3 SAAS SAAS CFA  CFA
     1013.25 20.0 50.0
E484 F Maketu Ecc NNN   NONE 100. 100. 100.  001- *   15.0 NNN 3 SAAS SAAS CFA  CFA
     1013.25 20.0 50.0

       << AUSLIG  & OTHER GLOBAL SITES >>
FRN2 Fern hill    NNN   NONE 100. 100. 100.  001- *   15.0 NNN 3 SAAS SAAS CFA  CFA
     1013.25 20.0 50.0
AREQ Arequipa     NNN   NONE 100. 100. 100.  001- *   15.0 NNN 3 SAAS SAAS CFA  CFA
     1013.25 20.0 50.0
```

Appendix D

The Station Information File: *station.info*

The following tabular information is a modified copy of the GAMIT station.info file which is used specify the antenna offsets, the instrument used and the range of applicability of the station information. Chapter 4 of the GAMIT manual describes the creation of the station information file.

The following explanations apply:

STATION CODE & NAME Redundant information for static positioning describing the station.

Ant Ht The height of the antenna. If the height is a reduced vertical height to the pre-amp base then this quantity is entered here. The height code, see later, then becomes DHPAB. This is the most common entry. Refer to the GAMIT manual for other codes.

Ant N North offset from the antenna sub-point to the required mark. This quantity is zero for instruments set up over the mark.

Ant E East offset from the antenna sub-point to the required mark. This quantity is zero for instruments set up over the mark.

Rcvr The receiver used for the observations.

AntCod The antenna code used for the observations.

HtCod The type of height observation reported in **Ant Ht**. DHPAB, direct height pre amp base is the most common being the vertical height from the mark or reference point to the pre amp base which is coincident with the RINEX point.

Ver The firmware version number used in the receiver.

Yr The year for which the information is relevant.

Doy The first day of year for which the entry is valid. It is assumed that the first entry is valid until a later specification is read. Thus a permanently mounted receiver will usually only have a single commencing entry. Single occupations will look like these entries until a subsequent occupation occurs.

Network participation Indication of network and dates of occupation.

D.1 Explanation of GAMIT codes used in *HISUB*

GAMIT solftware contains a subroutine called HISUB which is capable of computing the offsets between a given ground mark and the nominated electrical center. Both the L_1 and L_2 phase centers are held as well as offsets between these centers. It is normal to reference all observations to the L_1 phase center. The following list of codes are accepted by the HISUB routine. Note that L1PHC and DHPAB apply to all configurations.

L1PHC

This is the direct height to the L_1 phase center. It was usually used for fixed/permanent stations. It is no longer favoured. In this work it will be mainly encountered on the older style CIGNET stations where there is no associated ground mark and the L_1 phase center is the mark. Many field operators attempted to supply this information on their field sheets. In most cases we choose to use measurements to the RINEX point due to its physical definition.

DHPAB

This is the direct height to pre-amp base. This point is generally defined as the RINEX point. In this case HISUB uses the antenna geometry to correct the observation to the L_1 phase center. It is the preferred type of antenna offset information.

TRMSST: Trimble 4000 SST/SSE

SLBGP Slant height to bottom outer edge of ground plane.
SLMGP Slant height to middle outer edge of ground plane.
SLTGP Slant height to top outer edge of ground plane.
SLTGN Slant height to top of ground plane in notch.
SLBGN Slant height to bottom of ground plane in notch.

ASHXII: Ashtec XII

SLAGP Slant height to holes, closed holes, in old style XII ground plane.
SLHGP Slant height to holes, open holes, in new style XII ground plane.
SLBGP Slant height to bevel of bottom edge of ground plane.
SLLGP Slant height to holes in large ground plane antenna.

ROGSNR: Dorne-Margolin with JPL choke ring

This type of antenna is common on the older style Rogues. HISUB accepts both ROGSNR, commonly used at UC, and DMRG07 for this antenna. It is also to be noted that the bottom of the choke rings, DHBCR is coincident with the DHPAB position which is the RINEX point.
DHBCR Direct height to bottom of choke ring.
DHTCR Direct height to top of choke ring. This is the normal JPL default.
SLBCR Slant height to bottom edge of choke ring.

ROGAOA: Dorne-Magolin B with Allan Osborne design
The types are the same as listed for the ROGSNR. These antenna are differenciated by their different codes. It is to be noted that the RINEX point is DHBCR point.

TRBROG: The Turbo-Rogue choke ring antenna
This is the common Turbo-Rogue antenna. GAMIT accepts TRBROG, mainly used at UC, or DMRG10. The same same types as defined in ROGSNR are used. It is to be noted that the RINEX point is **DHPAB** for these antenna and that this point is offset from DHBCR

MIN6AT: The Mini-Mac 2816AT
This unit was located at Hobart. It is commonly called TASM. Only DHPAB or L1PHC are valid.

LEIGRT: Leica with GRT 44 carrier
This is the only Leica antenna currently coded in GAMIT. Only DHPAB or L1PHC are valid.

```
--- STATION CODE & NAME --- Ant Ht   Ant N    Ant E   Rcvr  AntCod HtCod  Ver  Yr DOY
  -- Network participation -
 ALIC ALIC Alice Springs    0.0345   0.0000   0.0000 ASHXII ASHXII DHPAB  6.0  92 206
     AFN IGS 92 days 206-216
 ALIC ALIC Alice Springs    0.0385   0.0000   0.0000 TRMSST TRMSST DHPAB  4.64 93 239
     ARN 93
 ALYA ALYA Groote Island    1.546    0.0000   0.0000 LEI200 LEIGRT DHPAB  1.43 93 239
     ARN 93
 ATKI ATKI Atkinson VIC     0.957    0.0000   0.0000 TRMSSE TRMSSE DHPAB  5.63 93 239
     ARN 93
 BANZ BANZ Barringun Zero   0.910    0.0000   0.0000 TRMSST TRMSST DHPAB  4.80 92 212
     NSW IGS 92 days 212-215
 BANZ BANZ Barringun Zero   0.758    0.0000   0.0000 TRMSST TRMSST DHPAB  4.80 92 217
     NSW IGS 92 days 218-221
 BARC BARC Barcaldine QLD   1.5454   0.0000   0.0000 TRMSST TRMSST DHPAB  4.70 92 206
     NSW IGS 92 days 207-210
 BARC BARC Barcaldine QLD   1.6296   0.0000   0.0000 TRMSST TRMSST DHPAB  4.70 92 211
     NSW IGS 92 days 212-214
 BARC BARC Barcaldine QLD   1.5225   0.0000   0.0000 TRMSST TRMSST DHPAB  4.70 92 215
     NSW IGS 92 days 216-217
 BASS BASS MY201 Mackay     1.401    0.0000   0.0000 TRMSST TRMSST SLBGP  4.70 93 157
     QLD Mini IGS
 BATE BATE Carnegie         1.529    0.0000   0.0000 ASHXII ASHXII DHPAB  7.00 93 239
     ARN 93
 BATH BATH Bathurst NSW     0.074    0.0000   0.0000 ASHXII ASHXII DHPAB  6.0  92 206
     NSW IGS 92 days 207-222
 BATH BATH Bathurst NSW     0.080    0.0000   0.0000 TRMSSE TRMSSE DHPAB  5.63 92 255
     NSW IGS 92 days 255-259
 BATH BATH Bathurst NSW     0.075    0.0000   0.0000 ASHXII ASHXII DHPAB  6.3  93 238
     ARN 93
 BENW BENW Lorne(Benwerrin) 1.573    0.0000   0.0000 TRMSST TRMSST DHPAB  4.64 92 206
     TIDE GAUGE IGS 92 day 207
 BENW BENW Lorne(Benwerrin) 1.505    0.0000   0.0000 TRMSST TRMSST DHPAB  4.64 92 208
     TIDE GAUGE IGS 92 day 208
 BENW BENW Lorne(Benwerrin) 1.609    0.0000   0.0000 TRMSST TRMSST DHPAB  4.64 92 209
     TIDE GAUGE IGS 92 day 209
 BENW BENW Lorne(Benwerrin) 1.565    0.0000   0.0000 TRMSST TRMSST DHPAB  4.64 92 210
     TIDE GAUGE IGS 92 day 210
 BM26 BM26 BM26 Simpson     1.445    0.0000   0.0000 TRMSST TRMSST DHPAB  4.64 92 212
     UNSW SIMPSON DESERT
 BM45 BM45 BM45 SIMPSON     1.265    0.0000   0.0000 TRMSST TRMSST DHPAB  4.70 92 212
     UNSW SIMPSON DESERT
 BM46 BM46 BM46 SIMPSON     1.221    0.0000   0.0000 TRMSST TRMSST DHPAB  4.70 92 212
     UNSW SIMPSON DESERT
 BM55 BM55 BM55 SIMPSON     1.141    0.0000   0.0000 TRMSST TRMSST DHPAB  4.70 92 212
     UNSW SIMPSON DESERT
 BRDV BRDV Birdsville       1.296    0.0000   0.0000 TRMSSE TRMSSE DHPAB  5.63 93 239
     ARN 93
 BREA BREA Breadalbane QLD  1.5606   0.0000   0.0000 TRMSST TRMSST DHPAB  4.70 92 206
     NSW IGS 92 days 207-209
 BREA BREA Breadalbane QLD  1.5002   0.0000   0.0000 TRMSST TRMSST DHPAB  4.64 92 215
     NSW IGS 92 days 216-217
 BROO BROO Broome WA        1.594    0.0000   0.0000 ASHXII ASHXII DHPAB  1.0  92 206
     TIDE GAUGE IGS 92 day 207-210
 BROO BROO Broome           1.717    0.0000   0.0000 TRMSST TRMSST DHPAB  5.63 93 239
     ARN 93
```

```
BRUN BRUN Brunswick NSW     0.139     0.0000    0.0000 TRMSST TRMSST DHPAB  4.80 92 218
    NSW IGS 92 days 218-221
BULL BULL Bullanginya NSW   0.080     0.0000    0.0000 TRMSST TRMSST DHPAB  4.70 92 206
    NSW IGS 92 days 207-210
BULL BULL Bullanginya NSW   0.074     0.0000    0.0000 TRMSST TRMSST DHPAB  4.64 92 212
    NSW IGS 92 days 212-215
CAIG CAIG Caiguna           1.443     0.0000    0.0000 TRMSSE TRMSSE DHPAB  5.63 93 239
    ARN 93
CAMW CAMW Cameron west      0.760     0.0000    0.0000 TRMSSE TRMSSE DHPAB  5.63 93 239
    ARN 93
CARN CARN Carnarvon         0.552     0.0000    0.0000 ASHXII ASHXII DHPAB  6.24 93 239
    ARN 93
CAS1 CAS1 Casey Pillar      0.0010    0.0000    0.0000 TRBROG TRBROG DHPAB  1.20 93 350
    ANT94
CAVE CAVE Caversham         1.4380    0.0000    0.0000 TRMSST TRMSST DHPAB  4.81 93 239
    ARN 93
CEDU CEDU Ceduna            0.032     0.0000    0.0000 ROGSNR ROGSNR DHPAB  7.4  93 239
    ARN 93
CHAR CHAR Charmouth hill    0.757     0.0000    0.0000 TRMSSE TRMSSE DHPAB  5.63 93 239
    ARN 93
CLIF CLIF Low cliff ecce    1.4033    0.0000    0.0000 TRMSSE TRMSSE DHPAB  5.60 93 239
    ARN 93
COCO COCO Cocos Island      0.076     0.0000    0.0000 ASHXII ASHXII DHPAB  6.0  92 206
    AFN IGS 92 days 207-226
COCO COCO Cocos Island      0.078     0.0000    0.0000 TRMSST TRMSST DHPAB  4.7  93 227
    ARN 93
COOL COOL Coolinbar         1.235     0.0000    0.0000 TRMSSE TRMSSE DHPAB  5.51 93 239
    ARN 93
CROW CROW Crowdy NSW        0.080     0.0000    0.0000 TRMSST TRMSST DHPAB  4.70 92 218
    NSW IGS 92 days 218-221
CULG CULG Culgoora NSW      0.871     0.0000    0.0000 TRMSSE TRMSSE DHPAB       92 255
    NSW IGS 92 days 255-259
D026 D026 Pukearenga No 2   1.3540    0.0000    0.0000 ASHXII ASHXII SLBGP  6.0  93 078
    NZD 93
D026 D026 Pukearenga No 2   1.3240    0.0000    0.0000 ASHXII ASHXII SLBGP  6.0  93 078
    NZD 93
D045 D045 Whangaparaoa      1.4270    0.0000    0.0000 ASHXII ASHXII SLBGP  6.0  93 074
    NZD 93
D045 D045 Whangaparaoa      1.4270    0.0000    0.0000 ASHXII ASHXII SLBGP  6.0  93 074
    NZD 93
D045 D045 Whangaparaoa      1.4280    0.0000    0.0000 ASHXII ASHXII SLBGP  6.0  93 075
    NZD 93
D045 D045 Whangaparaoa      1.4280    0.0000    0.0000 ASHXII ASHXII SLBGP  6.0  93 075
    NZD 93
D045 D045 Whangaparaoa      1.4260    0.0000    0.0000 ASHXII ASHXII SLBGP  6.0  93 077
    NZD 93
D045 D045 Whangaparaoa      1.4260    0.0000    0.0000 ASHXII ASHXII SLBGP  6.0  93 077
    NZD 93
D045 D045 Whangaparaoa      1.4280    0.0000    0.0000 ASHXII ASHXII SLBGP  6.0  93 078
    NZD 93
D072 D072 F Maketu          7.0130    0.0000    0.0000 ASHXII ASHXII DHPAB  6.0  93 077
    NZD 93
D072 D072 F Maketu          7.1170    0.0000    0.0000 LEI200 LEIGRT DHPAB  6.0  93 079
    NZD 93
D078 D078 201 Te Pohue      1.2450    0.0000    0.0000 ASHXII ASHXII DHPAB  6.0  93 078
    NZD 93
D100 D100 106 Okahuatiu     1.9350    0.0000    0.0000 ASHXII ASHXII SLBGP  6.0  93 078
```

```
    NZD 93
D100 D100 106 Okahuatiu      2.0690   0.0000   0.0000 ASHXII ASHXII SLBGP  6.0  93 078
    NZD 93
D100 D100 106 Okahuatiu      1.9390   0.0000   0.0000 ASHXII ASHXII SLBGP  6.0  93 079
    NZD 93
D105 D105 A Huirangi         1.4230   0.0000   0.0000 ASHXII ASHXII SLBGP  6.0  93 075
    NZD 93
D105 D105 A Huirangi         1.4730   0.0000   0.0000 ASHXII ASHXII SLBGP  6.0  93 077
    NZD 93
D131 D131 Mt Stewart         1.0490   0.0000   0.0000 ASHXII ASHXII SLBGP  6.0  93 075
    NZD 93
D131 D131 Mt Stewart         1.0490   0.0000   0.0000 ASHXII ASHXII SLBGP  6.0  93 076
    NZD 93
D143 D143 Eringa             1.4010   0.0000   0.0000 ASHXII ASHXII SLBGP  6.0  93 074
    NZD 93
D143 D143 Eringa             1.3620   0.0000   0.0000 ASHXII ASHXII SLBGP  6.0  93 076
    NZD 93
D158 D158 Jenkins Hill       1.3960   0.0000   0.0000 ASHXII ASHXII SLBGP  6.0  93 073
    NZD 93
D172 D172 Mt Murchison       1.6800   0.0000   0.0000 ASHXII ASHXII SLBGP  6.0  93 072
    NZD 93
D172 D172 Mt Murchison       1.6800   0.0000   0.0000 ASHXII ASHXII SLBGP  6.0  93 073
    NZD 93
D191 D191 Isolated Hill      1.8160   0.0000   0.0000 ASHXII ASHXII SLBGP  6.0  93 072
    NZD 93
D191 D191 Isolated Hill      1.8630   0.0000   0.0000 ASHXII ASHXII SLBGP  6.0  93 074
    NZD 93
D212 D212 Mt Pleasant        1.5770   0.0000   0.0000 ASHXII ASHXII SLBGP  6.0  93 071
    NZD 93
D212 D212 Mt Pleasant        1.5520   0.0000   0.0000 ASHXII ASHXII SLBGP  6.0  93 072
    NZD 93
D229 D229 Mt Mary            1.1930   0.0000   0.0000 ASHXII ASHXII SLBGP  6.0  93 068
    NZD 93
D229 D229 Mt Mary            1.1920   0.0000   0.0000 ASHXII ASHXII SLBGP  6.0  93 070
    NZD 93
D229 D229 Mt Mary            1.6070   0.0000   0.0000 ASHXII ASHXII SLBGP  6.0  93 070
    NZD 93
D229 D229 Mt Mary            1.6070   0.0000   0.0000 ASHXII ASHXII SLBGP  6.0  93 071
    NZD 93
D233 D233 A Mt Horrible      1.1520   0.0000   0.0000 ASHXII ASHXII SLBGP  6.0  93 068
    NZD 93
D233 D233 A Mt Horrible      1.6100   0.0000   0.0000 ASHXII ASHXII SLBGP  6.0  93 071
    NZD 93
D253 D253 T Hyde Rock        1.1700   0.0000   0.0000 ASHXII ASHXII SLBGP  6.0  93 067
    NZD 93
D253 D253 T Hyde Rock        1.1300   0.0000   0.0000 ASHXII ASHXII SLBGP  6.0  93 067
    NZD 93
D253 D253 T Hyde Rock        1.1200   0.0000   0.0000 ASHXII ASHXII SLBGP  6.0  93 068
    NZD 93
D253 D253 T Hyde Rock        1.1500   0.0000   0.0000 ASHXII ASHXII SLBGP  6.0  93 069
    NZD 93
D269 D269 A North Taieri     1.6120   0.0000   0.0000 ASHXII ASHXII SLBGP  6.0  93 067
    NZD 93
D269 D269 A North Taieri     1.4510   0.0000   0.0000 ASHXII ASHXII SLBGP  6.0  93 067
    NZD 93
D269 D269 A North Taieri     1.5020   0.0000   0.0000 ASHXII ASHXII SLBGP  6.0  93 068
    NZD 93
```

```
D286 D286 X The Bluff      2.6550   0.0000   0.0000 ASHXII ASHXII SLBGP  6.0  93 067
    NZD 93
D286 D286 X The Bluff      2.8120   0.0000   0.0000 ASHXII ASHXII SLBGP  6.0  93 067
    NZD 93
D302 D302 Mt York          1.4880   0.0000   0.0000 ASHXII ASHXII SLBGP  6.0  93 067
    NZD 93
D302 D302 Mt York          1.3320   0.0000   0.0000 ASHXII ASHXII SLBGP  6.0  93 067
    NZD 93
D302 D302 Mt York          1.4690   0.0000   0.0000 ASHXII ASHXII SLBGP  6.0  93 069
    NZD 93
D309 D309 HB Mt Greenland  1.3030   0.0000   0.0000 ASHXII ASHXII SLBGP  6.0  93 070
    NZD 93
D309 D309 HB Mt Greenland  1.4500   0.0000   0.0000 ASHXII ASHXII SLBGP  6.0  93 070
    NZD 93
D309 D309 HB Mt Greenland  1.3030   0.0000   0.0000 ASHXII ASHXII SLBGP  6.0  93 071
    NZD 93
D309 D309 HB Mt Greenland  1.4500   0.0000   0.0000 ASHXII ASHXII SLBGP  6.0  93 072
    NZD 93
D320 D320 JF               0.1140   0.0000   0.0000 ASHXII ASHXII DHPAB  6.0  93 069
    NZD 93
D320 D320 JF               0.1130   0.0000   0.0000 ASHXII ASHXII DHPAB  6.0  93 070
    NZD 93
D320 D320 JF               0.2800   0.0000   0.0000 ASHXII ASHXII DHPAB  6.0  93 070
    NZD 93
D338 D338 8741             1.2510   0.0000   0.0000 ASHXII ASHXII SLBGP  6.0  93 069
    NZD 93
D338 D338 8741             1.3400   0.0000   0.0000 ASHXII ASHXII SLBGP  6.0  93 070
    NZD 93
D338 D338 8741             1.2650   0.0000   0.0000 ASHXII ASHXII SLBGP  6.0  93 070
    NZD 93
D425 D425 A Cape Campbell  1.3250   0.0000   0.0000 ASHXII ASHXII SLBGP  6.0  93 073
    NZD 93
D425 D425 A Cape Campbell  1.3300   0.0000   0.0000 ASHXII ASHXII SLBGP  6.0  93 074
    NZD 93
D431 D431 Bluff Hill No 3  1.6300   0.0000   0.0000 ASHXII ASHXII SLBGP  6.0  93 076
    NZD 93
D431 D431 Bluff Hill No 3  1.5770   0.0000   0.0000 ASHXII ASHXII SLBGP  6.0  93 079
    NZD 93
D452 D452 79 Rangiriri     1.2160   0.0000   0.0000 ASHXII ASHXII SLBGP  6.0  93 077
    NZD 93
D469 D469 I Parapara       1.2970   0.0000   0.0000 ASHXII ASHXII SLBGP  6.0  93 073
    NZD 93
D469 D469 I Parapara       1.2960   0.0000   0.0000 ASHXII ASHXII SLBGP  6.0  93 075
    NZD 93
D473 D473 Marotiri No 2    1.4880   0.0000   0.0000 ASHXII ASHXII SLBGP  6.0  93 076
    NZD 93
D473 D473 Marotiri No 2    1.5240   0.0000   0.0000 LEI200 LEIGRT DHPAB  1.0  93 077
    NZD 93
D473 D473 Marotiri No 2    1.5380   0.0000   0.0000 LEI200 LEIGRT DHPAB  1.0  93 078
    NZD 93
D473 D473 Marotiri No 2    1.4330   0.0000   0.0000 LEI200 LEIGRT DHPAB  1.0  93 078
    NZD 93
D474 D474 Three Sisters    1.4760   0.0000   0.0000 ASHXII ASHXII SLBGP  6.0  93 067
    NZD 93
D474 D474 Three Sisters    1.4760   0.0000   0.0000 ASHXII ASHXII SLBGP  6.0  93 067
    NZD 93
D474 D474 Three Sisters    1.4760   0.0000   0.0000 ASHXII ASHXII SLBGP  6.0  93 071
```

```
    NZD 93
D474 D474 Three Sisters      1.4760   0.0000   0.0000 ASHXII ASHXII SLBGP  6.0  93 071
    NZD 93
D481 D481 Marotiri Ecc       1.6060   0.0000   0.0000 ASHXII ASHXII SLBGP  6.0  93 077
    NZD 93
D481 D481 Marotiri Ecc       1.5700   0.0000   0.0000 ASHXII ASHXII SLBGP  6.0  93 078
    NZD 93
D481 D481 Marotiri Ecc       1.5120   0.0000   0.0000 ASHXII ASHXII SLBGP  6.0  93 078
    NZD 93
D482 D482 HH R9              0.1770   0.0000   0.0000 LEI200 LEIGRT DHPAB  1.0  93 077
    NZD 93
D483 D483 HH R9A             0.6180   0.0000   0.0000 LEI200 LEIGRT DHPAB  1.0  93 078
    NZD 93
D484 D484 F Maketu Ecc       1.8080   0.0000   0.0000 ASHXII ASHXII SLBGP  6.0  93 079
    NZD 93
DARW DARW Darwin             0.031    0.0000   0.0000 ASHXII ASHXII DHPAB  6.0  92 206
    AFN IGS 92 days 207-221
DARW DARW Darwin             0.0350   0.0000   0.0000 ASHXII ASHXII DHPAB  2.00 93 227
    ARN 93
DAV1 DAV1 Davis NMS5         0.0035   0.0000   0.0000 TRBROG TRBROG DHPAB  1.20 93 350
    ANT94
DEAK DEAK Deakin ecce        1.570    0.0000   0.0000 TRMSST TRMSST SLBGP  4.70 93 239
    ARN 93
DILL DILL McDills Simpson    1.396    0.0000   0.0000 TRMSST TRMSST DHPAB  4.70 92 212
    UNSW Simpson Desert
DS40 DS40 Canberra           0.0000   0.0000   0.0000 ROGSNR ROGSNR DHPAB  5.60 91 004
DS41 DS41 Canberra temp      0.0000   0.0000   0.0000 ROGSNR ROGSNR DHPAB  7.00 92 044
DS42 DS42 Canberra new       0.0000   0.0000   0.0000 ROGSNR ROGSNR DHPAB  5.60 92 132
E072 D072 F Maketu           7.0130   0.0000   0.0000 ASHXII ASHXII DHPAB  6.0  93 077
    NZD 93
E072 E072 F Maketu           7.1170   0.0000   0.0000 LEI200 LEIGRT DHPAB  6.0  93 079
    NZD 93
E078 E078 201 Te Pohue       1.5160   0.0000   0.0000 ASHXII ASHXII DHPAB  6.0  93 078
    NZD 93
E100 E100 106 Okahuatiu      2.0730   0.0000   0.0000 ASHXII ASHXII SLBGP  6.0  93 079
    NZD 93
E105 D105 A Huirangi         1.5500   0.0000   0.0000 ASHXII ASHXII SLBGP  6.0  93 075
    NZD 93
E105 D105 A Huirangi         1.2530   0.0000   0.0000 ASHXII ASHXII SLBGP  6.0  93 077
    NZD 93
E131 D131 Mt Stewart         1.1890   0.0000   0.0000 ASHXII ASHXII SLBGP  6.0  93 075
    NZD 93
E131 D131 Mt Stewart         0.9240   0.0000   0.0000 ASHXII ASHXII SLBGP  6.0  93 076
    NZD 93
E143 D143 Eringa             1.2360   0.0000   0.0000 ASHXII ASHXII SLBGP  6.0  93 074
    NZD 93
E143 D143 Eringa             1.2110   0.0000   0.0000 ASHXII ASHXII SLBGP  6.0  93 076
    NZD 93
E158 D158 Jenkins Hill       1.5520   0.0000   0.0000 ASHXII ASHXII SLBGP  6.0  93 073
    NZD 93
E172 D172 Mt Murchison       1.7830   0.0000   0.0000 ASHXII ASHXII DHPAB  6.0  93 072
    NZD 93
E172 D172 Mt Murchison       1.8430   0.0000   0.0000 ASHXII ASHXII SLBGP  6.0  93 073
    NZD 93
E191 D191 Isolated Hill      1.8900   0.0000   0.0000 ASHXII ASHXII SLBGP  6.0  93 072
    NZD 93
E191 D191 Isolated Hill      1.7170   0.0000   0.0000 ASHXII ASHXII SLBGP  6.0  93 074
```

```
    NZD 93
E212 D212 Mt Pleasant      1.5440   0.0000   0.0000 ASHXII ASHXII SLBGP  6.0  93 071
    NZD 93
E212 D212 Mt Pleasant      1.4990   0.0000   0.0000 ASHXII ASHXII SLBGP  6.0  93 072
    NZD 93
E229 D229 Mt Mary          1.5880   0.0000   0.0000 ASHXII ASHXII SLBGP  6.0  93 067
    NZD 93
E229 D229 Mt Mary          1.1930   0.0000   0.0000 ASHXII ASHXII SLBGP  6.0  93 068
    NZD 93
E229 D229 Mt Mary          1.5200   0.0000   0.0000 ASHXII ASHXII SLBGP  6.0  93 071
    NZD 93
E233 D233 A Mt Horrible    1.1090   0.0000   0.0000 ASHXII ASHXII SLBGP  6.0  93 068
    NZD 93
E233 D233 A Mt Horrible    1.6780   0.0000   0.0000 ASHXII ASHXII SLBGP  6.0  93 071
    NZD 93
E253 D253 T Hyde Rock      1.0500   0.0000   0.0000 ASHXII ASHXII DHPAB  6.0  93 068
    NZD 93
E253 D253 T Hyde Rock      1.0600   0.0000   0.0000 ASHXII ASHXII SLBGP  6.0  93 069
    NZD 93
E269 D269 A North Taieri   1.1820   0.0000   0.0000 ASHXII ASHXII SLBGP  6.0  93 068
    NZD 93
E302 D302 Mt York          1.5970   0.0000   0.0000 ASHXII ASHXII SLBGP  6.0  93 069
    NZD 93
E309 D309 HB Mt Greenland  1.4500   0.0000   0.0000 ASHXII ASHXII SLBGP  6.0  93 071
    NZD 93
E309 D309 HB Mt Greenland  1.2280   0.0000   0.0000 ASHXII ASHXII SLBGP  6.0  93 072
    NZD 93
E320 D320 JF               0.2790   0.0000   0.0000 ASHXII ASHXII DHPAB  6.0  93 069
    NZD 93
E338 D338 8741             1.3410   0.0000   0.0000 ASHXII ASHXII SLBGP  6.0  93 069
    NZD 93
E425 D425 A Cape Campbell  1.4400   0.0000   0.0000 ASHXII ASHXII SLBGP  6.0  93 073
    NZD 93
E425 D425 A Cape Campbell  1.5350   0.0000   0.0000 ASHXII ASHXII SLBGP  6.0  93 074
    NZD 93
E431 D431 Bluff Hill No 3  1.5380   0.0000   0.0000 ASHXII ASHXII SLBGP  6.0  93 076
    NZD 93
E431 E431 Bluff Hill No 3  1.5150   0.0000   0.0000 ASHXII ASHXII SLBGP  6.0  93 079
    NZD 93
E452 D452 79 Rangiriri     1.0380   0.0000   0.0000 ASHXII ASHXII SLBGP  6.0  93 077
    NZD 93
E469 D469 I Parapara       1.4630   0.0000   0.0000 ASHXII ASHXII SLBGP  6.0  93 073
    NZD 93
E469 D469 I Parapara       1.4600   0.0000   0.0000 ASHXII ASHXII SLBGP  6.0  93 075
    NZD 93
E473 D473 Marotiri No 2    1.3920   0.0000   0.0000 ASHXII ASHXII SLBGP  6.0  93 076
    NZD 93
E473 D473 Marotiri No 2    1.5240   0.0000   0.0000 LEI200 LEIGRT DHPAB  1.0  93 077
    NZD 93
E481 D481 Marotiri Ecc     1.5710   0.0000   0.0000 ASHXII ASHXII SLBGP  6.0  93 077
    NZD 93
E482 D482 HH R9            0.1770   0.0000   0.0000 LEI200 LEIGRT DHPAB  1.0  93 077
    NZD 93
E483 E483 HH R9A           0.6180   0.0000   0.0000 LEI200 LEIGRT DHPAB  1.0  93 078
    NZD 93
E484 E484 F Maketu Ecc     1.7600   0.0000   0.0000 ASHXII ASHXII SLBGP  6.0  93 079
    NZD 93
```

```
EC19 EC19 UNSW Pillar 19    0.101    0.0000    0.0000 LEIGRT LEIGRT DHPAB  2.0   94 050
    ANT94
EDEN EDEN Eden NSW          0.137    0.0000    0.0000 TRMSST TRMSST DHPAB  4.69  92 206
    NSW IGS 92 days 207-221
ELDO ELDO Gove NT           1.549    0.0000    0.0000 LEI200 LEIGRT DHPAB  1.43  93 239
    ARN 93
EMUU EMUU Emu               1.6578   0.0000    0.0000 TRMSST TRMSST DHPAB  4.70  92 206
    NSW IGS 92 days 216-217
ESPE ESPE Esperance WA      1.6735   0.0000    0.0000 ASHXII ASHXII DHPAB  1.0   92 206
    TIDE GAUGE IGS 92 day 207-210
ESPE ESPE Esperance         1.475    0.0000    0.0000 TRMSST TRMSST DHPAB  4.7   93 239
    ARN 93
FLAG FLAG Port Kembla NSW   1.3397   0.0000    0.0000 TRMSST TRMSST DHPAB  4.80  92 206
    TIDE GAUGE IGS 92 day 207-210
FRN2 FRN2 FERN HILL ACT     0.0000   0.0000    0.0000 ROGSNR ROGSNR DHPAB  5.60  94 099
    AUSLIG SITE
GIBS GIBS Mcdougall         1.347    0.0000    0.0000 TRMSSE TRMSSE DHPAB  5.52  93 239
    ARN 93
GILG GILG Gilgunnia NSW     0.140    0.0000    0.0000 TRMSST TRMSST DHPAB  4.69  92 212
    NSW IGS 92 days 212-215
GOKA GOKA Goroka png        1.478    0.0000    0.0000 ASHXII ASHXII SLBGP  7.00  93 239
    ARN 93
GREN GREN Green Hill        1.278    0.0000    0.0000 ASHXII ASHXII DHPAB  6.00  92 206
    NSW IGS 92 days 219-220
GROO GROO Groote Is         1.534    0.0000    0.0000 LEI200 LEIGRT DHPAB  1.43  93 239
    ARN 93
HART HART Hartebeesthoek    9.7540   0.0000    0.0000 ROGSNR ROGSNR DHPAB  2.31  90 334
HOB1 HOB1 Hobart Cignet     0.0      0.0000    0.0000 ROGSNR ROGSNR DHPAB  7.4   93 239
    ARN 93
HOBA HOBA Hobart            0.038    0.0000    0.0000 ASHXII ASHXII DHPAB  6.0   92 206
    AFN IGS 92 days 206-221
HOBA HOBA Hobart AFN        0.097    0.0000    0.0000 ROGSNR ROGSNR DHPAB  1.0   93 239
    ARN 93
HOWI HOWI Howitt QLD        1.5858   0.0000    0.0000 TRMSST TRMSST DHPAB  4.64  92 211
    NSW IGS 92 days 212-214
HWKR HWKR Hawker            1.5641   0.0000    0.0000 TRMSSE TRMSSE DHPAB  5.60  93 239
    ARN 93
JOHN JOHN Johnston Origin   1.111    0.0000    0.0000 LEI200 LEIGRT DHPAB  1.43  93 239
    ARN 93
JUNC JUNC Junction          0.8840   0.0000    0.0000 TRMSSE TRMSSE DHPAB  5.60  93 239
    ARN 93
KALG KALG Coolgardie        1.299    0.0000    0.0000 TRMSSE TRMSSE DHPAB  5.60  93 239
    ARN 93
KARR KARR Karratha          0.035    0.0000    0.0000 ASHXII ASHXII DHPAB  6.0   92 206
    AFN IGS 92 days 206-
KARR KARR Karratha          0.0305   0.0000    0.0000 TRMSST TRMSST DHPAB  4.81  93 239
    ARN 93
KDMN KDMN Kidman springs    1.174    0.0000    0.0000 LEI200 LEIGRT DHPAB  4.43  93 239
    ARN 93
KILI KILI Tanami NT         1.461    0.0000    0.0000 LEI200 LEIGRT DHPAB  4.43  93 239
    ARN 93
LLTR LLTR Lake Littra NSW   0.112    0.0000    0.0000 TRMSST TRMSST DHPAB  4.64  92 206
    NSW IGS 92 days 208-210,212-215
LLTR LLTR Lake Littra NSW   0.1270   0.0000    0.0000 TRMSST TRMSST DHPAB  4.30  93 239
    ARN 93
MAC1 MAC1 Macquarie Island  0.1025   0.0000    0.0000 TRBROG TRBROG DHPAB  1.20  93 350
    ANT94
```

```
MAW1 MAW1 Mawson Pillar     0.0385   0.0000   0.0000 TRBROG TRBROG DHPAB  1.20 93 350
    ANT94
MCMU MCMU McMurdo           0.0000   0.0000   0.0000 ROGSNR ROGSNR DHPAB  6.11 92 052
    New Installation (on top of pole)
MORE MORE Port Moresby      6.335    0.0000   0.0000 ASHXII ASHXII DHPAB  6.0  92 206
    AFN IGS 92 days 206-222
MORE MORE Port Moresby      6.41     0.0000   0.0000 ASHXII ASHXII DHPAB  7.0  93 225
    ARN 93
MUCK MUCK Muckadilla QLD    1.4110   0.0000   0.0000 TRMSST TRMSST DHPAB  4.64 92 206
    NSW IGS 92 days 207-210
MUCK MUCK Muckadilla QLD    1.4794   0.0000   0.0000 TRMSST TRMSST DHPAB  4.70 92 211
    NSW IGS 92 days 219-220
MULA MULA Mulara QLD        1.545    0.0000   0.0000 TRMSST TRMSST SLBGP  4.70 93 157
    QLD Mini IGS
NORM NORM Normanton         1.5111   0.0000   0.0000 TRMSST TRMSST DHPAB  4.70 92 206
    NSW IGS 92 days 212-215
OAKS OAKS Rosslyn Tide QLD  1.4058   0.0000   0.0000 TRMSST TRMSST DHPAB  4.70 92 206
    TIDE GAUGE IGS 92 day 207-210
OAKS OAKS Rosslyn Tide QLD  1.442    0.0000   0.0000 TRMSST TRMSST SLBGP  4.70 93 157
    QLD Mini IGS
OLVE OLVE Olive NSW         1.384    0.0000   0.0000 TRMSST TRMSST DHPAB  4.64 92 212
    NSW IGS 92 days 212-215
OLVE OLVE Olive NSW         1.398    0.0000   0.0000 TRMSSE TRMSST DHPAB  5.63 93 239
    ARN 93
ORRO ORRO Orroral           0.0000   0.0000   0.0000 ASHXII ASHXII DHPAB  2.00 92 136
OTA1 OTA1 Otago New         0.687    0.0000   0.0000 ASHXII ASHXII DHPAB  7.00 93 239
    ARN 93
OTAG OTAG Dunedin NZ        0.075    0.0000   0.0000 ASHXII ASHXII DHPAB  6.0  92 208
    AFN IGS 92 days 200-221
OTAG OTAG Dunedin NZ        0.066    0.0000   0.0000 ASHXII ASHXII DHPAB  7.0  93 239
    ARN 93
PAMA PAMA Tahiti            8.4200   0.0000   0.0000 ROGSNR ROGSNR DHPAB  2.31 91 334
PER2 PER2 Hilary Tideg      1.617    0.0000   0.0000 TRMSSE TRMSSE DHPAB  5.63 93 239
    ARN 93
PER3 PER3 Hilary Tideg      1.611    0.0000   0.0000 ASHXII ASHXII DHPAB  6.0  92 206
    TIDE GAUGE IGS 92 day 207-210
PERT PERT Perth             0.0568   0.0000   0.0000 ROGSNR ROGSNR DHPAB  7.4  93 239
    ARN 94
PIEB PIEB Piebald           1.4592   0.0000   0.0000 TRMSST TRMSST DHPAB  4.70 92 206
    NSW IGS 92 day 219-220
PILL PILL Darwin Pillar     0.312    0.0000   0.0000 MIN6AT MIN6AT L1PHC  1.64 92 206
    TIDE GAUGE IGS 92 day 207-210
PIVT PIVT Wyndam            1.192    0.0000   0.0000 LEI200 LEIGRT DHPAB  4.43 93 239
    ARN 93
PORT PORT Portland VIC      1.493    0.0000   0.0000 TRMSST TRMSST DHPAB  4.64 92 206
    TIDE GAUGE IGS 92 day 207-210
QUT1 QUT1 QUT BNE QLD       0.070    0.0000   0.0000 TRMSST TRMSST DHPAB  4.64 92 206
    QUT Kinematic Base 207-221
RATH RATH Noreena Downs     0.620    0.0000   0.0000 ASHXII ASHXII DHPAB  7.60 93 239
    ARN 93
RAWL RAWL Rawlinson         1.469    0.0000   0.0000 TRMSST TRMSST DHPAB  4.70 93 239
    ARN 93
ROPE ROPE Roper River       1.579    0.0000   0.0000 LEI200 LEIGRT DHPAB  1.00 92 206
    NSW IGS 92 day 213-214
ROPE ROPE Roper River       1.555    0.0000   0.0000 LEI200 LEIGRT DHPAB  4.43 93 239
    ARN 93
SHAM SHAM Shamrock NT       0.3025   0.0000   0.0000 TRMSST TRMSST DHPAB  4.64 92 212
```

```
    NSW IGS 92 day 213-214
SHAM SHAM Shamrock NT        0.343    0.0000    0.0000 LEI200 LEIGRT DHPAB  4.43 93 239
    ARN 93
SML1 SML1 SML1 SIMPSON       1.485    0.0000    0.0000 TRMSST TRMSST DHPAB  4.70 92 212
    UNSW SIMPSON DESERT
SPM9 SPM9 Burnie             1.1830   0.0000    0.0000 MIN6AT MIN6AT L1PHC  1.64 92 206
    TIDE GAUGE IGS 92 day 207-210
STAN STAN Pt Stanvac SA      1.5252   0.0000    0.0000 TRMSST TRMSST DHPAB  4.30 92 206
    TIDE GAUGE IGS 92 day 207-210
STAN STAN Stanvac            1.314    0.0000    0.0000 TRMSST TRMSST DHPAB  4.30 93 239
    ARN 93
SUGA SUGA Sugarland QLD      1.598    0.0000    0.0000 TRMSST TRMSST SLBGP  4.70 93 157
    QLD Mini IGS
SUND SUND Sundown NSW        0.080    0.0000    0.0000 TRMSST TRMSST DHPAB  4.70 92 212
    NSW IGS 92 days 212-215
TAS1 TAS1 Tasmania           0.0000   0.0000    0.0000 MIN6AT MIN6AT L1PHC  1.64 91 243
    CIGNET
TEXA TEXA Texas Pillar QLD   0.076    0.0000    0.0000 TRMSST TRMSST DHPAB  4.70 92 206
    NSW IGS 92 days 207-210
TEXA TEXA Texas Pillar QLD   0.078    0.0000    0.0000 TRMSST TRMSST DHPAB  4.70 92 219
    NSW IGS 92 days 219-220
THEV THEV Thevenard SA       1.4402   0.0000    0.0000 TRMSST TRMSST DHPAB  4.30 92 206
    TIDE GAUGE IGS 92 day 207-210
TORB TORB Torbay             0.109    0.0000    0.0000 TRMSSE TRMSSE DHPAB  5.60 93 239
    ARN 93
TOWA TOWA Townsville         0.032    0.0000    0.0000 ASHXII ASHXII DHPAB  6.0  92 205
    ARN92 days 205-220
TOWA TOWA Townsville         0.0045   0.0000    0.0000 TRMSST TRMSST DHPAB  4.64 93 239
    ARN 93
TOWN TOWN Townsville         0.0000   0.0000    0.0000 TRMSST TRMSST L1PHC  4.30 90 271
TOWN TOWN Townsville         0.0010   0.0000    0.0000 TRMSST TRMSST L1PHC  4.81 93 239
    ARN 94
TRIA TRIA Triabunna          0.881    0.0000    0.0000 ASHXII ASHXII DHPAB  6.0  92 206
    TIDE GAUGE IGS 92 day 208
TRK1 TRK1 TRK1 SIMPSON       1.274    0.0000    0.0000 TRMSST TRMSST DHPAB  4.70 92 212
    UNSW SIMPSON DESERT
TRK3 TRK3 TRK3 SIMPSON       1.179    0.0000    0.0000 TRMSST TRMSST DHPAB  4.70 92 212
    UNSW SIMPSON DESERT
VANI VANI Vanimo PNG         1.399    0.0000    0.0000 ASHXII ASHXII SLAGP  6.0  92 217
    AFN IGS 92 days 218-221
WELL WELL Wellington NZ      0.0000   0.0000    0.0000 TRMSST TRMSST L1PHC  4.30 91 243
    CIGNET
WELL WELL Wellington NZ      0.062    0.0000    0.0000 ASHXII ASHXII DHPAB  7.0  93 239
    ARN 93
WILF WILF Mt Isa             1.5343   0.0000    0.0000 TRMSST TRMSST DHPAB  4.70 92 215
    NSW IGS 92 day 216-217
WILF WILF Mt Isa             1.4622   0.0000    0.0000 TRMSST TRMSST DHPAB  4.64 92 218
    NSW IGS 92 day 219-220
WILF WILF Mt Isa             0.929    0.0000    0.0000 TRMSSE TRMSSE DHPAB  5.64 93 239
    ARN 93
WINN WINN Winnellie          1.651    0.0000    0.0000 MIN6AT MIN6AT L1PHC  1.64 92 206
    TIDE GAUGE IGS 92 day 207-210
WOLL WOLL Wollogorang        1.506    0.0000    0.0000 LEI200 LEIGRT DHPAB  4.43 93 239
    ARN 93
XMAS XMAS Christmas Is       1.4674   0.0000    0.0000 TRMSST TRMSST DHPAB  4.64 92 207
    AFN IGS 92 days 208-230
YAR1 YAR1 Yaragadee          0.0732   0.0000    0.0000 ROGSNR ROGSNR DHPAB  5.60 91 103
```

```
YAR1 YAR1 Yaragadee        0.0732   0.0000   0.0000 ROGSNR ROGSNR DHPAB  7.00 92 138
YAR1 YAR1 Yaragadee        0.0732   0.0000   0.0000 ROGSNR ROGSNR DHPAB  7.4  93 225
```

Appendix E

The Earthquake File

The following listing is the earthquake file associated with the final GLOBK runs.

Lines 1 and 2 are due to the movement of the reference point from the L_1 phase center to the reference mark (see IGS Message Nos 420, 430).

Line 3 is due to a naming conflict at Gnangara. It equates the 1992 Trimble site to the 1993 occupation.

Lines 4 and 5 are at Hobart AFN Pillar. The first was necessitated due to an unaccounted metal spacer between the base of the antenna and the pillar. The second is the combination of the spacer and the move from L_1 phase center to reference mark.

Lines 6 to 11 are to account for metal spacers at these sites. In the case of Ceduna the thichness was different for the two occupations.

Lines 12 through 31 are associated with the New Zealand analysis where there were two independant station occupations in the same day. The station.info file is limited to single day entries and hence a change of name was instituted to correctly reduce the observations to the reference mark. It is now necessary to bring the two estimates to a single value by combining the results.

```
GLOBK EARTHQUAKE file: /data5/gps/soln/ds42_fixer

There were   32 site renames applied
 #   Orig      New      Period from    ----->      To          Position change (m)    Type
 1 DS4X_GPS->DS42_GPS 1994/ 7/24  0: 0  1994/ 8/ 1  0: 0  0.0000  0.0000 -0.0920 NEU
 2 DS42_GPS->DS42_GPS 1992/ 7/25  0: 0  1994/ 1/ 1  0: 0  0.0000  0.0000 -0.0920 NEU
 3 PER3_GPS->PER2_GPS 1900/ 1/ 1  1: 0  2100/ 1/ 1  1: 0  0.0000  0.0000  0.0000 XYZ
 4 HOBA_GPS->HOBA_GPS 1993/ 8/25  0: 0  1994/ 1/ 1  0: 0  0.0000  0.0000 -0.0320 NEU
 5 HOB2_GPS->HOBA_GPS 1994/ 7/26  0: 0  1994/ 7/31  0: 0  0.0000  0.0000  0.0648 NEU
 6 ALIC_GPS->ALIC_GPS 1994/ 7/26  0: 0  1994/ 7/31  0: 0  0.0000  0.0000 -0.0320 NEU
 7 CEDU_GPS->CEDU_GPS 1993/ 8/25  0: 0  1994/ 1/ 1  0: 0  0.0000  0.0000 -0.0320 NEU
 8 CEDU_GPS->CEDU_GPS 1994/ 7/26  0: 0  1994/ 7/31  0: 0  0.0000  0.0000 -0.0380 NEU
 9 DARW_GPS->DARW_GPS 1994/ 7/26  0: 0  1994/ 7/31  0: 0  0.0000  0.0000 -0.0320 NEU
10 KARR_GPS->KARR_GPS 1994/ 7/26  0: 0  1994/ 7/31  0: 0  0.0000  0.0000 -0.0340 NEU
11 TOWA_GPS->TOWA_GPS 1994/ 7/26  0: 0  1994/ 7/31  0: 0  0.0000  0.0000 -0.0380 NEU
12 E072_GPS->D072_GPS 1900/ 1/ 1  1: 0  2100/ 1/ 1  1: 0  0.0000  0.0000  0.0000 XYZ
13 E078_GPS->D078_GPS 1900/ 1/ 1  1: 0  2100/ 1/ 1  1: 0  0.0000  0.0000  0.0000 XYZ
14 E100_GPS->D100_GPS 1900/ 1/ 1  1: 0  2100/ 1/ 1  1: 0  0.0000  0.0000  0.0000 XYZ
15 E105_GPS->D105_GPS 1900/ 1/ 1  1: 0  2100/ 1/ 1  1: 0  0.0000  0.0000  0.0000 XYZ
16 E131_GPS->D131_GPS 1900/ 1/ 1  1: 0  2100/ 1/ 1  1: 0  0.0000  0.0000  0.0000 XYZ
17 E143_GPS->D143_GPS 1900/ 1/ 1  1: 0  2100/ 1/ 1  1: 0  0.0000  0.0000  0.0000 XYZ
18 E158_GPS->D158_GPS 1900/ 1/ 1  1: 0  2100/ 1/ 1  1: 0  0.0000  0.0000  0.0000 XYZ
19 E191_GPS->D191_GPS 1900/ 1/ 1  1: 0  2100/ 1/ 1  1: 0  0.0000  0.0000  0.0000 XYZ
20 E212_GPS->D212_GPS 1900/ 1/ 1  1: 0  2100/ 1/ 1  1: 0  0.0000  0.0000  0.0000 XYZ
21 E253_GPS->D253_GPS 1900/ 1/ 1  1: 0  2100/ 1/ 1  1: 0  0.0000  0.0000  0.0000 XYZ
22 E309_GPS->D309_GPS 1900/ 1/ 1  1: 0  2100/ 1/ 1  1: 0  0.0000  0.0000  0.0000 XYZ
23 E320_GPS->D320_GPS 1900/ 1/ 1  1: 0  2100/ 1/ 1  1: 0  0.0000  0.0000  0.0000 XYZ
24 E338_GPS->D338_GPS 1900/ 1/ 1  1: 0  2100/ 1/ 1  1: 0  0.0000  0.0000  0.0000 XYZ
25 E425_GPS->D425_GPS 1900/ 1/ 1  1: 0  2100/ 1/ 1  1: 0  0.0000  0.0000  0.0000 XYZ
26 E431_GPS->D431_GPS 1900/ 1/ 1  1: 0  2100/ 1/ 1  1: 0  0.0000  0.0000  0.0000 XYZ
27 E452_GPS->D452_GPS 1900/ 1/ 1  1: 0  2100/ 1/ 1  1: 0  0.0000  0.0000  0.0000 XYZ
28 E469_GPS->D469_GPS 1900/ 1/ 1  1: 0  2100/ 1/ 1  1: 0  0.0000  0.0000  0.0000 XYZ
29 E473_GPS->D473_GPS 1900/ 1/ 1  1: 0  2100/ 1/ 1  1: 0  0.0000  0.0000  0.0000 XYZ
30 E482_GPS->D482_GPS 1900/ 1/ 1  1: 0  2100/ 1/ 1  1: 0  0.0000  0.0000  0.0000 XYZ
31 E483_GPS->D483_GPS 1900/ 1/ 1  1: 0  2100/ 1/ 1  1: 0  0.0000  0.0000  0.0000 XYZ
32 MCMR_GPS->MCMU_GPS 1900/ 1/ 1  1: 0  2100/ 1/ 1  1: 0  0.0000  0.0000  0.0000 XYZ
```

Appendix F

Time Slice Tables & Maps

F.1 Introduction

This appendix aims to provide information in tabular and map form as to what data were collected, used and archived and its spatial relationship with other similar data.

Chapter 3, Strategy, has figures describing the hierarchy and lateral connections between the networks. Figure F.1 below is a summary of the most of the network connections

F.1.1 The Time Slice Tables

The time slice tables list all the stations assigned to a network. The networks are generally associated with geographic regions such as New South Wales or Northern Territory and Queensland. Consequently the time slice lists do not include those higher level stations that are reduced as part of the regional network in order to provide the strength for unified solution.

These time slice tables use the following symbols:

- · is used to indicate no available RINEX data.
- o is used to indicate that RINEX data are available but were not processed.
- • is used to indicate that RINEX data are available, was processed and that clean RINEX files are available.
- ⊕ is used to indicate that RINEX data are available but that it may pose problems in cleaning and integration. This category has only been used for Antarctic data at this stage.

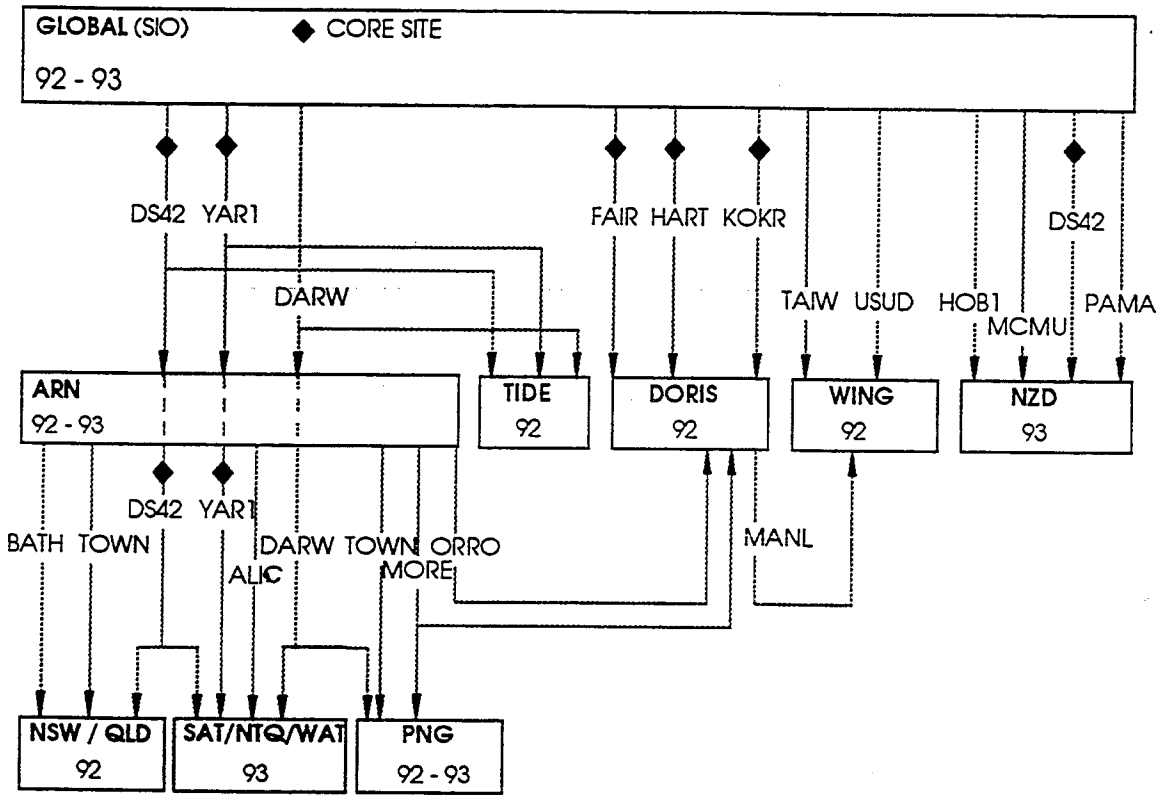

Figure F.1: Sketch of major network connections used in determining the solution

F.1.2 The Maps

Maps are placed on the same page, or the same page opening as the Time Slice Tables to provide spatial and geographical context of the stations. The maps use the following symbols:

- ◇ is used for global stations providing hierarchial connections between the network levels.
- o is used for stations providing lateral connections between the various sub class of the network.
- □ is the general site symbol.

F.2 TID92: Level 2

Table F.1: The 1992 Tide Array Time Slice Table

Station		Day of 1992				
		2	2	2	2	2
		0	0	0	0	1
		6	7	8	9	0
Benwerrin	BENW	·	●	●	●	●
Broome	BROO	o	●	●	·	·
Esperance	ESPE	o	●	●	·	·
Port Kembla	FLAG	o	●	●	●	●
Oaks	OAKS	·	●	●	●	●
Perth	PERT	o	●	●	●	●
Darwin Pillar	PILL	o	●	●	●	●
Portland	PORT	·	●	●	●	·
Burnie	SPM9	·	·	●	·	·
Port Stanvac	STAN	·	●	●	●	●
Thevenard	THEV	·	o	●	●	●
Triabunna	TRIA	·	●	●	●	●
Winnellie	WINN	o	●	●	●	●

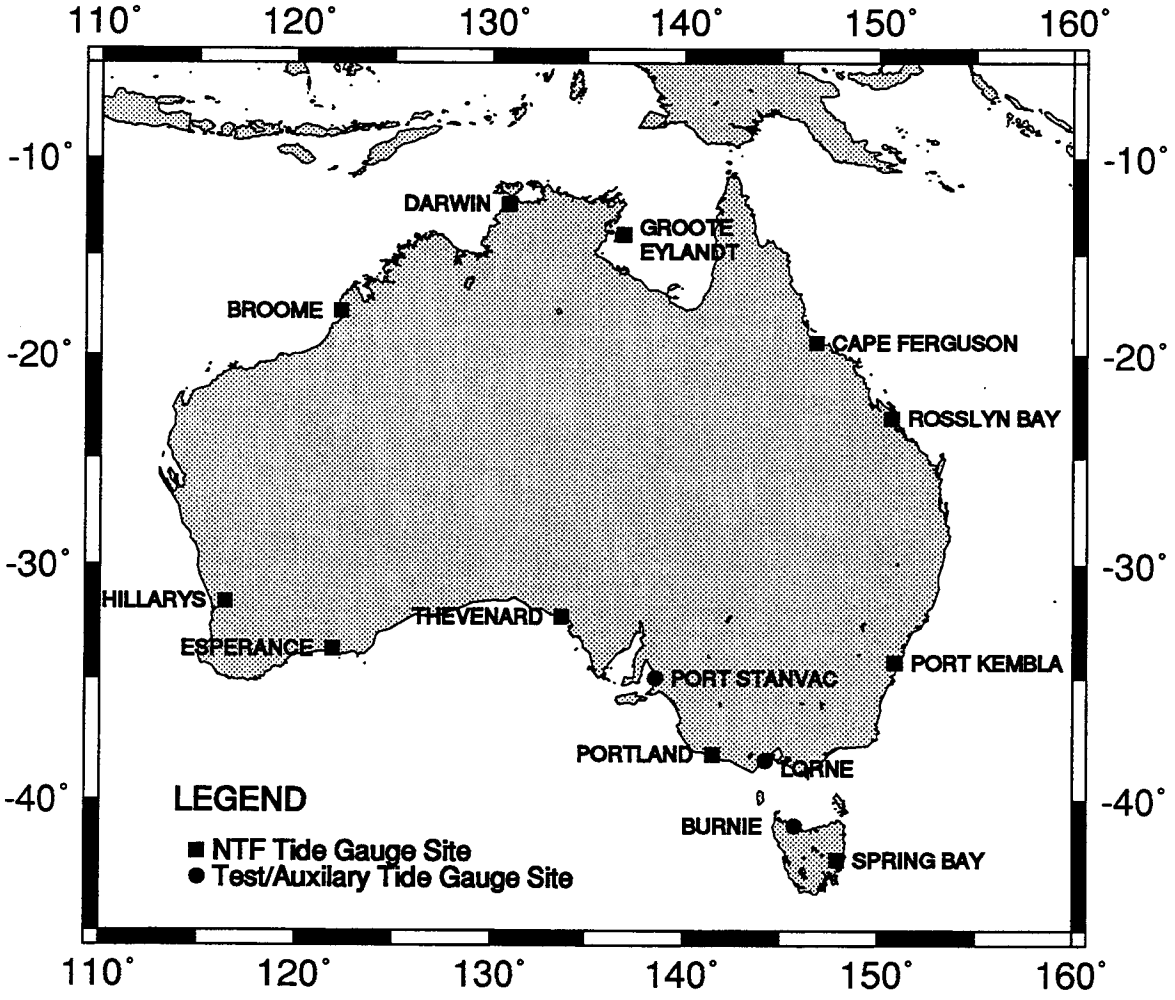

Figure F.2: Stations in the Australian Baseline Sea Level Monitoring Array

F.3 ARN92: Level 2

Table F.2: ARN92 Time Slice Table

Station		Day of 1992														
		207	208	209	210	211	212	213	214	215	216	217	218	219	220	221
Aiambak (PNG)	AIAM	·	·	·	·	·	·	·	o	o	●	●	·	·	·	·
Alice Springs	ALIC	●	●	●	●	●	o	o	o	o	●	●	●	●	●	o
Atkinson	ATKI	·	o	o	●	●	o	·	o	o	o	·	·	o	·	·
Smithfield	AUST	o	o	o	o	o	o	o	o	o	o	o	o	o	o	o
Bakosurtanal Indon	BAKO	·	·	●	●	·	·	·	·	·	·	·	·	·	·	·
Bathurst	BATH	●	●	●	●	●	●	●	●	●	●	●	●	●	●	o
Cocos Is	COCO	●	●	●	●	●	o	o	o	o	●	●	●	●	●	o
Tidbinbilla	DS42	●	●	●	●	●	o	o	o	o	●	●	●	●	●	o
Hobart, AFN	HOBA	●	●	●	●	●	o	o	o	o	●	●	●	●	●	o
Johnson Origin	JOHN	·	·	·	●	●	o	·	·	·	·	·	·	·	·	·
Karratha	KARR	●	●	●	●	●	o	o	o	o	●	●	●	●	●	o
Misima Is (PNG)	MISI	o	o	●	●	●	·	·	·	·	·	·	·	·	·	·
Port Moresby (PNG)	MORE	o	o	●	●	●	o	o	o	o	●	●	●	●	●	o
Orroral	ORRO	●	●	●	●	●	o	o	o	o	●	●	●	●	●	o
Dunedin, (NZ)	OTAG	·	·	●	●	●	o	o	o	o	●	●	●	●	●	o
Rawlinson	RAWL	·	·	·	·	·	·	·	·	·	·	·	·	·	●	·
Hobart, CIGNET	TASM	●	●	●	●	●	o	o	o	o	●	●	●	●	●	o
Townsville, AFN	TOWA	●	●	●	●	●	o	o	o	o	●	●	●	●	●	o
Townsville, CIGNET	TOWN	●	●	●	●	●	o	o	o	o	●	●	●	●	●	o
Vanima, (PNG)	VANI	·	·	·	·	·	·	·	·	·	·	·	●	●	●	o
Wellington, (NZ)	WELL	●	●	●	●	●	o	o	o	o	●	●	●	●	●	o
Christmas Is	XMAS	·	●	●	●	●	o	o	o	o	●	●	●	●	●	o
Yaragadee	YAR1	●	●	●	●	o	o	o	o	o	●	●	●	●	●	o

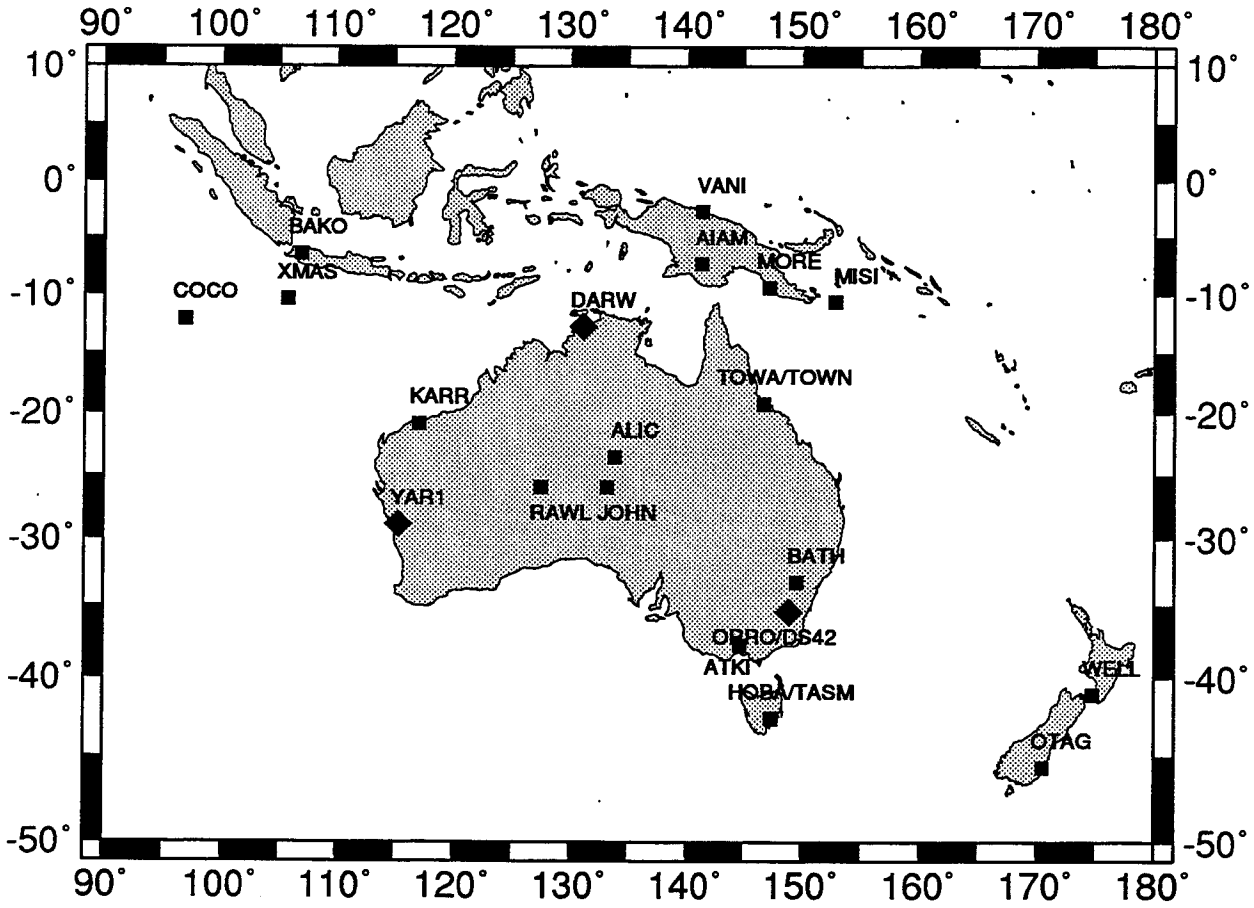

Figure F.3: Stations in the Australian Regional Network 1992

F.4 DOR92: Level 2

Table F.3: The DORIS 1992 Time Slice Table

Station		Day of 1992																		
		206	207	208	209	210	211	212	213	214	215	216	217	218	219	220	221	222	223	224
Addis Ababa	ADD1	·	·	·	·	·	·	·	·	·	·	·	·	·	·	·	·	·	·	·
Arlitt	ARLT	·	·	●	●	●	o	o	o	o	o	o	●	●	●	o	o	o	o	·
Arnagador	ARNA	·	·	●	●	●	o	o	o	o	o	o	●	·	·	·	·	·	·	·
Brasillia	BRAS	·	o	●	●	●	o	o	o	o	o	o	●	●	●	o	·	·	·	·
Cachoeira	CACH	·	·	·	·	·	·	·	·	·	·	·	·	·	·	·	·	·	·	·
Colombo	COLB	·	·	·	●	●	o	o	o	o	o	o	●	●	●	o	o	o	·	·
Djibouti	DJIB	·	o	●	●	●	o	o	o	o	o	o	●	●	·	o	o	o	·	·
Galapagos	GALA	·	·	·	·	o	o	o	o	o	o	o	●	●	●	o	o	o	·	·
Mexico	INEG	·	·	·	●	●	o	o	o	o	o	o	●	●	●	o	o	o	·	·
Kourou	KOUR	·	·	·	·	·	·	·	·	·	·	·	·	·	·	o	·	o	o	·
Libreville	LIBV	·	·	·	·	·	·	·	·	·	·	·	·	·	·	o	o	o	o	o
Manila	MANL	·	·	·	·	·	·	o	o	o	o	o	●	●	●	o	o	o	·	·
Noumea	NMN1	·	·	·	·	·	·	o	o	o	o	o	·	·	·	·	·	·	·	·
Paraguay	PARA	·	o	●	●	●	o	o	o	o	o	o	●	●	●	o	·	·	·	·
Reunion Is	REUN	o	o	●	●	●	o	o	o	o	o	o	●	●	●	o	o	·	·	·
Sakalinsk	SAKL	·	·	·	●	●	o	o	o	o	o	o	●	●	●	o	o	o	·	·
Soccoro	SOCO	·	·	·	●	●	o	o	o	o	o	o	●	●	●	o	o	o	·	·
St Helene	STHL	o	o	●	●	●	o	o	o	o	·	·	·	·	·	·	·	·	·	·

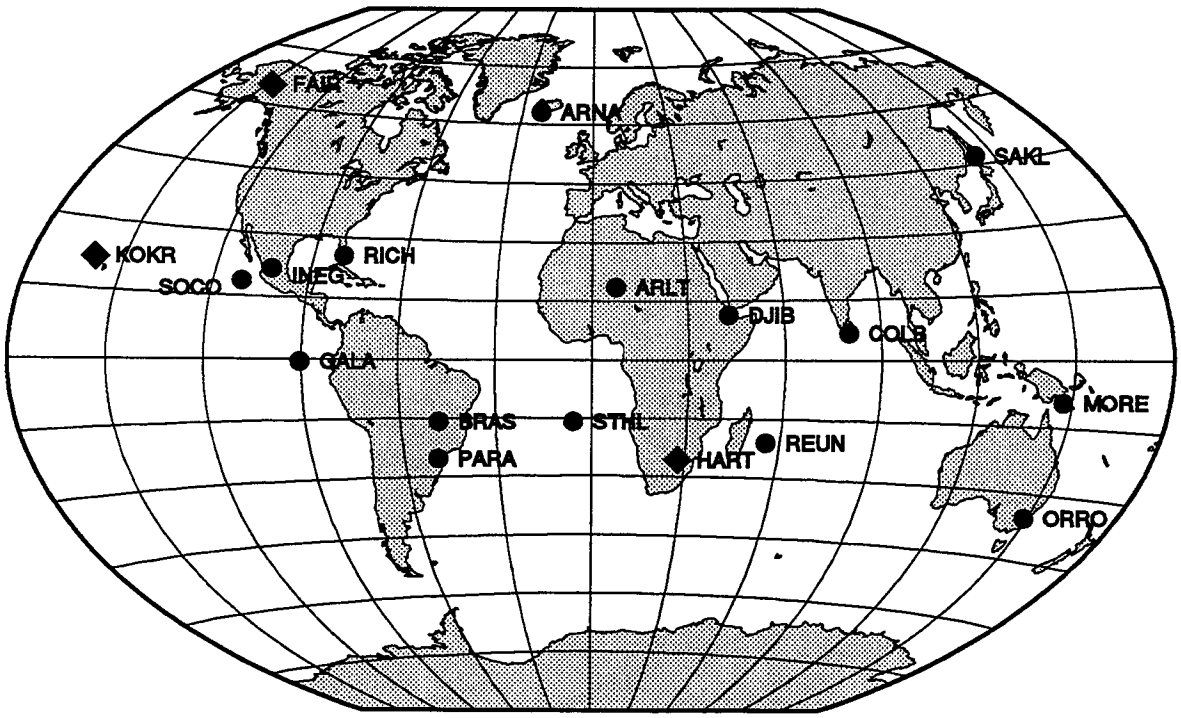

Figure F.4: Stations in the DORIS Network 1992

F.5 WNG92: Level 2

Table F.4: The Western Pacific, WNG, 1992 Time Slice Table

Station		Day of 1992														
		207	208	209	210	211	212	213	214	215	216	217	218	219	220	221
Beijing China	BEIJ	·	·	·	·	·	·	·	·	·	·	·	·	·	·	·
Daejeon Korea	DAEN	o	o	o	o	o	o	o	o	o	o	o	●	●	●	o
Manila Philippines	MANL	·	·	·	·	·	o	o	o	o	o	o	●	●	●	o
Manazuru Japan	MNZR	·	·	o	o	o	o	o	·	·	o	o	o	o	·	o
Nobeyama Japan	NBYM	o	o	o	o	o	o	o	·	·	·	·	·	·	·	·
Oshima Japan	OSMA	·	·	o	o	o	o	o	·	·	o	o	o	o	·	o
Nambersian Philippines	PNG5	·	·	·	·	·	·	·	·	·	·	·	·	·	·	·
Paisha China (Taiw)	S01R	o	o	o	o	o	o	o	o	o	o	o	o	o	o	o
Lanhsu China (Taiw)	S102	o	o	o	o	o	o	o	o	o	o	o	●	●	●	o
Shanghai China	SHAN	o	o	o	o	o	o	o	o	o	o	o	●	●	●	o
Turugisaki Japan	TURG	·	·	o	o	o	o	o	·	·	o	o	o	o	·	o
Wuhan China	WUHA	o	o	o	o	o	o	o	o	o	o	o	●	●	●	o

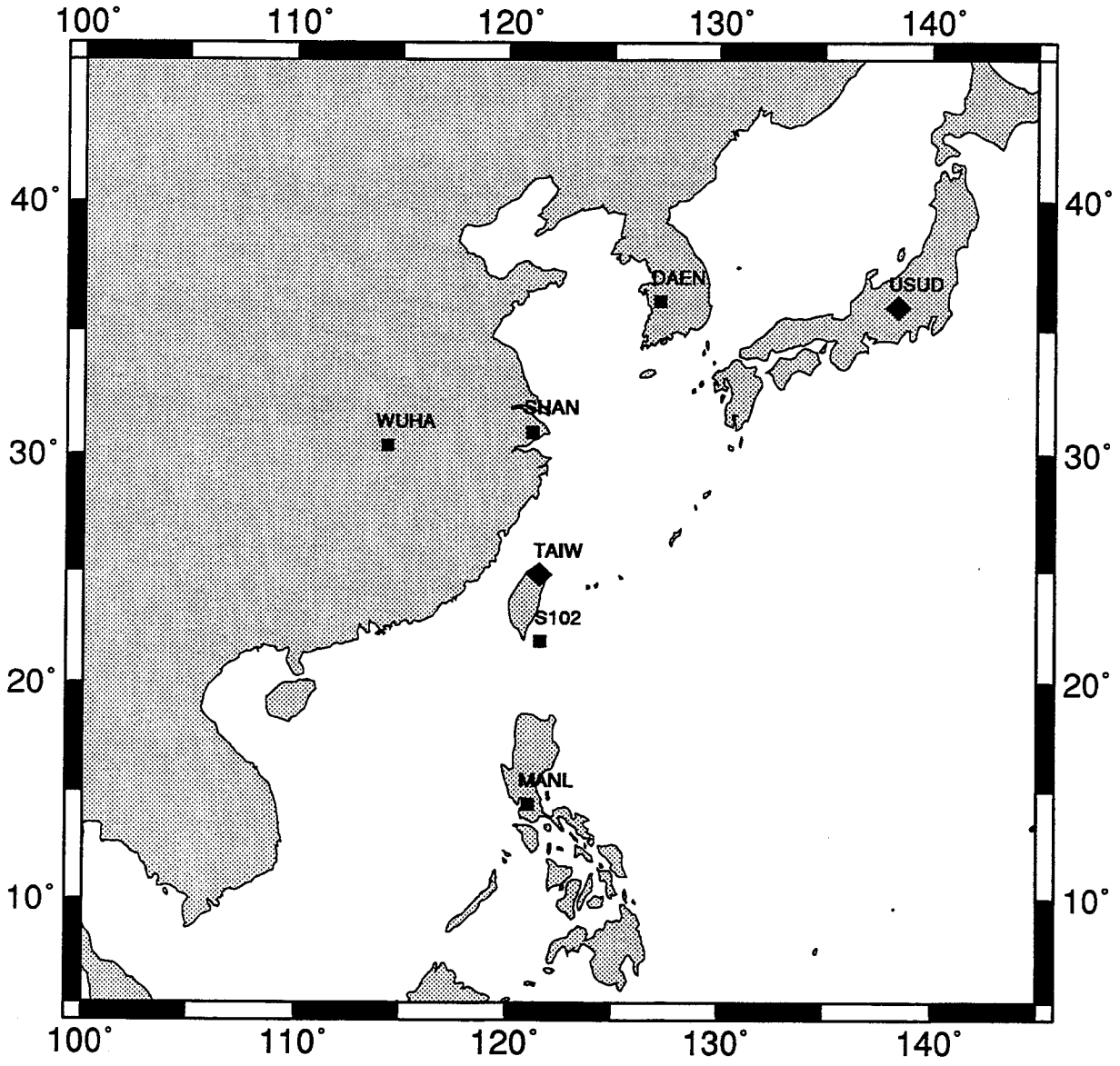

Figure F.5: Stations in the WING North East Asian campaign 1992

F.6 NSW92: Level 3

Table F.5: The New South Wales and Queensland 1992 Time Slice Table

Station		Day of 1992															
		206	207	208	209	210	211	212	213	214	215	216	217	218	219	220	221
Acres Dish	ACRE	·	·	·	·	·	·	·	·	·	·	○	·	·	·	·	·
Anzac Hill	ANZA	·	·	·	·	·	·	·	·	·	·	·	○	·	·	·	·
Atkinson	ATKI	·	·	○	○	○	○	○	·	●	○	○	·	·	○	·	·
Barringun Zero	BANZ	·	·	·	·	·	·	○	●	○	○	·	·	●	●	●	○
Barcaldine	BARC	·	○	○	●	○	·	○	●	○	·	●	●	·	·	·	·
BM26	BM26	·	·	·	·	·	·	·	●	·	·	·	·	·	·	·	·
BM45	BM45	·	·	·	·	·	·	·	·	·	●	·	·	·	·	·	·
BM46	BM46	·	·	·	·	·	·	·	·	·	●	·	·	·	·	·	·
BM55	BM55	·	·	·	·	·	·	·	·	●	·	·	·	·	·	·	·
Breadlbane	BREA	·	·	·	·	·	·	○	●	○	·	●	●	·	·	·	·
Brunswick	BRUN	·	·	·	·	·	·	·	·	·	·	·	·	●	●	●	○
Bullanginya	BULL	○	●	●	●	●	·	●	●	○	○	·	·	·	·	·	·
Bungalow	BUNG	·	·	·	·	·	·	·	·	·	·	·	○	·	·	·	·
Crowdy	CROW	·	·	·	·	·	·	·	·	·	·	·	·	●	●	●	○
McDills No1 Bore	DILL	·	·	·	·	·	·	·	●	●	●	○	·	·	·	·	·
Eden	EDEN	·	●	●	●	●	·	·	·	·	·	·	·	·	·	·	·
Emu	EMUU	·	·	·	·	·	·	·	·	·	·	●	●	·	·	·	·
Gilgunnia	GILG	·	·	·	·	·	·	●	●	●	○	·	·	·	·	·	·
Green Hill	GREN	·	·	·	·	·	·	·	·	·	·	·	·	·	●	●	·
Howitt	HOW1	·	·	·	·	·	·	●	●	●	·	·	·	·	·	·	·
Lake Littra	LLTR	○	·	●	●	●	·	●	●	○	○	·	·	·	·	·	·
Muckadilla	MUCK	·	○	○	●	○	·	●	●	○	○	·	·	·	·	·	·
Normanton	NORM	·	·	·	·	·	·	·	·	·	·	·	·	·	●	●	·
Olive	OLVE	·	·	·	·	·	·	●	●	●	○	·	·	·	·	·	·
Orroral Valley	ORRO	·	·	·	·	·	·	·	·	●	●	·	·	·	·	·	·
Piebald	PIEB	·	·	·	·	·	·	·	·	·	·	·	·	·	●	●	·
Qld Uni of Tech	QUT1	○	●	●	●	○	○	○	●	○	○	●	○	○	·	·	○
Roper River	ROPE	·	·	·	·	·	·	·	●	●	·	·	·	·	·	·	·
Shamrock	SHAM	·	·	·	·	·	·	·	●	●	·	·	·	·	·	·	·
Sundown	SUND	·	·	·	·	·	·	●	●	●	○	·	·	·	·	·	·
Texas Pillar	TEXA	·	●	●	●	●	·	·	·	·	·	·	·	·	●	●	○
Wilfred	WILF	·	·	·	·	·	·	·	·	·	·	●	●	·	●	●	·

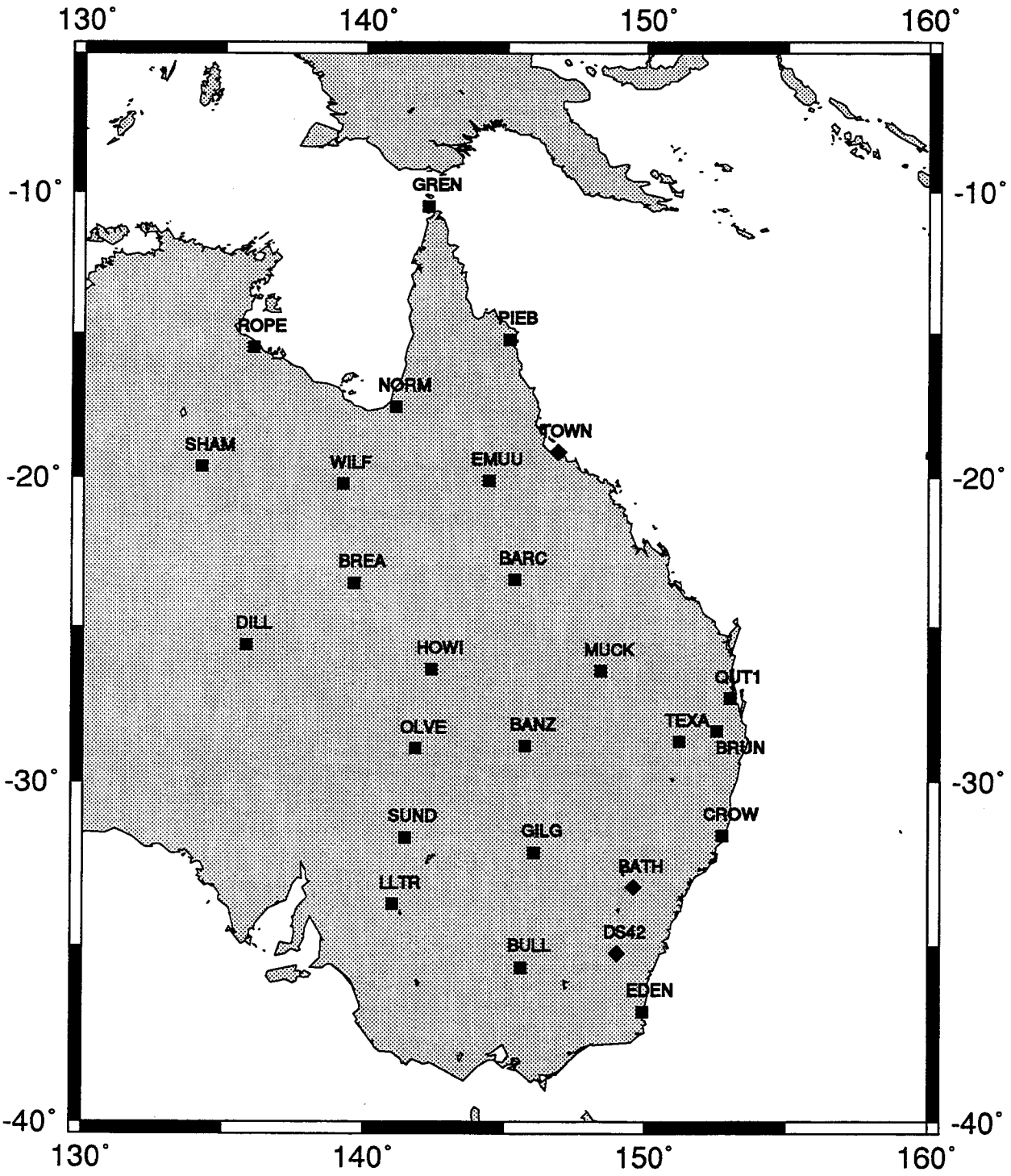

Figure F.6: Stations in the New South Wales and Queensland Network 1992

F.7 ARN93: Level 2

Table F.6: The Australian Region 1993 Time Slice Table

Station		Day of 1993																			
		234	235	236	237	238	239	240	241	242	243	244	245	246	247	248	249	250	251	252	253	254
Alice Springs	ALIC	·	·	·	·	·	·	●	●	●	●	●	●	●	●	●	·	·	·	·	·	·
Bakosurtanal	BAKO	·	o	·	o	o	o	·	·	●	·	●	●	·	·	·	·	·	·	o	·	·
Bathurst	BATH	·	·	·	·	·	o	●	●	●	●	●	●	●	●	●	o	o	·	·	·	·
Caversham-Perth	CAVE	·	·	·	·	·	·	·	·	●	●	●	●	·	·	·	·	·	·	·	·	·
Ceduna	CEDU	·	·	·	·	·	·	●	●	●	●	●	●	●	●	●	·	·	·	·	·	·
Cocos Island	COCO	o	o	o	o	o	o	●	●	●	●	●	●	o	·	·	·	·	·	·	·	·
Darwin	DARW	o	o	o	o	o	o	●	●	●	●	●	●	●	●	●	o	o	o	o	o	o
Canberra	DS42	o	o	o	o	o	o	●	●	●	●	●	●	●	●	●	o	o	o	o	o	o
Hobart,CIGNET	HOB1	o	o	o	o	o	o	●	●	●	●	●	●	●	●	●	o	o	o	o	·	·
Hobart,AFN	HOBA	o	o	o	o	o	o	●	●	●	●	●	●	●	●	●	o	o	o	o	o	o
Karratha	KARR	·	·	·	·	·	·	●	●	●	●	●	●	●	●	●	·	·	·	·	·	·
Port Moresby	MORE	o	o	o	o	o	o	●	●	●	●	●	●	●	●	●	o	o	o	o	o	·
Otago	OTA1	·	·	·	·	·	·	·	·	·	●	●	●	●	●	·	·	·	·	o	·	·
Dunedin	OTAG	·	·	·	·	·	o	·	●	●	●	●	●	●	●	●	o	o	o	·	·	·
Perth-Trimble	PER2	·	·	·	·	·	·	·	·	·	·	·	·	·	●	●	·	·	·	·	·	·
Perth-Rogue	PERR	·	·	·	·	·	·	●	●	●	●	●	●	●	·	·	·	·	·	·	·	·
Townsville,AFN	TOWA	·	·	·	·	·	·	●	●	●	●	●	●	●	●	●	·	·	·	·	·	·
Townsville,CIG	TOWN	o	o	o	o	o	o	●	●	●	●	●	●	●	●	●	o	o	o	o	o	o
Wellington	WELL	·	·	·	·	·	·	●	●	●	●	●	●	●	●	●	o	·	·	o	·	·
Yaragadee	YAR1	o	o	o	o	o	o	●	●	●	●	●	●	●	●	●	o	o	o	o	o	o

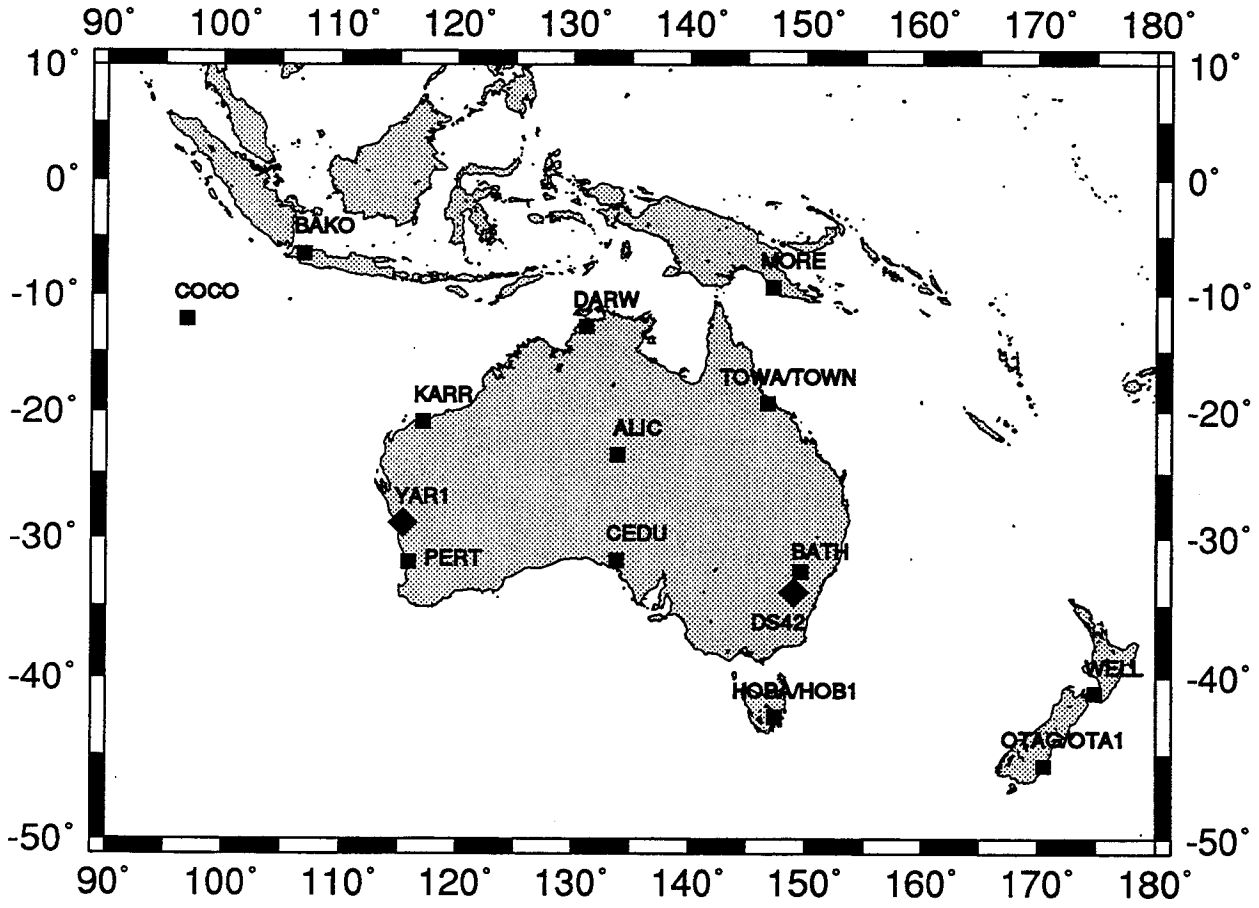

Figure F.7: Stations in the Australian Regional Network 1993

F.8 NZD93: Level 2

Table F.7: New Zealand 1993 Time Slice Table

Station		Day of 1993												
		067	068	069	070	071	072	073	074	075	076	077	078	079
Pukearenga No2	D026	·	·	·	·	·	·	·	·	·	·	·	●	·
XVII Whangaparaoa	D045	·	·	·	·	·	·	·	●	●	●	●	●	○
F Maketu	D072	·	·	·	·	·	·	·	·	·	·	●	·	●
201 Te Pohue	D078	·	·	·	·	·	·	·	·	·	·	·	●	●
106 Okahuatiu	D100	·	·	·	·	·	·	·	·	·	·	·	●	●
A Huirangi	D105	·	·	·	·	·	·	·	·	○	·	●	·	·
Mt Stewart	D131	·	·	·	·	·	·	·	·	●	●	·	·	·
Eringa	D143	·	·	·	·	·	·	·	●	·	●	·	·	·
Jenkins Hill No.2	D158	·	·	·	·	·	·	●	·	·	·	·	·	·
Isolated Hill	D191	·	·	·	·	·	●	·	○	·	·	·	·	·
Mt Pleasant	D212	·	·	·	·	●	●	·	·	·	·	·	·	·
Mt Mary	D229	·	●	·	●	●	·	·	·	·	·	·	·	·
A Mt Horrible	D233	·	●	·	·	○	·	·	·	·	·	·	·	·
T Hyde Rock	D253	●	●	●	·	·	·	·	·	·	·	·	·	·
X The Bluff	D286	●	·	·	·	·	·	·	·	·	·	·	·	·
A Nth Taieri	D269	○	○	·	·	·	·	·	·	·	·	·	·	·
Mt York	D302	●	·	○	·	·	·	·	·	·	·	·	·	·
HB Mt Greenland	D309	·	·	·	●	●	●	·	·	·	·	·	·	·
JF (Gillespies S.D.)	D320	·	·	●	●	·	·	·	·	·	·	·	·	·
8471	D338	·	·	●	○	·	·	·	·	·	·	·	·	·
A (Cape Campbell S.D.)	D425	·	·	·	·	·	·	●	●	·	·	·	·	·
Bluff Hill No.3	D431	·	·	·	·	·	·	·	·	·	●	·	·	●
79 (Rangiriri S.D.)	D452	·	·	·	·	·	·	·	·	·	·	●	·	·
I Parapara	D469	·	·	·	·	·	·	●	·	●	·	·	·	·
Marotiri No.2	D473	·	·	·	·	·	·	·	·	·	○	●	●	·
Three Sisters	D474	●	●	●	●	●	●	●	●	●	·	·	·	·
HHR9	D482	·	·	·	·	·	·	·	·	·	·	●	·	·
HHR9A	D483	·	·	·	·	·	·	·	·	·	·	·	●	●
Mt Murchison	D172	·	·	·	·	·	○	○	·	·	·	·	·	·
Maratiri Ecc	D481	·	·	·	·	·	·	·	·	·	·	○	○	·
F Maketu Ecc	D484	·	·	·	·	·	·	·	·	·	·	·	·	○
Wellington	WELL	○	○	○	●	●	●	●	●	●	●	●	●	●

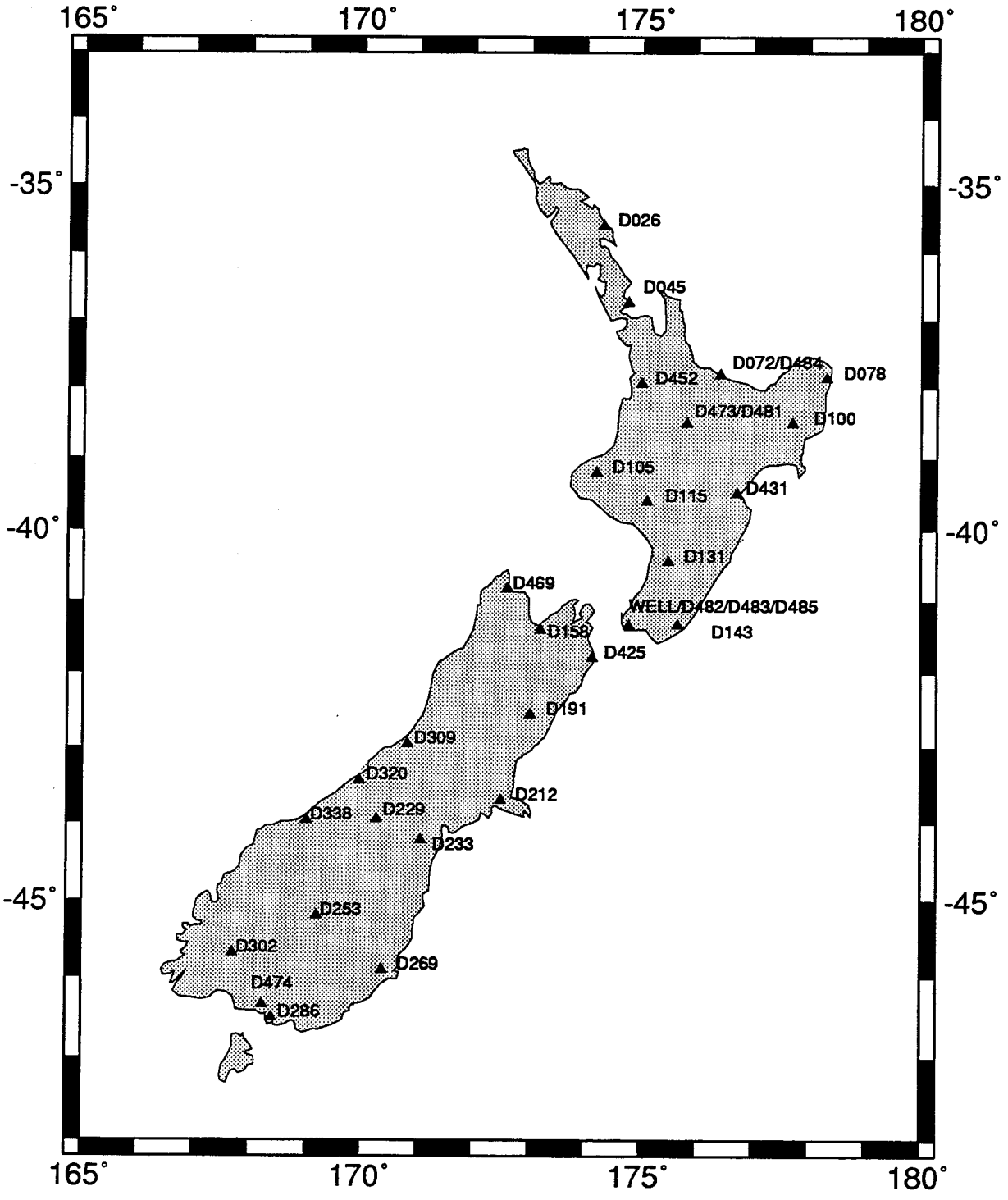

Figure F.8: Stations in the New Zealand Regional Network 1993

F.9 SAT93, NTQ93 & WAT93, Level 3 Networks

Table F.8: The State networks for the 500 km network in 1993 Time Slice Table

Station		Day of 1993														
		237	238	239	240	241	242	243	244	245	246	247	248	249	250	251
Atkinson	ATKI	·	·	·	●	●	●	·	·	·	·	·	·	·	·	·
Bathurst	BATH	·	·	·	●	●	●	·	·	·	·	·	·	·	·	·
Birdsville	BRDV	·	·	·	●	●	●	●	●	●	·	·	·	·	·	·
Broome	BROO	·	·	·	·	·	·	·	·	·	●	●	●	·	·	·
Caiguna	CAIG	·	·	·	·	·	·	·	·	·	●	●	●	·	·	·
Cameron West	CAMW	·	·	·	●	●	●	·	·	·	·	·	·	·	·	·
Carnarvon	CARN	·	·	·	·	·	·	·	·	·	●	●	●	·	·	·
Charmouth Hill	CHAR	·	·	·	●	●	●	·	·	·	·	·	·	·	·	·
Low Cliff	CLIF	·	·	·	●	●	●	·	·	·	·	·	·	·	·	·
Coolinbar	COOL	·	·	·	·	·	·	·	·	·	●	●	●	·	·	·
Deakin	DEAK	·	·	·	●	●	●	·	·	·	●	●	●	·	·	·
Esperance	ESPE	·	·	·	·	·	·	·	·	·	●	●	●	·	·	·
Gove	ELDO	·	·	·	·	·	·	●	●	●	·	·	·	·	·	·
McDougall	GIBS	·	·	·	·	·	·	·	·	·	·	·	·	·	·	·
Groote Island	GROO	·	·	·	·	·	·	●	●	●	·	·	·	·	·	·
Hawker	HWKR	·	·	·	●	●	●	·	·	·	·	·	·	·	·	·
Johnston Origin	JOHN	·	·	·	●	●	●	●	●	●	·	·	·	·	·	·
Junction	JUNC	·	·	·	●	●	●	·	·	·	·	·	·	·	·	·
Coolgardie	KALG	·	·	·	·	·	·	·	·	·	●	●	●	·	·	·
Kidman Springs	KDMN	·	·	·	·	·	·	●	●	●	·	·	·	·	·	·
Tanami	KILI	·	·	·	·	·	·	●	●	●	●	·	●	·	·	·
Lake Littra	LLTR	·	·	·	●	●	●	·	·	·	·	·	·	·	·	·
Olive	OLVE	·	·	·	●	●	●	·	·	·	·	·	·	·	·	·
Wyndam	PIVT	·	·	·	·	·	·	●	●	●	●	·	●	·	·	·
Noreena Down	RATH	·	·	·	·	·	·	·	·	·	●	●	●	·	·	·
Rawlinson	RAWL	·	·	·	●	●	●	●	●	●	●	●	●	·	·	·
Roper River	ROPE	·	·	·	·	·	·	●	●	●	·	·	·	·	·	·
Shamrock	SHAM	·	·	·	·	·	·	●	●	●	·	·	·	·	·	·
Port Stanvac	STAN	·	·	·	●	●	●	·	·	·	·	·	·	·	·	·
Torbay	TORB	·	·	·	·	·	·	·	·	·	●	●	●	·	·	·
Wilfred	WILF	·	·	·	·	·	·	●	●	●	·	·	·	·	·	·
Wollogorang	WOLL	·	·	·	·	·	·	●	●	●	·	·	·	·	·	·

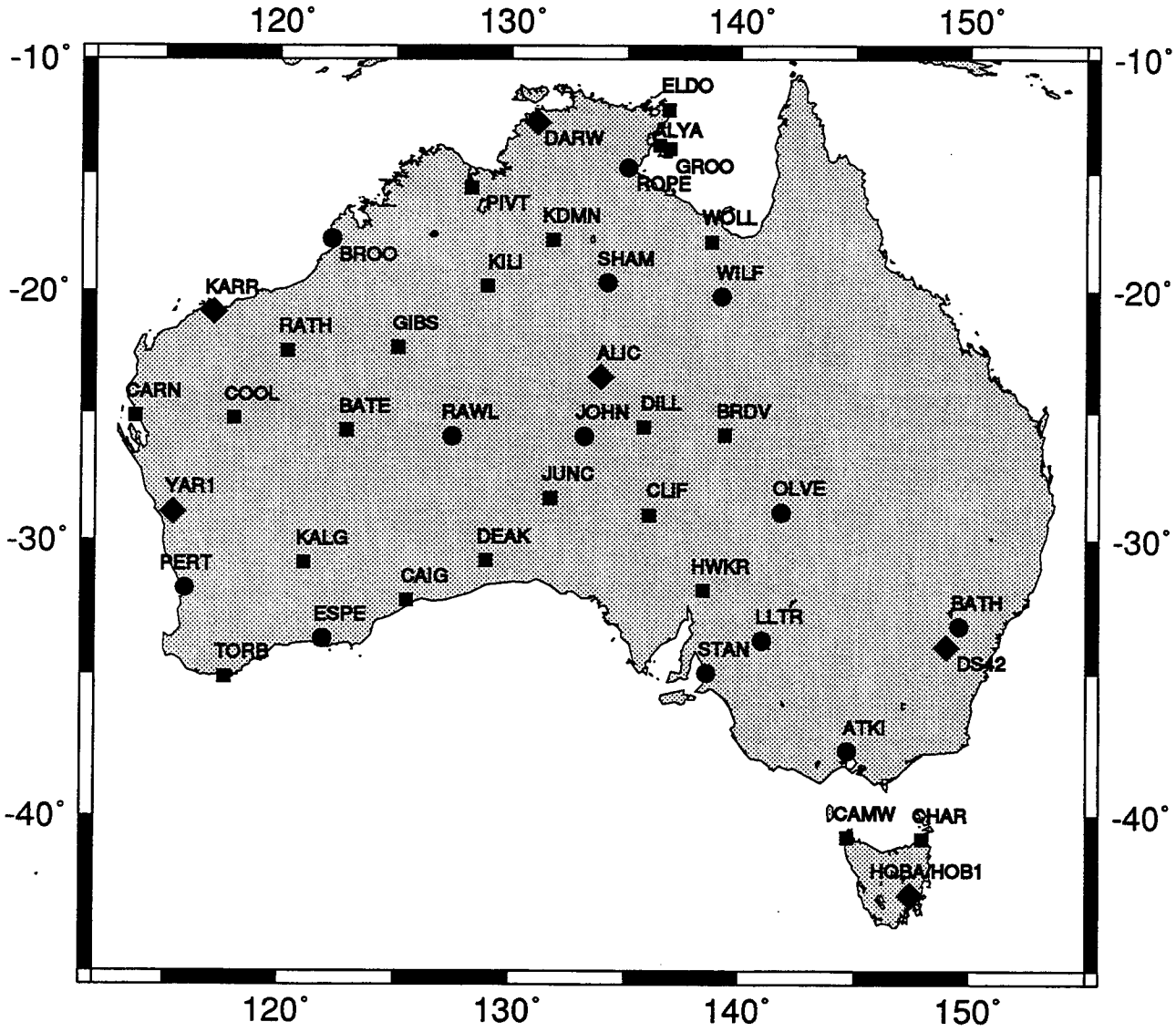

Figure F.9: Stations participating in the ANN 500 km network in 1993

F.10 PNG93: Level 3

Table F.9: The Papua New Guinea network in 1993 Time Slice Table

Station		Day of 1993																				
		230	231	232	233	234	235	236	237	238	239	240	241	242	243	244	245	246	247	248	249	250	251
Aiambak	AIAM	·	·	·	·	·	·	o	o	o	o	·	·	·	·	·	·	·	·	·	·	·	·
Amanab	AMAN	o	o	o	o	o	o	·	·	·	·	·	·	·	·	·	·	·	·	·	·	·	·
Goroka	GOKA	·	·	·	·	·	·	·	·	o	o	●	●	●	●	·	·	·	·	·	·	·	·
Gurney	GUNY	·	·	·	·	·	·	·	·	·	·	·	·	·	·	●	●	·	·	·	·	·	·
Kavieng	KAVI	·	·	·	·	·	·	·	·	·	·	·	·	·	·	·	·	●	●	●	o	·	·
Kikori	KIKO	·	·	·	·	·	·	·	·	·	·	●	●	●	·	·	·	·	·	·	·	·	·
Kopiago	KOPI	·	·	·	·	·	o	o	o	o	o	·	·	·	·	·	·	·	·	·	·	·	·
Madang	MADA	·	·	·	·	o	o	·	·	·	·	●	●	●	●	●	●	·	·	·	·	·	·
Manus	MANU	·	·	·	·	·	·	·	·	·	·	·	·	·	·	·	·	·	●	●	o	o	o
Mendi	MEND	·	·	·	·	·	·	·	·	o	o	●	●	·	·	·	·	·	·	·	·	·	·
Ningerum	NING	·	·	·	·	·	·	o	o	·	·	·	·	·	·	·	·	·	·	·	·	·	·
Unitech	UNIT	·	·	·	·	·	·	·	·	·	·	·	·	·	●	●	●	·	·	·	·	·	·
Vanimo	VANI	o	o	o	·	·	·	·	·	·	·	·	·	·	·	·	·	·	·	·	·	·	·
Wankun	WANK	·	·	·	·	·	·	·	·	·	·	·	·	·	●	●	●	·	·	·	·	·	·
Wewak	WEWK	·	o	o	o	o	o	o	o	·	·	·	·	·	·	·	·	·	·	·	·	·	·
Wuvulu	WUVU	o	o	o	o	o	·	·	·	·	·	·	·	·	·	·	·	●	●	●	·	·	·

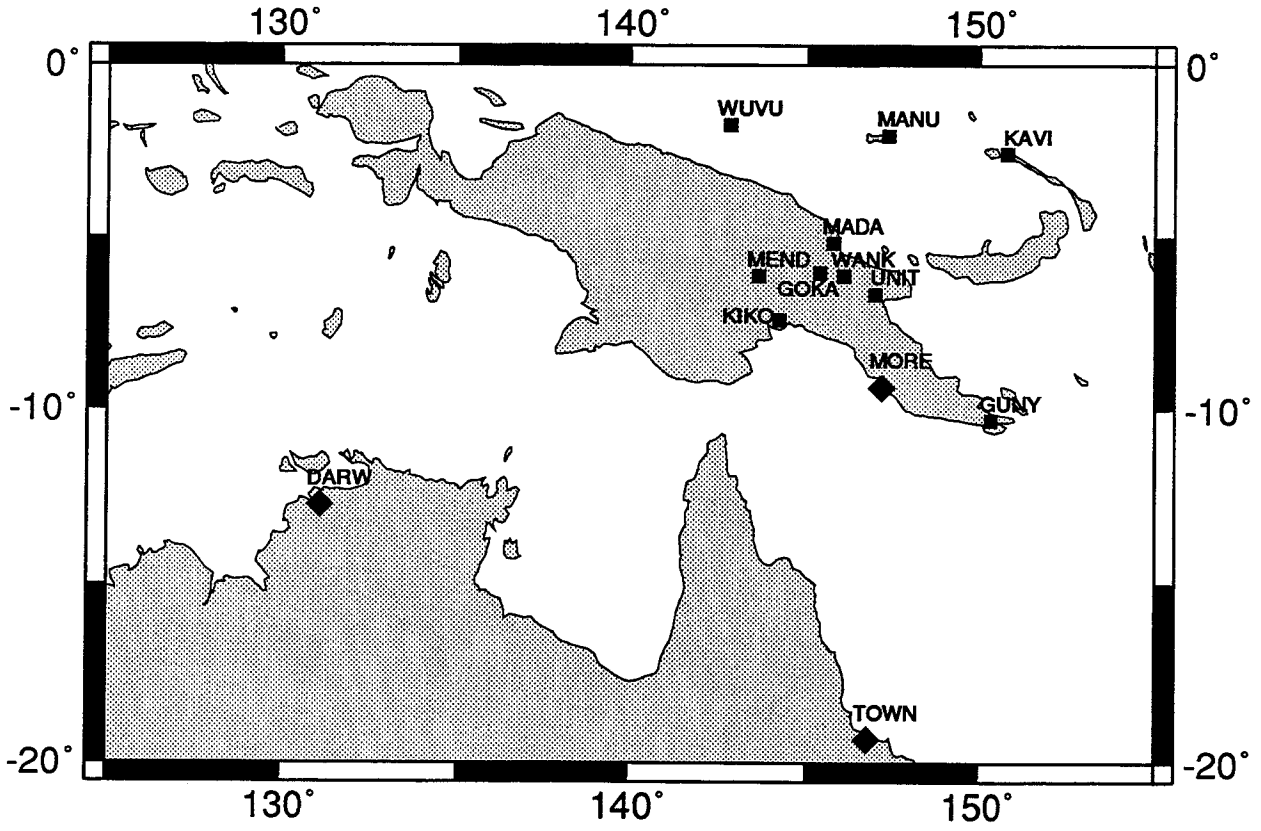

Figure F.10: Stations in the Papua New Guinea Network 1993

F.11 QLD93: Level 3

Table F.10: The Queensland network in 1993 Time Slice Table

Station		Day of 1993			
		1 5 8	1 5 9	1 6 0	1 6 1
Mackay	BASS	•	•	•	•
Mulara	MULA	•	•	•	•
Oaks	OAKS	·	·	·	•
Sugarland	SUGA	•	•	•	•

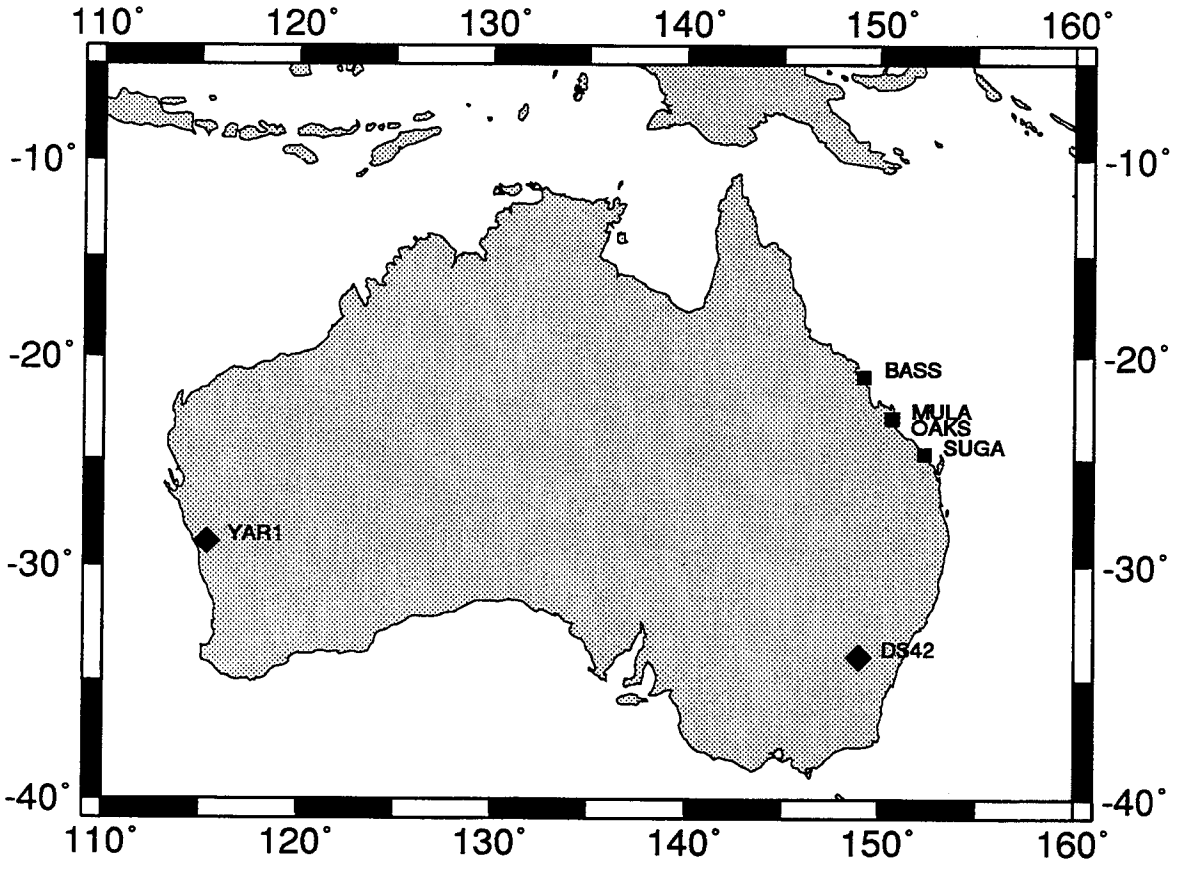

Figure F.11: Stations in the Queensland Network 1993

F.12 AUS94: Level 3

Table F.11: The Australian regional network in 1994 Time Slice Table

Station		Day of 1994						
		205	206	207	208	209	210	211
Alice Springs	ALIC	·	·	·	●	●	●	●
Atkinson	ATK1	·	·	·	●	●	●	·
Barringun Zero	BANZ	·	·	·	●	●	●	·
Bathurst	BATH	·	·	·	●	●	●	●
Bullanginya	BULL	·	·	·	●	●	●	·
Casey	CAS1	·	·	·	●	●	●	●
Ceduna	CEDU	·	·	·	●	●	●	·
Darwin	DARW	·	·	·	●	●	●	●
Davis	DAV1	·	·	·	●	●	●	●
Canberra	DS42	·	o	o	●	●	●	●
Gilgunnia	GILG	·	·	·	●	●	●	·
Hobart Cignet	HOB1	·	·	·	●	●	●	●
Hobart AFN	HOB2	·	·	·	·	·	●	●
Howitt	HOW1	·	·	·	●	●	●	·
Karratha	KARR	·	·	·	●	●	●	●
Lake Littra	LLTR	·	·	·	●	●	●	·
Macquarie Is	MAC1	·	·	·	●	●	●	●
McMurdo	MCM1	·	·	·	●	●	●	●
Port Moresby	MORE	·	o	o	●	●	●	·
Olive	OLVE	·	·	·	●	●	●	·
Perth Roque	PERT	·	·	·	●	●	●	●
Portland	PORT	·	·	·	●	●	●	·
Sundown	SUND	·	·	·	●	●	●	●
Townsville	TOWA	·	·	·	●	●	●	●
Lae Uni Tech	UNIT	·	o	o	●	●	·	·
Yaragadee	YAR1	·	·	·	●	●	●	●

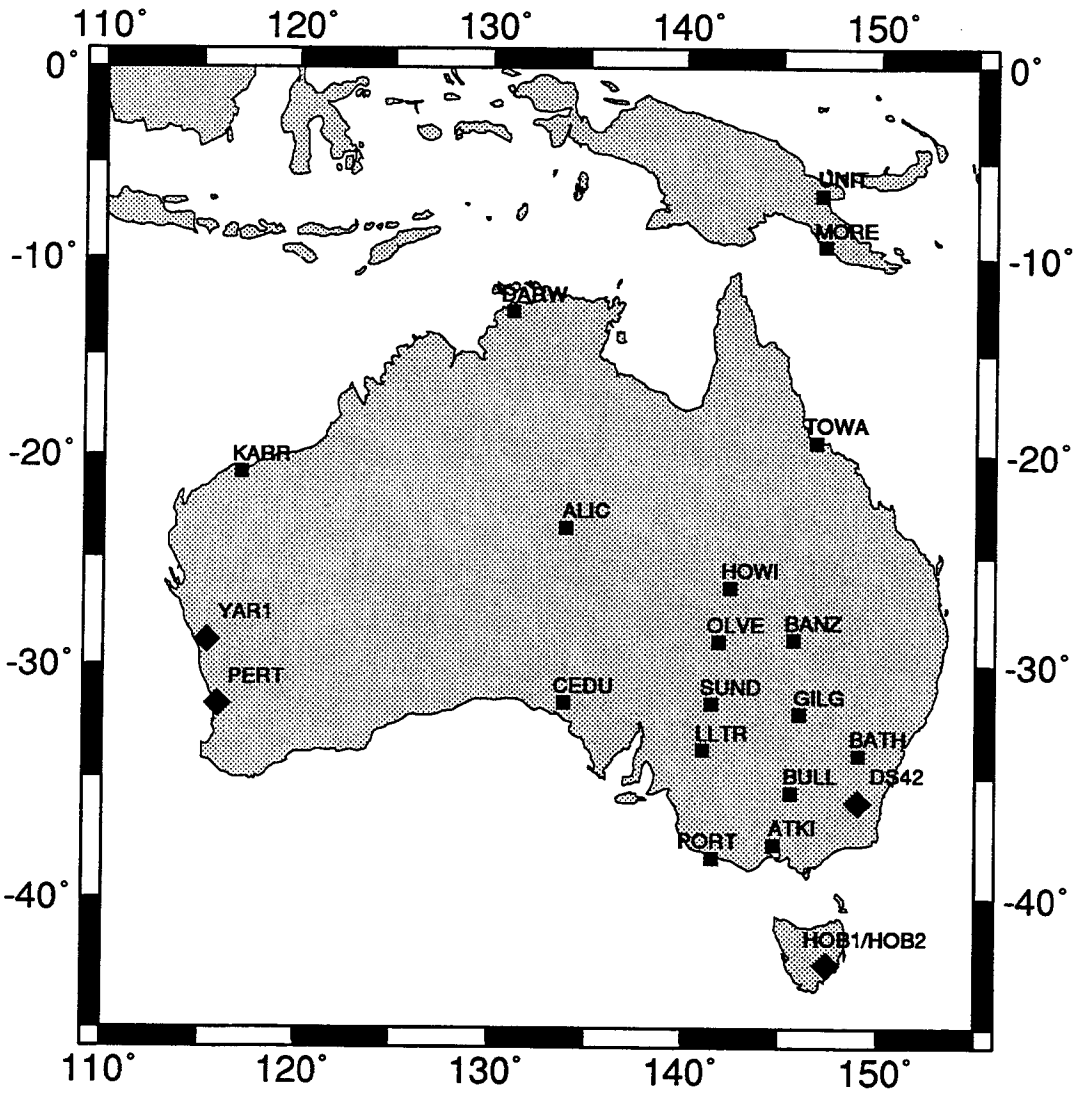

Figure F.12: Stations in the Australian Regional Network 1994

F.13 ANT94: Level 1

Table F.12: The Antarctic Stations in 1994 Time Slice Table

Station		Day of 1994															
		005	006	007	008	009	010	011	012	051	052	053	054	055	056	057	058
Algonquin	ALGO	·	·	●	●	●	●	·	·	·	·	●	●	·	●	·	·
Blyth PGGA	BLYT	·	·	·	·	·	·	·	·	·	·	·	●	●	●	·	·
Bermuda	BRMU	·	·	●	●	●	●	·	·	·	·	●	●	●	●	·	·
Casey Pillar	CAS1	·	·	●	●	●	●	·	·	·	·	●	●	●	●	·	·
Davis NMS5	DAV1	·	·	●	●	●	●	·	·	·	·	●	●	●	●	·	·
Penticton WC	DRAO	·	·	●	●	●	●	·	·	·	·	●	●	●	●	·	·
Goldstone PG	DS10	·	·	●	●	●	●	·	·	·	·	●	●	●	●	·	·
Tidbinbilla	DS42	·	·	●	●	●	●	·	·	·	·	●	●	●	●	·	·
Madrid	DS60	·	·	●	●	●	●	·	·	·	·	●	●	●	●	·	·
UNSW Pillar	EC19	·	·	·	·	·	·	·	·	·	·	●	·	●	●	·	·
Fairbanks	FAIR	·	·	●	●	●	●	·	·	·	·	●	●	●	●	·	·
Fortaleza	FORT	·	·	●	●	●	●	·	·	·	·	●	●	·	●	·	·
Hartebeestho	HART	·	·	●	●	●	●	·	·	·	·	●	●	●	●	·	·
Hobart	HOB1	·	·	●	●	●	●	·	·	·	·	●	●	●	●	·	·
JPLM7272 PGG	JPLM	·	·	●	●	●	●	·	·	·	·	●	●	●	●	·	·
Kokee Rogue	KOKR	·	·	●	●	●	●	·	·	·	·	●	●	●	●	·	·
Kootwijk	KOSG	·	·	●	●	●	●	·	·	·	·	●	·	·	·	·	·
Kourou Fr.G	KOUR	·	·	●	●	●	●	·	·	·	·	●	●	●	●	·	·
Macquarie Is	MAC1	·	·	●	●	●	●	·	·	·	·	●	●	●	●	·	·
Maspalomas	MASP	·	·	●	●	●	●	·	·	·	·	●	●	●	●	·	·
Lake Mathews	MATH	·	·	●	●	●	●	·	·	·	·	●	●	●	●	·	·
Mawson Pilla	MAW1	·	·	●	●	●	●	·	·	·	·	●	●	●	●	·	·
McMurdo	MCM1	·	·	·	·	·	·	·	·	·	·	·	●	●	●	·	·
Onsala	ONSA	·	·	●	●	●	●	·	·	·	·	●	·	●	●	·	·
Tahiti	PAMA	·	·	●	●	●	●	·	·	·	·	●	●	●	●	·	·
Perth	PERT	·	·	·	●	●	●	·	·	·	·	●	●	●	●	·	·
Pie Town NM	PIE1	·	·	●	●	●	●	·	·	·	·	●	●	●	●	·	·
PFO1 PGGA	PIN1	·	·	●	●	●	●	·	·	·	·	●	●	●	●	·	·
Palos Verdes	PVEP	·	·	●	●	●	●	·	·	·	·	●	●	●	●	·	·
Quincy CA	QUIN	·	·	●	●	●	●	·	·	·	·	●	●	●	●	·	·
Richmond 199	RCM5	·	·	●	●	●	●	·	·	·	·	●	●	●	●	·	·
Santiago	SANT	·	·	●	●	●	●	·	·	·	·	●	●	●	●	·	·
Scripps 3 PG	SIO3	·	·	●	●	●	●	·	·	·	·	●	●	●	●	·	·
St Johns	STJO	·	·	●	●	●	●	·	·	·	·	●	●	●	●	·	·
Taiwan	TAIW	·	·	●	●	●	●	·	·	·	·	●	●	●	●	·	·
Tromso	TROM	·	·	●	●	●	●	·	·	·	·	●	●	●	●	·	·
Usuda final	USU3	·	·	●	●	●	●	·	·	·	·	●	●	●	●	·	·
Vandenberg P	VNDP	·	·	●	●	●	●	·	·	·	·	●	●	●	●	·	·
Wellington	WELL	·	·	●	●	●	●	·	·	·	·	·	·	·	·	·	·
Wettzell	WTZ1	·	·	●	●	●	●	·	·	·	·	●	●	●	●	·	·
Yaragadee	YAR1	·	·	●	●	●	●	·	·	·	·	●	●	●	●	·	·
Yellowknife	YELL	·	·	●	●	●	●	·	·	·	·	●	●	●	●	·	·

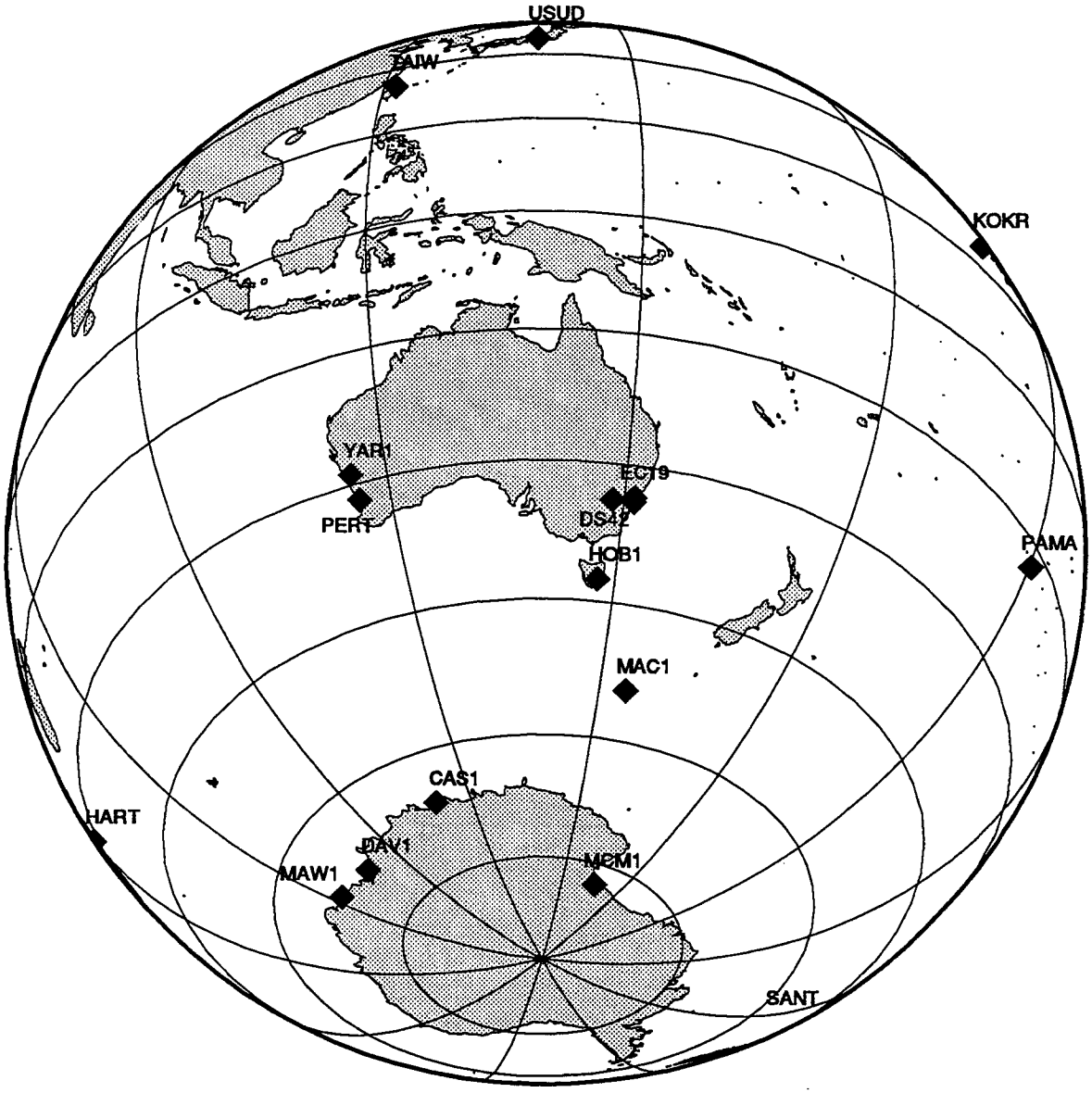

Figure F.13: Stations in the Antarctic Global Network 1994

Publications from

THE SCHOOL OF GEOMATIC ENGINEERING

(Formerly School of Surveying)

THE UNIVERSITY OF NEW SOUTH WALES

All prices include postage by surface mail. Air mail rates on application. (Effective September 1996)

To order, write to Publications Officer, School of Geomatic Engineering
The University of New South Wales, Sydney 2052, AUSTRALIA

NOTE: ALL ORDERS MUST BE PREPAID

UNISURV REPORTS - S SERIES

S8 - S20	Price (including postage) :		$10.00
S29 onwards	Price (including postage) :	Individuals	$25.00
		Institutions	$30.00

S8 A. Stolz, "Three-D Cartesian co-ordinates of part of the Australian geodetic network by the use of local astronomic vector systems", Unisurv Rep. S8, 182 pp, 1972.

S10 A.J. Robinson, "Study of zero error & ground swing of the model MRA101 tellurometer", Unisurv Rep. S10, 200 pp, 1973.

S12. G.J.F. Holden, "An evaluation of orthophotography in an integrated mapping system", Unisurv Rep. S12, 232 pp, 1974.

S14. Edward G. Anderson, "The Effect of Topography on Solutions of Stokes` Problem", Unisurv Rep. S14, 252 pp, 1976.

S16. K. Bretreger, "Earth Tide Effects on Geodetic Observations", Unisurv S16, 173 pp, 1978.

S17. C. Rizos, "The role of the gravity field in sea surface topography studies", Unisurv S17, 299 pp, 1980.

S18. B.C. Forster, "Some measures of urban residential quality from LANDSAT multi-spectral data", Unisurv S18, 223 pp, 1981.

S19. Richard Coleman, "A Geodetic Basis for recovering Ocean Dynamic Information from Satellite Altimetry", Unisurv S19,332 pp, 1981.

S20. Douglas R. Larden, "Monitoring the Earth's Rotation by Lunar Laser Ranging", Unisurv Report S20, 280 pp, 1982.

S29 Gary S Chisholm, "Integration of GPS into hydrographic survey operations", Unisurv S29, 190 pp, 1987.

S30. Gary Alan Jeffress, "An investigation of Doppler satellite positioning multi-station software", Unisurv S30, 118 pp, 1987.

S31. Jahja Soetandi, "A model for a cadastral land information system for Indonesia", Unisurv S31, 168 pp, 1988.

S33. R. D. Holloway, "The integration of GPS heights into the Australian Height Datum", Unisurv S33, 151 pp.,1988.

S34. Robin C. Mullin, "Data update in a Land Information Network", Unisurv S34, 168 pp. 1988.

S35. Bertrand Merminod, "The use of Kalman filters in GPS Navigation", Unisurv S35, 203 pp., 1989.

S36. Andrew R. Marshall, "Network design and optimisation in close range Photogrammetry", Unisurv S36, 249 pp., 1989.

S37. Wattana Jaroondhampinij, "A model of Computerised parcel-based Land Information System for the Department of Lands, Thailand," Unisurv S37, 281 pp., 1989.

S38. C. Rizos (Ed.), D.B. Grant, A. Stolz, B. Merminod, C.C. Mazur "Contributions to GPS Studies", Unisurv S38, 204 pp., 1990.

S39. C. Bosloper, "Multipath and GPS short periodic components of the time variation of the differential dispersive delay", Unisurv S39, 214 pp., 1990.

S40. John Michael Nolan, "Development of a Navigational System utilizing the Global Positioning System in a real time, differential mode", Unisurv S40, 163 pp., 1990.

S41. Roderick T. Macleod, "The resolution of Mean Sea Level anomalies along the NSW coastline using the Global Positioning System", 278 pp., 1990.

S42. Douglas A. Kinlyside, "Densification Surveys in New South Wales - coping with distortions", 209 pp., 1992.

S43. A. H. W. Kearsley (ed.), Z. Ahmad, B. R. Harvey and A. Kasenda, "Contributions to Geoid Evaluations and GPS Heighting", 209 pp., 1993.

S44. Paul Tregoning, "GPS Measurements in the Australian and Indonesian Regions (1989-1993)", 134 + xiii pp, 1996.

S45. Wan-Xuan Fu, "A study of GPS and other navigation systems for high precision navigation and attitude determinations", 332pp, 1996.

S46. Peter Morgan et al, "A zero order GPS network for the Australia region", 187 + xii pp, 1996.

MONOGRAPHS

Prices include postage by surface mail

M1.	R.S. Mather, "The theory and geodetic use of some common projections", (2nd edition), 125 pp., 1978.	Price	$15.00
M2.	R.S. Mather, "The analysis of the earth's gravity field", 172 pp., 1971.	Price	$8.00
M3.	G.G. Bennett, "Tables for prediction of daylight stars", 24 pp.,1974.	Price	$5.00
M4.	G.G. Bennett, J.G. Freislich & M. Maughan, "Star prediction tables for the fixing of position", 200 pp., 1974.	Price	$8.00
M8.	A.H.W. Kearsley, "Geodetic Surveying", 96 pp, (revised) 1988.	Price	$12.00
M11.	W.F. Caspary, "Concepts of Network and Deformation Analysis", 183 pp., 1988.	Price	$25.00
M12.	F.K. Brunner, "Atmospheric Effects on Geodetic Space Measurements", 110 pp., 1988.	Price	$16.00
M13.	Bruce R. Harvey, "Practical Least Squares and Statistics for Surveyors", (2nd edition), 319 pp., 1994.	Price	$30.00
M14.	Ewan G. Masters & John R. Pollard (Ed.), "Land Information Management", 269 pp., 1991. (Proceedings LIM Conference, July 1991).	Price	$20.00
M15/1	Ewan G. Masters & John R. Pollard (Ed.), "Land Information Management - Geographic Information Systems - Advance Remote Sensing Vol 1" 295 pp., 1993 (Proceedings of LIM & GIS Conference, July 1993).	Price	$30.00
M15/2	Ewan G. Masters & John R. Pollard (Ed.), "Land Information Management - Geographic Information Systems - Advance Remote Sensing Vol 2" 376 pp., 1993 (Proceedings of Advanced Remote Sensing Conference, July 1993).	Price	$30.00
M16.	A. Stolz, "An Introduction to Geodesy", 112 pp., 1994.	Price	$20.00